The role of unicellular cyanobacteria in nitrogen fixation and assimilation in subtropical marine waters

Dissertation
Zur Erlangung des Grades eines Doktors der Naturwissenschaften
– Dr. rer. Nat. –

Dem Fachbereich Geowissenschaften
der Universität Bremen

vorgelegt von

Andreas Krupke

Bremen, August 2013

Die vorliegende Arbeit wurde in der Zeit von April 2010 bis August 2013 am Max–Planck–Institut für marine Mikrobiologie in Bremen angefertigt.

1. Gutachter: Prof. Dr. Marcel Kuypers
2. Gutachter: PD Dr. Bernhard Fuchs

Tag des Promotionskolloquiums: 11.09.2013

La volunté ouvre la porte vers le succès

Louis Pasteur (1822 – 1895)

Abstract

Biological N_2 fixation constitutes the major source of nitrogen in open ocean systems, regulating the marine nitrogen inventory and primary productivity. Symbiotic relationships between phytoplankton and N_2 fixing microorganisms (diazotrophs) have been suggested to play a significant role in the ecology and biogeochemistry in these oceanic regions. The widely distributed, uncultured N_2 fixing cyanobacterium UCYN–A was suggested to live in symbiosis since it has unprecedented genome reduction, including the lack of genes encoding for oxygen–evolving photosystem II and the tricarboxylic acid cycle. This thesis aims to study carbon and nitrogen metabolism on field populations of UCYN–A using molecular biology, as well as mass spectrometry tools to visualize metabolic activity on a single cell scale.

The development of a 16S rRNA oligonucleotide probe specifically targeting UCYN–A cells and its successful application on environmental samples (Manuscript I and II) revealed a symbiotic partnership with a unicellular prymnesiophyte. We demonstrated a nutrient transfer in carbon and nitrogen compounds between these two partner cells, providing an explanation how these diazotrophs thrive in open ocean systems. Further, UCYN–A can also associate with globally abundant calcifying prymnesiophyte members, e.g. *Braarudosphaera bigelowii*, indicating that this symbiosis might impact the efficiency of the *biological carbon pump*.

In manuscript III, we provided quantitative information on the cellular abundance and distribution of UCYN–A cells in the North Atlantic Ocean and identified the eukaryotic partner cell as *Haptophyta* (including prymnesiophyte) via double Catalyzed Reporter Deposition–Fluorescence *In Situ* Hybridization (CARD–FISH). The UCYN–A–*Haptophyta* association was the dominant form (87.0±6.1%) over free–living UCYN–A cells. Interestingly, we also detected UCYN–A cells living in association with unknown eukaryotes and non–calcifying *Haptophyta* cells, raising questions about the host specificity.

During a follow up study (Manuscript IV), we conducted various nutrient amendment experiments (including iron, phosphorus, ammonium–nitrate and Saharan Dust) in order to examine physiological interactions between individual UCYN–A and *Haptophyta* cells. Single cell measurements using nanometer scale secondary ion mass spectrometry (nanoSIMS) revealed a tight physiological coupling in the transfer of carbon ($R^2 = 0.6232$; n = 44) and nitrogen ($R^2 = 0.9659$; n = 44) between host and symbiont. N_2 fixation was mainly stimulated when iron–rich Saharan Dust was added, emphasizing on aeolian dust deposition in seawater as a major parameter in constraining N_2 fixation of UCYN–A. Moreover, when fixed nitrogen species (ammonium and nitrate) were added, a third unknown microbial partner

cell was observed within individual UCYN–A–*Haptophyta* associations, but their menaing is unclear.

Based on this thesis work we revealed how UCYN–A cells thrive in the environment and established a culture–independent technique to assess the *in situ* activity in respect to CO_2 and N_2 fixation of this ecological relevant group of microorganisms. Furthermore, this unusual partnership between a cyanobacterium and a unicellular alga is a model for symbiosis and is analogous to plastid and organismal evolution, and if calcifying, may have important implications for past and present oceanic N_2 fixation.

Zusammenfassung

Die biologische Fixierung von atmosphärischem Stickstoffgas (N_2) stellt die Hauptquelle von verfügbarem Stickstoff im offenen Ozean dar und reguliert den marinen Stickstoffhaushalt und die Primärproduktion. Symbiotische Beziehungen zwischen Phytoplankton und N_2 fixierenden Mikroorganismen (Diazotrophe) spielen vermutlich eine entscheidende Rolle in der Ökologie und Biogeochemie innerhalb dieser marinen Gebiete. Die weit verbreitete, unkultivierte N_2 fixierende Cyanobakterie UCYN–A wurde vermutet in Symbiose zu leben wegen ihrer beispiellosen Genomreduktion, unter anderem fehlender Gene für das Sauerstoff produzierende Photosystem II und für den Tricarbonsäurezyklus. Der Schwerpunkt dieser Arbeit liegt auf das Studieren vom Kohlenstoff (C) und Stickstoff (N) Metabolismus in Feldpopulationen von UCYN–A unter der Benutzung von molekular–biologischen Techniken, als auch massen–spektroskopischen Geräten, um die metabolische Aktivität von Einzelzellen zu visualisieren.

Die Entwicklung einer 16S rRNA Oligonukleotid Sonde spezifisch für UCYN–A Zellen und ihrer erfolgreichen Applikation in Umweltproben (Manuskript I und II) führte zu der Entdeckung einer symbiotischen Partnerschaft mit einem einzelligen Prymnesiophyten. Wir zeigen einen Nährstofftransfer von C und N zwischen UCYN–A und deren Partnerzellen, und bieten eine Erklärung wie diese diazotrophe Organismen im offenen Ozean leben. Weiterhin, UCYN–A Zellen können auch mit global verbreiteten kalzifizierenden Prymnesiophyten, zum Beispiel *Braarudosphaera bigelowii*, assoziieren, was darauf hindeuten kann, dass diese Symbiose die Effizienz der biologischen Kohlenstoffpumpe beeinflussen kann.

In Manuskript III stellen wir quantitative Informationen zur zellulären Abundanz und Verteilung von UCYN–A Zellen im Nord Atlantik bereit und identifizieren den eukaryotischen Partner als *Haptophyta* (inklusive Prymnesiophyten). Hierbei haben wir die doppelte „Catalyzed Reporter Deposition–*In Situ* Hybridization“ (CARD–FISH) Methodik angewandt. Die UCYN–A–*Haptophyta* Assoziation war die dominante Form (87.0±6.1%) gegenüber frei–lebenden UCYN–A Zellen. Interessanterweise haben wir ebenfalls UCYN–A Zellen mit unbekannten Eukaryoten assoziiert gesehen und nicht kalzifizierenden *Haptophyta*, welche Fragen über die Host Spezifität aufwerfen.

In einer Folgestudie (Manuskript IV) führten wir Experimente mit verschiedenen Nährstoffzugaben durch (inklusive Eisen, Phosphat, Ammonium–Nitrat und Staub aus der Sahara Wüste), um die physiologischen Interaktionen zwischen UCYN–A und *Haptophyta*

Zellen zu untersuchen. Durch die nanoSIMS Technologie konnten wir Messungen an einzelnen Zellen durchführen, welche gezeigt haben, dass eine signifikante physiologische Kopplung im Transfer von C (R^2 = 0.6232; n = 44) und N (R^2 = 0.9659; n = 44) zwischen Host und Symbiont besteht. N_2 Fixierung war hauptsächlich durch eisenhaltige Staubzugabe stimuliert worden und unterstreicht dadurch die Bedeutung vom windtransportiertem Staubeintrag im Seewasser als Hauptfaktor für die Limitierung von N_2 Fixierung in UCYN–A Zellen. Sobald biologisch verfügbares N in den Experimenten verfügbar war, haben wir in einigen UCYN–A–*Haptopyhta* Assoziationen eine dritte unbekannte mikrobielle Struktur festgestellt, deren Bedeutung unklar ist.

Auf Grund dieser Doktorarbeit konnten wir zeigen wie UCYN–A Zellen in der Umwelt leben und haben eine Methodik etabliert, welche die *in situ* Aktivität in Bezug auf CO_2 und N_2 Fixierung dieser einzigartigen Assoziation messen kann. Weiterhin, diese ungewöhnliche Partnerschaft zwischen einer Cyanobakterie und einer einzelligen Alge stellt ein Model für Symbiose dar und ist ein Analogon zur Plastid– und Organismusevolution. Zusätzlich, wenn UCYN–A Zellen mit kalzifizierenden Eukaryoten assoziieren, können solche Partnerschaften einen entscheidenden Einfluss auf vergangene und aktuelle marine N_2 Fixierung haben.

Table of Contents

1 Introduction ... 1
1.1 Nitrogen fixation in marine systems ... 1
1.2 Nitrogen fixing microorganisms ... 4
1.2.1 Trichodesmium ... 6
1.2.2 Heterocyst forming cyanobacteria ... 8
1.2.3 Unicellular cyanobacterial groups (UCYN) ... 9
1.3 Parameters controlling N_2 fixation ... 13
1.4 Assessing N_2 fixation activity ... 14
1.5 Aims of thesis ... 18
1.6 References ... 21

2 Manuscripts ... 31
2.1 Manuscript I: Unicellular Cyanobacterium Symbiotic with a Single-Celled Eukaryotic Alga ... 33
2.1.1 Manuscript I: Supplementary Materials ... 39
2.2 Manuscript II: *In situ* identification and N_2 and C fixation rates of uncultivated cyanobacteria populations ... 59
2.2.1 Manuscript II: Supplementary Information ... 73
2.3 Manuscript III: Distribution of the association between unicellular algae and the dinitrogen (N_2) fixing cyanobacterium UCYN–A in the North Atlantic Ocean ... 83
2.3.1 Manuscript III: Supplementary Information ... 113
2.4 Manuscript IV: The effect of nutrients on carbon and nitrogen fixation by the UCYN–A–*Haptophyta* symbiosis ... 119
2.4.1 Manuscript IV: Supplementary Information ... 145

3 General Discussion and outlook ... 149
3.1 References ... 155

4 Appendix ... 159
4.1 Responses of the coastal bacterial community to viral infection of the algae *Phaeocystis globosa* ... 159
4.2 Draft genome sequence of marine alphaproteobacterial strain HIMB11, the first cultivated representative of a unique lineage within the Roseobacter clade possessing a remarkably small genome ... 161
4.3 *In situ* oxygenic photosynthesis fuels aerobic oxidation of methane in the anoxic water of Lago di Cadagno ... 164
4.4 Experimental and single cell approaches to understanding microbial life in subsurface sediments underlying the extremely oligotrophic South Pacific Gyre ... 166

5 Acknowledgements ... 169

6 Erklärung ... 171

1 Introduction

1.1 Nitrogen fixation in marine systems

Dinitrogen gas (N_2) accounts for approximately 80% of the Earth's atmosphere, but due to its relatively inert chemical properties most organisms are not able to convert this gas into bioavailable nitrogen (Zehr and Paerl, 2008). Nitrogen (N) is indispensable for life since it constitutes a critical component of cellular biomass such as nucleic acids, lipids and proteins. The reduction of N_2 gas into bioavailable ammonia (NH_3) is commonly referred to as N_2 fixation and only a few microorganisms (diazotrophs) possess the metabolic repertoire to perform this process (Dixon and Kahn, 2004). Advancements in new methodologies including culture–independent techniques coupled to high throughput quantitative assays and genome sequencing efforts have revealed greater species diversity within the N_2 fixing community than previously known. However, our knowledge about the physiology and activity of these diazotrophs is limited.

Primary productivity in the world's oceans is considered to be mainly limited by N. Microbial mediated N_2 fixation is the major process that provides bioavailable nitrogen. Nitrates (i.e. NH_3, NO_3^- and NO_2^-), taken up along with CO_2 by photosynthetic phytoplankton, are converted into cellular organic compounds, forming the base of the marine food web (Capone, 2000). Phytoplankton turnover in surface waters causes a flux of sinking organic matter containing cellular biomass and organically rich N compounds (e.g. amino acids), leading to the formation of particulate organic nitrogen (PON). The biological degradation of PON results in the formation of nitrate (NO_3^-) in deeper water layers, which can fuel surface phytoplankton blooms by physical upwelling and mixing events. The amount of primary production supported by the regeneration and upwelling of nutrients within the euphotic zone is minor compared to the impact of newly fixed N (Capone et al., 1997; Capone et al., 2005) (Fig. 1).

Understanding the magnitude of marine N_2 fixation is of crucial interest because it influences ocean–atmosphere fluxes of carbon and other nutrients and ultimately regulates the concentrations of the greenhouse gas CO_2 (Sundquist and Broecker, 1985; Karl et al., 1997). Therefore, N_2 fixation represents a globally significant process that structures marine ecosystems by providing "new" N and by controlling the export and sequestration of organic carbon, a process known as the *biological pump*.

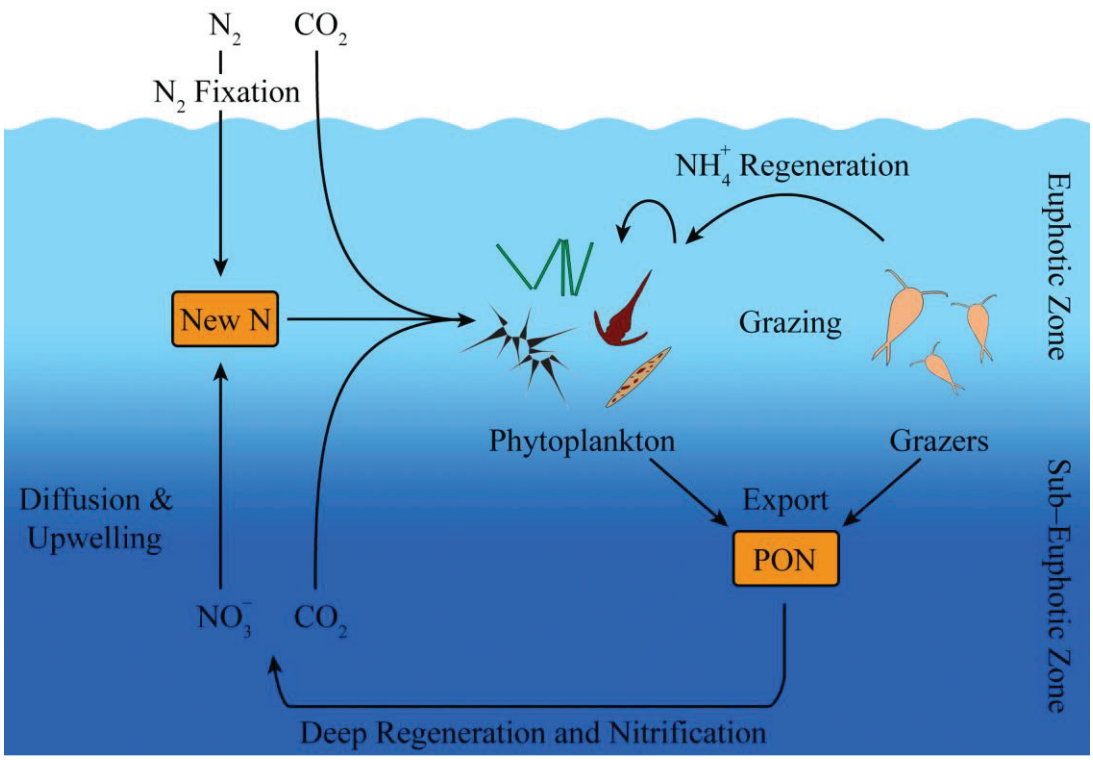

Fig. 1: Generalized marine N cycle with emphasis on N_2 fixation. The supply of "new" N based on N_2 fixation and nitrate from deep waters determines the amount of CO_2 fixation (primary productivity). The latter process defines how much fixed carbon and particulate organic nitrogen (PON) is exported to deeper water layers. Additionally, primary productivity is also fuelled by the regeneration of organic material to ammonia within surface waters. Modified after Sohm et al. (2011)

The marine N cycle is complex and involves a variety of nitrogen species such as N_2, NO_3^-, ammonium (NH_4^+), nitrite (NO_2^-), nitrous oxide (N_2O) and organic N ranging in oxidation states from +V to –III (Fig. 2). Due to the plurality of N species and oxidation states, various microbial transformation pathways exist that are used to acquire N for growth and as an energy source during respiration (Gruber, 2008). The assimilation of NO_3^- and NH_4^+ by phytoplankton is the dominant process in the marine N cycle, because its uptake and incorporation into biomass requires a low energy input, especially NH_4^+ which does not involve a redox reaction (Zehr and Ward, 2002). Fixed organic nitrogen can be converted into inorganic nitrogen species through ammonification and nitrification, and they represent important remineralization processes that link the most oxidized form of nitrogen (NO_3^-) with the most reduced form (NH_4^+) (Goldman et al., 1987; Bronk and Steinberg, 2008; Ward, 2008). Microbial denitrification and anaerobic oxidation of ammonium (anammox) describe major processes that remove bioavailable N (N–loss) from the marine environment by releasing N_2 gas to the atmosphere (Mulder et al., 1995; Kuypers et al., 2003; Lam and

Kuypers, 2011). These pathways play a critical role in the bioavailability of organic nitrogen compounds in the ocean.

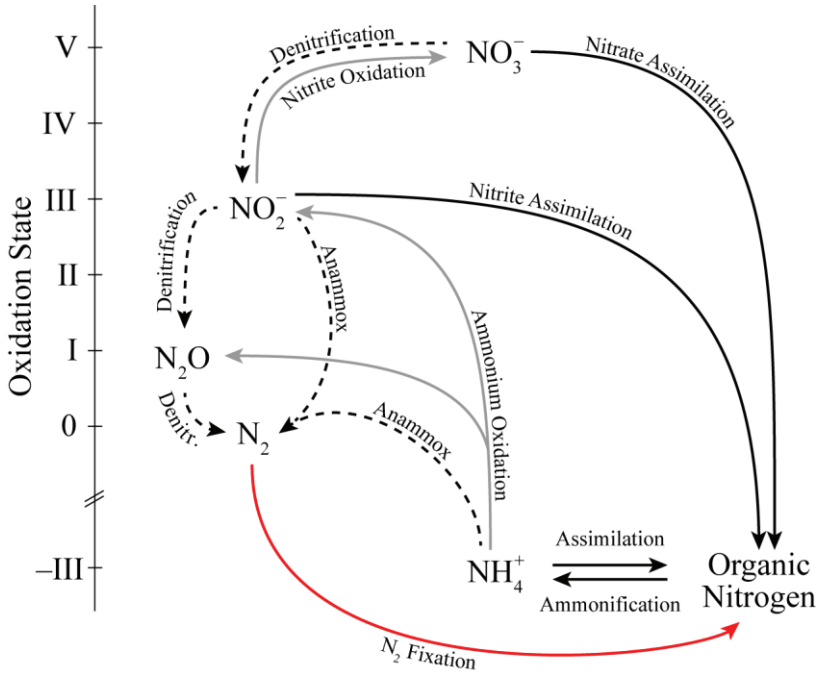

Fig. 2: Overview of different nitrogen species, correlating oxidation states and major transformation pathways in the marine environment. The dashed lines indicate processes that are carried out under anaerobic conditions, whereas the grey lines represent nitrification processes. The red line emphasizes N_2 fixation activity, the focus of this thesis. Modified after Gruber (2008).

Biologically fixed N in the oceans sum up to about 6.6 x 10^5 Tg N (Gruber, 2008). Aside from N_2 fixation, "new" N is also delivered through atmospheric deposition. The latter source has been estimated to be around 67 Tg N a^{-1} and is expected to rise approximately 10% up to 77 Tg N a^{-1} over the next two decades due to increasing anthropogenic influences from for example the burning of fossil fuels and the extensive use of fertilizers in agriculture. This will inevitably effect the surface ocean productivity (Duce et al., 2008). Other additional N sources originate in benthic environments and rivers, but these inputs are constrained to coastal areas (Capone and Carpenter, 1982; Boyer et al., 2006). Combined estimates of fixed N sources result in a global gain of ~200–300 Tg N a^{-1} (Table 1). On a global scale, marine N_2 fixation is estimated to provide 100–200 Tg N a^{-1} (Karl et al., 2002; Gruber, 2008), exceeding all other N sources, hence, playing a pivotal role in regulating the marine N inventory and primary productivity.

Estimates of N–loss processes outweigh N–gain processes, leading to an imbalanced marine N–budget (Codispoti, 1995; Michaels et al., 1996; Gruber, 2005; Capone and Knapp, 2007). The ongoing controversy about this discrepancy has been one of the main driving

forces for investigating the marine N cycle. Newly discovered diazotrophs reveal a greater diversity within the N_2 fixers than previously known, suggesting that N_2 fixation rates are likely underestimated in the marine environment (Zehr et al., 1998; Zehr et al., 2001). Therefore, the identification of microorganisms involved in N_2 fixation and understanding the factors that regulate their activity is crucial in order to balance the marine N budget, as well as to better understand ecosystem.

Table 1: Global estimates N–gain and N–loss in marine waters. Adapted from Gruber (2008)

Process	**Codispoti et al. (2001)**	**Galloway et al. (2004)**	**Gruber (2004)**
		Nitrogen sources (Tg N a^{-1})	
Pelagic N_2 fixation	117	106	120
Benthic N_2 fixation	15	15	15
River input (DON*)	34	18	35
River input (PON**)	42	30	45
Atmospheric deposition	86	33	50
Total sources	**294**	**202**	**265**
		Nitrogen sinks (Tg N a^{-1})	
Organic N export	1		1
Benthic denitrification	300	206	180
Pelagic denitrification	150	116	65
Sedimentation	25	16	25
N_2O loss	6	4	4
Total sinks	**482**	**342**	**275**

* Dissolved organic nitrogen

** Particulate organic nitrogen

1.2 Nitrogen fixing microorganisms

Biological N_2 fixation is an ancient process carried out by diazotrophic microorganisms of bacterial and archaeal lineages in a wide range of environments (Staal et al., 2003; Zehr et al., 2003; Zehr and Paerl, 2008). The term diazotroph implies a chemical reaction with two N atoms (*diazo–*) used for nourishishment (*–troph*). Most diazotrophs are photoautotrophic as they are able to fix CO_2 and N_2 gas (Capone et al., 2008). During CO_2 fixation, the

photosystem II (PSII) is used to split two water molecules into two hydrogens and one oxygen (O_2), the release of energy is used to synthesize carbohydrates with O_2 as the terminal electron acceptor. These carbohydrates provide an energy reservoir that can be utilized for the subsequent N_2 fixation process.

The nitrogenase is the key enzyme used for N_2 fixation by diazotrophs (Postgate, 1982); it contains two multisubunit metallo–proteins. The first protein encoded by the *nifD* and *nifK* genes has molecular weight of about 220 kDa and is composed of O_2 sensitive molybdenum–iron–clusters (Mo–Fe) that contain the active site. The second protein is considerably smaller (~70 kDa), and it is composed of Fe–clusters that exhibit the active binding site of adenosintriphosphate (ATP) and an inorganic aggregate formed by four Fe and sulfur (S) atoms, which are responsible for ATP hydrolysis and electron transfer (Bulen and LeComte, 1966; Hageman and Burris, 1978). This component is encoded by the *nifH* gene (Zehr et al., 2003). Due to the triple bond within the N_2 molecule (N≡N) it costs energy to reduce this form to NH_4^+ (Gallon, 1992). Eight reducing equivalents and 16 ATP molecules are required to accomplish this reaction:

$$N_2 + 8\ H^+\ 8\ e^- + 16\ ATP \rightarrow 2\ NH_3 + H_2 + 16\ ADP + 16\ P_i \qquad \text{Eq. 1.1}$$

Because the nitrogenase enzyme complex is O_2 sensitive, some diazotrophs separate CO_2 fixation from N_2 fixation by spatial segregating the two processes. Some diazotrophs have evolved specialized cellular compartments, known as heterocysts, which keep the nitrogenase enzyme in an active stage for catalyzing the N_2 fixation and prevent this enzyme from inactivation by O_2 contact via photosynthesis (Stewart, 1969; Rippka et al., 1971; Berman–Frank et al., 2003). This distinct morphological feature makes it possible to identify certain filamentous heterocyst–forming diazotrophs. However, the majority of the diazotrophic community does not contain this morphological feature. Instead, diversity is distinguished by genetic approaches that target the *nifH* gene; an approach which has recently gained in popularity because this marker gene is well conserved among the diazotrophic community (Zehr et al., 2003). Cyanobacteria are considered the main diazotrophs in marine waters, but functional *nifH* gene assays also revealed non–cyanobacterial phylotypes, highlighting the potential ecological importance of heterotrophic N_2 fixing microorganisms (Zehr et al., 1998; Farnelid and Riemann, 2008; Farnelid et al., 2011; Halm et al., 2012). Most heterotrophic diazotrophs are not light–dependent and can inhabit deeper water layers

compared to other diazotrophs. Nonetheless, actual heterotrophic N_2 fixing activity has not been proven and its ecological significance remains unclear.

Known open ocean N_2 fixing cyanobacteria have been assigned into three major groups according to the *nifH* gene phylogeny:

(I) Filamentous non–heterocyst forming *Trichodesmium*

(II) Filamentous heterocyst forming symbionts with unicellular eukaryotic algae (*Richelia*, *Calothrix* and relatives)

(III) Unicellular cyanobacteria (*Crocosphaera* and relatives of *Cyanothece*)

In open ocean systems, the cyanobacterium *Trichodesmium* sp. and filamentous cyanobacterial symbionts of diatoms are considered the dominant diazotrophs that significantly influence the marine N cycle (Villareal and Carpenter, 1988; Capone et al., 1997; Carpenter et al., 1999). Recent studies detected novel *nifH* gene phylotypes of unicellular cyanobacteria (UCYN), showing that these groups of organism are present in all major oceanic basins and believed to be ecologically relevant (Zehr et al., 2001; Zehr et al., 2003; Montoya et al., 2004; Moisander et al., 2010). However, since very few diazotrophs representatives have been successfully cultivated (Waterbury and Rippka, 1989; Prufert–Bebout et al., 1993; Zehr et al., 2001; Falcón et al., 2004b), it is difficult to know the conditions and parameters that allow them to thrive in the environment. Instead we rely on culture independent techniques to infer N_2 fixing activity and estimate their contribution to the marine N budget.

1.2.1 Trichodesmium

The filamentous non–heterocyst forming *Trichodesmium* sp. is considered the most abundant diazotroph in the oceans and global estimates of N_2 fixation activity has been mainly attributed to these cyanobacteria (Capone et al., 1997; Karl et al., 1997; Capone et al., 2005). *Trichodesmium* was first isolated in pure culture by Prufert–Bebout (1993) from the North Atlantic. These microorganisms either appear as free–living trichomes or they form extensive colonies and aggregates, which sometimes can be observed from space (Capone et al., 1997; Subramaniama et al., 2002) (Fig. 3).

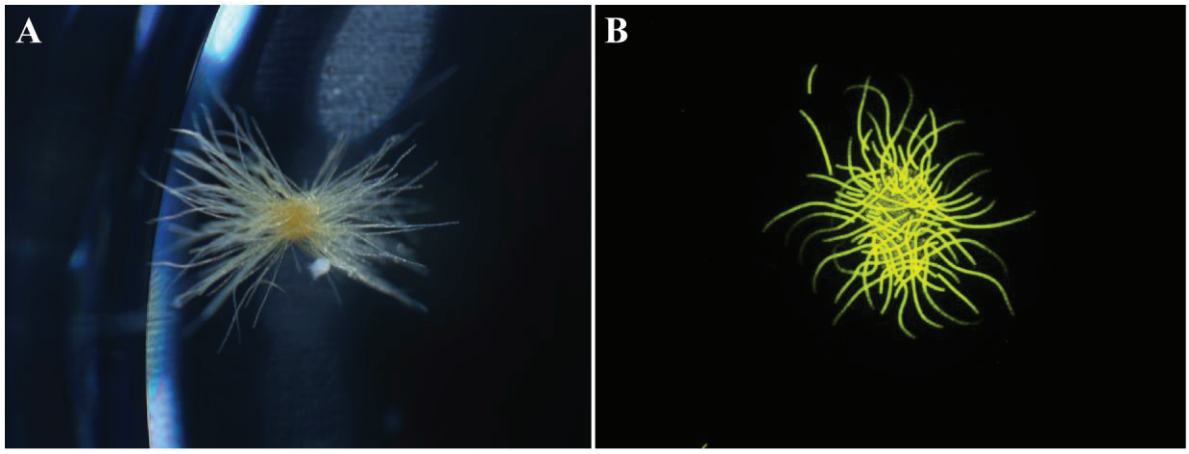

Fig. 3: Individual filaments of *Trichodesmium* that form two different aggregates under (A) a binocular microscope and (B) an epifluorescent microscope collected near the Hawaiian Islands from station ALOHA (22° 45' N, 158° 00'W) on board the RV *Kilo Moana* (KM 0210) during a research cruise in July 2011. Pictures taken by the C–MOORE class 2011.

Quantifying *Trichodesmium* and accurately assessing their biomass is challenging due to different forms, leading to further uncertainties in estimating global N_2 fixation (Capone et al., 1997). The distribution of different forms plays a critical role in estimating N_2 fixation activity since free trichomes of *Trichodesmium* have been reported to fix less N_2 than colony forming *Trichodesmium* when normalized to individual filaments (Saino and Hattori, 1980; Letelier and Karl, 1998). *Trichodesmium* is globally abundant and thrives best in oligotrophic open ocean environments with water temperatures ≥25 °C, i.e. most subtropical and tropical regions (Capone et al., 1997; Breitbarth et al., 2007; White et al., 2007a). This cyanobacterium exhibits special physiological properties to grow in nutrient depleted environments. For instance, these microorganisms can store and sequester carbohydrates and phosphate inside their trichomes to survive during low nutrient periods (White et al., 2006; Orchard et al., 2010). These storage compounds essentially provide energy during N_2 fixation (Sohm and Capone, 2006; White et al., 2006). *Trichodesmium* has also been shown to harbour epibiotic bacteria that support the acquisition of phosphate (Van Mooy et al., 2012), and it also possess the genetic ability to utilize phosphonates in order to scavenge additional phosphate (Dyhrman et al., 2006). Phosphonates constitute organically bound phosphorus, which is usually not accessible to other marine microorganisms. *Trichodesmium* is also able to generate gas vacuoles and control their buoyancy, which allows these microorganisms to migrate vertically along the water column in order to acquire better light conditions and obtain nutrients that are exhausted in surface waters (Villareal and Carpenter, 2003; Karl et al., 2008). Further studies suggest that this behaviour can be used to evade grazing pressure, giving *Trichodesmium* a distinct advantage with respect to microbial fitness.

Intriguingly, *Trichodesmium* can fix CO_2 and N_2 simultaneously during the day, despite the lack of heterocyst. It was suggested that the nitrogenase is active in distinct regions that are depleted in cellular oxygen, but rich in reductants (Bryceson and Fay, 1981; Paerl and Bland, 1982; Paerl and Bebout, 1988). Others suggested that *Trichodesmium* is capable of fixing CO_2 via the Mehler reaction, where the oxygen produced by PSII is rapidly reduced back to photosystem I (PSI). Such a mechanism would allow for the quick separation of photosynthesis from N_2 fixation using altering microzones during the day (Berman–Frank et al., 2001b; Küpper et al., 2004).

1.2.2 Heterocyst forming cyanobacteria

The heterocyst forming cyanobacteria represent a group that include both free–living and symbiotic cells. Heterocyst–forming cyanobacteria are commonly observed in estuaries and brackish water; in open ocean environments these microorganisms are less abundant. A possible explanation for these observations is turbulence sensitivity in open ocean systems, which is hypothesizes to cause a decrease in the organisms' biological fitness (Howarth et al., 1993). In the brackish waters of the Baltic Sea cyanobacteria such as *Nodularia* spp, *Aphanizomenon* spp. and *Anabaena* spp. are commonly present. *Nodularia* spp. and *Aphanizomenon* spp. show temperature preferences ranging between 16–22 °C and 25–28 °C, respectively (Lehtimaki et al., 1997) and can reach abundances of 10^4 heterocyst L^{-1} during blooming events (Laamanen and Kuosa, 2005). In tropical and subtropical marine waters, heterocystous diazotrophs are frequently encountered living symbiotically with diatoms (Venrick, 1974; Carpenter et al., 1999; Zeev et al., 2008). Some heterocystous forming cyanobacteria have been encountered in a free–living stage, but their abundances are considerably low (Gómez et al., 2005; White et al., 2007b; Grabowski et al., 2008). These diatom–diazotroph associations (DDAs) are mainly represented by *Richelia intracellularis* living symbiotically within diatoms like *Hemiaulus* spp. or *Rhizolsolenia* (Fig. 4) and filaments of *Calothrix* spp. that live associated with the diatom *Chaetoceros* (Carpenter and Foster, 2003).

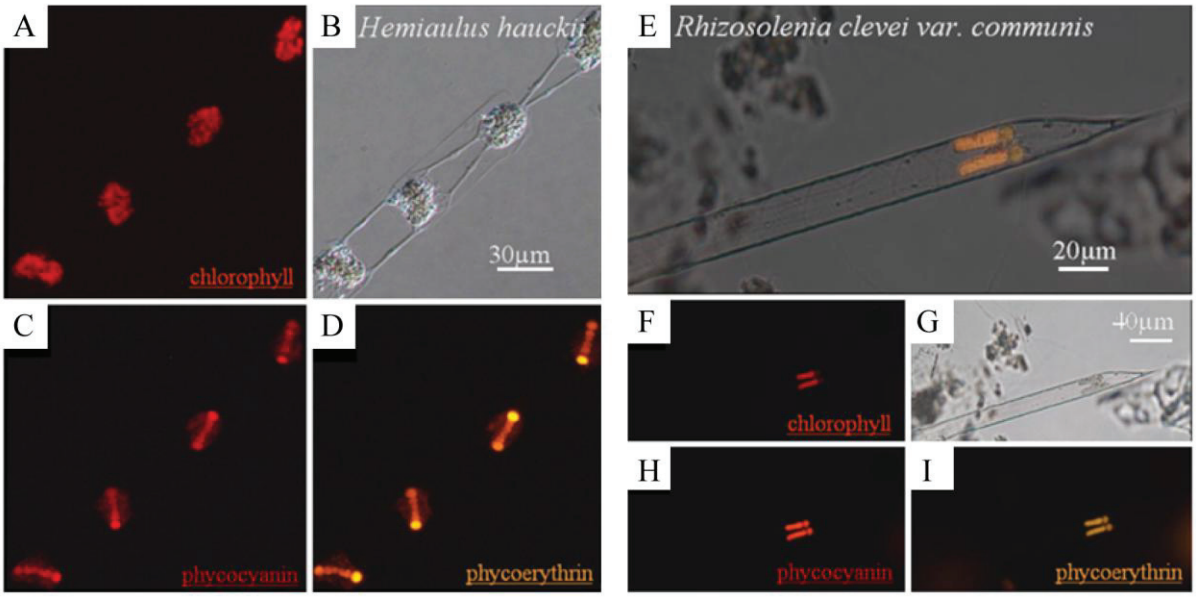

Fig. 4: Compilation of symbioses between diatoms and diazotrophs. (A–D) The diatom *Hemiaulus hauckii* and its endosymbiotic cyanobacterium *Richelia intracellularis* and (E–I) the diatom *Rhizosolenia* spp. and its endosymbiotic cyanobacterium *Richelia intrace*. (B,G) Bright–field microscopy, fluorescence pattern of (A–F) chlorophyll (excitation: 450 nm; emission: 680 nm), (D,I) phycoerythrin (excitation: 490 nm; emission: 580 nm) and (C,H) phycocyanin (excitation: 620 nm; emission: 660 nm). Source Zeev et al. (2008).

These associations are widely distributed in warm oligotrophic environments and appear in numbers averaging around 10^3 heterocyst L^{-1} (Venrick, 1974; Carpenter et al., 1999; Zeev et al., 2008). Diatoms commonly form silica frustules, which make them heavier compared to most other phytoplankton. Enhanced sinking rate of diatoms fuel the *biological pump* as cell aggregates or fecal pellets from zooplankton (Smetacek, 1999; Buesseler, 2012).

Recent work observed host specificity among different symbiotic associations, and suggested that the diatoms use distinct physiological mechanisms to interact with their diazotrohic partners (Foster and Zehr, 2006). Foster et al (2011) demonstrated that the symbiotic diazotrophs can fix extensive amounts of N_2 and transport this rapidly to their host, fuelling growth. These findings are intriguing and show the importance of these interactions, and give attention to an understudied group of organisms that may have a profound impact on the marine C and N cycles (Foster et al., 2011). Presently, little is known about the ecophysiology of these symbiotic cyanobacteria and their host; however, the recently cultivated epibiont *Calothrix* (from the diatom *Chaetoceros*) has made it possible to study the interactions and mechanisms behind this symbiosis in more detail (Foster et al., 2010).

1.2.3 Unicellular cyanobacterial groups (UCYN)

The recently characterized UCYN group of unicellular cyanobacteria have been shown to have high rates of N_2 fixation within a cell–size fraction below 10 µm, emphasizing their

importance within the diazotrophic community (Zehr et al., 2001). According to their *nifH* gene phylogeny, these unicellular cyanobacteria have been divided into three groups, namely UCYN–A, UCYN–B and UCYN–C (Zehr et al., 1998; Zehr et al., 2008) (Fig. 5).

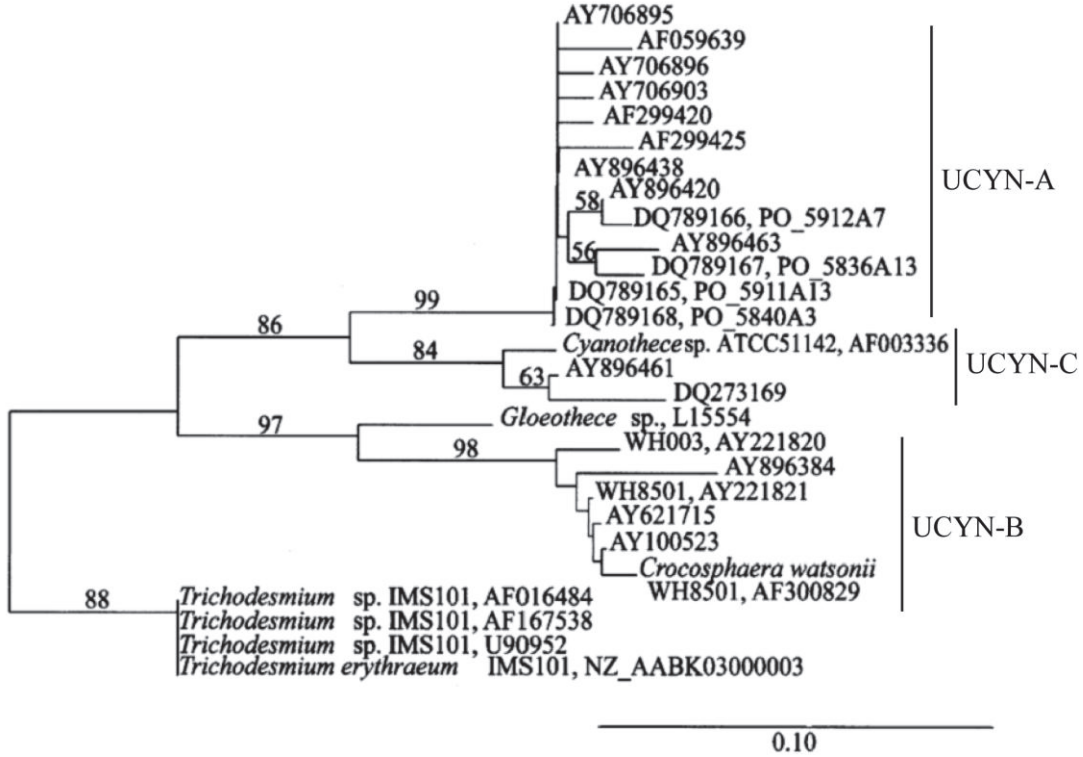

Fig. 5: Maximum–Likelihood phylogenetic reconstruction inferred from selected *nifH* gene sequences from the North Pacific showing the three uncultured unicellular cyanobacterial groups UCYN–A, UCYN–B and UCYN–C (Needoba et al., 2007).

Over the past decade, each of these groups have been identified and quantified using group specific *nifH* gene primers via quantitative polymerase chain reaction (qPCR) assays. From this work, we now know that these cyanobacteria are widely distributed in marine waters, especially within tropical and subtropical regions (Langlois et al., 2005; Zehr et al., 2008; Moisander et al., 2010). Their abundances can sometimes dominate the diazotrophic community (Montoya et al., 2004; Church et al., 2008; Langlois et al., 2008; Goebel et al., 2010). The *nifH* gene sequence of UCYN–C shares a high similarity with *Cyanothece* sp ATCC 51142 and some diatom endosymbionts (Zehr, 2011). In comparison to UCYN–B and UCYN–A, little is known about the UCYN–C, except that it co–occurs with the other two UCYN populations.

The only cultivated representative of the UCYN–B population is *Crocosphaera watsonii*. *Crocosphaera* was originally isolated from the South Atlantic Ocean by Waterbury and Rippka (1989), and subsequent genetic surveys on its specific *nifH* gene sequence showed

that these diazotrophs are also widely distributed in marine waters (Moisander et al., 2010). *Crocosphaera* sp. can be easily identified by microscopy since it features distinct autofluorescence pattern due to its pigmented cells that contain phycoerythrin (Webb et al., 2009) (Fig. 6). Studies on cultured strains of *Crocosphaera* sp. revealed temperature preferences ranging between 22–36 °C and showed spherically shaped cells appearing in two distinct phenotypic groups characterized by size differences (2–4 um and 4–8 um) (Webb et al., 2009; Foster et al., 2013). This diazotroph is capable of producing an extra polymer saccharide matrix (EPS) (Webb et al., 2009; Foster et al., 2013), it is believed that these compounds provide C sources during nutrient limitation, aiding in nutrient acquisition from surrounding water and serve as O_2 protection for the nitrogenase enzyme (Reddy et al., 1996; Corzo et al., 2000).

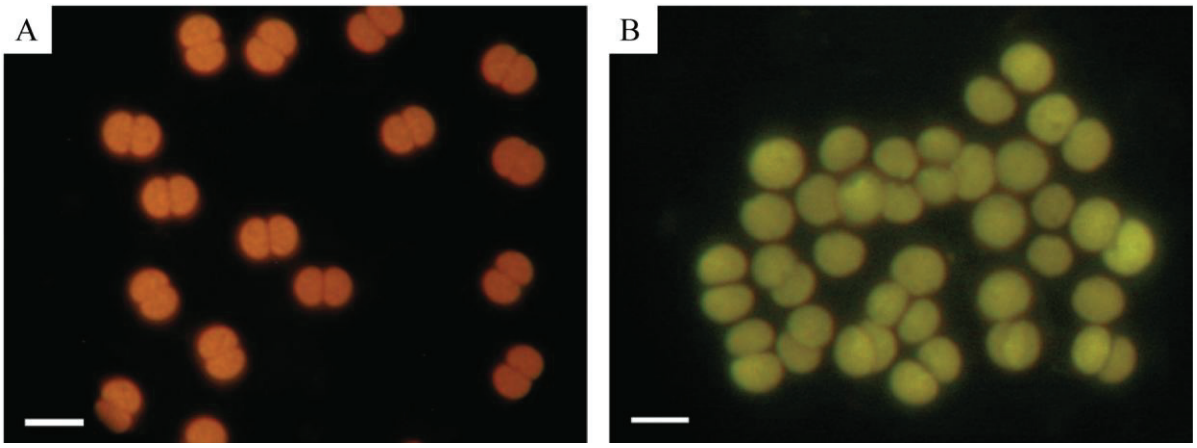

Fig. 6: Epifluorescence microscopic evaluation on *Crocosphaera watsonii*–like cells under blue excitation on field samples collected from station ALOHA (22° 45' N, 158° 00'W) near the Hawaiian Islands. (A) The free–living phenotype, and (B) the colonial phenotype. Scale bars 5 µm. Source Foster et al. (2013).

Quantitative measurements on *nifH* genes specific for *Crocosphaera* sp. demonstrated a linear increase between gene copies (10^3–10^4 L^{-1}) and temperature (Church et al., 2008; Langlois et al., 2008). *Crocosphaera* sp. temporarily separates CO_2 and N_2 fixation during the day and night, respectively. The synthesized carbohydrates stored during the day are partially utilized for the more energy demanding N_2 fixation process. The temporal separation has also been confirmed in field samples analysing *nifH* gene transcripts when numbers peaked during the night (Church et al., 2004). The segregation between C and N metabolism is tightly regulated by complex gene expression mechanisms including a circadian clock (Chen et al., 1996; Mohr et al., 2010a). The latter was confirmed by the genome analysis of *Crocosphaera watsonii*, which closely follows a 12:12 h light–dark cycle (Shi et al., 2010). Here, the production of the nitrogenase enzyme is initiated shortly before the dark phase in preparation

for the upcoming N_2 fixation activity during dark hours (Dron et al., 2011). The length of the light period is directly coupled to the length of the N_2 fixation period because the light length determines the reservoir of carbohydrates that fuel N_2 fixation activity at night (Dron et al., 2013).

In contrast, our knowledge about physiological characteristics of the UCYN–A group is limited since there is no cultured representative strain available. UCYN–A usually inhabits subtropical and tropical oligotrophic regions with water regimes that range in temperatures between 15–30 °C, indicating a broader distribution then other UCYN groups (Needoba et al., 2007; Church et al., 2008; Moisander et al., 2010). In addition, UCYN–A *nifH* gene copy numbers are usually more abundant compared to other UCYN groups (Church et al., 2008; Moisander et al., 2010). It is puzzling, however, that UCYN–A expresses *nifH* gene transcripts mostly during the day. This contradicts the common assumption that unicellular diazotrophs temporally separate CO_2 fixation from N_2 fixation (Gallon, 1992; Berman–Frank et al., 2003; Dron et al., 2011).

Technical improvements in fluorescence activated cell sorting (FACS) in combination with subsequent 16S and nested *nifH* gene sequencing attempts resulted in successfully separating the UCYN–A population (Zehr et al., 2008). This work detected UCYN–A cell diameters of approximately 1 µm, and through genetic analyses, revealed that these microorganisms lack genes for photosystem II (PSII) and C fixation, characteristic for cyanobacteria. Sorted UCYN–A cells and subsequent sequencing efforts succeeded in closing its genome and demonstrated that other genes that encode essential metabolic pathways are missing, e.g. RuBisCo, TCA cycle genes and some genes connected to amino acid and purine synthesis (Tripp et al., 2010). These findings explain how UCYN–A is able to actively express most *nifH* genes during the light period. Other studies suggest that UCYN–A might be photoheterotrophic since it lacks photosynthetic genes, or that is may live in association with other phototrophic microorganisms (Bothe et al., 2010; DeLong, 2010; Tripp et al., 2010). The mechanisms that this cyanobacterium utilizes to thrive in the environment without performing CO_2 fixation are still unknown.

Attempts to visualize the globally abundant uncultured cyanobacterium UCYN–A have so far been unsuccessful; furthermore research currently lacks activity measurements of N_2 fixation by UCYN–A. This thesis work aims to improve our understanding of, (1) how UCYN–A cells thrive in the environment and, (2) estimating their contribution to marine N_2 fixation. Here we establish a method to identify these microorganisms by fluorescence microscopy and then to link their phylogeny with *in situ* metabolic activity on a single cell

scale. This work primarily assesses the physiological activity of this ecological important group of microorganisms through culture–independent techniques.

1.3 Parameters controlling N_2 fixation

Understanding the factors that control the activity of diazotrophs and determining their temporal–spatial distribution in marine waters is of crucial interest in order to improve N_2 fixation estimates and to identify high productive marine areas that can be linked to high C export (Karl et al., 2002; Karl et al., 2012). Better predictions will also improve flux calculations of parameters that impact climate change, e.g. atmospheric CO_2 levels.

The availability of nutrients such as trace metals has been suggested to play a major role in constraining N_2 fixation activity. For instance, the availability of phosphorus (P) and iron (Fe), important for nitrogenase activity, have been the main focus of N_2 fixation research. For instance, studies on cultured strains of *Trichodesmium* spp. revealed higher N_2 fixation rates under higher Fe concentrations, due to elevated Fe requirements for the activity of their nitrogenase enzyme (Berman–Frank et al., 2001a; Kustka et al., 2003). In contrast, low Fe concentrations have shown to decrease N_2 fixation rates in concert with the expression of distinct proteins involved in Fe stress and down regulate proteins containing Fe involved in CO_2 and N_2 fixation (Berman–Frank et al., 2001b; Küpper et al., 2008; Chappell and Webb, 2010). Similarly, the cultured diazotroph *Crocosphaera watsonii* expresses distinct proteins under Fe stress, i.e. *idiA* homologues, which are proposed to protect PSII against O_2 stress and have been shown to be dominant components of metatranscriptomes of *Crocosphaera* sp. (Webb et al., 2001; Hewson et al., 2009). The North Atlantic is characterized by elevated Fe supply originating mainly from Saharan dust, that stimulates the abundance, distribution and activity of diazotrophs (Capone et al., 2005; LaRoche and Breitbarth, 2005; Moore et al., 2009) (Fig. 7).

The availability of P is another important parameter that limits *Trichodesmium* N_2 fixation activity in the Atlantic ocean (Sañudo–Wilhelmy et al., 2001). Elevated N_2 fixation activity leads to decreasing P concentrations, hence, causing P limitations (Wu et al., 2000; Cavender–Bares et al., 2001). The Atlantic Ocean has been shown to be more P limited than Fe, while the opposite is seen in the Pacific Ocean (Cavender–Bares et al., 2001; Karl et al., 2001; Mahowald et al., 2005; Moutin et al., 2008; Moore et al., 2009). It appears that a stoichiometric balance of P and Fe concentrations may limit N_2 fixation, and in some instances, a co–limitation of N_2 fixation by the availability of P and Fe may exist (Mills et al (2004).

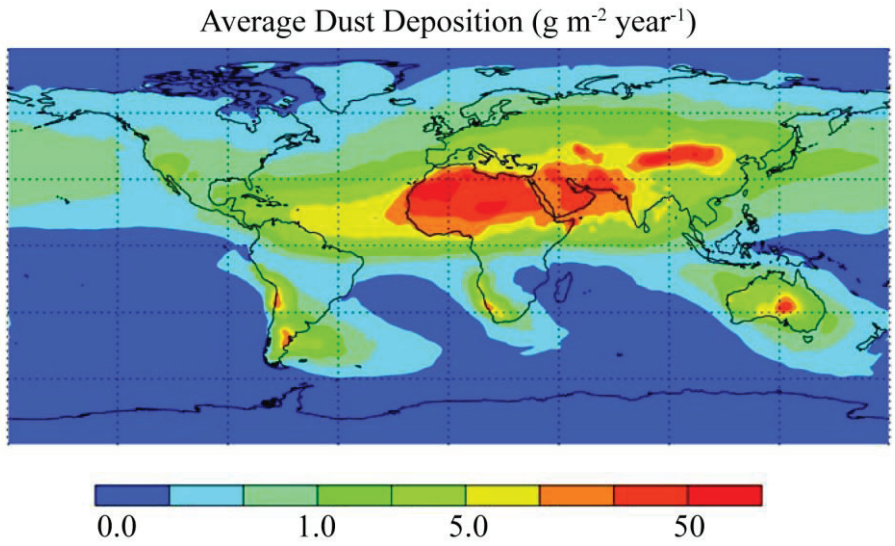

Fig. 7: Global distribution of dust deposition leading to P and Fe input in marine environments. Source Jickells et al. (2005).

1.4 Assessing N_2 fixation activity

There are several methodologies available to determine N_2 fixation activity, including geochemical and modelling approaches, as well as measurements through mass spectrometry and molecular tools.

Quantitative methods to determine N_2 fixation rates are based on geochemical and modelling estimates, and mass spectrometry approaches that use the acetylene reduction assay (Capone, 1993; Capone and Montoya, 2001) and stable isotope $^{15}N_2$ tracer (Montoya et al., 1996). Geochemical and modelling estimates of N_2 fixation are based on abundances, C:N requirements and growth rates of distinct N_2 fixing microorganisms. These factors are most accurately obtained when the investigated population is in culture, which is only the case for a few representative strains (Waterbury and Rippka, 1989; Chen et al., 1996). For instance, C:N requirements of uncultured diazotrophs are derived using equations and empirical data that describe the relationship between cellular C:N content, cell size and morphology of different phytoplankon populations (Strathmann, 1967; Liu et al., 1997; Goebel et al., 2008). This empirical data is needed to determine cellular N_2 fixation rates and can be extrapolated on a regional or global scale if abundance data for the targeted diazotrophic population in that respective region is available. Abundance data can be acquired through microscopic counts, quantitative information on functional genes or remote sensing techniques (Subramaniama et al., 2002; Tyrrell et al., 2003; Church et al., 2005a).

Another approach for estimating N_2 fixation is based on models that use algorithms to describe anomalies in the stoichiometry of N:P ratios. Early work by Redfield (1958) revealed

that the organic matter composition of marine phytoplankton follows a constant stoichiometric ratio between C, N and P:

$$106\ CO_2 + 16\ HNO_3 + H_3PO_4 + 122\ H_2O \leftrightarrow (CH_2O)_{106}\ (NH_3)_{16}\ (H_3PO_4) + 138\ O_2 \qquad \text{Eq. 1.2}$$

The classical Redfield N:P stoichiometry of 16:1 is used as a proxy to distinguish from N or P limitation, where ratios in water less than 16 indicate N limitation and ratios above 16 indicate P limitation. This ratio has been revaluated recently and may change substantially between different phytoplankton populations and marine regions (Broecker and Henderson, 1998; Klausmeier et al., 2004). For example, varying N:P ratios for algae ranging from 5–19 under nutrient–replete growth conditions have been shown by Geider and LaRoche (2002). Further studies revealed higher N:P ratios for cyanobacteria and lower values for diatoms, indicating taxonomic differences in respect to the Redfield ratio (Bertilsson et al., 2003; Heldal et al., 2003; Ho et al., 2003; Fu et al., 2005). Despite the variability of the N:P ratio in the elemental composition of phytoplankton, this ratio remains stable throughout most of the deep ocean (Takahashi et al., 1985) because of feedback mechanisms between denitrification and N_2 fixation processes. Since both processes transform fixed N compounds in marine systems, but do not alter the P concentration, these biogeochemical pathways are considered to be the main factors that control the N:P stoichiometry (Redfield, 1958; Brandes and Devol, 2002; Gruber, 2008). In order to detect deviations from the classical 16:1 ratio, the term N* was invented:

$$N^* = [NO_3^-] - 16\ [PO_4^{3-}] + 2.9\ \mu mol\ kg^{-1} \qquad \text{Eq. 1.3}$$

The constant of 2.9 $\mu mol\ kg^{-1}$ was added to achieve zero values for global means of N* according to Gruber and Sarmiento (1997; 2002). Obtained values for N* can be used to emphasize areas with elevated N (positive values) or depleted N concentrations (negative values). This approach cannot distinguish between anomalies originating from denitrification or N_2 fixation because this equation describes the sum of both processes. However, since both processes are often spatially and temporarily separated, obtained results can be well interpreted and used to estimate global N budgets. Modelling approaches based on this anomaly concept suggested that the Atlantic Ocean represents a net source of fixed N, whereas the Pacific Ocean serves as a net sink of fixed N (Gruber, 2008). On the other hand, higher N_2 fixation rates have been proposed for the Pacific Ocean compared to the Atlantic Ocean using similar modelling approaches (Deutsch et al., 2007).

Determining the natural abundance of ^{15}N isotopes represents another geochemical approach to estimate N_2 fixation. This stable isotope represents a minor fraction of the N element constituting only 0.365% of all N atoms (Nier, 1950), but is sufficient to quantify differences in isotope ratio abundances between the sample material and the atmosphere. In biological systems, enzymatically–catalyzed reactions can lead to isotopic fractionation because lighter isotopes react more readily, leading to products that are lighter than the reactants (Teece et al., 1999). Denitrification and N_2 fixation, for instance, are generally considered to control the size and isotopic composition of the oceanic NO_3^- pool (Brandes and Devol, 2002), where the former process lowers the pool size of NO_3^- while increasing its $\delta^{15}N$ signature and the latter process results in opposite effects. These isotopic variations can be monitored as they transform into different nitrogen compounds within the euphotic zone (Voss et al., 2001; Montoya et al., 2002; McClelland et al., 2003) and benthic sediments (Altabet et al., 1995; Ganeshram et al., 1995). These findings can be used to study the marine N cycle across broad spatial and temporal scales (Fig. 8).

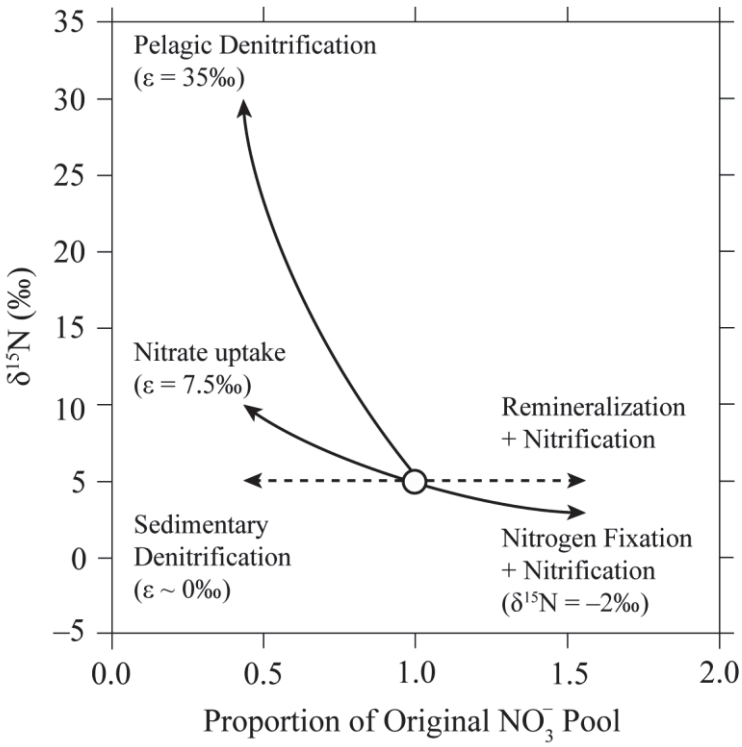

Fig. 8: Schematic overview of different processes and their isotopic fractionation effect on $\delta^{15}N$ of oceanic NO_3^-. Source Montoya (2008)

Direct measurements of N_2 fixation are commonly carried out by applying the acetylene reduction approach (ARA) and the $^{15}N_2$ tracer method. The former method was introduced more than five decades ago (Neess et al., 1962; Dugdale et al., 1964) and is based

on the ability of the nitrogenase enzyme (crucial for N_2 fixation) to reduce small triple bonded molecules, chemically similar to N_2 (N≡N), such as cyanide, azide, nitrous oxide and acetylene. Acetylene (H–C≡C–H) is saturated in liquid and added to the incubation bottle (Capone, 1993; Montoya et al., 1996). Acetylene is reduced to ethylene in a theoretical molar ratio of 3:1 relative to N_2 gas and ethylene is measured via flame ionization gas chromatography, measuring N_2 fixation by assessing the activity of the nitrogenase enzyme.

N_2 fixation activity can be measured via the $^{15}N_2$ gas tracer method that is commonly carried out by injecting the tracer into gas tight incubation bottles and after determination of the incubation period, the sample water is filtered and subsequently analysed via mass spectrometry. N_2 fixation rates are then calculated by the change in ^{15}N labelled particulate organic nitrogen (^{15}N–PON) between the beginning of the incubation and at the end of the incubation according to following equation (Montoya et al., 1996; Capone and Montoya, 2001):

$$N_2 \text{ fixation } \left[\text{nmol N t}^{-1}\right] = \frac{\left(\text{AT\% PN}_{\text{final}} - \text{AT\% PN}_{\text{initial}}\right)}{\left(\text{AT\% N}_2 - \text{AT\% PN}_{\text{initial}}\right)} \text{ x } \frac{\text{PN}_{\text{final}}\left[\text{nmol}\right]}{\Delta \text{ t}} \qquad \text{Eq. 1.4}$$

where AT% stands for the atomic percentage of the ^{15}N isotope in PON at the end (PN_{final}) or at the beginning ($PN_{initial}$) or the incubation and in the dissolved N_2 pool. The only parameter that is not measured is the amount of the labeled $^{15}N_2$ pool, which is derived from equations describing the dissolution coefficient of N_2 gas in seawater (Weiss, 1970). The dissolution of the $^{15}N_2$ gas within the incubated seawater is of crucial importance to measure N_2 fixation rates precisely. Recent studies demonstrated a methodological underestimation of N_2 fixation by using this tracer method compared to an improved protocol (Mohr et al., 2010b; Großkopf et al., 2012). These authors dissolved $^{15}N_2$ gas into liquid prior to its injection into the incubation bottles, aiming an improved distribution and accessibility of the ^{15}N tracer for the diazotrophic community. This approach might lead to a more balanced N_2 budget in the oceans.

The ARA method requires less laboratory work and is more sensitive compared to the classical $^{15}N_2$ tracer method. However, the latter approach does not need a conversion factor of 3:1, which undergoes an ongoing debate about its accuracy. Recent findings showed that the conversion factor between the acetylene reduction and N_2 fixation deviated away from a 3:1 ratio (Mulholland et al., 2004; Capone et al., 2005; Mulholland and Bernhardt, 2005), emphasizing the need to improve methods to assess N_2 fixation activity.

The abundance of diazotrophs also can provide insight into N_2 fixation distribution. The key enzyme for N_2 fixation is nitrogenase and its iron subunit is encoded by the *nifH* gene. The development of functional gene assays targeting the *nifH* gene via qPCR is commonly applied and provides information on abundance and distribution of distinct diazotrophic community members (Zehr and McReynolds, 1989; Zehr et al., 2003; Church et al., 2005a). Nonetheless, the results obtained via these approaches have to be interpreted with caution because they are based on the assumption that each diazotrophic cell contains only one *nifH* gene copy per cell. This has only been confirmed for *Trichodesmium*, *Cyanothece* and *Crocosphaera* (Zehr et al., 2008), but does not hold necessarily true for other diazotrophic microorganisms including UCYN–A (Bombar et al., 2011; Ininbergs et al., 2011; Bombar et al., 2013). Therefore, the *nifH* gene assay is semi–quantitative because it does not provide exact cell abundances, but is a useful approach to assess diazotrophic community structure. These functional gene assays can also serve to target *nifH* gene expression as mRNA in order to infer N_2 fixation activity (Church et al., 2005b; Short and Zehr, 2007). This is convenient for identifying diazotrophs that are actively expressing the *nifH* gene, and therefore the nitrogenase enzyme, but cannot provide actual rates of N_2 fixation.

Developments in culture–independent techniques coupled with secondary ion mass spectrometry (nanoSIMS) made it possible to acquire precise information about the uptake of stable isotopes within single microbial cells, linking biological activity with phylogenetic identification (Orphan et al., 2001; Musat et al., 2008). Thus, quantifying rates of uptake at the single cell level would be more accurate and reliable. These findings emphasize the powerful approach of enumerating cellular abundances of distinct populations and quantifying their activity by detecting their isotopic enrichment on a single cell level. This is a useful tool for visualizing N_2 fixation activity on a single cell level and for assigning it to distinct diazotrophic populations (Foster et al., 2011; Thompson et al., 2012; Krupke et al., 2013). In combination with the newly optimized $^{15}N_2$ tracer method, this technique will further improve our estimates of N_2 fixation.

1.5 Aims of thesis

Microbial mediated conversion of atmospheric N_2 gas into bioavailable NH_3 constitutes an important N source in oligotrophic open ocean systems controlling primary productivity. The discovery of new N_2 fixing microorganisms based on functional *nifH* gene assays revealed a higher diversity within the diazotrophic community than previously known. These phylotypes were divided into three uncultured unicellular cyanobacterial groups, i.e. UCYN–A, UCYN–B and UCYN–C. These groups are globally abundant and the detection of high N_2 fixation

rates in cell–size fractions with high abundances of UCYN groups indicated their ecological importance within the diazotrophic community.

In particular, *nifH* gene phylotypes of UCYN–A can dominate diazotrophic communities and reveal highest *nifH* expression during the day, which is unusual since unicellular diazotrophs perform N_2 fixation during the night. Further investigations succeeded in closing the genome of UCYN–A showing that these microorganisms lack genes for PSII, any known CO_2 fixation pathway and other metabolic features characteristic for cyanobacteria. These findings explain elevated *nifH* gene transcription during the day, but questions how these microorganisms thrive in the environment remained unanswered. Our knowledge about the UCYN–A group and their physiological activity is limited since this group has not been obtained in culture and we depend on field measurements to estimate their contribution to N_2 fixation.

My doctoral thesis work focuses on studying C and N metabolism on field populations of UCYN–A using molecular biology, as well as mass spectrometry tools to visualize metabolic activity on a single cell scale. As part of my thesis, I worked on the development of a 16S rRNA oligonucleotide probe that specifically targets the UCYN–A population, allowing us to link the phylogenetic identity of UCYN–A with its metabolic activity on a single cell scale using nanoSIMS technology. The successful application of this genus–specific probe (Manuscript I and II) enabled us to asses these microorganisms microscopically and image their CO_2 and N_2 fixation activity for the first time. In parallel, we revealed that these cyanobacteria live in association with globally important calcifying nanoplankton (Manuscript I). These findings have implications for our understanding of the marine C and N cycles since associations between cyanobacteria and eukaryotes have been shown to play a critical role in ocean productivity and carbon sequestration.

Another component of my thesis was to quantify cellular abundances of the UCYN–A association via double CARD–FISH (Catalyzed Reporter Deposition–Fluorescence *In Situ* Hybridization) assays in the North Atlantic Ocean (Manuscript III). We simultaneously identified UCYN–A and their eukaryotic partner as *Haptophyta* cells, demonstrating that UCYN–A live in association with a unicellular alga, and that this association is the dominant form versus free–living UCYN–A cells.

Finally, I studied the impact of various nutrients on physiological interactions between individual UCYN–A cells and their partner eukaryote (i.e. *Haptophyta*). This work aimed to gather detailed information about the environmental factors that constrain UCYN–A N_2 fixation activity, and identify environmental factors that affect the nutrient transfer between

these two partner cells (Manuscript IV). This work forms the foundation for detailed culture independent studies on a widely distributed group of microorganisms and underlines the importance of measuring *in situ* activity. This work enhances our understanding of the importance and distribution of UCYN-A in the marine environment, the role of their associations with a eukaryotic partner cell in mediating C and N fixation, and the environmental factors that influence their presence and metabolic activity.

1.6 References

Altabet, M.A., Francois, R., Murray, D.W., and Prell, W.L. (1995) Climate–related variations in denitrification in the Arabian Sea from sediment $^{15}N/^{14}N$ ratios. *Nature* **373**: 506–509.

Berman–Frank, I., Lundgren, P., and Falkowski, P. (2003) Nitrogen fixation and photosynthetic oxygen evolution in cyanobacteria. *Res Microbiol* **154**: 157–164.

Berman–Frank, I., Cullen, J.T., Shaked, Y., Sherrell, R.M., and Falkowski, P.G. (2001a) Iron availability, cellular iron quotas, and nitrogen fixation in *Trichodesmium*. *Limnol Oceanogr* **46**: 1249–1260.

Berman–Frank, I., Lundgren, P., Chen, Y.–B., Küpper, H., Kolber, Z., Bergman, B., and Falkowski, P. (2001b) Segregation of nitrogen fixation and oxygenic photosynthesis in the marine cyanobacterium *Trichodesmium*. *Science* **294**: 1534–1537.

Bertilsson, S., Berglund, O., Karl, D.M., and Chisholm, S.W. (2003) Elemental composition of marine *Prochlorococcus* and *Synechococcus*: Implications for the ecological stoichiometry of the sea. *Limnol Oceanogr* **48**: 1721–1731.

Bombar, D., Turk–Kubo, K.A., Robidart, J., Carter, B.J., and Zehr, J.P. (2013) Non-cyanobacterial *nifH* phylotypes in the North Pacific Subtropical Gyre detected by flow–cytometry cell sorting. *Environ Microbiol Rep*: 1–11.

Bombar, D., Moisander, P.H., Dippner, J.W., Foster, R.A., Voss, M., Karfeld, B., and Zehr, J.P. (2011) Distribution of diazotrophic microorganisms and *nifH* gene expression in the Mekong River plume during intermonsoon. *Mar Ecol Prog Ser* **424**: 39–52.

Bothe, H., Tripp, H.J., and Zehr, J.P. (2010) Unicellular cyanobacteria with a new mode of life: The lack of photosynthetic oxygen evolution allows nitrogen fixation to proceed. *Arch Microbiol* **192**: 783–790.

Boyer, E.W., Howarth, R.W., Galloway, J.N., Dentener, F.J., Green, P.A., and Vörösmarty, C.J. (2006) Riverine nitrogen export from the continents to the coasts. *Glob Biogeochem Cycles* **20**: 1–9.

Brandes, J.A., and Devol, A.H. (2002) A global marine–fixed nitrogen isotopic budget: Implications for Holocene nitrogen cycling. *Glob Biogeochem Cycles* **16**: 1–14.

Breitbarth, E., Oschlies, A., and LaRoche, J. (2007) Physiological constraints on the global distribution of *Trichodesmium*–effect of temperature on diazotrophy. *Biogeosciences* **4**: 53–61.

Broecker, W.S., and Henderson, G.M. (1998) The sequence of events surrounding Termination II and their implications for the cause of glacial–interglacial CO_2 changes. *Paleoceanography* **13**: 352–364.

Bronk, D.A., and Steinberg, D.K. (2008) Nitrogen Regeneration. In *In Nitrogen in the marine environment*. Ed., Capone, D.G., Bronk, D.A., Mulholland, M.R., and Carpenter, E.J. (eds): Burlington, MA: Academic, pp. 385–467.

Bryceson, I., and Fay, P. (1981) Nitrogen fixation in *Oscillatoria* (*Trichodesmium*) erythraea in relation to bundle formation and trichome differentiation. *Mar Biol* **61**: 159–166.

Buesseler, K.O. (2012) Biogeochemistry: The great iron dump. *Nature* **487**: 305–306.

Bulen, W.A., and LeComte, J.R. (1966) The nitrogenase system from Azotobacter: two-enzyme requirement for N_2 reduction, ATP-dependent H_2 evolution, and ATP hydrolysis. *Proceedings of the National Academy of Sciences* **56**: 979–986.

Capone, D.G. (1993) Determination of nitrogenase activity in aquatic samples using the acetylene reduction procedure. In *Handbook of methods in aquatic microbial ecology*. Kemp, P.F., Sherr, B.F., Sherr, E.B., and Cole, J.J. (eds). Boca Raton: Lewis Publishers, pp. 621–631.

Capone, D.G. (2000) The marine microbial nitrogen cycle. In *Microbial ecology of the oceans*. Kirchman, D.L. (ed). Ne York: Wiley-Liss, pp. 455–494.

Capone, D.G., and Carpenter, E.J. (1982) Nitrogen fixation in the marine environment. *Science* **217**: 1140–1142.

Capone, D.G., and Montoya, J.P. (2001) Nitrogen fixation and denitrification. *Methods Microbio* **30**: 501–515.

Capone, D.G., and Knapp, A.N. (2007) Oceanography: A marine nitrogen cycle fix? *Nature* **445**: 159–160.

Capone, D.G., Bronk, D.A., Mulholland, M.R., and Carpenter, E.J. (2008) *Nitrogen in the marine environment*: Academic Press.

Capone, D.G., Zehr, J.P., Paerl, H.W., Bergman, B., and Carpenter, E.J. (1997) *Trichodesmium*, a globally significant marine cyanobacterium. *Science* **276**: 1221–1229.

Capone, D.G., Burns, J.A., Montoya, J.P., Subramaniam, A., Mahaffey, C., Gunderson, T. et al. (2005) Nitrogen fixation by *Trichodesmium* spp.: An important source of new nitrogen to the tropical and subtropical North Atlantic Ocean. *Glob Biogeochem Cycles* **19**: 1–17.

Carpenter, E.J., and Foster, R.A. (2003) Marine cyanobacterial symbioses. In *Cyanobacteria in symbiosis*. Rai, A.N., Bergman, B., and Rasmussen, U. (eds): Kluwer Academic Publishers, pp. 11–17.

Carpenter, E.J., Montoya, J.P., Burns, J., Mulholland, M.R., Subramaniam, A., and Capone, D.G. (1999) Extensive bloom of a N_2–fixing diatom/cyanobacterial association in the tropical Atlantic Ocean. *Mar Ecol Prog Ser* **185**: 273–283.

Cavender–Bares, K.K., Karl, D.M., and Chisholm, S.W. (2001) Nutrient gradients in the western North Atlantic Ocean: Relationship to microbial community structure and comparison to patterns in the Pacific Ocean. *Deep-Sea Res Pt I* **48**: 2373–2395.

Chappell, P.D., and Webb, E.A. (2010) A molecular assessment of the iron stress response in the two phylogenetic clades of *Trichodesmium*. *Environ Microbiol* **12**: 13–27.

Chen, Y.–B., Zehr, J.P., and Mellon, M. (1996) Growth and nitrogen fixation of the diazotrophic filamentous nonheterocystous cyanobacterium *Trichodesmium* sp. IMS 101 in defined media: Evidence for a circadian rhythm. *J Phycol* **32**: 916–923.

Church, M.J., Ducklow, H.W., and Karl, D.M. (2004) Light dependence of [^{3}H] leucine incorporation in the oligotrophic North Pacific Ocean. *Appl Environ Microbiol* **70**: 4079–4087.

Church, M.J., Jenkins, B.D., Karl, D.M., and Zehr, J.P. (2005a) Vertical distributions of nitrogen-fixing phylotypes at stn ALOHA in the oligotrophic North Pacific Ocean. *Aquat Microb Ecol* **38**: 3–14.

Church, M.J., Short, C.M., Jenkins, B.D., Karl, D.M., and Zehr, J.P. (2005b) Temporal patterns of nitrogenase gene (*nifH*) expression in the oligotrophic North Pacific Ocean. *Appl Environ Microbiol* **71**: 5362–5370.

Church, M.J., Björkman, K.M., Karl, D.M., Saito, M.A., and Zehr, J.P. (2008) Regional distributions of nitrogen–fixing bacteria in the Pacific Ocean. *Limnol Oceanogr* **53**: 63–77.

Codispoti, L.A. (1995) Is the ocean losing nitrate? *Nature* **376**: 724.

Codispoti, L.A., Brandes, J.A., Christensen, J.P., Devol, A.H., Naqvi, S.W.A., Paerl, H.W., and Yoshinari, T. (2001) The oceanic fixed nitrogen and nitrous oxide budgets: Moving targets as we enter the anthropocene? *Scientia Marina* **65**: 85–105.

Corzo, A., Morillo, J.A., and Rodríguez, S. (2000) Production of transparent exopolymer particles (TEP) in cultures of *Chaetoceros calcitrans* under nitrogen limitation. *Aquat Microb Ecol* **23**: 63–72.

DeLong, E.F. (2010) Interesting things come in small packages. *Genome Biol* **11**: 118.

Deutsch, C., Sarmiento, J.L., Sigman, D.M., Gruber, N., and Dunne, J.P. (2007) Spatial coupling of nitrogen inputs and losses in the ocean. *Nature* **445**: 163–167.

Dixon, R., and Kahn, D. (2004) Genetic regulation of biological nitrogen fixation. *Nat Rev Microbiol* **2**: 621–631.

Dron, A., Rabouille, S., Claquin, P., and Sciandra, A. (2013) Photoperiod length paces the temporal orchestration of cell cycle and carbon–nitrogen metabolism in *Crocosphaera watsonii*. *Environ Microbiol*: doi:10.1111/1462-2920.12163.

Dron, A., Rabouille, S., Claquin, P., Le Roy, B., Talec, A., and Sciandra, A. (2011) Light–dark (12:12) cycle of carbon and nitrogen metabolism in *Crocosphaera watsonii* WH8501: relation to the cell cycle. *Environ Microbiol* **14**: 967–981.

Duce, R.A., LaRoche, J., Altieri, K., Arrigo, K.R., Baker, A.R., Capone, D.G. et al. (2008) Impacts of atmospheric anthropogenic nitrogen on the open ocean. *Science* **320**: 893–897.

Dugdale, R.C., Goering, J.J., and Ryther, J.H. (1964) High nitrogen fixation rates in the Sargasso Sea and the Arabian Sea. *Limnol Oceanogr* **9**: 507–510.

Dyhrman, S.T., Chappell, P.D., Haley, S.T., Moffett, J.W., Orchard, E.D., Waterbury, J.B., and Webb, E.A. (2006) Phosphonate utilization by the globally important marine diazotroph *Trichodesmium*. *Nature* **439**: 68–71.

Falcón, L.I., Lindvall, S., Bauer, K., Bergman, B., and Carpenter, E.J. (2004) Ultrastructure of unicellular N_2 fixing cyanobacteria from the tropical North Atlantic and subtropical North Pcific Oceans. *J Phycol* **40**: 1074–1078.

Farnelid, H., and Riemann, L. (2008) Heterotrophic N_2–fixing bacteria: Overlooked in the marine nitrogen cycle? In *Nitrogen fixation research progress. Nova Science Publishers, New York, NY*. Couto, G.N. (ed). New York: Nova Science Publisher, pp. 409–423.

Farnelid, H., Andersson, A.F., Bertilsson, S., Al-Soud, W.A., Hansen, L.H., Sørensen, S. et al. (2011) Nitrogenase Gene Amplicons from Global Marine Surface Waters Are Dominated by Genes of Non–Cyanobacteria. *PLoS ONE* **6**: e19223.

Foster, R.A., and Zehr, J.P. (2006) Characterization of diatom–cyanobacteria symbioses on the basis of *nifH*, *hetR* and 16S rRNA sequences. *Environ Microbiol* **8**: 1913–1925.

Foster, R.A., Goebel, N.L., and Zehr, J.P. (2010) Isolation of the *Calothrix Rhizosoleniae* (cyanobacteria) strain SC01 from *Chaetoceros* (Bacillariophyta) spp. diatoms of the subtropical North Pacific Ocean. *J Phycol* **46**: 1028–1037.

Foster, R.A., Sztejrenszus, S., and Kuypers, M.M. (2013) Measuring carbon and N_2 fixation in field populations of colonial and free–living unicellular cyanobacteria using nanometer-scale secondary ion mass spectrometry. *J Phycol*: 1–15.

Foster, R.A., Kuypers, M.M.M., Vagner, T., Paerl, R.W., Musat, N., and Zehr, J.P. (2011) Nitrogen fixation and transfer in open ocean diatom–cyanobacterial symbioses. *ISME J* **5**: 1484–1493.

Fu, F., Zhang, Y., Leblanc, K., Sanudo–Wilhelmy, S.A., and Hutchins, D.A. (2005) The biological and biogeochemical consequences of phosphate scavenging onto phytoplankton cell surfaces. *Limnol Oceanogr* **50**: 1459–1472.

Gallon, J.R. (1992) Reconciling the incompatible: N_2 fixation and O_2. *New Phytol* **122**: 571–609.

Galloway, J.N., Dentener, F.J., Capone, D.G., Boyer, E.W., Howarth, R.W., Seitzinger, S.P. et al. (2004) Nitrogen cycles: Past, present, and future. *Biogeochemistry* **70**: 153–226.

Ganeshram, R.S., Pedersen, T.F., Calvert, S.E., and Murray, J.W. (1995) Large changes in oceanic nutrient inventories from glacial to interglacial periods. *Nature* **376**: 755–758.

Geider, R., and La Roche, J. (2002) Redfield revisited: variability of C: N: P in marine microalgae and its biochemical basis. *Europ J Phycol* **37**: 1–17.

Goebel, N.L., Edwards, C.A., Carter, B.J., Achilles, K.M., and Zehr, J.P. (2008) Growth and carbon content of three different sized diazotrophic cyanobacteria observed in the subtropical North Pacific. *J Phycol* **44**: 1212–1220.

Goebel, N.L., Turk, K.A., Achilles, K.M., Paerl, R., Hewson, I., Morrison, A.E. et al. (2010) Abundance and distribution of major groups of diazotrophic cyanobacteria and their potential contribution to N_2 fixation in the tropical Atlantic Ocean. *Environ Microbiol* **12**: 3272–3289.

Goldman, J.C., Caron, D.A., and Dennett, M.R. (1987) Regulation of gross growth efficiency and ammonium regeneration in bacteria by substrate C: N ratio. *Limnol Oceanogr* **32**: 1239–1252.

Gómez, F., Furuya, K., and Takeda, S. (2005) Distribution of the cyanobacterium *Richelia intracellularis* as an epiphyte of the diatom *Chaetoceros compressus* in the western Pacific Ocean. *J Plank Res* **27**: 323–330.

Grabowski, M.N.W., Church, M.J., and Karl, D.M. (2008) Nitrogen fixation rates and controls at Stn ALOHA. *Aquat Microb Ecol* **52**: 175–183.

Großkopf, T., Mohr, W., Baustian, T., Schunck, H., Gill, D., Kuypers, M.M.M. et al. (2012) Doubling of marine dinitrogen-fixation rates based on direct measurements. *Nature* **488**: 361–364.

Gruber, N. (2004) The dynamics of the marine nitrogen cycle and its influence on atmospheric CO_2 variations. In *The ocean carbon cycle and climate*: Springer, pp. 97–148.

Gruber, N. (2005) Oceanography: A bigger nitrogen fix. *Nature* **436**: 786–787.

Gruber, N. (2008) The marine nitrogen cycle: Overview and challenges. In *In Nitrogen in the marine environment*. Capone, D.G., Bronk, D.A., Mulholland, M.R., and Carpenter, E.J. (eds): Burlington, MA: Academic, pp. 1–50.

Gruber, N., and Sarmiento, J.L. (1997) Global patterns of marine nitrogen fixation and denitrification. *Glob Biogeochem Cycles* **11**: 235–266.

Gruber, N., and Sarmiento, J.L. (2002) Large–scale biogeochemical-physical interactions in elemental cycles. *The sea* **12**: 337–399.

Hageman, R.V., and Burris, R.H. (1978) Nitrogenase and nitrogenase reductase associate and dissociate with each catalytic cycle. *P Natl Acad Sci USA* **75**: 2699–2702.

Halm, H., Lam, P., Ferdelman, T.G., Lavik, G., Dittmar, T., LaRoche, J. et al. (2012) Heterotrophic organisms dominate nitrogen fixation in the South Pacific Gyre. *ISME J* **6**: 1238–1249.

Heldal, M., Scanlan, D.J., Norland, S., Thingstad, F., and Mann, N.H. (2003) Elemental composition of single cells of various strains of marine *Prochlorococcus* and *Synechococcus* using X–ray microanalysis. *Limnol Oceanogr* **48**: 1732–1743.

Hewson, I., Poretsky, R.S., Beinart, R.A., White, A.E., Shi, T., Bench, S.R. et al. (2009) *In situ* transcriptomic analysis of the globally important keystone N_2–fixing taxon *Crocosphaera watsonii*. *ISME J* **3**: 618–631.

Ho, T.Y., Quigg, A., Finkel, Z.V., Milligan, A.J., Wyman, K., Falkowski, P.G., and Morel, F.M.M. (2003) The elemental composition of some marine phytoplankton. *J Phycol* **39**: 1145–1159.

Howarth, R.W., Butler, T., Lunde, K., Swaney, D., and Chu, C.R. (1993) Turbulence and planktonic nitrogen fixation: A mesocosm experiment. *Limnol Oceanogr* **38**: 1696–1711.

Ininbergs, K., Bay, G., Rasmussen, U., Wardle, D.A., and Nilsson, M.-C. (2011) Composition and diversity of *nifH* genes of nitrogen–fixing cyanobacteria associated with boreal forest feather mosses. *New Phytol* **192**: 507–517.

Jickells, T.D., An, Z.S., Andersen, K.K., Baker, A.R., Bergametti, G., Brooks, N. et al. (2005) Global iron connections between desert dust, ocean biogeochemistry, and climate. *Science* **308**: 67–71.

Karl, D., Letelier, R., Tupas, L., Dore, J., Christian, J., and Hebel, D. (1997) The role of nitrogen fixation in biogeochemical cycling in the subtropical North Pacific Ocean. *Nature* **388**: 533–538.

Karl, D., Michaels, A., Bergman, B., Capone, D., Carpenter, E., Letelier, R. et al. (2002) Dinitrogen fixation in the world's oceans. *Biogeochemistry* **57**: 47–98.

Karl, D.M., Letelier, R.M., Rkman, K., and Letelier, R.M. (2008) Nitrogen fixation–enhanced carbon sequestration in low nitrate, low chlorophyll seascapes. *Mar Ecol Prog Ser* **364**: 257–268.

Karl, D.M., Church, M.J., Dore, J.E., Letelier, R.M., and Mahaffey, C. (2012) Predictable and efficient carbon sequestration in the North Pacific Ocean supported by symbiotic nitrogen fixation. *P Natl Acad Sci USA* **109**: 1842–1849.

Karl, D.M., Björkman, K.M., Dore, J.E., Fujieki, L., Hebel, D.V., Houlihan, T. et al. (2001) Ecological nitrogen–to–phosphorus stoichiometry at station ALOHA. *Deep-Sea Res Pt II* **48**: 1529–1566.

Klausmeier, C.A., Litchman, E., Daufresne, T., and Levin, S.A. (2004) Optimal nitrogen–to–phosphorus stoichiometry of phytoplankton. *Nature* **429**: 171–174.

Krupke, A., Musat, N., LaRoche, J., Mohr, W., Fuchs, B.M., Amann, R.I. et al. (2013) *In situ* identification and N_2 and C fixation rates of uncultivated cyanobacteria populations. *Syst Appl Microbiol* **36**: 259–271.

Küpper, H., Ferimazova, N., Šetlík, I., and Berman–Frank, I. (2004) Traffic lights in *Trichodesmium*. Regulation of photosynthesis for nitrogen fixation studied by chlorophyll fluorescence kinetic microscopy. *Plant Physiol* **135**: 2120–2133.

Küpper, H., Šetlík, I., Seibert, S., Prášil, O., Šetlikova, E., Strittmatter, M. et al. (2008) Iron limitation in the marine cyanobacterium *Trichodesmium* reveals new insights into regulation of photosynthesis and nitrogen fixation. *New Phytol* **179**: 784–798.

Kustka, A.B., Sanudo–Wilhelmy, S.A., Carpenter, E.J., Capone, D., Burns, J., and Sunda, W.G. (2003) Iron requirements for dinitrogen–and ammonium–supported growth in cultures of *Trichodesmium* (IMS 101): Comparison with nitrogen fixation rates and iron: carbon ratios of field populations. *Limnol Oceanogr* **48**: 1869–1884.

Kuypers, M.M.M., Sliekers, A.O., Lavik, G., Schmid, M., Jørgensen, B.B., Kuenen, J.G. et al. (2003) Anaerobic ammonium oxidation by anammox bacteria in the Black Sea. *Nature* **422**: 608–611.

Laamanen, M., and Kuosa, H. (2005) Annual variability of biomass and heterocysts of the N_2–fixing cyanobacterium Aphanizomenon flos–aquae in the Baltic Sea with reference to *Anabaena* spp. and *Nodularia spumigena*. *Boreal Environ Res* **10**: 19–30.

Lam, P., and Kuypers, M.M.M. (2011) Microbial nitrogen cycling processes in oxygen minimum zones. *Annu Rev Mar Sci* **3**: 317–345.

Langlois, R.J., LaRoche, J., and Raab, P.A. (2005) Diazotrophic diversity and distribution in the tropical and subtropical Atlantic Ocean. *Appl Environ Microbiol* **71**: 7910–7919.

Langlois, R.J., Hummer, D., and LaRoche, J. (2008) Abundances and distributions of the dominant *nifH* phylotypes in the Northern Atlantic Ocean. *Appl Environ Microbiol* **74**: 1922–1931.

LaRoche, J., and Breitbarth, E. (2005) Importance of the diazotrophs as a source of new nitrogen in the ocean. *J Sea Res* **53**: 67–91.

Lehtimaki, J., Moisander, P., Sivonen, K., and Kononen, K. (1997) Growth, nitrogen fixation, and nodularin production by two baltic sea cyanobacteria. *Appl Environ Microbiol* **63**: 1647–1656.

Letelier, R.M., and Karl, D.M. (1998) *Trichodesmium* spp. physiology and nutrient fluxes in the North Pacific subtropical gyre. *Aquat Microb Ecol* **15**: 265–276.

Liu, H., Nolla, H.A., and Campbell, L. (1997) *Prochlorococcus* growth rate and contribution to primary production in the equatorial and subtropical North Pacific Ocean. *Aquat Microb Ecol* **12**: 39–47.

Mahowald, N.M., Baker, A.R., Bergametti, G., Brooks, N., Duce, R.A., Jickells, T.D. et al. (2005) Atmospheric global dust cycle and iron inputs to the ocean. *Glob Biogeochem Cycles* **19**: 1–15.

McClelland, J.W., Holl, C.M., and Montoya, J.P. (2003) Relating low $\delta^{15}N$ values of zooplankton to N_2–fixation in the tropical North Atlantic: Insights provided by stable isotope ratios of amino acids. *Deep-Sea Res Pt I* **50**: 849–861.

Michaels, A.F., Olson, D., Sarmiento, J.L., Ammerman, J.W., Fanning, K., Jahnke, R. et al. (1996) Inputs, losses and transformations of nitrogen and phosphorus in the pelagic North Atlantic Ocean. *Biogeochemistry* **35**: 181–226.

Mills, M.M., Ridame, C., Davey, M., La Roche, J., and Geider, R.J. (2004) Iron and phosphorus co–limit nitrogen fixation in the eastern tropical North Atlantic. *Nature* **429**: 292–294.

Mohr, W., Intermaggio, M.P., and LaRoche, J. (2010a) Diel rhythm of nitrogen and carbon metabolism in the unicellular, diazotrophic cyanobacterium *Crocosphaera watsonii* WH8501. *Environ Microbiol* **12**: 412–421.

Mohr, W., Großkopf, T., Wallace, D.W.R., and LaRoche, J. (2010b) Methodological underestimation of oceanic nitrogen fixation rates. *PLoS ONE* **5**: e12583.

Moisander, P.H., Beinart, R.A., Hewson, I., White, A.E., Johnson, K.S., Carlson, C.A. et al. (2010) Unicellular cyanobacterial distributions broaden the oceanic N_2 fixation domain. *Science* **327**: 1512–1514.

Montoya, J.P. (2008) Nitrogen stable isotopes in marine environments. In *In Nitrogen in the marine environment*. Capone, D.G., Bronk, D.A., Mulholland, M.R., and Carpenter, E.J. (eds): Burlington, MA: Academic, pp. 1277–1302.

Montoya, J.P., Carpenter, E.J., and Capone, D.G. (2002) Nitrogen fixation and nitrogen isotope abundances in zooplankton of the oligotrophic North Atlantic. *Limnol Oceanogr* **47**: 1617–1628.

Montoya, J.P., Voss, M., Kahler, P., and Capone, D.G. (1996) A Simple, High–Precision, High–Sensitivity Tracer Assay for N_2–Fixation. *Appl Environ Microbiol* **62**: 986–993.

Montoya, J.P., Holl, C.M., Zehr, J.P., Hansen, A., Villareal, T.A., and Capone, D.G. (2004) High rates of N_2 fixation by unicellular diazotrophs in the oligotrophic Pacific Ocean. *Nature* **430**: 1027–1032.

Moore, C.M., Mills, M.M., Achterberg, E.P., Geider, R.J., LaRoche, J., Lucas, M.I. et al. (2009) Large–scale distribution of Atlantic nitrogen fixation controlled by iron availability. *Nat Geosci* **2**: 867–871.

Moutin, T., Karl, D.M., Duhamel, S., Rimmelin, P., Raimbault, P., Van Mooy, B.A.S., and Claustre, H. (2008) Phosphate availability and the ultimate control of new nitrogen input by nitrogen fixation in the tropical Pacific Ocean. *Biogeosciences* **5**: 95–109.

Mulder, A., Graaf, A.A., Robertson, L.A., and Kuenen, J.G. (1995) Anaerobic ammonium oxidation discovered in a denitrifying fluidized bed reactor. *FEMS Microbiol Ecol* **16**: 177–184.

Mulholland, M.R., and Bernhardt, P.W. (2005) The effect of growth rate, phosphorus concentration, and temperature on N_2 fixation, carbon fixation, and nitrogen release in continuous cultures of *Trichodesmium* IMS101. *Limnol Oceanogr* **50**: 839–849.

Mulholland, M.R., Bronk, D.A., and Capone, D.G. (2004) Dinitrogen fixation and release of ammonium and dissolved organic nitrogen by *Trichodesmium* IMS101. *Aquat Microb Ecol* **37**: 85–94.

Musat, N., Halm, H., Winterholler, B., Hoppe, P., Peduzzi, S., Hillion, F. et al. (2008) A single–cell view on the ecophysiology of anaerobic phototrophic bacteria. *P Natl Acad Sci USA* **105**: 17861–17866.

Needoba, J.A., Foster, R.A., Sakamoto, C., Zehr, J.P., and Johnson, K.S. (2007) Nitrogen fixation by unicellular diazotrophic cyanobacteria in the temperate oligotrophic North Pacific Ocean. *Limnol Oceanogr* **52**: 1317–1327.

Neess, J.C., Dugdale, R.C., Dugdale, V.A., and Goering, J.J. (1962) Nitrogen metabolism in lakes. I. Measurement of nitrogen fixation with N^{15}. *Limnol Oceanogr* **7**: 163–169.

Nier, A.O. (1950) A redetermination of the relative abundances of the isotopes of carbon, nitrogen, oxygen, argon, and potassium. *Phys Rev* **77**: 789–793.

Orchard, E.D., Benitez–Nelson, C.R., Pellechia, P.J., Lomas, M.W., and Dyhrman, S.T. (2010) Polyphosphate in *Trichodesmium* from the low-phosphorus Sargasso Sea. *Limnol Oceanogr* **55**: 2161–2169.

Orphan, V.J., House, C.H., Hinrichs, K.–U., McKeegan, K.D., and DeLong, E.F. (2001) Methane-consuming archaea revealed by directly coupled isotopic and phylogenetic analysis. *Science* **293**: 484–487.

Paerl, H.W., and Bland, P.T. (1982) Localized tetrazolium reduction in relation to N_2 fixation, CO_2 fixation, and H_2 uptake in aquatic filamentous cyanobacteria. *Appl Environ Microbiol* **43**: 218–226.

Paerl, H.W., and Bebout, B.M. (1988) Direct measurement of O_2–depleted microzones in marine *Oscillatoria*: Relation to N_2 fixation. *Science* **241**: 442–445.

Postgate, J.R. (1982) *The fundamentals of nitrogen fixation*. Cambridge University Press.

Prufert–Bebout, L., Paerl, H.W., and Lassen, C. (1993) Growth, nitrogen fixation, and spectral attenuation in cultivated *Trichodesmium* species. *Appl Environ Microbiol* **59**: 1376–1375.

Reddy, K.J., Soper, B.W., Tang, J., and Bradley, R.L. (1996) Phenotypic variation in exopolysaccharide production in the marine, aerobic nitrogen–fixing unicellular cyanobacterium *Cyanothece* sp. *World J Microbiol Biotechnol* **12**: 311–318.

Redfield, A.C. (1958) The biological control of chemical factors in the environment. *Am J Sci* **46**: 205–221.

Rippka, R., Neilson, A., Kunisawa, R., and Cohen-Bazire, G. (1971) Nitrogen fixation by unicellular blue–green algae. *Arch Mikrobiol* **76**: 341–348.

Saino, T., and Hattori, A. (1980) Nitrogen fixation by *Trichodesmium* and its significance in nitrogen cycling in the Kuroshio area and adjacent waters. In *The Kuroshio IV*. Takenouti, A.Y. (ed): Saikon Publishing, Tokyo, pp. 697–709.

Sañudo–Wilhelmy, S.A., Kustka, A.B., Gobler, C.J., Hutchins, D.A., Yang, M., Lwiza, K. et al. (2001) Phosphorus limitation of nitrogen fixation by *Trichodesmium* in the central Atlantic Ocean. *Nature* **411**: 66–69.

Shi, T., Ilikchyan, I., Rabouille, S., and Zehr, J.P. (2010) Genome-wide analysis of diel gene expression in the unicellular N_2-fixing cyanobacterium *Crocosphaera watsonii* WH 8501. *ISME J* **4**: 621–632.

Short, S.M., and Zehr, J.P. (2007) Nitrogenase gene expression in the Chesapeake Bay Estuary. *Environ Microbiol* **9**: 1591–1596.

Smetacek, V. (1999) Diatoms and the ocean carbon cycle. *Protist* **150**: 25–32.

Sohm, J.A., and Capone, D.G. (2006) Phosphorus dynamics of the tropical and subtropical north Atlantic: *Trichodesmium* spp. versus bulk plankton. *Mar Ecol Prog Ser* **317**: 21–28.

Sohm, J.A., Webb, E.A., and Capone, D.G. (2011) Emerging patterns of marine nitrogen fixation. *Nat Rev Microbiol* **9**: 499–508.

Staal, M., Meysman, F.J.R., and Stal, L.J. (2003) Temperature excludes N_2–fixing heterocystous cyanobacteria in the tropical oceans. *Nature* **425**: 504–507.

Stewart, W.D.P. (1969) Biological and ecological aspects of nitrogen fixation by free–living micro-organisms. *Proc R Soc Lond B Bio* **172**: 367–388.

Strathmann, R.R. (1967) Estimating the organic carbon content of phytoplankton from cell volume or plasma volume. *Limnol Oceanogr* **12**: 411–418.

Subramaniama, A., Brownb, C.W., Hoodc, R.R., Carpenter, E.J., and Capone, D.G. (2002) Detecting *Trichodesmium* blooms in SeaWiFS imagery. *Deep Sea Res* **2**: 107–121.

Sundquist, E.T., and Broecker, W.S. (1985) The carbon cycle and atmospheric CO_2: Natural variations Archean to present. In: American Geophysical Union.

Takahashi, T., Broecker, W.S., and Langer, S. (1985) Redfield ratio based on chemical data from isopycnal surfaces. *J Geophys Res* **90**: 6907–6924.

Teece, M.A., Fogel, M.L., Dollhopf, M.E., and Nealson, K.H. (1999) Isotopic fractionation associated with biosynthesis of fatty acids by a marine bacterium under oxic and anoxic conditions. *Org Geochem* **30**: 1571–1579.

Thompson, A.W., Foster, R.A., Krupke, A., Carter, B.J., Musat, N., Vaulot, D. et al. (2012) Unicellular cyanobacterium symbiotic with a single–celled eukaryotic alga. *Science* **337**: 1546–1550.

Tripp, H.J., Bench, S.R., Turk, K.A., Foster, R.A., Desany, B.A., Niazi, F. et al. (2010) Metabolic streamlining in an open–ocean nitrogen–fixing cyanobacterium. *Nature* **464**: 90–94.

Tyrrell, T., Marañón, E., Poulton, A.J., Bowie, A.R., Harbour, D.S., and Woodward, E.M.S. (2003) Large-scale latitudinal distribution of *Trichodesmium* spp. in the Atlantic Ocean. *J Plank Res* **25**: 405–416.

Van Mooy, B.A.S., Hmelo, L.R., Sofen, L.E., Campagna, S.R., May, A.L., Dyhrman, S.T. et al. (2012) Quorum sensing control of phosphorus acquisition in *Trichodesmium* consortia. *The ISME journal* **6**: 422–429.

Venrick, E.L. (1974) The distribution and significance of *Richelia intracellularis* Schmidt in the North Pacific Central Gyre. *Limnol Oceanogr* **19**: 437–445.

Villareal, T.A., and Carpenter, E.J. (1988) Nitrogen fixation, suspension characteristics, and chemical composition of *Rhizosolenia* mats in the central North Pacific gyre. *Biol Oceanogr* **6**: 327–345.

Villareal, T.A., and Carpenter, E.J. (2003) Buoyancy regulation and the potential for vertical migration in the oceanic cyanobacterium *Trichodesmium*. *Microb Ecol* **45**: 1–10.

Voss, M., Dippner, J.W., and Montoya, J.P. (2001) Nitrogen isotope patterns in the oxygen-deficient waters of the Eastern Tropical North Pacific Ocean. *Deep-Sea Res Pt I* **48**: 1905–1921.

Ward, W.B. (2008) Nitrification in Marine Systems. In *In Nitrogen in the marine environment*. Capone, D.G., Bronk, D.A., Mulholland, M.R., and Carpenter, E.J. (eds): Burlington, MA: Academic, pp. 199–261.

Waterbury, J.B., and Rippka, R. (1989) Subsection I. Order *Chroococcales*. In *Bergey`s Manual of Systematic Bacteriology*. Krieg NR, and (eds), H.J. (eds): Williams & Wilkins:Baltimore., pp. 1728–1746.

Webb, E.A., Moffett, J.W., and Waterbury, J.B. (2001) Iron stress in open–ocean cyanobacteria (*Synechococcus*, *Trichodesmium*, and *Crocosphaera* spp.): Identification of the IdiA protein. *Appl Environ Microbiol* **67**: 5444–5452.

Webb, E.A., Ehrenreich, I.M., Brown, S.L., Valois, F.W., and Waterbury, J.B. (2009) Phenotypic and genotypic characterization of multiple strains of the diazotrophic cyanobacterium, *Crocosphaera watsonii,* isolated from the open ocean. *Environ Microbiol* **11**: 338–348.

Weiss, R.F. (1970) The solubility of nitrogen, oxygen and argon in water and seawater. In *Deep Sea Research and Oceanographic Abstracts*: Elsevier, pp. 721–735.

White, A.E., Spitz, Y.H., and Letelier, R.M. (2007a) What factors are driving summer phytoplankton blooms in the North Pacific Subtropical Gyre? *J Geophys Res* **112**: 1–11.

White, A.E., Spitz, Y., Karl, D., and Letelier, R.M. (2006) Flexible elemental stoichiometry in *Trichodesmium* spp. and its ecological implications. *Limnol Oceanogr* **51**: 1777–1790.

White, A.E., Prahl, F.G., Letelier, R.M., and Popp, B.N. (2007b) Summer surface waters in the Gulf of California: Prime habitat for biological N_2 fixation. *Glob Biogeochem Cycles* **21**: 1–11.

Wu, J., Sunda, W., Boyle, E.A., and Karl, D.M. (2000) Phosphate depletion in the western North Atlantic Ocean. *Science* **289**: 759–762.

Zeev, E.B., Yogev, T., Man-Aharonovich, D., Kress, N., Herut, B., Béjà, O., and Berman-Frank, I. (2008) Seasonal dynamics of the endosymbiotic, nitrogen–fixing cyanobacterium *Richelia intracellularis* in the eastern Mediterranean Sea. *The ISME Journal* **2**: 911–923.

Zehr, J.P. (2011) Nitrogen fixation by marine cyanobacteria. *Trends Microbiol* **19**: 162–173.

Zehr, J.P., and McReynolds, L.A. (1989) Use of degenerate oligonucleotides for amplification of the *nifH* gene from the marine cyanobacterium *Trichodesmium thiebautii*. *Appl Environ Microbiol* **55**: 2522–2526.

Zehr, J.P., and Ward, B.B. (2002) Nitrogen cycling in the ocean: New perspectives on processes and paradigms. *Appl Environ Microbiol* **68**: 1015–1024.

Zehr, J.P., and Paerl, H.W. (2008) Molecular ecological aspects of nitrogen fixation in the marine environment. In *Microbial Ecology of the Oceans*. Kirchman, D. (ed): John Wiley & Sons, Inc, pp. 481–525.

Zehr, J.P., Mellon, M.T., and Zani, S. (1998) New nitrogen–fixing microorganisms detected in oligotrophic oceans by amplification of nitrogenase (*nifH*) genes. *Appl Environ Microbiol* **64**: 3444–3450.

Zehr, J.P., Jenkins, B.D., Short, S.M., and Steward, G.F. (2003) Nitrogenase gene diversity and microbial community structure: a cross system comparison. *Environ Microbiol* **5**: 539–554.

Zehr, J.P., Waterbury, J.B., Turner, P.J., Montoya, J.P., Omoregie, E., Steward, G.F. et al. (2001) Unicellular cyanobacteria fix N_2 in the subtropical North Pacific Ocean. *Nature* **412**: 635–637.

Zehr, J.P., Bench, S.R., Carter, B.J., Hewson, I., Niazi, F., Shi, T. et al. (2008) Globally distributed uncultivated oceanic N_2–fixing cyanobacteria lack oxygenic photosystem II. *Science* **322**: 1110–1112.

2 Manuscripts

2.1 Manuscript I: Unicellular Cyanobacterium Symbiotic with a Single-Celled Eukaryotic Alga

Anne W. Thompson, Rachel A. Foster, **Andreas Krupke**, Brandon J. Carter, Niculina Musat, Daniel Vaulot, Marcel M. M. Kuypers, Jonathan P. Zehr

Published 2012 in *Science* **337**: 1546–1550

Contribution: A.W.T., R.A.F and J.P.Z. designed the research and were responsible for sample collection. A.W.T, R.A.F. and A.K prepared samples and were responsible for data acquisition. Experimental data contribution by D.V.; The manuscript was written by A.W.T. and R.A.F. with editorial assistance from N.M., M.M.M.K. and J.P.Z.

2.2 Manuscript II : In situ identification and N_2 and C fixation rates of uncultivated cyanobacteria populations

Andreas Krupke, Niculina Musat, Julie LaRoche, Wiebke Mohr, Bernhard M. Fuchs, Rudolf I. Amann, Marcel M.M. Kuypers, Rachel A. Foster
Published 2013 in *Systematics and Applied Microbiology* **36**: 259–271.

Contribution: A.K., N.M. and R.A.F. designed the research and were responsible for sample collection. J.L.R. and W.M. were involved in sample collection. B.M.F., R.I.A. and M.M.M K. gave scientific and technical input. Sample preparation and experimental work was done by A.K., N.M. and R.A.F.; The manuscript was written by A.K. with editorial assistance from N.M., M.M.M.K. and R.A.F.

2.3 Manuscript III: Distribution of the association between unicellular algae and the N_2 fixing cyanobacterium UCYN–A in the North Atlantic Ocean

Andreas Krupke, Gaute Lavik, Hannah Halm, Bernhard M Fuchs, Rudolf I Amann, Marcel MM Kuypers

In preparation for *The ISME Journal*

Contribution: G.L. and M.M.M.K. designed the research and H.H. and B.M.F. were responsible for sample collection. Technical feedback was provided by G.L. and B.M.F. Sample preparation and data acquisition was done by A.K.; The manuscript was written by A.K. with editorial assistance from G.L., B.M.F., R.I.A. and M.M.M.K.

2.4 Manuscript IV: The effect of nutrients on carbon and nitrogen fixation by the UCYN–A–*Haptophyta* symbiosis

Andreas Krupke, Bernhard M Fuchs and Marcel M.M. Kuypers

In preparation for *Environmental Microbiology*

Potential co–authors: Wiebke Mohr, Julie LaRoche, Rudolf I Amann

Contribution: W.M., J.L.R. and M.M.M.K. designed the research. A.K., W.M and J.L.R. were responsible for sample collection. Sample preparation and data acquisition was done by A.K.; RIA provided scientific feedback and comments. The manuscript was written by A.K. with editorial assistance from B.M.F. and M.M.M.K.

2.1 Manuscript I: Unicellular Cyanobacterium Symbiotic with a Single-Celled Eukaryotic Alga

Anne W. Thompson,[1]* Rachel A. Foster,[2]* Andreas Krupke,[2] Brandon J. Carter,[1] Niculina Musat,[2]† Daniel Vaulot,[3] Marcel M. M. Kuypers,[2] Jonathan P. Zehr[1]‡

[1]Ocean Sciences, University of California, Santa Cruz, CA 95064, USA
[2] Max–Planck–Institut für Marine Mikrobiologie, 28359 Bremen, Germany
[3]UPMC (Paris-06) and CNRS, UMR 7144, Station Biologique, Place G. Tessier 29680 Roscoff, France

* These authors contributed equally to this work.
† Present address: Department of Isotope Biogeochemistry, UFZ–Helmholtz Centre for Environmental Research, Leipzig 04318, Germany.
‡ To whom correspondence should be addressed. E-mail: zehrj@ucsc.edu

Unicellular Cyanobacterium Symbiotic with a Single-Celled Eukaryotic Alga

Anne W. Thompson,[1]* Rachel A. Foster,[2]* Andreas Krupke,[2] Brandon J. Carter,[1] Niculina Musat,[2]† Daniel Vaulot,[3] Marcel M. M. Kuypers,[2] Jonathan P. Zehr[1]‡

Symbioses between nitrogen $(N)_2$–fixing prokaryotes and photosynthetic eukaryotes are important for nitrogen acquisition in N-limited environments. Recently, a widely distributed planktonic uncultured nitrogen-fixing cyanobacterium (UCYN-A) was found to have unprecedented genome reduction, including the lack of oxygen-evolving photosystem II and the tricarboxylic acid cycle, which suggested partnership in a symbiosis. We showed that UCYN-A has a symbiotic association with a unicellular prymnesiophyte, closely related to calcifying taxa present in the fossil record. The partnership is mutualistic, because the prymnesiophyte receives fixed N in exchange for transferring fixed carbon to UCYN-A. This unusual partnership between a cyanobacterium and a unicellular alga is a model for symbiosis and is analogous to plastid and organismal evolution, and if calcifying, may have important implications for past and present oceanic N_2 fixation.

Nitrogen (N) is a primary nutrient whose availability constrains the productivity of the biosphere (*1*). Some bacteria and archaea can fix N_2 into biologically available ammonium and are important in the N cycle of terrestrial ecosystems and the global ocean. Although photosynthetic carbon (C) fixation evolved in eukaryotes through endosymbiosis of cyanobacteria that resulted in the chloroplast, no N_2-fixing plastids or N_2-fixing eukaryotes are known. Nonetheless, N_2-fixing symbioses are common in terrestrial environments between bacteria or cyanobacteria and multicellular plants. In the oceans, there are microscopic observations of probable symbioses between N_2-fixing cyanobacteria and single-celled eukaryotic algae (*2*), although the nature of the interactions, if any, are unclear, except between the heterocystous N_2-fixing cyanobacteria and their associated diatoms (*3*).

Recently, a geographically widespread uncultivated diazotrophic cyanobacterium (UCYN-A) (*4*) was found to have an unusual degree of genomic streamlining suggestive of obligate symbiosis. The streamlined genome of UCYN-A (1.44 million base pairs) lacks photosystem II (PS II: the oxygen-evolving component of the photosynthetic apparatus), RuBisCo (ribulose-1,5-bisphosphate carboxylase-oxygenase that fixes CO_2), and the tricarboxylic acid cycle (TCA), features that usually define cyanobacteria (*5*, *6*). UCYN-A requires organic carbon for energy (although it may obtain some energy through cyclic photophosphorylation around PS I) and biosynthesis, as well as a number of specific amino acids and nucleotides (*5*, *6*). We propose the name *Candidatus* Atelocyanobacterium thalassa for UCYN-A. Dissolved organic carbon concentrations in the ocean are typically low, particularly for labile compounds such as glucose that UCYN-A would require (it has a complete gly-

[1]Ocean Sciences, University of California, Santa Cruz, CA 95064, USA. [2]Max-Planck-Institut für Marine Mikrobiologie, Bremen, Germany D-28359. [3]UPMC (Paris-06) and CNRS, UMR 7144, Station Biologique, Place G. Tessier 29680 Roscoff, France.

*These authors contributed equally to this work.
†Present address: Department of Isotope Biogeochemistry, UFZ–Helmholtz Centre for Environmental Research, Leipzig 04318, Germany.
‡To whom correspondence should be addressed. E-mail: zehrj@ucsc.edu

colysis pathway). Because UCYN-A has a complete suite of nitrogenase genes and related genes required for nitrogen fixation, it was hypothesized that UCYN-A provides fixed nitrogen in exchange for fixed carbon from a symbiotic partner (*5*, *7*).

We tested different possible partner phytoplankton populations in seawater samples from the North Pacific Ocean (Fig. 1, fig. S1, and table S1) for the presence of symbiotic UCYN-A by screening flow-cytometrically sorted cells with a UCYN-A–specific quantitative PCR (qPCR) assay for the nitrogenase gene (*nifH*) (*8*). The UCYN-A genome had been obtained with this approach (*6*), but the seawater was first concentrated by vacuum filtration before sorting, which dislodged the UCYN-A from their associated cells (fig. S1). Here, we used a similar flow sorting procedure, but instead, raw seawater that had not been preserved or concentrated was immediately sorted and resulted in detection of most (63 to 94%) of the UCYN-A *nifH* genes in the sorted photosynthetic picoeukaryote population (PPE) (1- to 3-μm-diameter cells) rather than other pigmented and nonpigmented cells (sorted populations displayed in Fig. 1). The data unequivocally showed that UCYN-A is associated with photosynthetic picoeukaryotic cells. These results explain the reports of UCYN-A *nifH* in filter-fractionated samples from the California Coast (0.8- to 3-μm and 3- to 200-μm fractions) (*9*) and Station ALOHA (1- to 3-μm fraction) (*5*). We now only observe an enriched population of free UCYN-A cells (0.2 to 1 μm) after seawater concentration by vacuum filtration, freezing for storage purposes, and resuspension in sterile seawater, which apparently disrupts the fragile association (fig. S1). UCYN-A appears to be in a loose extracellular association (epiphytic) that is easily dislodged, which explains why there is some amplification of UCYN-A *nifH* from outside the region of the sorted photosynthetic picoeukaryote population (table S1). This delicate association is similar to microscopic observations of other probable marine plankton symbioses, including the mixed populations of unicellular *Synechococcus*- and *Crocosphaera*-like unicellular cyanobacteria housed in the girdle of *Dinophysis* (dinoflagellates) (*10*).

The marine picoeukaryotic population defined by flow cytometry is extremely diverse (*11*–*13*). Therefore, to identify the specific cells associated with UCYN-A, we compared universal 18*S* ribosomal RNA (rRNA) and 16*S* rRNA gene clone libraries that were amplified from sorted samples of the entire picoeukaryote population to those from sorted single picoeukaryote cells (table S1). Single cells and the entire picoeukaryote population were initially screened for UCYN-A by *nifH* qPCR. As expected, the partial 18*S* rRNA gene sequences [~730 base pairs (bp)] derived from the entire picoeukaryote population sorts were diverse and included sequences from several classes of marine picoeukaryotes (Fig. 2 and table S3). 16*S* rRNA gene sequences amplified from the entire picoeukaryote population sorts were also diverse and confirmed the presence of UCYN-A in these populations (table S3). However, amplification of the 18*S* rRNA gene (using nested PCR) from single UCYN-A *nifH*-positive sorted picoeukaryote cells yielded exclusively prymnesiophyte sequences (Fig. 2 and table S4).

The partial 18*S* rRNA gene sequences [or "partner" sequences from the Ek555/1269 primer amplicon, GenBank accession nos. JX291679 to JX291804 and JX291547 to JX291678], derived from 12 single UCYN-A–*nifH*–positive picoeukaryotic cells, were greater than 99.5% identical to each other and had best BLASTn hits (>99% identical) to a sequence derived from sorted picoplankton from the oligotrophic South Pacific Ocean (GenBank accession no. FJ537341, BIOSOPE T60.34, sample T60, Station STB11, –107.29°E, –27.77°S) (*14*) (Fig. 2). A metagenome from sorted photosynthetic picoeukaryotes of the same sample (BIOSOPE, sample T60) also contained numerous DNA sequence reads (mean length of 340 bp) that were almost identical (99 to 100%) to the UCYN-A genome. Samples from an adjacent station (STB7, samples T39 and T40) contained neither good matches to the UCYN-A genome nor the partner partial 18*S* rRNA gene sequence we identified (table S2 and fig. S2). Assembly of the UCYN-A reads from sample T60 covered 12.4% of the UCYN-A genome (table S2), providing additional evidence that UCYN-A is associated with the picoeukaryotes and that the UCYN-A partner is the same in the oligotrophic North and South Pacific Oceans.

We examined the phylogeny of the full-length 18*S* rRNA gene of the BIOSOPE environmental sequence (T60.34) (UCYN-A partner sequence best BLASTn hit) relative to the diverse prymnesiophyte class (*11*, *15*, *16*). The BIOSOPE T60.34 sequence clustered with the calcareous nanoplankton *Braarudosphaera bigelowii* (*17*–*20*) and with *Chrysochromulina parkeae* (*21*, *22*), which may contain calcified scales as well (*23*) (Fig. 2). *B. bigelowii* appears to represent several pseudo-cryptic species that are all easily differentiated from other calcareous phytoplankton by their distinct pentagonal plates (*19*). Production of calcified plates by the UCYN-A partner is an intriguing possibility, because calcareous phytoplankton are important in the vertical flux of carbon and nitrogen in the oceans. Sedimentary records from the late Cretaceous show fossils of *Braarudosphaera* species in open ocean sediments (*24*, *25*), suggesting that the UCYN-A symbiosis could be ancient and could potentially be studied in a paleo-oceanographic context. However, prymnesiophytes (for example, *Emiliania huxleyi*) have complex life histories in which form (in particular calcification) and behavior change dramatically between haploid and diploid life stages [references in (*26*)]. Because the life-history stage of the partner cells in the natural populations of this study is unknown and sample processing could have dissolved or removed plates, whether or not the partner is calcifying could not be determined. Calcification of the partner cell could be an important facet in its symbiosis with UCYN-A, because it could provide a mechanism for stabilizing an extracellular association.

Prymnesiophytes are typically free-living and photosynthetic and therefore could provide organic C for an associated photoheterotroph like UCYN-A. To test this hypothesis, we applied a halogenated in situ hybridization nanometer-scale secondary ion mass spectrometry (HISH-SIMS) approach to natural phytoplankton populations

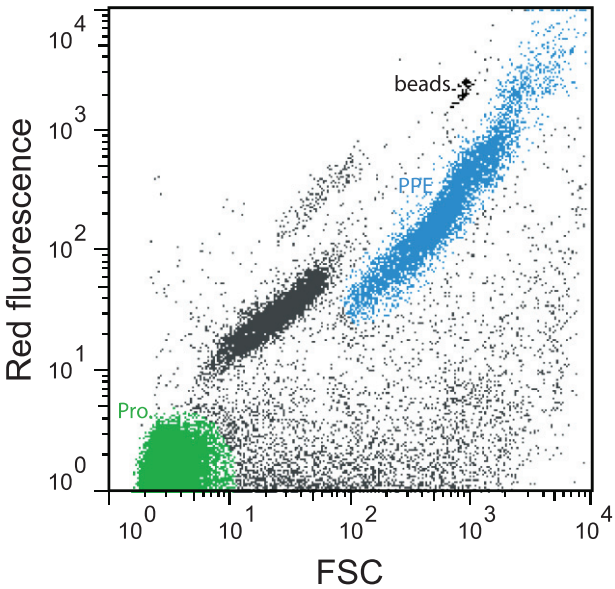

Fig. 1. Example flow cytogram of cell populations in unpreserved seawater that were targeted in this study. Red fluorescence is a measure of chlorophyll a concentration per cell. Forward scatter (FSC) is a proxy for cell size. Beads 3 μm in diameter (black) were used for reference. Cell populations indicated are photosynthetic picoeukaryotes (PPE, blue), *Prochlorococcus* (*Pro.*, green.), and cells (gray) that are not PPE or *Pro*. Coloring of each population indicates the sort gates used. Most UCYN-A *nifH* gene copies (63 to 94%) were amplified from the PPE population (table S1). Flow cytograms of all samples used in this study are presented in fig. S1.

from Station ALOHA (*27*) that were amended with $^{15}N_2$ and ^{13}C-bicarbonate ($H^{13}CO_3$) and incubated under in situ conditions. The photosynthetic picoeukaryote cells (diameter 1 to 3 μm) were subsequently sorted by flow cytometry, preserved, and processed for HISH-SIMS (*27*, *28*). A highly specific oligonucleotide probe for the UCYN-A 16*S* rRNA gene (UCYN-732) (*27*) confirmed the presence of 278 UCYN-A cells among the sorted photosynthetic picoeukaryote population. Most (163, 59%) of the UCYN-A cells (diameter 0.31 to 0.92 μm) remained associated with a larger partner cell (diameter 0.99 to 1.76 μm) during sample processing. UCYN-A cells were mainly observed at one end of the partner cell in what appeared to be an indentation (Fig. 3A). Numerous UCYN-A cells (107, 38%) were dislodged from their eukaryotic partners during HISH-SIMS sample processing (the cells were initially attached, otherwise they would not have been sorted by flow cytometry) and observed without an associated cell. Some (3%) of the UCYN-A cells identified by HISH were present as pairs located at opposite ends of a single partner cell (Fig. 3A). In other planktonic symbioses involving cyanobacteria (e.g., diatom symbionts with filamentous heterocyst-forming cyanobacteria), the cyanobacteria migrate to polar ends of the larger partner cells before cell division of the host (*29*). Similarly, the partner cells with multiple associated UCYN-A cells may have been dividing, because the incubation period was longer than a typical cell division cycle (36 hours). Measurements of scanning electron micrographs (SEMs) of individual *B. bigelowii* cells from enrichments of coastal waters show three size classes, the smallest of which corresponds

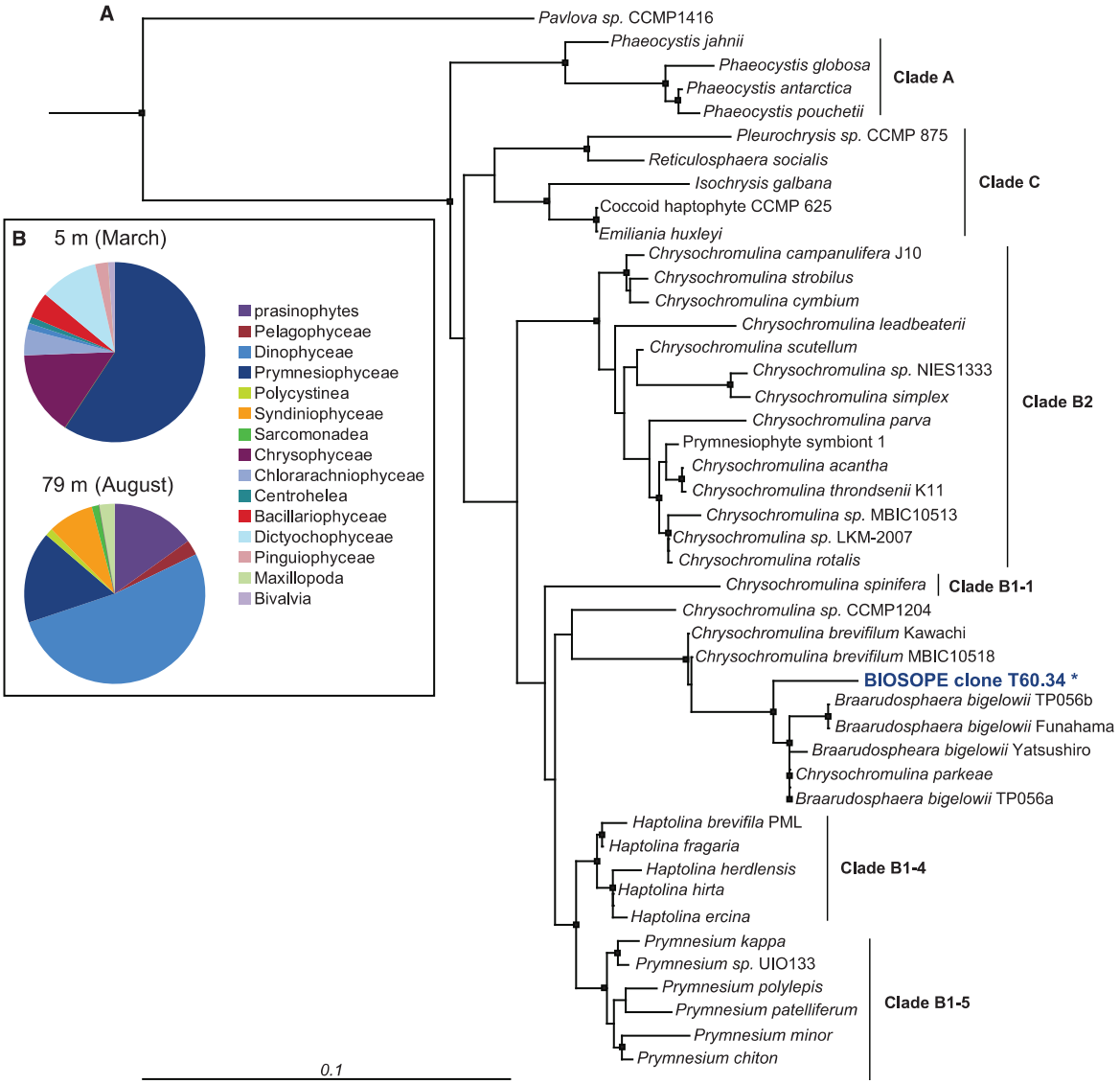

Fig. 2. Diversity and phylogeny of UCYN-A *nifH*-positive sorted picoeukaryote populations and single cells from 5-m and 79-m depths at Station ALOHA. (**A**) Maximum-likelihood tree (PhyML) of selected cultured prymnesiophyte 18*S* rRNA gene sequences with clade assignments and genus names per (*15*). "BIOSOPE T60.34" sequence (blue type and asterisk) is the best BLASTn hit of the UCYN-A partner sequence amplified from UCYN-A *nifH*-positive single photosynthetic picoeukaryotes. Node support greater than 75% is marked by black squares. (**B**) 18*S* rRNA gene diversity of the entire sorted picoeukaryote population that was the source of single cell sorts from March (5-m depth, cruise KM1110) and August (79-m depth, cruise HOT234) that were positive for UCYN-A *nifH* and the BIOSOPE T60.34 sequence.

to cell diameters of about 5 μm, which is larger than the UCYN-A partner cell measured here (*18*, *19*). If calcareous plates are present on the UCYN-A partner, loss of the plates during sample processing for HISH-SIMS may result in measurement of a smaller cell diameter than cells measured by SEM. Alternatively, the UCYN-A partner may represent an additional smaller-size class of *B. bigelowii* adapted to the oligotrophic ocean.

Ten partner cells and their associated UCYN-A cells were chosen for quantitative isotopic analysis with nanoSIMS. On average, $^{13}C/^{12}C$ enrichment was lower in the UCYN-A cells than in the partner cells (average ^{13}C atom % of 1.8139 and 2.4602, respectively; Fig. 3, B and C, and table S6). Because the UCYN-A genome does not contain carbon-fixation pathways (*5*, *6*), but photosynthetic picoeukaryotes do, we conclude that the ^{13}C enrichment in UCYN-A was due to transfer of fixed C from the eukaryotic partner. Both partner and UCYN-A were strongly ^{15}N-enriched (Fig. 3, C and D, and table S6). As only some bacteria and some archaea can fix N_2, our nanoSIMS data provide direct evidence for active N_2 fixation by the uncultivated UCYN-A. The average $^{15}N/^{14}N$ enrichment was higher in the partner cells than in the UCYN-A cells (average ^{15}N atom % of 1.5308 and 1.2081, respectively), showing that extensive amounts (we estimate up to 95%) of fixed N were transferred from UCYN-A to the partner cell. In contrast, little of the C (1 to 17%) fixed by the partner cell was transferred to the UCYN-A, consistent with the lower C requirements of a small slow-growing heterotrophic symbiont. The large fraction of N transferred to the partner is consistent with results from known symbioses, such as between heterocystous cyanobacteria and marine planktonic diatoms (*3*).

The symbiosis reported here is unusual in that it is a partnership between a prymnesiophyte and a unicellular cyanobacterium. The results provide an explanation for how the metabolically streamlined UCYN-A survives in the oligotrophic ocean, despite the lack of the TCA cycle, PS II, and some biosynthetic pathways. Tracer experiments using ^{15}N and ^{13}C clearly show that the cyanobacterium provides fixed N to the eukaryotic partner and conversely that C fixation by the eukaryotic partner can provide C to UCYN-A. Thus, the association appears to be at least a mutualistic and facultative, if not an obligate, association. It is still not known whether the cyanobacterium is an endosymbiont or lives on the surface of the prymnesiophyte. However, the sensitivity to disruption and the HISH-SIMS imaging indicates that it is a loose cell-surface association. Many of the dislodged cells observed after HISH-SIMS were located near a picoeukaryotic cell. Because *B. bigelowii*, the closest known relative of the sequence amplified from our single-cell sorts, has calcareous plates that are easily dislodged, it is conceivable that UCYN-A is somehow associated with these plates. Sample handling and processing, in particular the HISH assay, could have dislodged or dissolved the calcium carbonate plates, releasing UCYN-A.

The association of UCYN-A with prymnesiophytes suggests that N fixed by UCYN-A may enter the microbial loop through this group of relatively abundant and globally relevant primary producers and mixotrophs (*11*, *16*, *30*, *31*) and has other important implications. The UCYN-A partner may be calcifying, which has implications for the contributions of N_2-based new production to vertical carbon fluxes (*32*), the sensitivity of the UCYN-A partner to ocean acidification (*33*), and paleo-oceanographic microfossils in sediments. Equally interesting is the existence of a planktonic unicellular N_2-fixing symbiosis and its implications for evolution and adaptation. The presence of these simple interactions between single-celled organisms are reminiscent of those earlier primary endosymbiotic events and underscores the enigmatic absence of N_2-fixing plastids in evolution as N_2 fixation is an energetically expensive oxygen-sensitive reaction, and nitrogenase is an ancient enzyme. Thus, the UCYN-A association is a symbiosis with a prymnesiophyte and provides an intriguing model for the evolution of N_2 fixation, and the mutualistic interactions between planktonic microorganisms.

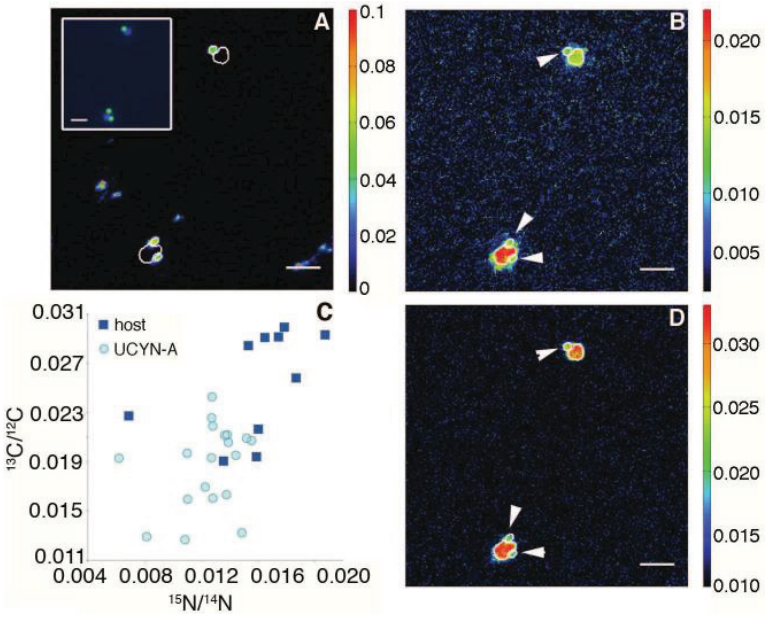

Fig. 3. Microscopy and elemental composition of two UCYN-A partner cells and their associated UCYN-A cells detected in samples from sorted picoeukaryotes analyzed by HISH-SIMS. (**A**) $^{19}F/^{12}C$ (HISH) labeling of UCYN-A. Inset displays labeling of the same UCYN-A cells by catalyzed reporter deposition—fluorescence in situ hybridization (green) and DAPI (4′,6-diamidino-2-phenylindole) staining of partner cell nucleus (blue). (**B**) The $^{13}C/^{12}C$ ratio image of UCYN-A and partner cell. (**C**) The $^{13}C/^{12}C$ and $^{15}N/^{14}N$ in 10 selected partner cells and their associated UCYN-A cells (table S6). (**D**) The $^{15}N/^{14}N$ image ratio of UCYN-A and partner cell. The white lines define regions of interest that were used for calculating $^{13}C/^{12}C$ and $^{15}N/^{14}N$ ratios. UCYN-A cells are indicated by white arrows in (B) and (D). Scale bar, 3 μm.

References and Notes

1. N. Gruber, J. N. Galloway, *Nature* **451**, 293 (2008).
2. E. J. Carpenter, R. A. Foster, in *Cyanobacteria in Symbiosis*, A. N. Rai, B. Bergman, U. Rasmussen, Eds. (Springer, Dordrecht, Netherlands, 2003), pp. 11–17.
3. R. A. Foster *et al.*, *ISME J.* **5**, 1484 (2011).
4. P. H. Moisander *et al.*, *Science* **327**, 1512 (2010).
5. H. J. Tripp *et al.*, *Nature* **464**, 90 (2010).
6. J. P. Zehr *et al.*, *Science* **322**, 1110 (2008).
7. H. Bothe, H. J. Tripp, J. P. Zehr, *Arch. Microbiol.* **192**, 783 (2010).
8. M. J. Church, C. M. Short, B. D. Jenkins, D. M. Karl, J. P. Zehr, *Appl. Environ. Microbiol.* **71**, 5362 (2005).
9. L. Z. Allen *et al.*, *ISME J.* **6**, 1403 (2012).
10. R. A. Foster, B. Bergman, E. J. Carpenter, *J. Phycol.* **42**, 453 (2006).
11. L. Jardillier, M. V. Zubkov, J. Pearman, D. J. Scanlan, *ISME J.* **4**, 1180 (2010).
12. S. Y. Moon-van der Staay, R. De Wachter, D. Vaulot, *Nature* **409**, 607 (2001).
13. D. Vaulot, W. Eikrem, M. Viprey, H. Moreau, *FEMS Microbiol. Rev.* **32**, 795 (2008).
14. X. L. Shi, D. Marie, L. Jardillier, D. J. Scanlan, D. Vaulot, *PLoS ONE* **4**, e7657 (2009).
15. B. Edvardsen *et al.*, *Eur. J. Phycol.* **46**, 202 (2011).
16. M. L. Cuvelier *et al.*, *Proc. Natl. Acad. Sci. U.S.A.* **107**, 14679 (2010).
17. H. H. Gran, T. Braarud, *J. Biol. Board Can.* **1**, 279 (1935).
18. K. Hagino, Y. Takano, T. Horiguchi, *Mar. Micropaleontol.* **72**, 210 (2009).
19. Y. Takano, K. Hagino, Y. Tanaka, T. Horiguchi, H. Okada, *Mar. Micropaleontol.* **60**, 145 (2006).
20. G. Deflandre, *C. R. Hebd. Seances Acad. Sci.* **225**, 439 (1947).
21. J. C. Green, B. S. C. Leadbeater, *J. Mar. Biol. Assoc. U. K.* **52**, 469 (1972).

22. L. K. Medlin, A. G. Sáez, J. R. Young, *Mar. Micropaleontol.* **67**, 69 (2008).
23. A. Sáez *et al.*, in *Coccolithophores: From Molecular Processes to Global Impact*, H. R. Y. Thierstein, J. R. Young, Eds. (Springer, Berlin, 2004), pp. 251–269.
24. P. R. Bown, J. A. Lees, J. R. Young, Eds., *Calcareous Nannoplankton Evolution and Diversity Through Time* (Springer, Berlin and Heidelberg, 2004), pp. 481–508.
25. W. G. Siesser, T. J. Bralower, E. H. Carlo, *Proc. Ocean Drill. Prog. Sci. Results* **122**, 653 (1992).
26. E. Paasche, *Phycologia* **40**, 503 (2001).
27. Materials and methods are available as supplementary materials on *Science* Online.
28. N. Musat *et al.*, *Proc. Natl. Acad. Sci. U.S.A.* **105**, 17861 (2008).
29. F. J. R. Taylor, *Ann. Inst. Oceanogr.* **58**, 61 (1982).
30. M. V. Zubkov, G. A. Tarran, *Nature* **455**, 224 (2008).
31. F. Unrein, R. Massana, L. Alonso-Sáez, J. M. Gasol, *Limnol. Oceanogr.* **52**, 456 (2007).
32. D. M. Karl, M. J. Church, J. E. Dore, R. M. Letelier, C. Mahaffey, *Proc. Natl. Acad. Sci. U.S.A.* **109**, 1842 (2012).
33. S. C. Doney, V. J. Fabry, R. A. Feely, J. A. Kleypas, *Annu. Rev. Mar. Sci.* **1**, 169 (2009).

Acknowledgments: D. Bottjer and M. Hogan provided advice for $^{15}N_2$ additions. Water samples were collected with the help of S. Curless, M. Church, S. Wilson, S. Tozzi, and the captain and crew of the research vessel *Kilo Moana*. On-board flow cytometry was made possible by K. Doggett and D. Karl. Funding was provided by the Gordon and Betty Moore Foundation (J.P.Z.) and the NSF Center for Microbial Oceanography: Research and Education (C-MORE). The Max Planck Society sponsored the HISH-SIMS analysis. We thank G. Lavik (Max Planck Institute, Bremen) for advice and suggestions for data analysis. J. Waterbury provided the scientific name for UCYN-A. D.V. was supported by PHYTOMETAGENE (JST-CNRS), METAPICO (Genoscope), and Micro B3 (funded by the European Union, contract 287589). BIOSOPE metagenome sequencing was performed at Genoscope (French National Sequencing Center) by J. Poulain. We thank H. Claustre, A. Sciandra, D. Marie, and all other BIOSOPE cruise participants. GenBank accession nos.: JX291679 to JX291804 and JX291547 to JX291678 (see table S4 for details).

Supplementary Materials

www.sciencemag.org/cgi/content/full/337/6101/1546/DC1
Materials and Methods
Figs. S1 and S2
Tables S1 to S6
References (*34*–*46*)

2 April 2012; accepted 20 July 2012
10.1126/science.1222700

2.1.1 Manuscript I: Supplementary Materials

www.sciencemag.org/cgi/content/full/337/6101/1546/DC1

Supplementary Materials for

Unicellular Cyanobacterium Symbiotic with a Single-Celled Eukaryotic Alga

Anne W. Thompson, Rachel A. Foster, Andreas Krupke, Brandon J. Carter, Niculina Musat Daniel Vaulot, Marcel M. M. Kuypers, Jonathan P. Zehr*

*To whom correspondence should be addressed. E-mail: zehrj@pmc.ucsc.edu

Published 21 September 2012, *Science* **337**, 1546 (2012)
DOI: 10.1126/science.1222700

This PDF file includes:

Materials and Methods
Figs. S1 and S2
Tables S1 to S6
References (*34–46*)

Figure S1: Flow cytograms and target cell populations for all samples used in this study. Red fluorescence is measured at 692-40 nm after excitation with a 488 nm laser and is a proxy for chlorophyll *a* content and forward scatter (FSC) is a proxy for cell size. All samples are unpreserved seawater except for (F), which is seawater concentrated 100X by vacuum filtration then preserved by freezing in liquid nitrogen for storage before analysis by flow cytometry. 3µm beads (B) were used for reference in some samples. Note the appearance of the dislodged UCYN-A (U) in the flow cytogram from concentrated seawater (F) and the absence of the UCYN-A population in un-concentrated water from the same sample (E). Other cell populations indicated are photosynthetic picoeukaryotes (PPE), *Synechococcus* (*Syn.*), and *Prochlorococcus* (*Pro.*). Light blue coloring indicates a greater density of events of a cell population. See Supplementary Table 1 for additional information on each sample and use in the experiments described in this study.

Figure S2: Presence of UCYN-A genome fragments in metagenomes prepared from sorted picoeukaryotes from three samples (T39, T41, and T60) from two stations (STB7 and STB11) from the South East Pacific Ocean (*14, 42*). Using BLASTN, numerous reads matching the UCYN-A genome at 99-100% similarity were found only at sample T60 (STB11) (Table S2). Notably, the partner 18S rRNA gene sequences were absent at Station STB7 and hits to the UCYN-A genome were relatively low (90-95% similar) with best hits to distantly related organisms such as *Cyanothece* and *Prochlorococcus* (Table S2).

Table S1: Sources, experiments conducted, and UCYN-A *nifH* quantification for samples utilized in this study. Experiments conducted: (A) UCYN-A *nifH* screens of sorted cell populations, (B) ^{15}N and ^{13}C incubations and HISH-SIMS, (C) 18S universal rRNA gene PCR from single and entire-population picoeukaryotes. Population abbreviations are *Prochlorococcus* (*Pro*) and photosynthetic picoeukaryotes (PPE).

Table S2: UCYN-A representation in metagenomes from sorted photosynthetic picoeukaryotes from two BIOSOPE stations.

Table S3: BLASTn hits of18S and 16S rRNA gene sequences derived from sorts of the entire picoeukaryote population from samples KM1110 (Accession numbers JX291805 - JX291865) (A) and HOT234 (Accession numbers JX291866 - JX291959) (B).

Table S4: Numbers and best BLASTn identity of 18S rRNA gene sequences derived from nested PCR of single *nifH*-positive picoeukaryotes from HOT234 and KM1110. Cruises are KM1110 (5 m March 2011, accession numbers JX291679 - JX291804) and HOT234 (79 m August 2011, accession numbers JX291547 - JX291678). Asterisk (*****) indicates the only marine species amplified. All others are suspected contaminants from terrestrial sources. Full species names are *Chrysochromulina acantha, Pinus armandii, Pinus luchuensis, Pinus morrisonicola, Lithocarpus rufovillosus, Ralstonia solanacearum, and Cunninghamia lanceolata.*

Table S5: The UCYN-732 and Helpers A and B oligonucleotide (5' to 3') shown with other closely related free-living and symbiotic cyanobacterial sequences. Mismatches are highlight in red.

Table S6: Summary of cell dimensions and nanoSIMS analyses for UCYN-A and partner cells measured by nanoSIMS.

1. *Environmental sampling:* Seawater samples were collected by 24-Niskin bottle CTD rosette at the hydrographic Station ALOHA in the North Pacific Ocean (*35*) during cruises KM1110 in March 2011 (25 meter depth), HOT234 (79 meter depth) in August 2011, and HOT239 (25 meter depth) in January 2012 and at a coastal site off the island of Hawai'i (20 2.047' N 155 57.394' W) on cruise KOK 11-15 (40 meter depth) in December 2011 (Table S1).

2. *Cell sorting:* All cell sorting was performed with a BD Biosciences Influx Cell Sorter equipped with a 488 nm laser (Sapphire Coherent), 70 µm diameter nozzle, and using BioSure Sheath fluid (BioSure, Grass Valley, CA USA) at 1X concentration. Sorting took place in a laboratory van equipped for flow cytometry either on board the ship (HOT234), on land directly following the cruise (KM1110), or on land following incubation in an on-deck flow-through seawater incubator and expedited shipping to California (HOT239 and KOK 11-15). All seawater samples were pre-filtered with a 50 µm filter (Partec Celltrics, Swedesboro, NJ USA) prior to sorting to prevent large particles from clogging the nozzle. Cells were sorted by gating on red fluorescence (692-40 nm) and forward scatter (FSC) using the BD cytometry software programs Spigot and FACS Sortware. The sort mode of "1.0 Drop Purity" was employed to ensure pure sorting of target populations. FlowJo (Tree Star, Ashland OR USA) was used to analyze cell counts and create dot plots (Fig. 1, Fig. S1).

3. *UCYN-A nifH screening of sorted cell populations:* Sorted cells were screened for UCYN-A nitrogenase (*nifH*) by qPCR using the UCYN-A-specific *nifH* primer/probe Taqman assay (Applied Biosystems, Carlsbad, CA USA) (*36*) for 45 cycles in 25 µL reactions. Three cell populations were screened for UCYN-A *nifH* including photosynthetic picoeukaryotes (PPE) (50-200 cells per sort replicate), *Prochlorococcus* (*Pro.*) (5,000 cells per sort replicate), and cells not PPE and not *Prochlorococcus* (at least 1,000 cells per replicate). At least four replicate sorts were analyzed by qPCR for each population and sample. Cells were sorted directly into Fast Step qPCR strips (Applied Biosystems) with 10 µL of 5 kD filtered water for direct use in qPCR following addition of the qPCR reagents on a StepOne qPCR machine (Applied Biosystems). No amplification of *nifH* in *Prochlorococcus* cell sorts indicated no *nifH* contamination of reagents or materials used. We relied on high temperatures in the first stages of qPCR to lyse cells rather than a DNA extraction step, which would have resulted in loss of material.

4. *Entire picoeukaryote population PCR with universal 18S/16S rRNA gene primers:* Sorts of the entire picoeukaryote population were carried out for each sample to assess the 18S and 16S rRNA gene diversity of the picoeukaryote population that was targeted in this study. Duplicate samples of 2500 cells (HOT234) and 500 cells (KM1110) were sorted into 10 µL 5 kD filtered water and amplified with 18S rRNA gene universal primers Ek555F and Ek1269R (*37*) in 50 µL reactions for 35 cycles using Platinum Taq reagents (Invitrogen, Grand Island, NY USA). PCR products were run on a 1% agarose gel for 90 minutes at 90V. Gel bands from approximately 500 bp and 700 bp positions were excised from the gel extracted using the QiaQuick Gel Extraction Kit (Qiagen).

   Purified PCR products were cloned using the pGEM-T Easy Kit (Promega, Madison, WI USA) following manufacturer's protocols and plasmid preps were performed using the Montage Plasmid MiniprepHTS Kit (Millipore, Billerica, MA USA). The UC Berkeley DNA Sequencing Facility (http://mcb.berkeley.edu/barker/dnaseq/) carried out Sanger sequencing. Sequences were checked for quality in Sequence Scanner (Applied Biosystems) and BLASTn was run against BLAST database nr (includes all GenBank, EMBL, DDBJ, and PDB sequences) in April 2011 to identify the sequences. Numerous 16S rRNA sequences (~500 bp) were picked up in addition to the 18S rRNA gene sequences (~730 bp) targeted by the primer set and these were included in analysis and confirmed the presence of UCYN-A in the photosynthetic picoeukaryote population (Table S3).

5. *UCYN-A nifH screening and nested PCR of single picoeukaryotes with 18S rRNA gene universal primers:* To identify the specific partner cell of UCYN-A (from the diverse picoeukaryote population) single picoeukaryotes from KM1110 (5 m) and HOT234 (79 m) were sorted into 10 µL of 5 kD water in 72

wells of 96-well qPCR plates. 24 wells were left empty for qPCR standards and no template controls (NTC). Plates were covered with AluminaSeal (Diversified Biotech, Dedham, MA USA) and stored at -80°C until processing. Whole plates were thawed at room temperature then screened for UCYN-A *nifH* as above.

Thirty single cell sorts with UCYN-A *nifH* gene copy of approximately 1 were selected for use in the nested PCR with 18S rRNA gene universal primers. The entire volume of the qPCR *nifH*-positive wells were used as template in 100 µL reactions with Platinum Taq reagents (Invitrogen). First, universal primers EukA/EukB (*38*) were applied for 35 cycles then 1 µL of the EukA/B PCR product used as template in 25 µL reactions with internal 18S rRNA gene primers 555F/1269R (*37*). Gel bands were extracted, purified, cloned (20-30 clones were picked for each single cell), and sequenced as above. For KM1110 samples, universal 16S rRNA gene primers (27F/1492R) and an internal unicellular diazotroph specific primer set (cya359F/nitro821R) (*39*) were applied to a subset of UCYN-A *nifH* positive single cells. All cya359F/nitro821R amplicons were identical to the UCYN-A 16S rRNA gene.

Sequences were compared to BLAST database nr (April 2011) by BLASTn for identification (Table S4). The great majority of sequences matched either the environmental prymnesiophyte clone from BIOSOPE T60.34 or *Pinus armandii* (Chinese White Pine). A few sequences matched other terrestrial tree species (Table S4). We believe the tree sequences are contaminants that are amplified when PCR template is in very low concentration (as in these single cell sorts) as no such tree sequences were derived from 18S rRNA gene clones libraries that were made from hundreds of sorted cells to assess the diversity of the entire picoeukaryote population (described above and Figure 2). Thus, we do not think they are an abundant sequence in our samples, but are due to reagent contamination acquired during sorting or PCR. To test this further, nested PCR with 18S rRNA gene universal primers (EukA/B) was applied to 5 kD-filtered water or *nifH*-negative cell sorts. *P. armandii* sequences were present only in the reactions made from the *nifH*-negative cell sorts, indicating that the pine sequences are a contaminant from sorting (likely in the sheath fluid or dust) rather than from PCR reagents. The only other marine sequence found in the 18S rRNA gene nested PCR sequences besides the BIOSOPE T60.34 sequence is from the prymnesiophyte *Chrysochromulina acantha.* This single sequence came from the clone library of one single cell sort from HOT234 that also contained *P.armandii* and BIOSOPE T60.34 sequences (sort ID 11D12,Table S4). Because we did not find this sequence in any other of the 30 single cell sorts, we presume that it is DNA contamination from the seawater sample amplified when template is in low concentration, rather than a specific associate of UCYN-A, as it did not appear in the clone library for the entire picoeukaryote population from samples HOT234 (Figure 2, Table S3).

6. *Prymnesiophyte 18S rRNA gene phylogeny*: Determining the phylogeny of the UCYN-A partner sequence was accomplished by constructing a tree of the full length 18S rRNA gene sequences of the UCYN-A partner best nucleotide hit (BIOSOPE T60.34, FJ537341, Uncultured *Chrysochromulina* clone) and selected cultured and environmental prymnesiophyte sequences (Fig. 2). Sequence alignments were created using SINA (v1.2.9) online with the SILVA SEED for the reference alignment (*40*). PhyML 3.0 was used to construct a maximum likelihood tree (*41*) using the HKY85 substitution model and bootstrapped with 100 replicates. Outgroups were chosen as in Cuvelier et al. (*16*) and included *Thalassiosira weissflogii* (AY485445), *Chlamydomonas reinhardtii* (AY665726), *Rhodomonas salina* (EU926158), *Compsopogon coeruleus* (AF342748), and *Chondrus crispus* (Z14140). Other species included in the tree (Fig. 2) are: *Pavlova sp.* CCMP1416 (AJ243369), *Phaeocystis globosa* (EU077556), *Phaeocystis pouchetii* isolate P360 (AF182114), *Phaeocystis antarctica* Karsten SK23 (X77481), *Phaeocystis jahnii* (AF163148), *Pleurochrysis sp.* CCMP 875 (AJ246265), *Reticulosphaera socialis* (X90992), Coccoid haptophyte CCMP 625 (U40924), *Isochrysis galbana* (ZJ246266), *Emiliania huxleyi* (AF184167), *Chrysochromulina campanulifera* strain J10 (AJ246273), *Chrysochromulina strobilus* (FN599060), *Chrysochromulina cymbium* (AM491018), *Chrysochromulina leadbeateri* (AM491017), *Chrysochromulina scutellum* (AJ246274), *Chrysochromulina sp.* NIES-1333 (DQ980478), *Chrysochromulina simplex* (AM491021), *Chrysochromulina parva* (AB601109), *Prymnesiophyte symbiont* 1 (AF166377), *Chrysochromulina acantha* strain T20 (AJ246278), *Chrysochromulina*

trondsenii K11 (AJ246279), *Chrysochromulina sp.* MBIC10513 (AB199882), *Chrysochromulina sp.* LKM-2007-1 (AM491020), *Chrysochromulina rotalis* (AM491025), *Chrysochromulina spinifera* (AB601108), *Chrysochromulina sp.* CCMP1204 (AM491016), *Chrysochromulina brevifilum* strain Kawachi (AM490995), *Chrysochromulina brevifilum* MBIC10518 (AB058358), *Chrysochromulina parkeae* (AM490994) , *Haptolina hirta*‡ (A5246272), *Haptolina ericina*‡ (AM491030), *Haptolina fragaria*‡ (AM491013), *Haptolina herdlensis*‡ (AM491011), *Haptolina brevifila PML* (AM491012), *Prymnesium chiton°* (AM491029), *Prymnesium minor°* (AM491010), *Prymnesium kappa°* (AJ246271), *Prymnesium polylepis°* (AJ004866), *Prymnesium* sp. UIO133, *Prymnesium patelliferum* (L34671), *Braarudosphaera bigelowii*, Funahama-T3 (AB478412), *Braarudosphaera bigelowii*, TP05-6-b (AB250785), *Braarudosphaera bigelowii*, TP05-6-a (AB250784), *Braarudosphaera bigelowii* Furue-15 (AB478413), *Braarudosphaera bigelowii* Yatsushiro-1 (AB478414), Genus names are changed to *Prymnesium* for species marked with (°) and to *Haptolina* for species marked with (‡) as in Edvardsen *et al.* (15) .

7. *Whole genome amplification of BIOSOPE sorted picoeukaryotes and comparison to UCYN-A genome:* Samples from Station B7 (STB7 - samples T39 and T40) and Station B11 (STB11- sample T60) were collected by tangential flow concentration, which is much less disruptive than other concentration methods, and cell sorting and DNA was extracted as described previously (*14*). Whole genome amplification was performed as described before (*42*). Each sample (T39, T40, and T60) was sequenced on a single 454 Titanium run (*34*). Raw reads were trimmed as described (*34*) and BLASTed (BLASTN) against the genome of UCYN-A (NC_013771) using a maximum e-value of e^{-100}. Raw reads were also mapped against the genome of UCYN-A using the software Geneious (http://www.geneious.com/) with the Medium-Low Sensitivity (Table S2).

8. *^{15}N and ^{13}C incubations, HISH-SIMS, calculations:* Seawater for isotope incubations was collected from 25 m during cruise KM1110 at Station ALOHA (22° 45'N, 158° 00'W). Water was pre-filtered through 10µm nylon mesh (Nitex 03-10/2) to remove larger diazotrophs (i.e. *Trichodesmium*, diatom-*Richelia* symbioses). *Crocosphaera nifH* and UCYN-A *nifH* gene abundances measured by qPCR were 5,752 and 183,569 copies L^{-1}, respectively. Water was dispensed into 4 acid-cleaned and sterile 500 mL polycarbonate bottles (Nalgene). Two bottles were left un-amended as controls and two bottles were amended with 125 µL of 500 mM ^{13}C-bicarbonate (Cambridge Isotopes, Andover, MA USA) and 1.5 mL $^{15}N_2$ (Cambridge Isotopes) at 21:00 hours. All bottles were shaken to dissolve the $^{15}N_2$ bubbles then were immediately placed in an on-deck incubator temperature-regulated by continuously flowing surface seawater and shaded to approximately 30% of photosynthetically active radiation (PAR) for 36-hours before processing by flow cytometry for HISH-SIMS measurements and filtration for bulk isotope measurements.

For HISH-SIMS analysis, 15,403 cells from the picoeukaryote sort region (Fig. S1) were sorted into separate tubes containing 2% paraformaldehyde (PFA) prepared in sterile-filtered seawater. After fixation for at least one hour at room temperature, sorted samples were divided into triplicates and applied by pipette to a small area (5 mm) marked by an ink circle in triplicate on gold-palladium sputtered 0.2 m filters. Gentle vacuum pressure (<5 psi) was used to draw the cells onto the filter. Cells on the filter were then rinsed with 1X Phosphate Buffered Saline (PBS) applied by pipette and gentle vacuum pressure, and allowed to dry. Filters were folded gently and placed into sterile microfuge tubes and stored at -20°C until further processing for the HISH-nanoSIMS.

A previously described HISH assay was applied to the PFA-fixed flow sorted picoeukaryote population samples with minor modifications (*28*). A highly specific oligonucleotide probe mixture and assay was developed based on the 16S rRNA gene of UCYN-A (CP001842 FJ170277). A mixture of a 5´-horseradish peroxidase (HRP)-labelled oligonucleotide UCYN-732 probe and helper A and B oligonucleotides were used and followed by the deposition of fluorine-containing tyramides (Oregon Green 488 dissolved in dimethylformamide containing 20 mg mL^{-1} 4-iodophenyl boronic acid) (Table

S6). Helper probes A and B (Table S5) were used to increase the accessibility and subsequent intensity of the UCYN-732 probe. A non-probe (NON338) (*43*) was used as a negative control.

The 5 mm ink-marked circles were excised with a knife and the cells were embedded in 0.1% low gelling point agarose to avoid cell loss. The cell wall was permeabilized at 37°C with a lysozyme solution (10 mg mL^{-1} in 0.05 M EDTA, pH 8.01, 0.1 M Tris-HCl, pH 7.5; Fluka, Taufkirchen, Germany). After permeabilization, filter samples were washed with ultrapure water (MQ, Millipore) and transferred to a 0.01 M HCl solution for 10 min at room temperature (RT) in order to bleach endogenous peroxidases. Hybridization conditions were as follows: 8.5 h at 35°C in a hybridization buffer containing: 0.9 M NaCl, 40 mM Tris-HCl (pH 7.5), 10 % dextran sulfate (wt/vol), 0.01 % (wt/vol) sodium dodecyl sulfate (SDS), 50% formamide (Fluka) (vol/vol), 10 % (wt/vol) Blocking Reagent (Boehringer, Mannheim, Germany), 1X Denhard's reagent, 0.26 mg mL^{-1} sheared salmon sperm DNA (Ambion), 0.2 mg mL^{-1} yeast RNA (Ambion). Post-hybridization, samples were incubated at 37°C for 15 min in pre-warmed (37°C) washing buffer containing 20 mM NaCl, 5 mM EDTA (pH 8.0), 20 mM Tris-HCl (pH 7.5), and 0.01 % SDS and subsequently transferred to 1X PBS (pH 7.6) for 20 min. Under dark conditions and at 46°C, a tyramide signal amplification (TSA) solution (5 % 20 x PBS; 2 M NaCl; 0.1 % blocking reagent; 10 % dextran sulfate; 0.0015 % (vol/vol) H_2O_2, 1 % Oregon Green 488 tyramide (Molecular Probes, Leiden, The Netherlands), 1 µL of tyramide solution) was applied to the samples for 20 min. Samples were rinsed twice at RT in 1X PBS (pH 7.6) and MQ water for 15 min each rinse. Cells were air dried, and stained with 1 µg mL^{-1} 4',6'-diamidino-2-phenylindole (DAPI) for 10 min at RT in the dark, then washed three times in MQ water and air dried. The total number of UCYN-A cells was enumerated on 2 of the 3 replicate samples prior to nanoSIMS analysis. All hybridized UCYN-A cells were counted as associated with partner cells or as dislodged. In addition, the partner cells, which were associated with 1, or 2 UCYN-A cells were further enumerated. For sample 1, 259 total UCYN-A cells were counted, with 83 (32%) UCYN-A cells dislodged, 166 (64%) UCYN-A cells were in association with 1 partner cell, and 5 partner cells (or 10 (4%) UCYN-A cells) were found with 2 UCYN-A cells attached. For sample two 278 UCYN-A cells were counted, and 107 (38 %) UCYN-A cells were dislodged, 163 (59 %) UCYN-A cells were in association with 1 partner cell, and 4 partner cells (or 8 (3%) UCYN-A cells) were found with 2 UCYN-A cells.

After enumeration, areas on the filter sections with UCYN-A cells were marked with arrows and numbers using a Laser Microdissection (LMD) Microscope 6500 (Leica, Berlin, Germany) fitted with appropriate filter set for the Oregon Green 488 tyramides (excitation max 498nm). Subsequently, the filters were mounted on a new glass slide coated with a 4:1 (v/v) embedding solution (low fluorescence glycerol mountant (Citifluor AF1, Citifluor Ldt, London, United Kingdom) and mounting fluid Vecta Shield (Vecta Laboratories, Burlingame, CA USA) and examined with an Axioplan II microscope (Carl Zeiss, Jena, Germany) fitted with the appropriate filter sets for the Oregon Green 488 tyramides and for DAPI (excitation max 390 nm). Microscopic pictures were taken and used for orientation purposes during subsequent nanoSIMS analysis and for post-processing using *look@nanosims* software (*44*).

NanoSIMS analysis was performed using a Cameca NanoSIMS 50L instrument. Ten individuals cells were analysed which were found in association with 1-2 UCYN-A cells, and 6 unattached UCYN-A cells were also measured. Analysis time, including tuning of detectors, was equivalent to 150h. Carbon (C), fluorine (F), nitrogen (as CN) and sulfur (S) isotopes (^{12}C, ^{13}C, ^{19}F, $^{12}C^{14}N$, $^{12}C^{15}N$ and ^{32}S) were measured simultaneously in raster imaging mode. Sample surfaces were rastered with a 16 keV Cesium (Cs^+) beam and a current between 25-35 pA. Primary ions were focused into a nominal ~50 nm spot diameter. The primary ion beam was used to raster the analyzed area with 2000 counts per pixel over the chosen raster size and a dwelling time of 1 or 3 ms per pixel. Areas ranged in size from 5 x 5 to 20 x 20 μm^2 depending on the distribution of the targeted cells (most areas were 10 x 10 μm^2). Negative secondary ions were collected simultaneously in electron multiplier detectors. Prior to analysis, the area was pre-sputtered for 1-2 min with a high-current Cs^+ beam to implant Cs and remove surface contaminants.

All scans were corrected for drift of the beam and sample stage after acquisition. Isotope ratio images were created as the ratio of a sum of total counts for each pixel over all recorded planes (40-100

planes) of the investigated isotope and the main isotope. Regions of interest (ROIs) around cell structures and cell diameter were manually circled and calculated using *look@nanosims* software (*44*).

The biovolume (V) of the UCYN-A and the associated cells were calculated according to the volume of a sphere:

$$V = (\pi/6) \times Ø^3 \quad (1)$$

where Ø is the cell diameter, and π is 3.14. The cell diameter was determined by the length of the ROI using the look@nanoSIMS software. As previously published (*45*), the carbon (C) content per cell was estimated by:

$$\text{Log [C]} = -0.363 + (0.863 \times \text{Log (V)} \quad (2)$$

The C content per cell (C_{con}) was converted into N content per cell (N_{con}) based on conversion factors provided by Tuit et al. (*46*) assuming a modified Redfield ratio (C:N) of 8.6. The C_{con} and N_{con} represent the initial C and N content. The isotopic ratios ($R_C = {}^{13}C/{}^{12}C$ and $R_N = {}^{15}N/{}^{14}N$) based on ROI selections and nanoSIMS analysis were used to calculate atom percent (AT %) enrichment of ^{13}C or ^{15}N by:

$$A_C = R_C/(1+R_C) \times 100 \quad (3)$$

$$A_N = R_N/(1+R_N) \times 100 \quad (4)$$

where A_C is the atom (AT) % ^{13}C and A_N is the AT % ^{15}N. The cell specific C and N_2 assimilation (F_C or F_N) was calculated for by:

$$F_C = ({}^{13}C_{ex} \times C_{con})/C_{SR} \quad (5)$$

$$F_N = ({}^{15}N_{ex} \times N_{con})/N_{SR} \quad (6)$$

where ${}^{13}C_{ex}$ and ${}^{15}N_{ex}$ are the ${}^{13}C/{}^{12}C$ and ${}^{15}N/{}^{14}N$ ratio of the individual ROIs corrected for by the mean ${}^{13}C/{}^{12}C$ and ${}^{15}N/{}^{14}N$ ratios in time zero samples divided by 100. The initial time zero ratios (${}^{13}C/{}^{12}C$ and ${}^{15}N/{}^{14}N$) were measured on bulk particulate samples (seawater collected onto a combusted GFF from the same depth of experiment) by a standard PDZ Europa ANCA-GSL elemental analyzer interfaced to a PDZ Europa 20-20 isotope ratio mass spectrometer (Sercon Ltd., Cheshire, UK). The bulk measurements were made at the stable isotope facility of University of California, Davis. The C_{SR} and N_{SR} are the calculated AT % of ^{13}C or ^{15}N in the experimental bottle and the C_{con} and N_{con} are described above (equation 2). The assimilated N or C was then divided by incubation time to determine cell-specific C and N_2 fixation rates. The percentage of fixed N transferred to the eukaryotic partners was determined by dividing the N assimilated into the associated cell as calculated above by the sum of N assimilated into the UCYN-A and the associated cell and multiplying by 100. Similarly, the percentage of C fixed and transferred to the UCYN-A cell was determined by dividing the C assimilated by UCYN-A as described above by the sum of C assimilated by the UCYN-A and the associated cell and multiplying by 100.

Table S1. Sample sources, experiments conducted, and UCYN-A *nifH* quantification for samples utilized in this study. Experiments conducted: (A) UCYN-A *nifH* screens of sorted cell populations, (B) ^{15}N and ^{13}C incubations and HISH-SIMS, (C) 18S universal rRNA gene PCR from single and entire-population picoeukaryotes. Population abbreviations are *Prochlorococcus* (Pro) and photosynthetic picoeukaryotes (PPE). 'NA' indicates the absence of quantitative measurements required for calculations.

Cruise	Date	Location	Depth	Experiments conducted	UCYN-A *nifH* detected in PPE?	%PPE with UCYN-A *nifH*	UCYN-A *nifH* gene copies per mL (PPE)	UCYN-A *nifH* gene copies per mL (*Pro*)	UCYN-A *nifH* gene copies per mL (not *Pro,* not PPE)	% Total UCYN-A *nifH* from PPE
KM1110	Mar-11	Station ALOHA	5m	(A), (C)	Yes	20.6±4.5	NA	NA	NA	NA
KM1110	Mar-11	Station ALOHA	25m	(A), (B)	Yes	NA	NA	NA	NA	NA
HOT234	Aug-11	Station ALOHA	79m	(A), (C)	Yes	109.8±34.0	1267.7(±392.1)	0	469.6(±354.6)	73.0
KOK 11-15	Dec-11	Coastal Hawai'i	40m	(A)	Yes	39.4±8.6	403.8(±88.4)	0	229.6(±81.0)	63.8
HOT239	Jan-12	Station ALOHA	25m	(A)	Yes	23.5±11.5	256.2(±125.8)	0	14.2(±14.0)	94.7

Table S2 : UCYN-A representation in metagenomes from sorted photosynthetic picoeukaryotes from two BIOSOPE stations.

Sample code	**T39**	**T41**	**T60**
Station	STB7	STB7	STB11
Longitude	-120.38	-120.38	-107.29
Latitude	-22.05	-22.05	-27.77
Depth	175	40	0
Number of reads	1,054,607	1,381,023	1,154,137
Number of reads matching UCYN-A genome			
- BLASTN hits P < e-100 and > 95% ID	0	1	730
Reads assembling to UCYN-A genome			
- Number of reads assembled	4	10	980
- % identity	90.8%	94.5%	99.7%
- genome coverage bp	444	820	178,405
- genome coverage %	0.0%	0.1%	12.4%

Table S3. BLASTn hits of18S and 16S rRNA gene sequences derived from sorts of the entire picoeukaryote population from samples KM1110 (Accession numbers JX291805 - JX291865) (A) and HOT234 (Accession numbers JX291866 - JX291959) (B).

(A) 18S rRNA gene hits

Cruise ID	Hit ID	Hit Description	# Hits	Category
KM1110	gb|AF290085.2|	Uncultured marine diatom 48-5-EKD54 18S ribosomal RNA gene partial sequence	4	Bacillariophyta
KM1110	gb|L33449.1	Mytilus californianus 18S small subunit ribosomal RNA gene complete sequence	1	Bivalvia
KM1110	gb|AY749516.1|	Uncultured eukaryote clone H30.5 18S ribosomal RNA gene partial sequence	1	Centrohelea
KM1110	gb|EF622558.1|	Chlorarachniophyceae sp. RCC337 small subunit ribosomal RNA gene partial sequence; nucleomorph	4	Chlorarachniophyceae
KM1110	gb|EF172998.1|	Uncultured eukaryote clone SSRPE02 18S ribosomal RNA gene partial sequence	2	Chrysophyceae
KM1110	gb|AY046860.1|	Uncultured eukaryote isolate C3_E031 18S ribosomal RNA gene partial sequence	4	Chrysophyceae
KM1110	gb|FJ537322.1|	Uncultured marine chrysophyte clone Biosope_T39.120 18S ribosomal RNA gene partial sequence	3	Chrysophyceae
KM1110	gb|FJ537350.1|	Uncultured marine chrysophyte clone Biosope_T65.146 18S ribosomal RNA gene partial sequence	2	Chrysophyceae
KM1110	gb|FJ537356.1|	Uncultured marine chrysophyte clone Biosope_T84.071 18S ribosomal RNA gene partial sequence	1	Chrysophyceae
KM1110	gb|AY129063.1|	Uncultured marine eukaryote clone UEPAC48p3 18S small subunit ribosomal RNA gene partial sequence	1	Chrysophyceae
KM1110	gb|EU247836.1|	Pedinellales sp. CCMP2098 18S ribosomal RNA gene partial sequence	3	Dictyochophyceae
KM1110	gb|EU500103.1|	Uncultured eukaryote clone hotxp1a10 18S ribosomal RNA gene partial sequence	1	Dictyochophyceae
KM1110	gb|AY426832.1|	Uncultured marine eukaryote clone BL000921.5 18S ribosomal RNA gene partial sequence	1	Dictyochophyceae
KM1110	gb|GQ344723.1|	Uncultured marine eukaryote clone cRFM1.39 18S ribosomal RNA gene partial sequence	**3**	Dictyochophyceae
KM1110	gb|GQ382424.1|	Uncultured marine eukaryote clone MO010_1.00340 18S ribosomal RNA gene partial sequence	1	Dictyochophyceae
KM1110	gb|EU780594.1|	Uncultured eukaryote clone AMT15_1B_25 18S ribosomal RNA gene partial sequence	1	Dinophyceae
KM1110	gb|EU106739.1|	Stramenopile sp. RCC853 18S ribosomal RNA gene partial sequence	1	Pinguiophyceae
KM1110	gb|GQ913175.1|	Uncultured eukaryote clone 111.2.81 18S ribosomal RNA gene partial sequence	1	Pinguiophyceae
KM1110	emb|AM491010.2|	Chrysochromulina minor partial 18S rRNA gene strain PLY 304	2	Prymnesiophyceae
KM1110	emb|AJ402351.1|	eukaryote clone OLI11056 18S rRNA gene	1	Prymnesiophyceae
KM1110	gb|FJ537341.1|	Uncultured Chrysochromulina clone Biosope_T60.034 18S ribosomal RNA gene partial sequence	37	Prymnesiophyceae
KM1110	gb|EF172993.1|	Uncultured eukaryote clone SSRPD92 18S ribosomal RNA gene partial sequence	1	Prymnesiophyceae
KM1110	gb|HM581630.1|	Uncultured marine eukaryote clone EN351CTD040_09Apr01_20m 18S small subunit ribosomal RNA gene partial sequence	2	Prymnesiophyceae
KM1110	gb|HM581628.1|	Uncultured marine eukaryote clone EN351CTD040_16_09Apr01_4m 18S small subunit ribosomal RNA gene partial sequence	5	Prymnesiophyceae
KM1110	gb|HM581603.1|	Uncultured marine eukaryote clone FS04R13_10_27Feb07_75m_sort 18S small subunit ribosomal RNA gene partial sequence	1	Prymnesiophyceae
KM1110	gb|EF539131.1|	Uncultured marine eukaryote clone MB07.26 18S ribosomal RNA gene partial sequence	1	Prymnesiophyceae
KM1110	gb|HM581615.1|	Uncultured marine eukaryote clone OC413BATS_P053_15m 18S small subunit ribosomal RNA gene partial sequence	1	Prymnesiophyceae

(A) 16S rRNA gene hits

Cruise ID	Hit ID	Hit Description	# Hits	Category
KM1110	gb|EF574323.1|	Uncultured bacterium clone S25_667 16S ribosomal RNA gene partial sequence	1	plastid (Bacillariophyceae)
KM1110	gb|EU394568.1|	Uncultured diatom clone PEACE2006/111_P3 16S ribosomal RNA gene partial sequence; chloroplast	1	plastid (Bacillariophyceae)
KM1110	gb|AY702151.1|	Dictyochophyte sp. RCC332 16S ribosomal RNA gene partial sequence; plastid	1	plastid (Dictyochophyceae)
KM1110	gb|GQ863844.1|	Uncultured eukaryote clone Ellett_IB4_32m_260 16S ribosomal RNA gene partial sequence; chloroplast	2	plastid (Dictyochophyceae)
KM1110	gb|FJ649290.1|	Uncultured phototrophic eukaryote clone STB11_25m_F8 16S ribosomal RNA gene partial sequence; chloroplast	2	plastid (Dictyochophyceae)
KM1110	gb|FJ649286.1|	Uncultured phototrophic eukaryote clone STB11_25m_E12 16S ribosomal RNA gene partial sequence; chloroplast	6	plastid (Dinophyceae)
KM1110	gb|GU119713.1|	Uncultured organism clone Gven_I11 16S ribosomal RNA gene partial sequence; chloroplast	4	plastid (Eustigmatophyceae)
KM1110	gb|HQ672102.1|	Uncultured bacterium clone F9P2610_S_H04 16S ribosomal RNA gene partial sequence	1	plastid (Pelagophyceae)
KM1110	gb|GQ863828.1|	Uncultured eukaryote clone Ellett_IB4_32m_102 16S ribosomal RNA gene partial sequence; chloroplast	1	plastid (Pelagophyceae)
KM1110	gb|FJ649259.1|	Uncultured phototrophic eukaryote clone UPW1_5m_B9 16S ribosomal RNA gene partial sequence; chloroplast	1	plastid (Prasinophyceae)
KM1110	gb|HQ672120.1|	Uncultured bacterium clone F9P2610_S_I09 16S ribosomal RNA gene partial sequence	1	plastid (Prymnesiophyceae)
KM1110	gb|EF574915.1|	Uncultured bacterium clone S25_1259 16S ribosomal RNA gene partial sequence	1	plastid (Prymnesiophyceae)
KM1110	gb|EF574086.1|	Uncultured bacterium clone S25_430 16S ribosomal RNA gene partial sequence	2	plastid (Prymnesiophyceae)
KM1110	gb|EF574441.1|	Uncultured bacterium clone S25_785 16S ribosomal RNA gene partial sequence	1	plastid (Prymnesiophyceae)
KM1110	gb|EF052026.1|	Uncultured haptophyte clone 250304-27 16S ribosomal RNA gene partial sequence; plastid	1	plastid (Prymnesiophyceae)
KM1110	gb|EF052003.1|	Uncultured haptophyte clone 250304-3 16S ribosomal RNA gene partial sequence; plastid	2	plastid (Prymnesiophyceae)
KM1110	gb|CP001068.1|	Ralstonia pickettii 12J chromosome 1 complete sequence	6	*Ralstonia pickettii*
KM1110	gb|CP001842.1|	Cyanobacterium UCYN-A complete genome	11	UCYN-A

Table S3. BLASTn hits of18S and 16S rRNA gene sequences derived from sorts of the entire picoeukaryote population from samples KM1110 (Accession numbers JX291805 - JX291865) (A) and HOT234 (Accession numbers JX291866 - JX291959) (B).

(B) 18S rRNA gene hits

Cruise ID	Hit ID	Hit Description	# Hits	Category
HOT234	gb|AY429070.1|	Uncultured dinoflagellate clone W159G6 18S ribosomal RNA gene partial sequence	1	Dinophyceae
HOT234	gb|AY664893.1|	Uncultured eukaryote clone SCM28C40 18S ribosomal RNA gene partial sequence	6	Dinophyceae
HOT234	gb|AY664957.1|	Uncultured eukaryote clone SCM15C83 18S ribosomal RNA gene partial sequence	1	Dinophyceae
HOT234	gb|AY664961.1|	Uncultured eukaryote clone SCM28C60 18S ribosomal RNA gene partial sequence	1	Dinophyceae
HOT234	gb|AY665023.1|	Uncultured eukaryote clone SCM27C47 18S ribosomal RNA gene partial sequence	1	Dinophyceae
HOT234	gb|DQ499645.1|	Lepidodinium viride 18S ribosomal RNA gene internal transcribed spacer	4	Dinophyceae
HOT234	gb|DQ504314.1|	Uncultured alveolate clone LC22_4EP_19 18S ribosomal RNA gene partial sequence	1	Dinophyceae
HOT234	gb|EU418969.1|	Dinophyceae sp. GD1590bp26 18S ribosomal RNA gene partial sequence	17	Dinophyceae
HOT234	gb|EU818044.1|	Uncultured marine alveolate clone ZZ0053262 18S ribosomal RNA gene partial sequence	1	Dinophyceae
HOT234	gb|EU818520.1|	Uncultured marine alveolate clone ZZ0053129 18S ribosomal RNA gene partial sequence	1	Dinophyceae
HOT234	gb|FJ914456.1|	Uncultured marine dinoflagellate clone S7 18S ribosomal RNA gene partial sequence	1	Dinophyceae
HOT234	gb|GQ382900.1|	Uncultured marine eukaryote clone MO010_42.00029 18S ribosomal RNA gene partial sequence	2	Dinophyceae
HOT234	gb|AY665124.1|	Uncultured eukaryote clone SCM27C27 18S ribosomal RNA gene partial sequence	6	Maxillopoda
HOT234	gb|AY749516.1|	Uncultured eukaryote clone H30.5 18S ribosomal RNA gene partial sequence	1	Maxillopoda
HOT234	gb|GU969200.1|	Clausocalanus furcatus 18S ribosomal RNA gene partial sequence	1	Maxillopoda
HOT234	gb|U40927.1|	Coccoid pelagophyte CCMP1395 nuclear 18S ribosomal RNA gene	2	Pelagophyceae
HOT234	gb|EU287795.1|	Uncultured marine Polycystinea clone OLI011-75m.50 18S ribosomal RNA gene partial sequence	1	Polycystinea
HOT234	gb|FJ537305.1|	Uncultured Prasinophyceae clone Biosope_T19.017 18S ribosomal RNA gene partial sequence	1	Prasinophyceae
HOT234	gb|FJ537318.1|	Uncultured Prasinophyceae clone Biosope_T39.095 18S ribosomal RNA gene partial sequence	2	Prasinophyceae
HOT234	gb|FJ537324.1|	Uncultured Prasinophyceae clone Biosope_T41.030 18S ribosomal RNA gene partial sequence	4	Prasinophyceae
HOT234	gb|FJ537325.1|	Uncultured Prasinophyceae clone Biosope_T41.051 18S ribosomal RNA gene partial sequence	1	Prasinophyceae
HOT234	gb|FJ537354.1|	Uncultured Prasinophyceae clone Biosope_T84.034 18S ribosomal RNA gene partial sequence	1	Prasinophyceae
HOT234	gb|HM474512.1|	Uncultured Prasinophyceae clone T41_W01D.032 18S ribosomal RNA gene partial sequence	1	Prasinophyceae
HOT234	gb|U40921.1|	Coccoid green alga CCMP1205 nuclear 18S ribosomal RNA gene	1	Prasinophyceae
HOT234	dbj|AB183618.1|	Emiliania sp. MBIC10582 gene for 18S rRNA partial sequence strain: MBIC10582	7	Prymnesiophyceae
HOT234	emb|AM490987.2|	Syracosphaera pulchra partial 18S rRNA gene strain ALGO GK 17	1	Prymnesiophyceae
HOT234	gb|FJ537341.1|	Uncultured Chrysochromulina clone Biosope_T60.034 18S ribosomal RNA gene partial sequence	4	Prymnesiophyceae
HOT234	gb|DQ314809.1|	Uncultured marine eukaryote clone NOR26.10 18S ribosomal RNA gene partial sequence	1	Sarcomonadea
HOT234	gb|EF172987.1|	Uncultured eukaryote clone SSRPD85 18S ribosomal RNA gene partial sequence	1	Syndiniophyceae
HOT234	gb|EF172989.1|	Uncultured eukaryote clone SSRPD87 18S ribosomal RNA gene partial sequence	1	Syndiniophyceae
HOT234	gb|EU793392.1|	Uncultured syndiniales clone PROSOPE.E5-55m.20 18S ribosomal RNA gene partial sequence	2	Syndiniophyceae
HOT234	gb|EU793689.1|	Uncultured syndiniales clone PROSOPE.ED-50m.193 18S ribosomal RNA gene partial sequence	1	Syndiniophyceae
HOT234	gb|EU793933.1|	Uncultured syndiniales clone PROSOPE.EM-5m.190 18S ribosomal RNA gene partial sequence	1	Syndiniophyceae

(B) 16S rRNA gene hits

Cruise ID	Hit ID	Hit Description	# Hits	Category
HOT234	gb|EF572495.1|	Uncultured bacterium clone S23_594 16S ribosomal RNA gene partial sequence	1	*Actinobacteria*
HOT234	gb|GU061498.1|	Uncultured bacterium clone CE1-DCM-27 16S ribosomal RNA gene partial sequence	1	*Actinobacteria*
HOT234	gb|DQ438491.1|	Uncultured bacterium clone ECS-P7-D55 16S ribosomal RNA gene partial sequence	2	plastid (Prasinophyceae)
HOT234	gb|AY702115.1|	Emiliania huxleyi strain CCMP625 16S ribosomal RNA gene partial sequence; plastid	1	plastid (Prymnesiophyceae)
HOT234	gb|EF052031.1|	Uncultured haptophyte clone 250304-32 16S ribosomal RNA gene partial sequence; plastid	1	plastid (Prymnesiophyceae)
HOT234	gb|EU802928.1|	Uncultured bacterium clone 4C230321 16S ribosomal RNA gene partial sequence	1	*Prochlorococcus*
HOT234	gb|EU804095.1|	Uncultured bacterium clone 6C231987 16S ribosomal RNA gene partial sequence	1	*Prochlorococcus*
HOT234	gb|EU805328.1|	Uncultured bacterium clone 6C233331 16S ribosomal RNA gene partial sequence	11	*Prochlorococcus*
HOT234	gb|GU061741.1|	Uncultured bacterium clone CEP-5m-43 16S ribosomal RNA gene partial sequence	1	*Prochlorococcus*
HOT234	gb|CP001842.1|	Cyanobacterium UCYN-A complete genome	1	UCYN-A

Table S4: Numbers and best BLASTn identity of 18S rRNA gene sequences derived from nested PCR of single *nifH*-positive picoeukaryotes from HOT234 and KM1110. Cruises are KM1110 (5 m March 2011, accession numbers JX291679 - JX291804) and HOT234 (79 m August 2011, accession numbers JX291547 - JX291678). Asterisk (*****) indicates the only marine species amplified. All others are suspected contaminants from terrestrial sources. Full species names are *Chrysochromulina acantha, Pinus armandii, Pinus luchuensis, Pinus morrisonicola, Lithocarpus rufovillosus, Ralstonia solanacearum, and Cunninghamia lanceolata*.

		Marine species		***Terrestrial species and suspected contaminants***								
Cruise	**Single Cell ID**	**BIOSOPE T60.34***	***C. acantha****	***P. armandii***	***P. luchuensis***	***P. morrisonicola***	***L. rufovillosus***	**environmental embryophyte**	***R. solanacearum***	***C. lanceolata***	**TOTAL sequences**	**Majority of sequences from each single cell**
KM1110	3	0	0	13	0	0	0	0	1	0	14	*P. armandii*
KM1110	4	0	0	14	0	0	0	0	0	0	14	*P. armandii*
KM1110	5	0	0	14	0	0	0	0	0	0	14	*P. armandii*
KM1110	6	12	0	1	1	0	0	0	0	0	14	Biosope_T60.034
KM1110	7	1	0	11	0	1	0	0	0	1	14	*P. armandii*
KM1110	8	0	0	14	0	0	0	0	0	0	14	*P. armandii*
KM1110	9	0	0	12	0	0	1	0	0	0	13	*P. armandii*
KM1110	10	0	0	12	0	1	1	0	0	0	14	*P. armandii*
KM1110	11	0	0	13	0	0	0	0	0	0	13	*P. armandii*
KM1110	12	17	0	0	0	0	0	0	0	0	17	Biosope_T60.034
KM1110	13	0	0	17	1	0	0	0	0	0	18	*P. armandii*
KM1110	14	0	0	16	1	1	0	0	0	0	18	*P. armandii*
KM1110	15	17	0	2	0	0	0	0	0	0	19	Biosope_T60.034
KM1110	16	18	0	1	0	0	0	0	0	0	19	Biosope_T60.034
KM1110	17	16	0	2	0	0	0	0	0	0	18	Biosope_T60.034
KM1110	18	18	0	0	0	0	0	0	0	0	18	Biosope_T60.034
KM1110	19	19	0	0	0	0	0	0	0	0	19	Biosope_T60.034
KM1110	20	0	0	19	0	0	0	0	0	0	19	*P. armandii*
KM1110	21	0	0	18	0	0	0	2	0	0	20	*P. armandii*
KM1110	22	20	0	0	0	0	0	0	0	0	20	Biosope_T60.034
HOT234	16E7	0	0	14	1	0	0	0	0	0	15	*P. armandii*
HOT234	11D12	5	1	11	0	0	0	0	0	0	17	*P. armandii*
HOT234	11D6	0	0	16	0	0	0	0	0	0	16	*P. armandii*
HOT234	16C10	7	0	3	0	1	0	0	0	0	11	Biosope_T60.034
HOT234	16C9	10	0	10	0	0	0	0	0	0	20	Biosope_T60.034
HOT234	16D11	0	0	8	0	0	0	0	0	0	8	*P. armandii*
HOT234	16F10	11	0	5	0	0	0	0	0	0	16	Biosope_T60.034
HOT234	11A9	0	0	15	1	1	1	0	0	0	18	*P. armandii*
HOT234	15F1	17	0	1	0	0	0	0	0	0	18	Biosope_T60.034
HOT234	16B2	13	0	14	0	0	0	0	0	0	27	*P. armandii*

Table S5. The UCYN-732 and Helpers A and B oligonucleotide (5’ to 3’) shown with other closely related free-living and symbiotic cyanobacterial sequences. Mismatches are highlighted in red.

	Helper A	UCYN-732	Helper B	
UCYN-A	5’ AGCTTTCGTCCCTGAGTGTCA	GTTACGGTCCAGTAGCAC	GCCTTCGCCACCGATGTT	3’
Cyanothece ATCC 51142	5’ AGCTTTCGTCCCTGAGTGTCA	GTTCCGGTCCAGTAGCGC	GCCTTCGCCACCGATGTT	3’
endosymbiont of *Climacodium frauenfeldianum*	5’ AGCTTTCGTCCCTGAGTGTCA	GTTTCGGTCCAGTAGCGC	GCCTTCGCCACCGATGTT	3’
endosymbiont of *Rhopalodia gibba*	5’ AGCTTTCGTCCCTGAGTGTCA	GTTCCGGCCCAGTAGCGC	GCTTTCGCCACCGATGTT	3’

Cell Type	Cell diameter (µm)	AT% ^{13}C	AT % ^{15}N
UCYN-A and partner			
Partner 1	1.47	2.8853	1.7218
UCYN-A	0.60	1.9108	1.0577
Partner 2	1.34	2.2014	0.6538
UCYN-A	0.71	1.8723	0.5854
Partner 3	1.35	2.4951	1.8019
UCYN-A	0.92	1.8752	1.2248
Partner 4	1.12	2.0990	1.5448
UCYN-A	0.52	2.0501	1.3155
Partner 5	1.22	2.8060	1.5893
UCYN-A	0.52	2.1220	1.2336
Partner 6	1.47	2.7436	1.4769
UCYN-A	0.79	2.3495	1.2287
Partner 7	1.65	2.8107	1.6822
UCYN-A	0.75	2.1861	1.2258
Partner 8	1.23	1.8838	1.5322
UCYN-A	0.31	1.2862	1.4322
UCYN-A	0.40	1.5864	1.3271
Partner 9	0.99	1.8501	1.3067
UCYN-A	0.45	1.2316	1.0430
UCYN-A	0.38	1.5583	1.2236
Partner 10	1.76	2.8268	1.9983
UCYN-A	0.76	1.9954	1.3398
UCYN-A	0.65	2.0280	1.4642
Dislodged UCYN-A			
UCYN-A	0.60	1.8954	1.3914
UCYN-A	0.69	1.6464	1.1809
UCYN-A	0.68	2.0098	1.4992
UCYN-A	0.86	2.0549	1.3330
UCYN-A	0.57	1.2560	0.7777
UCYN-A	0.56	1.5506	1.0606

Figure S1

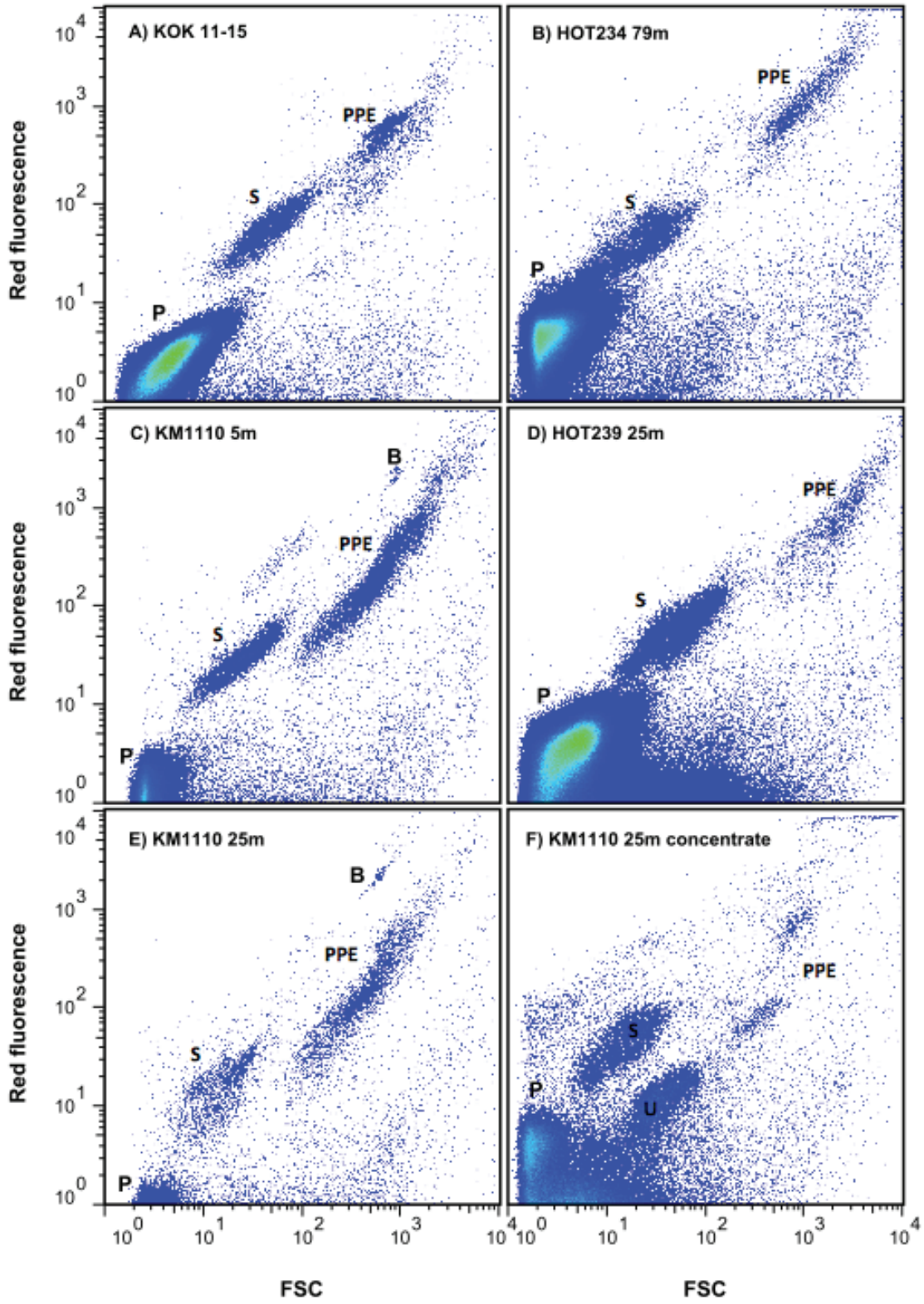
A) KOK 11-15
B) HOT234 79m
C) KM1110 5m
D) HOT239 25m
E) KM1110 25m
F) KM1110 25m concentrate
PPE
S
P
B
U
Red fluorescence
FSC
10^0
10^1
10^2
10^3
10^4

Figure S2

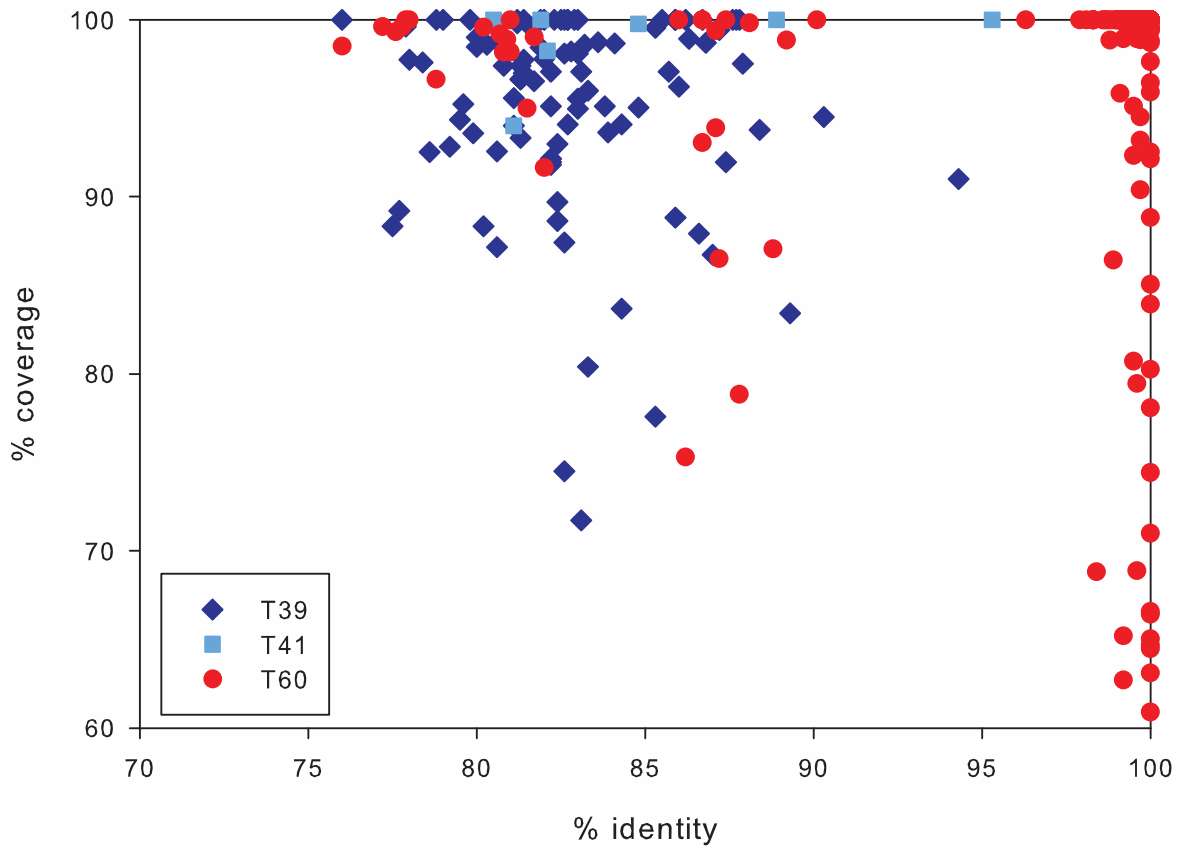
100
90
80
70
60
% coverage
70
75
80
85
90
95
100
% identity
T39
T41
T60

References and Notes

1. N. Gruber, J. N. Galloway, An Earth-system perspective of the global nitrogen cycle. *Nature* **451**, 293 (2008). doi:10.1038/nature06592 Medline

2. E. J. Carpenter, R. A. Foster, in *Cyanobacteria in Symbiosis*, A. N. Rai, B. Bergman, U. Rasmussen, Eds. (Springer, Netherlands, 2003), pp. 11–17.

3. R. A. Foster *et al*., Nitrogen fixation and transfer in open ocean diatom-cyanobacterial symbioses. *ISME J.* **5**, 1484 (2011). doi:10.1038/ismej.2011.26 Medline

4. P. H. Moisander *et al*., Unicellular cyanobacterial distributions broaden the oceanic N_2 fixation domain. *Science* **327**, 1512 (2010). doi:10.1126/science.1185468 Medline

5. H. J. Tripp *et al*., Metabolic streamlining in an open-ocean nitrogen-fixing cyanobacterium. *Nature* **464**, 90 (2010). doi:10.1038/nature08786 Medline

6. J. P. Zehr *et al*., Globally distributed uncultivated oceanic N_2-fixing cyanobacteria lack oxygenic photosystem II. *Science* **322**, 1110 (2008). doi:10.1126/science.1165340 Medline

7. H. Bothe, H. J. Tripp, J. P. Zehr, Unicellular cyanobacteria with a new mode of life: The lack of photosynthetic oxygen evolution allows nitrogen fixation to proceed. *Arch. Microbiol.* **192**, 783 (2010). doi:10.1007/s00203-010-0621-5 Medline

8. M. J. Church, C. M. Short, B. D. Jenkins, D. M. Karl, J. P. Zehr, Temporal patterns of nitrogenase gene (*nifH*) expression in the oligotrophic North Pacific Ocean. *Appl. Environ. Microbiol.* **71**, 5362 (2005). doi:10.1128/AEM.71.9.5362-5370.2005 Medline

9. L. Z. Allen *et al*., Influence of nutrients and currents on the genomic composition of microbes across an upwelling mosaic. *ISME J.* **6**, 1403 (2012). doi:10.1038/ismej.2011.201 Medline

10. R. A. Foster, E. J. Carpenter, B. Bergman, Unicellular cyanobionts in open ocean dinoflagellates, radiolarians, and tintinnids: Ultrastructural characterization and immunolocalization of phycoerythrin and nitrogenase. *J. Phycol.* **42**, 453 (2006). doi:10.1111/j.1529-8817.2006.00206.x

11. L. Jardillier, M. V. Zubkov, J. Pearman, D. J. Scanlan, Significant CO_2 fixation by small prymnesiophytes in the subtropical and tropical northeast Atlantic Ocean. *ISME J.* **4**, 1180 (2010). doi:10.1038/ismej.2010.36 Medline

12. S. Y. Moon-van der Staay, R. De Wachter, D. Vaulot, Oceanic 18S rDNA sequences from picoplankton reveal unsuspected eukaryotic diversity. *Nature* **409**, 607 (2001). doi:10.1038/35054541 Medline

13. D. Vaulot, W. Eikrem, M. Viprey, H. Moreau, The diversity of small eukaryotic phytoplankton (≤3 μm) in marine ecosystems. *FEMS Microbiol. Rev.* **32**, 795 (2008). doi:10.1111/j.1574-6976.2008.00121.x Medline

14. X. L. Shi, D. Marie, L. Jardillier, D. J. Scanlan, D. Vaulot, Groups without cultured representatives dominate eukaryotic picophytoplankton in the oligotrophic South East Pacific Ocean. *PLoS ONE* **4**, e7657 (2009). doi:10.1371/journal.pone.0007657 Medline

15. B. Edvardsen *et al*., Ribosomal DNA phylogenies and a morphological revision provide the basis for a revised taxonomy of the Prymnesiales (Haptophyta). *Eur. J. Phycol.* **46**, 202 (2011). doi:10.1080/09670262.2011.594095

16. M. L. Cuvelier *et al*., Targeted metagenomics and ecology of globally important uncultured eukaryotic phytoplankton. *Proc. Natl. Acad. Sci. U.S.A.* **107**, 14679 (2010). doi:10.1073/pnas.1001665107 Medline

17. H. H. Gran, T. Braarud, A quantitative study of the phytoplankton in the Bay of Fundy and the Gulf of Maine (including observations on hydrography, chemistry and turbidity). *J. Biol. Board Can.* **1**, 279 (1935). doi:10.1139/f35-012

18. K. Hagino, Y. Takano, T. Horiguchi, Pseudo-cryptic speciation in *Braarudosphaera bigelowii* (Gran and Braarud) Deflandre. *Mar. Micropaleontol.* **72**, 210 (2009). doi:10.1016/j.marmicro.2009.06.001

19. Y. Takano, K. Hagino, Y. Tanaka, T. Horiguchi, H. Okada, Phylogenetic affinities of an enigmatic nannoplankton, *Braarudosphaera bigelowii* based on the SSU rDNA sequences. *Mar. Micropaleontol.* **60**, 145 (2006). doi:10.1016/j.marmicro.2006.04.002

20. G. Deflandre, *C R Hebd. Seances Acad. Sci.* **225**, 439 (1947).

21. J. C. Green, B. S. C. Leadbeater, *Chrysochromulina Parkeae* Sp.Nov. [Haptophyceae] a New Species Recorded From S.W. England and Norway. *J. Mar. Biol. Assoc. U. K.* **52**, 469 (1972). doi:10.1017/S002531540001883X

22. L. K. Medlin, A. G. Sáez, J. R. Young, A molecular clock for coccolithophores and implications for selectivity of phytoplankton extinctions across the K/T boundary. *Mar. Micropaleontol.* **67**, 69 (2008). doi:10.1016/j.marmicro.2007.08.007

23. A. Sáez *et al*., in *Coccolithophores: From Molecular Processes to Global Impact*, H. R. Y. Thierstein, J. R. Young, Eds. (Springer, Berlin, 2004), pp. 251–269.

24. P. R. Bown, J. A. Lees, J. R. Young, Eds., *Calcareous Nannoplankton Evolution and Diversity Through Time* (Springer, Berlin and Heidelberg, 2004), pp. 481–508.

25. W. G. Siesser, T. J. Bralower, E. H. Carlo, *Proc. Ocean Drill. Prog. Sci. Results* **122**, 653 (1992).

26. E. Paasche, A review of the coccolithophorid *Emiliania huxleyi* (Prymnesiophyceae), with particular reference to growth, coccolith formation, and calcification-photosynthesis interactions. *Phycologia* **40**, 503 (2001). doi:10.2216/i0031-8884-40-6-503.1

27. Materials and methods are available as supplementary materials on *Science* Online.

28. N. Musat *et al*., A single-cell view on the ecophysiology of anaerobic phototrophic bacteria. *Proc. Natl. Acad. Sci. U.S.A.* **105**, 17861 (2008). doi:10.1073/pnas.0809329105 Medline

29. F. J. R. Taylor, *Ann. Inst. Oceanogr.* **58**, 61 (1982).

30. M. V. Zubkov, G. A. Tarran, High bacterivory by the smallest phytoplankton in the North Atlantic Ocean. *Nature* **455**, 224 (2008). doi:10.1038/nature07236 Medline

31. F. Unrein, R. Massana, L. Alonso-Sáez, J. M. Gasol, Significant year-round effect of small mixotrophic flagellates on bacterioplankton in an oligotrophic coastal system. *Limnol. Oceanogr.* **52**, 456 (2007). doi:10.4319/lo.2007.52.1.0456

32. D. M. Karl, M. J. Church, J. E. Dore, R. M. Letelier, C. Mahaffey, Predictable and efficient carbon sequestration in the North Pacific Ocean supported by symbiotic nitrogen fixation. *Proc. Natl. Acad. Sci. U.S.A.* **109**, 1842 (2012). doi:10.1073/pnas.1120312109 Medline

33. S. C. Doney, V. J. Fabry, R. A. Feely, J. A. Kleypas, Ocean acidification: The other CO_2 Problem. *Annu. Rev. Mar. Sci.* **1**, 169 (2009). doi:10.1146/annurev.marine.010908.163834

34. D. Vaulot *et al.*, Metagenomes of the picoalga bathycoccus from the Chile Coastal Upwelling. *PLoS ONE* **7**, e39648 (2012). doi:10.1371/journal.pone.0039648 Medline

35. D. M. Karl, R. Lukas, The Hawaii Ocean Time-series (HOT) program: Background, rationale and field implementation. *Deep Sea Res. Part II Top. Stud. Oceanogr.* **43**, 129 (1996). doi:10.1016/0967-0645(96)00005-7

36. M. J. Church, B. D. Jenkins, D. M. Karl, J. P. Zehr, Vertical distributions of nitrogen-fixing phylotypes at Stn Aloha in the oligotrophic North Pacific Ocean. *Aquat. Microb. Ecol.* **38**, 3 (2005). doi:10.3354/ame038003

37. P. López-García, H. Philippe, F. Gail, D. Moreira, Autochthonous eukaryotic diversity in hydrothermal sediment and experimental microcolonizers at the Mid-Atlantic Ridge. *Proc. Natl. Acad. Sci. U.S.A.* **100**, 697 (2003). doi:10.1073/pnas.0235779100 Medline

38. L. Medlin, H. J. Elwood, S. Stickel, M. L. Sogin, The characterization of enzymatically amplified eukaryotic 16S-like rRNA-coding regions. *Gene* **71**, 491 (1988). doi:10.1016/0378-1119(88)90066-2 Medline

39. S. L. Mazard, N. J. Fuller, K. M. Orcutt, O. Bridle, D. J. Scanlan, PCR analysis of the distribution of unicellular cyanobacterial diazotrophs in the Arabian Sea. *Appl. Environ. Microbiol.* **70**, 7355 (2004). doi:10.1128/AEM.70.12.7355-7364.2004 Medline

40. E. Pruesse *et al.*, SILVA: A comprehensive online resource for quality checked and aligned ribosomal RNA sequence data compatible with ARB. *Nucleic Acids Res.* **35**, 7188 (2007). doi:10.1093/nar/gkm864 Medline

41. S. Guindon, F. Lethiec, P. Duroux, O. Gascuel, PHYML Online—a web server for fast maximum likelihood-based phylogenetic inference. *Nucleic Acids Res.* **33** (Web Server issue), W557 (2005). doi:10.1093/nar/gki352 Medline

42. C. Lepère, D. Vaulot, D. J. Scanlan, Photosynthetic picoeukaryote community structure in the South East Pacific Ocean encompassing the most oligotrophic waters on Earth. *Environ. Microbiol.* **11**, 3105 (2009). doi:10.1111/j.1462-2920.2009.02015.x Medline

43. G. Wallner, R. Amann, W. Beisker, Optimizing fluorescent in situ hybridization with rRNA-targeted oligonucleotide probes for flow cytometric identification of microorganisms. *Cytometry* **14**, 136 (1993). doi:10.1002/cyto.990140205 Medline

44. L. Polerecky *et al.*, Look@NanoSIMS—a tool for the analysis of nanoSIMS data in environmental microbiology. *Environ. Microbiol.* **14**, 1009 (2012). doi:10.1111/j.1462-2920.2011.02681.x Medline

45. P. G. Verity *et al.*, Relationships between cell volume and the carbon and nitrogen content of marine photosynthetic nanoplankton. *Limnol. Oceanogr.* **37**, 1434 (1992). doi:10.4319/lo.1992.37.7.1434

46. C. Tuit, J. Waterbury, G. Ravizza, Diel variation of molybdenum and iron in marine diazotrophic cyanobacteria. *Limnol. Oceanogr.* **49**, 978 (2004). doi:10.4319/lo.2004.49.4.0978

2.2 Manuscript II: *In situ* identification and N_2 and C fixation rates of uncultivated cyanobacteria populations

Andreas Krupke[a,1], Niculina Musat[a,1,2], Julie LaRoche[b,3], Wiebke Mohr[b,4], Bernhard M. Fuchs[a], Rudolf I. Amann[a], Marcel M.M. Kuypers[a], Rachel A. Foster[a,*]

[a] Max Planck Institute for Marine Microbiology, Bremen D-28359, Germany

[b] Marine Biogeochemie, Helmholtz Center for Ocean Research (GEOMAR), Kiel 24105, Germany

* Corresponding author: Rachel Foster, Department of Biogeochemistry, Max Planck Institute for Marine Microbiology, Celsiusstr. 1, 28359 Bremen, Germany
E-mail address: rfoster@mpi-bremen.de (R.A. Foster)

[1]Contributed equally.

[2]Current address: Department of Isotope Biogeochemistry Helmholtz Centre for Environmental Research – UFZ Permoserstraße 15, Leipzig 04318, Germany.

[3]Current address: Biology Department, Dalhousie University, Halifax Nova Scotia, B3H4R2, Canada

[4]Current address: Harvard University, Department of Earth and Planetary Sciences, 20 Oxford Street, Cambridge, MA 02138, USA.

Systematic and Applied Microbiology 36 (2013) 259–271

Contents lists available at SciVerse ScienceDirect

Systematic and Applied Microbiology

journal homepage: www.elsevier.de/syapm

In situ identification and N_2 and C fixation rates of uncultivated cyanobacteria populations

Andreas Krupke[a,1], Niculina Musat[a,1,2], Julie LaRoche[b,3], Wiebke Mohr[b,4], Bernhard M. Fuchs[a], Rudolf I. Amann[a], Marcel M.M. Kuypers[a], Rachel A. Foster[a,*]

[a] Max Planck Institute for Marine Microbiology, Bremen D-28359, Germany
[b] Marine Biogeochemie, Helmholtz Center for Ocean Research (GEOMAR), Kiel 24105, Germany

ARTICLE INFO

Article history:
Received 29 October 2012
Received in revised form 12 February 2013
Accepted 15 February 2013

Keywords:
N_2 fixation
UCYN-A
UCYN-B
CARD-FISH
HISH-SIMS
nanoSIMS
Cyanobacteria

ABSTRACT

Nitrogen (N_2) fixation is a globally important process often mediated by diazotrophic cyanobacteria in the open ocean. In 2010, seawater was collected near Cape Verde to identify and measure N_2 and carbon (C) fixation by unicellular diazotrophic cyanobacteria. The *nifH* gene abundance (10^4–10^6 *nifH* L^{-1}) and *nifH* gene transcript abundance (10^2–10^4 cDNA *nifH* L^{-1}) for two unicellular groups, UCYN-A and UCYN-B, were detected. UCYN-A was also identified and quantified (10^4–10^5 cells L^{-1}) by new probes (UCYN-A732 and UCYN-A159) using Catalyzed Reporter Deposition-Fluorescence In Situ Hybridization (CARD-FISH) assays. The UCYN-A were observed as free cells or attached to a larger unidentified eukaryotic cell. A Halogen In Situ Hybridization-Secondary Ion Mass Spectrometry (HISH-SIMS) assay using the UCYN-A732 probe was applied on samples previously incubated with ^{13}C-bicarbonate and $^{15}N_2$. Free UCYN-A cells were enriched in both ^{13}C and ^{15}N and estimated C and N_2 fixation rates for UCYN-A were lower compared to co-occurring unicellular cyanobacteria cells similar in size (3.1–5.6 μm) and pigmentation to diazotroph *Crocosphaera watsonii*. Here, we identify and quantify two common co-occurring unicellular groups and measure their cellular activities by nanoSIMS.

© 2013 Elsevier GmbH. All rights reserved.

Introduction

A large fraction (80%) of the Earth's atmosphere is composed of di-nitrogen gas (N_2), yet only a few microorganisms are capable of converting N_2 into bio-available nitrogen (N) [28,73]. Since dissolved inorganic nitrogen (DIN) is often considered the major limiting nutrient in many open ocean environments [26,52], N_2 fixation is an important new source of N that alleviates N limitation in the upper water column [8,28]. The biological conversion of N_2 to ammonia (NH_3) is catalyzed by the nitrogenase enzyme complex in a small and diverse group of microorganisms commonly referred to as diazotrophs [71]. Advancements in culture-independent techniques coupled to high throughput quantitative assays and genome sequencing efforts have provided new insights on the diversity, distribution, and activity of diazotrophic microorganisms.

Several widely distributed cyanobacteria populations, such as the filamentous non-heterocystous *Trichodesmium* spp. and the heterocystous diatom symbiont *Richelia intracellularis* are most often considered the dominant N_2 fixers in open ocean habitats [7,33]. However, more recent work indicates that the smaller size fraction (<10 μm) of diazotrophs, which is comprised of co-occurring archaeal and bacterial lineages including heterotrophic and photoheterotrophic bacteria, and unicellular cyanobacterial populations are an equally important component of the diazotrophic community [25,38,39,70,73]. Both UCYN-A and UCYN-B are unicellular cyanobacteria groups, which have been identified by the presence of their *nifH* gene, which encodes for the nitrogenase enzyme complex [73]. On the basis of *nifH* phylogenetic studies, the unicellular diazotroph *Crocosphaera watsonii* is the closest relative and only cultured representative in the UCYN-B phylogeny [73]. UCYN-A was recently identified as symbiotic with a single-celled eukaryotic alga (Prymnesiophyte) [57]. UCYN-A and UCYN-B can co-occur but differ greatly with respect to distribution in the water column, cell diameter, the time of day when *nifH* transcript abundance is highest and the content of their genomes [3,38,64,68,72].

Despite a wide distribution and abundance of UCYN-A *nifH* gene copies, as well as UCYN-A *nifH* gene transcripts [11,29,32,38], UCYN-A has evaded isolation, and therefore we know very little

* Corresponding author at: Department of Biogeochemistry, Max Planck Institute for Marine Microbiology, Celsiusstr. 1, D-28359 Bremen, Germany.
Tel.: +49 421 2028 655.
E-mail address: rfoster@mpi-bremen.de (R.A. Foster).

[1] Contributed equally.
[2] Current address: Department of Isotope Biogeochemistry Helmholtz Centre for Environmental Research – UFZ Permoserstraße 15, Leipzig 04318, Germany.
[3] Current address: Biology Department, Dalhousie University, Halifax Nova Scotia, Canada, B3H4R2.
[4] Current address: Harvard University, Department of Earth and Planetary Sciences, 20 Oxford Street, Cambridge, MA 02138, USA.

0723-2020/$ – see front matter © 2013 Elsevier GmbH. All rights reserved.
http://dx.doi.org/10.1016/j.syapm.2013.02.002

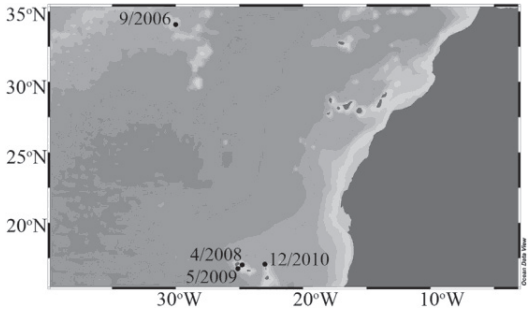

Fig. 1. Map of sampling locations in the subtropical North Atlantic Ocean. Incubation experiments were performed on surface seawater samples collected in December 2010.

about its metabolism and contribution to the C and N cycles. More is known of UCYN-B because10 different strains of *C. watsonii* have been isolated from the open ocean allowing laboratory and genome comparison studies [64,69]. Yet little is known of their activity in the environment since single cell measurements have not been possible until recently. Thus, the primary objective of this study was to make single cell measurements of UCYN-A and UCYN-B populations as they represent an important component of the smaller size fraction of diazotrophs.

Here we describe a new Catalyzed Reporter Deposition-Fluorescence In Situ Hybridization (CARD-FISH) assay highly specific for UCYN-A, which was applied to multiple samples from distant locations in the subtropical North Atlantic. Cells, similar in size and pigmentation to *C. watsonii* (hereafter referred to as *Crocosphaera*-like) were observed and easily identified by standard epifluoresence microscopy. Standard qPCR assays for *nifH* abundance and *nifH* transcript abundance were used to initially screen for the presence and potential nitrogenase activity of both UCYN-A and UCYN-B. The CARD-FISH assay was then used in combination with stable isotope labelling experiments and high-resolution nanometer scale secondary ion mass spectrometry (nanoSIMS) to simultaneously identify UCYN-A cells and to directly measure their metabolic activity. Similarly we measured the N_2 and C fixation for the individual *Crocosphaera*-like cells identified by microscopy using nanoSIMS. We focused on the two unicellular populations that have attracted attention due to their potential importance in the global N and C budgets. A field site in the subtropical North Atlantic near the Cape Verdean (CV) Islands was chosen for experimentation since the site was easily accessible and both UCYN-A and UCYN-B are common year round (LaRoche, unpublished results).

Materials and methods

Sampling sites

Our primary study site was a field location (16.76 N, 25.12 W) near Sao Vicente, Cape Verde (CV). We sampled in December 2010 from the fishing vessel Syngoga (Fig. 1). Surface seawater was collected using 5 L buckets lowered by hand to the surface (0–1 m) and in addition we collected samples from depth (30 and 60 m) using a GO-FLO bottle (General Oceanics, Miami, FL, USA). The near surface seawater from CV was sampled for bottle incubations, nucleic acid samples, and CARD-FISH samples; the samples from depth were limited in volume (10 L) and therefore collections were limited to CARD-FISH and DNA samples.

Additional CARD-FISH samples were collected earlier in 2006, 2008 and 2009 in other locations of the subtropical North Atlantic (Fig. 1, Supplementary Table 1). In September 2006, 500 mL of seawater was collected from 30 m using a conductivity-temperature-depth (CTD) sampler at station 18 (34.07 N, 30.00 W) of the Vision cruise. In April 2008 seawater was collected during the MSM 08/1 cruise from 10 m depth using a CTD sampler at station 7 (17.08 N 23.00 W). In May 2009, 4.5 L of seawater was sampled from the surface near the CV site (17.03 N, 24.78 W) using a trace metal clean sampler.

N_2 and C fixation

Rates of N_2 fixation were measured with the $^{15}N_2$ label method [40] and primary production was measured simultaneously by adding 4% of the ambient TCO_2 as 98% ^{13}C-labelled bicarbonate. Three replicate experiments were performed in December 2010 where 4 replicate light transparent, acid washed 2.75 L polycarbonate bottles were filled with surface seawater from CV. Three bottles were used for whole water analysis and the 4th replicate for nanoSIMS analysis.

The bottles were filled without air bubbles, closed with caps fitted with septa and kept in coolers until returned to the laboratory (within 2 h of collection). At the laboratory, 250 μL of 500 mM ^{13}C (98% + $^{13}CO_2$, Sigma–Aldrich, St. Louis, MO, USA) bicarbonate ($^{13}HCO_3^-$) solution and the tracer $^{15}N_2$ (98% $^{15}N_2$, Sigma–Aldrich) was added to each 2.75 L incubation bottle (1.5 mL, or 5.4% of ambient N_2) with gas tight syringes. The time of injection for experiments 1–3 was between 9:30 and 10:00 AM and each experiment had 3 incubation periods: time 0 (0 h), 1 (7.5–12.1 h) and 2 (19.6–22.2 h). The incubation periods 1 and 2 corresponded approximately to sunset and sunrise, respectively. After amendment with isotopes, the bottles were inverted several times and placed on their sides in an incubator with continuously flowing surface seawater and shaded to 25% surface irradiance. The temperature was checked during the incubation (4–5 times) and fluctuated by +/− 2 °C. After each incubation period (0–2), 3 bottles were filtered for whole water analysis using a peristaltic pump (Cole-Parmer, Vernon Hills, IL, USA) onto pre-combusted 25 mm diameter Glass Fiber Filters (Whatman GF/F; Sigma–Aldrich) held in a swinnex filter holder. The GF/F filters were freeze-dried over night, acid–fumed (37% HCl) for 24 h in a desiccator, and packaged for combustion analysis. Carbon (C) and nitrogen (N) content was analysed by an automated elemental analyser (Thermo Flash EA, 1112 Series) coupled to a Delta Plus Advantage mass spectrometer (Thermo Finnigan, Dreieich, Germany). Fixation rates were calculated as a function of the change in the tracer concentration of the particulate organic pool relative to the size of the pool between time 0 and the two subsequent time periods (1 and 2), as described in detail elsewhere [40].

Nucleic acid collection and extraction

In order to quickly estimate the abundance of UCYN-A and UCYN-B in the incubation experiments, DNA samples were collected and used in previously described qPCR assays [19]. For each experiment, 3 additional acid-washed light transparent polycarbonate bottles (2.75 L) were filled and incubated as described above. After each time period (0, 1, 2), one of the three 2.75 L bottles was filtered for DNA. Between 1.0–2.75 L was filtered directly onto a 0.2 μm pore size Supor filter (Pall Corporation; East Hills, NY, USA) held within a 25 mm swinnex filter holder using a peristaltic pump.

Two size fractionation experiments were performed on 5 December 2010, where 1.8–2.0 L of whole surface water was filtered through an in-line system of 5.0, 3.0 and 0.2 μm pore size filters held within 25 mm diameter swinnex filter holder using a peristaltic pump. On 10 December, a diel experiment of *nifH* gene expression was performed where 14 acid-washed light transparent polycarbonate bottles (2.75 L) were filled with surface sea water from CV and incubated as described above. Two bottles were

filtered approximately every 4–5 h (10:00, 14:00, 18:30, 22:00, 2:00, 6:00 and 10:00 am) onto a 0.2 μm pore size Supor filter as described above. One bottle was used for DNA and the second bottle for RNA.

The time of filtration for all DNA and RNA samples was limited to 1 h and then samples were immediately flash frozen in a −80 °C dry shipper. The DNA was extracted following the DNeasy plant mini kit (Qiagen, Hilden, Germany) protocol with some minor modifications [60]. Total RNA was extracted using the Qiagen RNeasy protocol (Qiagen) with minor modifications and was reverse transcribed using the Super-Script III cDNA synthesis kit (Invitrogen, Darmstadt, Germany) following manufacturer's recommendations. The reaction mixtures and necessary negative controls used were as described previously [19].

Quantitative PCR

nifH gene transcript abundance and *nifH* gene abundance was quantified using previously described TaqMAN oligonucleotides and optimized assays for UCYN-A and UCYN-B [10,38]. The standard curves for each primer and probe set were made from 10-fold dilution series of linearized plasmids containing the *nifH* gene ranging from 1 to 10^8 gene copies per reaction. Regression analyses of the number of cycles (Ct) of the standard curve were done in Excel. The PCR efficiency for each sample was determined as previously described by Short et al. [55].

CARD-FISH samples

In order to identify and estimate the abundance of UCYN-A in the incubation experiments and the size-fractionation experiments described above, 0.5–1.0 L of incubated seawater was filtered through an in line system of 5.0, 3.0 and 0.2 μm pore size filters (GTTP) held within 25 mm diameter swinnex filter holder using a peristaltic pump. One sample was taken after each incubation period (0–2). The CARD-FISH filters were covered with 200 μL of 1% paraformaldehyde (PFA). After 1–4 h at room temperature (RT), the filters were rinsed in 1 × phosphate buffered saline (PBS) solution (130 mM NaCl; 10 mM Na_2HPO_4; pH 7.6) and stored at −20 °C until further processing.

For the CARD-FISH samples collected earlier in 2006, 2008 and 2009, whole seawater (20–500 mL) was fixed prior to filtration at a final concentration of 1–2% PFA for 1 h at RT. The seawater was filtered using a vacuum pump onto a 0.2 μm pore size GTTP filter (47 or 25 mm diameter), rinsed in 1 × PBS, and stored frozen (−20 °C) until further processing.

CARD-FISH assay

The UCYN-A specific probes, UCYN-A732 and UCYN-A159, and the corresponding helpers and competitor oligonucleotides used in the CARD-FISH assays are listed in Table 1. The 16S rRNA sequence of the competitor oligonucleotides for UCYN-A732 and UCYN-A159 contain 1 mismatch with the 16S rRNA of the target UCYN-A cells and were named according to their matching targets, *C. watsonii*-732 and *Prochlorococcus marinus*-159 (Table 1). In addition, we list the general bacterial probe (EUB338) [1] and the Nitro821 probe [4,34], which were used as additional positive controls, and the NON338 probe [63] was used as a negative control. All hybridizations were performed at optimal formamide (FA) concentrations to ensure high stringency (Table 1) (Supplementary Methods). Each hybridization assay contained a mixture of HRP-oligonucleotide probe, the corresponding helper oligonucleotides A and B, and the competitor oligonucleotide (each at working solutions of 50 ng μL^{-1}) diluted in hybridization buffer (1:300; v:v).

CARD-FISH identification and cell counts were performed using standard protocols [47,48] in single and double hybridization assays on filter pieces. The 25 mm and 47 mm diameter filters (5.0, 3.0, 0.2 μm pore size) were cut into 8 and 16, respectively, equally sized filter pieces. The cell wall was permeabilized by treatment with lysozyme solution (10 mg mL^{-1} in 0.05 M EDTA, pH 8.0; 0.1 M TrisHCl; Fluka, Taufkirchen, Germany) for 1 h at 37 °C, followed by the inactivation of endogenous peroxidases using 30% H_2O_2 or 0.01 M HCl for 10 min at RT [47,49]. The cells were hybridized 3 h at 35 °C and washed in washing buffer for 15 min at 37 °C [47]. CARD was performed for 20 min at 46 °C using Alexa488 or Alexa594 tyramides (Molecular probes, Leiden, The Netherlands). The cells were counterstained with 1 mg mL^{-1} 4′,6-diamidino-2-phenylindol (DAPI) for 10 min at RT in the dark. For microscopy counts, filter pieces were embedded in a mixture of low fluorescence glycerol mountant (Citifluor AF1, Citifluor Ltd., London, United Kingdom) and mounting fluid Vecta Shield (Vecta Laboratories, Burlingame, CA, USA) in a 4:1 ratio.

Two dual hybridizations were performed using a combination of HRP-UCYN-A732 and HRP-UCYN-A159 in the first assay and HRP-UCYN-A732 and HRP-*C. watsonii*-732 competitor oligonucleotide in the second assay (Supplementary Methods).

HISH-SIMS assays

After each time period (0–2), the 4th replicate incubation bottle was filtered with the in-line filtration system described above, but through 2 size fractions (3.0 and 0.2 μm pore size filters). Prior to filtration, filters were pre-sputtered with gold (Au) and palladium (Pd). Between 1.5 and 2.75 L was filtered onto the 3.0 μm filter and 0.5–1.25 L was filtered onto the 0.2 μm filter. The filters were placed in petri dishes with 200 μL of 1% PFA for 1–4 h, washed with 1 × PBS and stored at −20 °C until further processing. For cell identification during nanoSIMS analysis, filters were sectioned into 5 mm diameter round pieces and hybridized with a mix of HRP-labelled UCYN-A732 and helper A and B followed by the deposition of fluorine-containing tyramides. Sample treatment and hybridizations were performed as described above for the CARD-FISH assay with some modifications. The embedded and permeabilized filter pieces were hybridized for 8.5 h at 35 °C. Longer hybridizations were required in order to increase the number of probe molecules hybridizing to the target rRNA and to increase the amount of fluorine containing tyramides deposited in the cell [44]. The CARD step was performed using Oregon Green 488 tyramides dissolved in dimethylformamide containing 20 mg mL^{-1} of 4-iodophenyl boronic acid. Filter pieces were incubated at 46 °C for 20 min in the dark [47,49]. Afterwards, filters were washed in 1 × PBS for 10–20 min in the dark and air-dried. The filter pieces were then counterstained with DAPI (1 μg mL^{-1}) as described above.

Microscopy and cell abundances

Microscopic evaluation and counting was performed with a Zeiss Axioskop II fluorescence microscope (Zeiss, Berlin, Germany). After each time period (0–2), between 100 and 200 grids (grid area = 15,625 μm^2) for each pore size filter piece (0.2, 3.0, and 5.0 μm) were counted separately and abundances from each pore size were pooled for a total UCYN-A count. Due to our intensive CARD-FISH optimization assay and probe design (e.g. various FA concentrations tested for probe stringency and specificity, assays with and without helpers, the test of competitor oligonucleotides, numerous positive and negative controls required for each hybridization assay), we had limited filter material for duplicate counts. Therefore, a larger filter surface area was used when counting to give more confidence to our CARD-FISH counts. Cell dimensions were estimated using the CARD-FISH microscopy images and Image J software [50].

Marking and mapping for nanoSIMS

The filter pieces containing hybridized UCYN-A cells were marked with a Laser Micro-dissection (LMD) Microscope 6500

Table 1
Summary of 16S rRNA targeted oligonucleotide probes, competitors, helpers, and recommended formamide (FA) concentrations used in the CARD-FISH assays. The corresponding target microorganisms and references are also listed.

Probe**	Target organism	Sequence (5′ → 3′)	% FA	Reference
UCYN-A 732	Unicellular cyanobacteria GROUP A	GTTACGGTCCAGTAGCAC	50	This study
C. watsonii-732	*C. watsonii* WH8501, used as competitor	GTTTCGGTCCAGTAGCAC*	50	This study
Helper A-732	Unicellular cyanobacteria GROUP A	GCCTTCGCCACCGATGTTCTT	50	This study
Helper B-732	Unicellular cyanobacteria GROUP A	AGCTTTCGTCCCTGAGTGTCA	50	This study
UCYN-A159	Unicellular cyanobacteria GROUP A	GGGTGTTAGCGGTCGTTT	60	This study
P. marinus-A159	*P. marinus*, used as competitor	GGGTATTAGCGGTCGTTT*	60	This study
Helper A-159	Unicellular cyanobacteria GROUP A	CCAACCGTTATCCCCATCCTA	60	This study
Helper B-159	Unicellular cyanobacteria GROUP A	TTTTTCACCTTACGGCATATT	60	This study
EUB338 I	Most Bacteria	GCTGCCTCCCGTAGGAGT	35	[1]
EUB338-II	supplement to EUB 338: *Planctomycetales*	GCAGCCACCCGTAGGTGT	35	[12]
EUB338-IIII	supplement to EUB 338: *Verrucomicrobiales*	GCTGCCACCCGTAGGTGT	35	[12]
NON338	Antisense of EUB338	ACTCCTACGGGAGGCAGC	35	[63]

* Highlighted in grey in the competitor oligonucleotide sequence are the corresponding mismatches to the target UCYN-A 16S rRNA;
** Hybridization temperature for all probes was 35 °C and FA is the optimal recommended formamide concentration.

(Leica, Berlin, Germany) using a filter set suitable for the Oregon Green 488 tyramides (excitation maximum: 498 nm; emission maximum: 526 nm). *Crocosphaera*-like cells were identified based on cell diameter, morphology, and excitation pattern under blue (450–490 nm) and green (510–560 nm) excitation filters and were also marked for analyses.

Laser markings (arrows and numbers) were made near the positively hybridized UCYN-A and the *Crocosphaera*-like cells. Microscopic pictures were taken and used for orientation purposes during subsequent nanoSIMS analysis and for post-processing using look@nanoSIMS software [49]. The filter pieces were then thoroughly washed with ultrapure water and ethanol and air dried prior to nanoSIMS analysis.

NanoSIMS analysis

NanoSIMS analysis was performed using a Cameca NanoSIMS 50 L instrument (Cameca, Gennevilliers France). Carbon (C), fluorine (F), nitrogen (as CN) and sulfur (S) secondary ions (^{12}C, ^{13}C, ^{19}F, $^{12}C^{14}N$, $^{12}C^{15}N$ and ^{32}S) were measured simultaneously in raster imaging mode. Sample surfaces were rastered with a 16 keV Cesium (Cs^+) beam and a current between 0.8 and 1.2 pA was applied on the sample surface. Primary ions were focused into a nominal ~100–120 nm spot diameter. The primary ion beam was used to raster the analyzed area with an image size of 256 × 256 pixels and a dwelling time of 1 or 3 ms per pixel. Raster areas were 5 μm × 5 μm, 10 μm × 10 μm or 30 μm × 30 μm depending on the size and distribution of the targeted cells (most areas were 5 μm × 5 μm). Negative secondary ions were collected simultaneously in electron multiplier detectors. Prior to analysis, the area was pre-sputtered for 1–2 min with a rastered high-current Cs^+ beam to implant Cs and remove surface contaminants.

All scans (20–150 planes) were corrected for drift of the beam and sample stage after acquisition. Isotope ratio images were created as the ratio of a sum of total counts for each pixel over all recorded planes of the investigated isotope and the main isotope. Regions of interest (ROIs) around cell structures were circled and calculated using *look@nanosims* software [49]. The cell dimensions were estimated from the ROIs and the *look@nanosims* software. The nanoSIMS images were processed using the first 25 planes and threshold option in Cameca WinImage software. The equations for C and N assimilation by individual cells were described previously [18] (Supplementary Methods).

Results

Identification and enumeration of UCYN-A cells by CARD-FISH

UCYN-A cells were identified and quantified using newly designed and optimized oligonucleotide probes and the CARD-FISH assay (Table 1). The UCYN-A732 and UCYN-A159 probes were designed to target specific regions of the 16S rRNA sequence of UCYN-A (*E. coli* 16S rRNA positions: 732–749 and, 159–177, respectively). Both probes were used in combination with helper oligonucleotides located up and downstream to their respective probe sites (Table 1). The helpers were designed to increase the probes' access to 16S rRNA target regions and thus, to enhance the signal intensity of the hybridized cells (Supplementary Fig. 1(A–D)). Competitor oligonucleotides were designed to avoid cross-hybridizations with co-occurring populations of *C. watsonii* and *P. marinus*, and were therefore named accordingly: *C. watsonii*-732 and *P. marinus*-159.

FA concentrations of 50% for UCYN-A732 and 60% for UCYN-A159 ensured both stringent specificity and strong fluorescent signals for positively hybridized cells (Supplementary Fig. 2(A) and (B)). Both probes were equally successful in identifying UCYN-A in the field samples. As a proof of concept for the specificity of both UCYN-A732 and UCYN-A159, we used a dual hybridization approach with 2 different tyramide dyes (Alexa488 and Alexa594, respectively) (Supplementary Methods) and observed that the UCYN-A732 and UCYN-A159 probes hybridized to morphologically similar cells (Fig. 2(C) and (D)).

Using the UCYN-A732 probe with helpers A-732 and B-732 and competitor *C. watsonii*-732 we identified and estimated cell abundances for UCYN-A in surface samples, depth profile samples and size fractionated (5.0, 3.0 and 0.2 μm) water samples collected at the CV field site in December 2010. We also estimated UCYN-A abundance in stable isotope amendment experiments (3 time periods: time 0–2) conducted in December 2010 (Table 2) and water samples collected earlier from the subtropical North Atlantic in September 2006 and near our CV site in April 2008 and May 2009 (Fig. 2(E)–(H)).

The positively hybridized UCYN-A cells were coccoid in shape and were observed as free cells or attached to a larger, unidentified eukaryote cell type (2.0–5.6 μm) (Fig. 2(A)–(H), Supplementary Table 2). Based on microscopy, the free UCYN-A cells had an average cell diameter of 1.2 ± 0.2 μm, which was smaller than the mean cell diameter of the attached UCYN-A cells (2.0 ± 0.7 μm) (Supplementary Table 2). Although we have few measurements for the cell diameters of associated UCYN-A and its partner, we found a

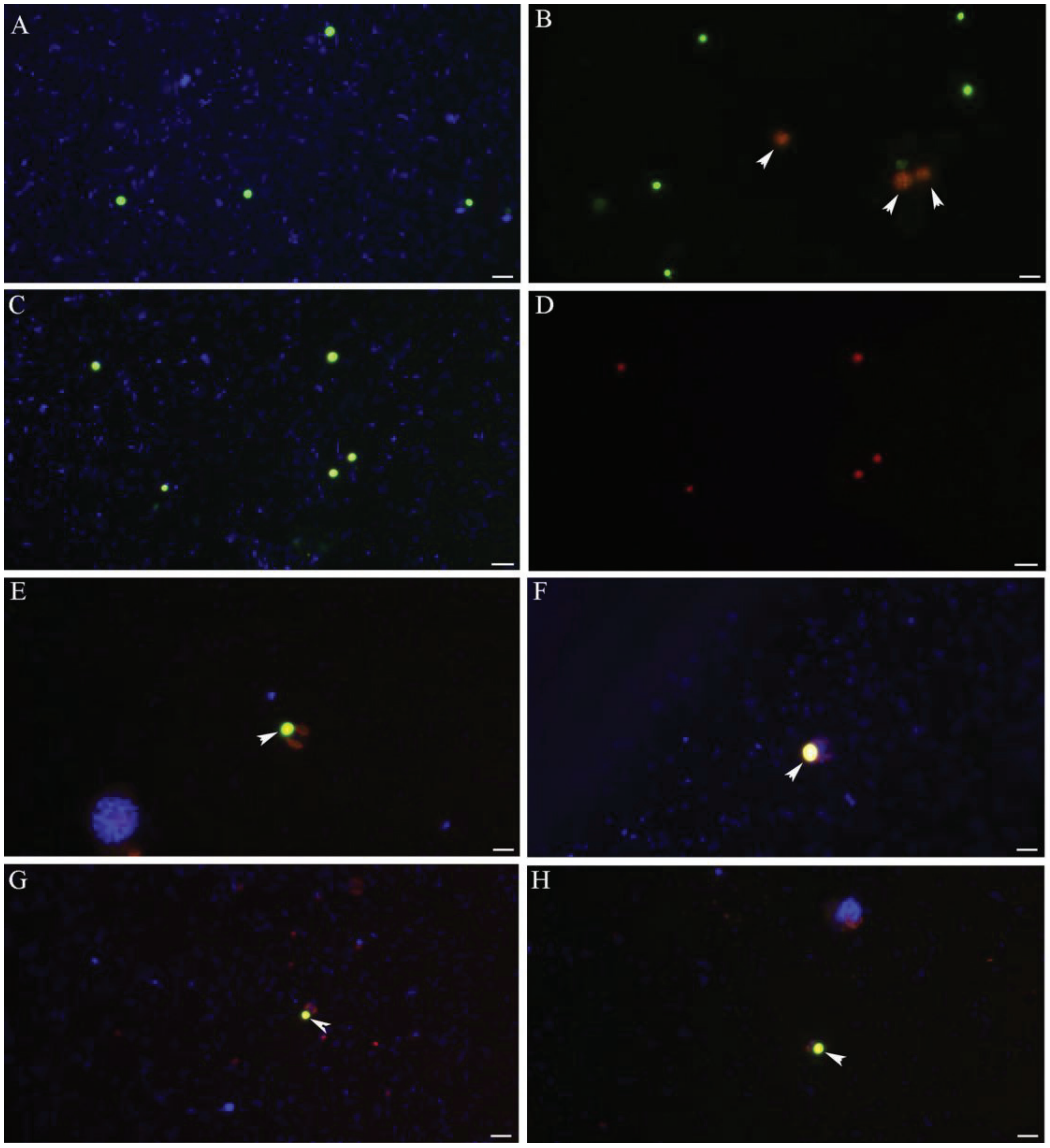

Fig. 2. Epifluorescence micrographs of UCYN-A cells hybridized with the specific HRP-labelled oligonucleotide probe UCYN-A732 and/or UCYN-159 followed by deposition of tyramides. Most images (A, C, E–H) are overlays of hybridized (green) and DAPI- stained cells (blue). (A) UCYN-A cells collected from surface waters at Cape Verde in December 2010 hybridized with UCYN-732, competitor *C. watsonii*-732, and helpers A and B. (B) Dual hybridization of field surface water samples from Cape Verde December 2010 hybridized to UCYN-A (green) and *C.watsonii*-like cells (orange and indicated with arrows) using UCYN-A 732, *C. watsonii*-732 with 2 different tyramide dyes and helpers A and B. (C-D) Dual hybridization of UCYN-A cells from Cape Verde December 2010 (0 m) using UCYN-A-159 (green) and UCYN-A732 (red) with 2 different tyramide dyes. (E, G) Attached UCYN-A cells (designated with arrows) collected from 30 m in the North Atlantic in September 2006 hybridized with the UCYN-732 shows 2 different sized hosts and associated UCYN-A cells. (F, H) Hybridized UCYN-A cells (designated with arrows) attached to two difference sized hosts (designated with arrows) collected from 10 m during the MSM cruise (F) in April 2008 and from the surface waters near the Cape Verdean Islands in May 2009 (H). Note in (E)–(H), the chloroplasts of the eukaryotic partner fluoresce red. Scale bar = 2 μm.

positive and linear correlation between the cell diameter of the attached UCYN-A cells and their associated partner cell ($r^2 = 0.93$; n = 7). The cell diameters (0.7–1.7 μm) measured after CARD-FISH for the free UCYN-A cells were similar to the range in cell diameters (0.5–1.0 μm) estimated by the nanoSIMS images and the look@nanoSIMS software (Table 3, Supplementary Table 2). One has to take into account that cell dimensions determined after CARD-FISH could be overestimated due to the strong fluorescent signals produced during the tyramide deposition step.

Free UCYN-A cells were observed in all field samples, while UCYN-A cells attached to a eukaryote were only recovered in the samples collected earlier in September 2006 in the North Atlantic and in April 2008 and May 2009 at the site near CV (Fig, 1, Fig. 2(E)–(H)). The attached UCYN-A cells were located at the polar ends of a larger eukaryotic cell that possessed two bright fluorescent chloroplasts (Fig. 2(E)–(H)).

CARD-FISH counts for UCYN-A cells from the incubation experiments in December 2010 ranged 1.76×10^3–8.19×10^5 cells L^{-1} (Table 2). Abundances were higher at the beginning of the expedition (3 and 5 December 2010, 1.73 and 8.19×10^5 cells L^{-1}) than at the end of the field trip (8 December 2010, 1.44×10^4 cells L^{-1}) (Table 2). The cell abundances for

Table 2
Summary of whole water (bulk) C and N_2 fixation rates, CARD-FISH counts, and *nifH* gene copy abundances from incubation experiments performed on surface seawater collected from Cape Verde field site in December 2010. The range, mean and standard deviation (in parenthesis) are provided for the rate measurements.

Exp	Date	Time (h)	C fixation, nmol C L^{-1} h^{-1} range (mean ± SE)	N_2 fixation nmol N L^{-1} h^{-1} range (mean ± SE)	UCYN-A cells L^{-1}	UCYN-A *nifH* gene copies L^{-1}	UCYN-B *nifH* gene copies $^{-1}$
1	12/3	0	Not applicable	Not applicable	1.73×10^5	3.69×10^6	6.31×10^4
	12/3	10.2	32.4–54.2 (40.6 ± 11.8)	0.40–0.62 (0.54 ± 0.12)	1.87×10^4	5.20×10^5	2.67×10^4
	12/4	19.6	9.9–16.7 (13.7 ± 3.5)	0.17–0.44 (0.29 ± 0.14)	5.04×10^4	5.98×10^5	3.43×10^4
2	12/5	0	Not applicable	Not applicable	8.19×10^5	4.03×10^5	6.84×10^4
	12/5	12.1	42.8–82.6 (58.7 ± 21.1)	0.18–0.52 (0.30 ± 0.19)	9.03×10^4	7.17×10^5	6.20×10^4
	12/6	22.2	17.0–49.1 (36.0 ± 16.8)	0.11–0.24 (0.19 ± 0.07)	2.61×10^4	5.88×10^5	7.71×10^4
3	12/8	0	Not applicable	Not applicable	1.44×10^4	1.23×10^5	6.06×10^4
	12/8	7.5	58.3–105.4 (85.7 ± 24.4)	0.39–1.56 (0.82 ± 0.65)	1.19×10^4	3.40×10^4	4.62×10^3
	12/9	20.1	19.0–72.0 (45.3 ± 26.5)	0.42–1.72(1.08 ± 0.65)	1.76×10^3	3.72×10^4	3.92×10^3

* CARD-FISH counts are pooled values from 3.0 and 0.2 μm size fractions.

UCYN-A were higher in the upper 30 m (5.14×10^3 cells L^{-1} at 0 m; 5.20×10^3 cells L^{-1} at 30 m), and decreased with depth (Fig. 3(A)). The UCYN-A cells were also enumerated from the sample collected earlier in September 2006 in the subtropical North Atlantic. Abundances of 3.6×10^4 cells L^{-1} and 3.2×10^4 cells L^{-1} were estimated using the UCYN-A732 and UCYN-A159 probes, respectively (data not shown). Thus, the cell counts obtained by hybridizations using the two probes independently were consistent.

In December 2010, water samples for CARD-FISH and HISH-SIMS assays were collected by size fractionation and UCYN-A was only observed as free cells (Fig. 2(A)–(D)). In two separate experiments, whole surface water was sequentially size fractionated (5.0, 3.0, 0.2 μm) and resulted in the majority (74% and 96%) of UCYN-A cells collected on the 0.2 μm filters, while 8% and 2% of UCYN-A cells were enumerated on the 3.0 μm filters, and 18% and 2% of UCYN-A cells were found on the 5 μm filters. All the filters for the HISH-SIMS analyses were also size fractionated in a 0.2–3.0 μm and a > 3.0 μm fraction, and resulted in the majority (92% and 98%) of the UCYN-A identified and enumerated on the 0.2 μm filter, while 8% and 2%, respectively, of the UCYN-A were found on the 3.0 μm filter.

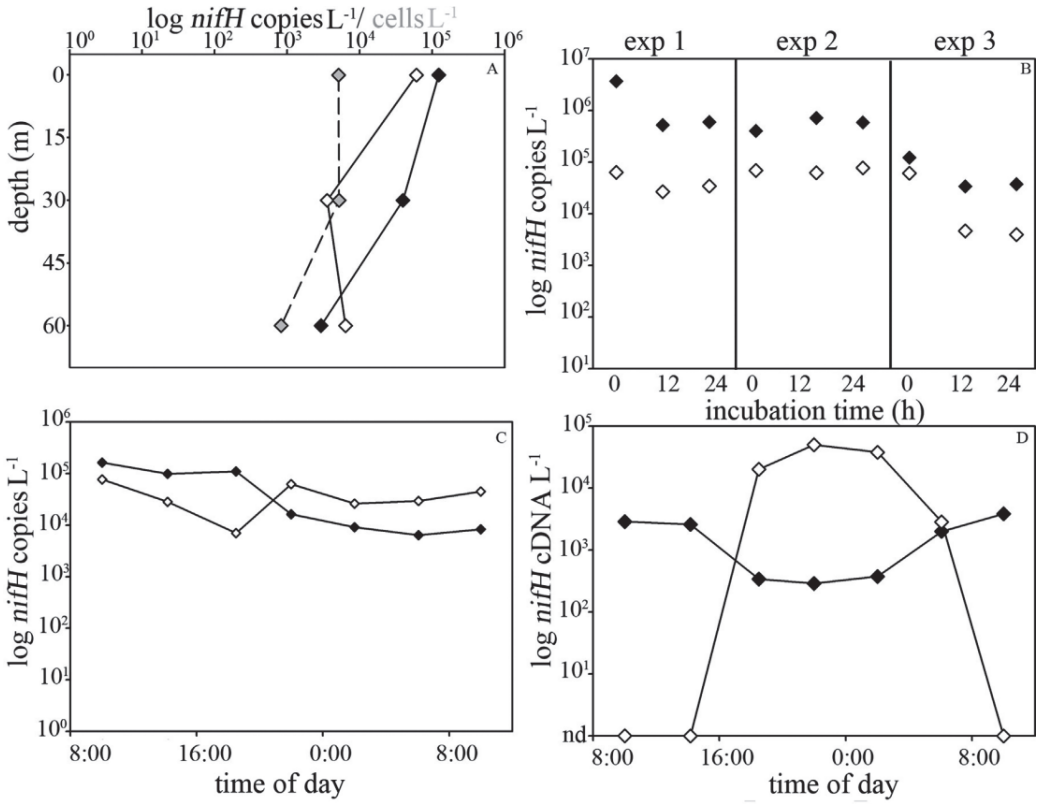

Fig. 3. Summary of results from qPCR assays for detecting unicellular groups: UCYN-A and UCYN-B in the field samples and incubation experiments from the Cape Verde field site in December 2010. UCYN-A are designated as filled diamonds (♦) and UCYN-B are open diamonds (◊). (A) The depth profile of *nifH* gene copies L^{-1} for UCYN-A and UCYN-B and abundances of UCYN-A cells (L^{-1}) from CARD-FISH counts designated as filled gray diamonds (◆). (B) The abundance of *nifH* gene copies L^{-1} for UCYN-A and UCYN-B at the three time periods (0–2) from the three separate $^{15}N_2$ and $^{13}CO_2$ amendment experiments. (C–D) The results from the diel experiment of *nifH* gene copy abundance (C) and *nifH* gene copy expression (D) for UCYN-A and UCYN-B detected in the bottles incubated on 10–11 December 2010.

Table 3
Summary of cell dimensions and nanoSIMS analysis for UCYN-A and *C. watsonii*-like cells from incubation experiments performed on surface seawater collected from Cape Verde field site in December 2010. Natural abundance values measured by EA-IRMS on triplicate time 0 bottles are also listed. The range, mean and standard deviation (SD) (in parenthesis) are provided for cell diameter, ^{13}C atom % and ^{15}N atom % (AT%) measured in individual cells. The individual carbon and N_2 fixation rate estimates are calculated based on the nanoSIMS and cell dimension analysis.

Exp.	Time (h)	Target	*n*	Cell diameter (μm) range (mean ± SE)	Atom % ^{13}C range (mean ± SD)	C fixation rate* fmol C cell^{-1} h^{-1}	Atom % ^{15}N range (mean ± SD)	N_2 fixation rate* (fmol N cell^{-1} h^{-1})
1	0	Bulk	–	–	1.0656–1.0671 (1.0662 ± 0.0008)	Not applicable	0.3661–0.3665 (0.3664 ± 0.0002)	Not applicable
2	0	Bulk	–	–	1.0672–1.0680 (1.0677 ± 0.0005)	Not applicable	0.3675–0.3679 (0.3677 ± 0.0002)	Not applicable
3	0	Bulk	–	–	1.0684–1.0692 (1.0687 ± 0.0005)	Not applicable	0.3682–0.3688 (0.3685 ± 0.0003)	Not applicable
3	0	UCYN-A	4	0.53–0.75 (0.65 ± 0.08)	1.0060–1.0400 (1.0228 ± 0.0140)	Not applicable	0.3670–0.3920 (0.3790 ± 0.0130)	Not applicable
1	10.1	UCYN-A	3	0.60–1.02 (0.77 ± 0.22)	1.1369–1.3515 (1.2241 ± 0.1128)	1.47×10^{-2}–5.22×10^{-2} ($3.31 \times 10^{-2} \pm 0.02$)	0.3959–0.4417 (0.4164 ± 0.0233)	4.70×10^{-4}–2.83×10^{-3} ($1.63 \times 10^{-3} \pm 0.001$)
1	19.8	UCYN-A	4	0.62–0.86 (0.76 ± 0.11)	1.4244–1.7402 (1.5736 ± 0.1559)	2.90×10^{-2}–1.02×10^{-1} ($6.69 \times 10^{-2} \pm 0.03$)	0.4127–0.5304 (0.4752 ± 0.0615)	8.39×10^{-4}–3.19×10^{-3} ($1.59 \times 10^{-3} \pm 0.001$)
2	12.9	UCYN-A	10	0.49–0.79 (0.66 ± 0.10)	1.0675–1.8395 (1.4993 ± 0.2966)	3.09×10^{-2}–1.56×10^{-1} ($8.37 \times 10^{-2} \pm 0.05$)	0.3744–0.5893 (0.4851 ± 0.0814)	6.35×10^{-5}–5.14×10^{-3} ($2.09 \times 10^{-3} \pm 0.002$)
2	23.0	UCYN-A	6	0.61–0.86 (0.72 ± 0.10)	1.2950–1.8675 (1.6124 ± 0.2081)	2.86×10^{-2}–9.91×10^{-2} ($5.39 \times 10^{-2} \pm 0.03$)	0.4202–0.6194 (0.5549 ± 0.0749)	8.05×10^{-4}–4.04×10^{-3} ($2.07 \times 10^{-3} \pm 0.001$)
2	0	*C. watsonii*-like	8	3.10–5.56 (4.29 ± 0.96)	1.0200–1.0480 (1.0336 ± 0.0096)	Not applicable	0.3600–0.3796 (0.3704 ± 0.0077)	Not applicable
2	13.2	*C. watsonii*-like	6	4.03–5.28 (4.75 ± 0.45)	2.1431–2.3304 (2.2196 ± 0.0682)	16.7–32.2 (25.7 ± 5.2)	0.3640–0.5300 (0.4264 ± 0.0744)	5.16×10^{-3}–3.68×10^{-1} ($1.73 \times 10^{-1} \pm 0.17$)
2	23.0	*C. watsonii*-like	5	4.02–.50 (4.32 ± 0.21)	2.5598–2.9899 (2.7570 ± 0.1675)	13.7–19.3 (16.8 ± 2.2)	0.8212 – 0.9235 (0.8641 ± 0.0382)	4.96×10^{-1}– 6.34×10^{-1} ($5.59 \times 10^{-1} \pm 0.06$)

* Cells showing C and N ratio values at natural abundance were not included in estimating the mean and standard deviation.

nifH abundance and nifH transcript abundance of UCYN-A and UCYN-B by quantitative PCR.

In order to estimate the distribution and abundance for UCYN-A and UCYN-B at the CV study site in December 2010, qPCR assays were applied to DNA extracts from depth profile samples (Fig. 3(A)). Abundances of UCYN-A and UCYN-B were also estimated from the three time periods (time 0–2) of the stable isotope incubation experiments (Fig. 3(B) and Table 2). And in parallel with the CARD-FISH assays, we estimated UCYN-A and UCYN-B *nifH* abundance in size-fractionation samples. The UCYN-A cell abundances determined by CARD-FISH were usually an order of magnitude less than the *nifH* copy abundance for UCYN-A determined by qPCR estimates (Table 2).

Both UCYN-A and UCYN-B were detected by qPCR at moderate abundances in the surface water of the CV site. UCYN-A *nifH* copies were more abundant at 0 m and 30 m (3.94×10^4 and 1.23×10^5 *nifH* L^{-1}) compared to UCYN-B *nifH* copies (3.57×10^3 and 6.06×10^4 *nifH* L^{-1}). UCYN-A *nifH* gene copies decreased with depth and were less abundant than UCYN-B *nifH* gene copies at 60 m depth (Fig. 3(A)). In general, UCYN-A was more abundant than UCYN-B in the incubation experiments of December 2010 (Table 2). However, during the incubation, the abundances of UCYN-A and UCYN-B *nifH* copies (L^{-1}) were subject to fluctuations in abundance and it varied according to each experiment (Fig. 3B, Table 2).

The temporal variation of *nifH* abundance and *nifH* gene expression for both UCYN-A and UCYN-B was investigated over a 24 h period in a separate diel experiment performed on 10–11 December 2010 (Fig. 3(C) and (D)). Both unicellular groups were detected throughout the diel experiment. The *nifH* gene transcript abundance for UCYN-A was higher during the day and early morning (2.00×10^3–3.86×10^3 cDNA *nifH* L^{-1}), and declined during the dark period (2.88×10^2–3.73×10^2 cDNA *nifH* L^{-1}), while *nifH* transcription for UCYN-B was only detected during the dark period and a maximum transcription was estimated at 22:40 h (5.02×10^4 cDNA *nifH* L^{-1}) (Fig. 3(D)).

Quantitative PCR of UCYN-A *nifH* gene copies on size fractionated (5.0, 3.0, 0.2 μm) samples estimated 98% of the *nifH* gene copies were derived from 0.2–3.0 μm size fraction (1.24×10^5 *nifH* L^{-1}) and 1% on the 3.0–5.0 μm (9.36×10^2 *nifH* L^{-1}) and 1% on the >5.0 μm (1.96×10^3 *nifH* L^{-1}) size fraction (data not shown).

C and N_2 fixation: whole water and single cell fixation rates

Bulk C fixation and N_2 fixation were measured in triplicate on surface water collected from the CV site in December 2010. Bulk C and N_2 fixation rates were higher during the day (32.4–105.4 nmol C L^{-1} h^{-1} and 0.18–0.62 nmol N L^{-1} h^{-1}) and lower in the bottles incubated overnight (9.9–72.0 nmol C L^{-1} h^{-1} and 0.11–0.44 nmol N L^{-1} h^{-1}). The average C fixation and N_2 fixation rates were higher in experiments 2 and 3 than during experiment 1 (Table 2). However, in experiment 3, the average N_2 fixation rate in the bottles incubated overnight was slightly higher (1.08 ± 0.65 nmol N L^{-1} h^{-1}) than the activity in bottles sampled immediately after the light period (0.82 ± 0.65 nmol N L^{-1} h^{-1}) (Table 2). Although differences in rates were observed between experiments and also in bottles incubated during the day as opposed to overnight, the differences were not statistically significant (ANOVA, $p > 0.08$, *t*-test, $p > 0.07$) (Fig. 4).

Twenty-seven positively hybridized UCYN-A cells were imaged for isotopic ratios of ^{13}C/^{12}C and ^{15}N/^{14}N from experiments 1–3, where 4 cells were analyzed from the time 0 samples, 13 cells were analyzed after the incubation in the light (time period 1), and 10 cells were measured after the overnight incubation (time period 2) (Table 3, Fig. 5). A smaller number of *C. watsonii*-like cells were

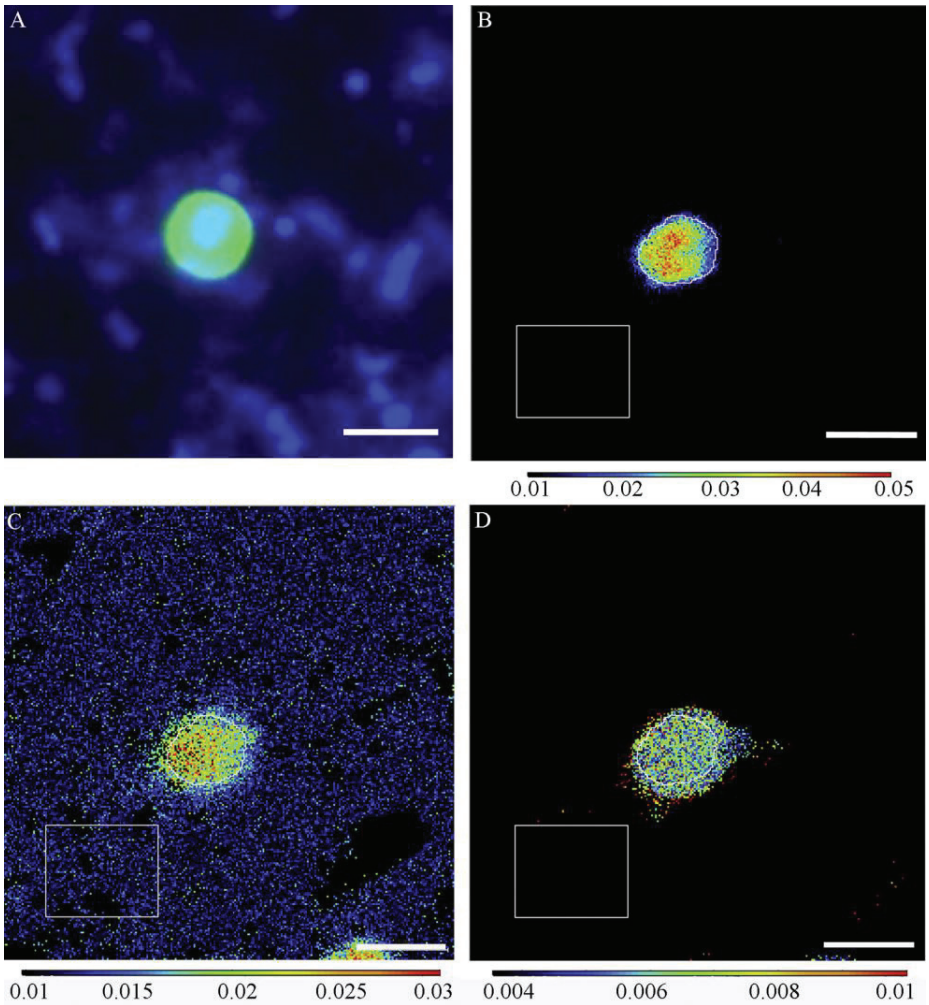

Fig. 4. Epifluorescence micrograph and nanoSIMS images of a UCYN-A cell from the stable isotope incubation experiments. (A) An overlay of hybridized (green) and DAPI stained (blue) UCYN-A cell using the UCYN-A732 probe. (B) The $^{19}F/^{12}C$ ratio (C) the $^{13}C/^{12}C$ ratio (D) the $^{15}N/^{14}N$ ratio. The white markings indicate the regions of interest (ROIs), which were used for calculating the $^{13}C/^{12}C$ and $^{15}N/^{14}N$ ratios of the cell. Scale bar = 1 μm.

observed and as such our nanoSIMS measurements were limited to 8, 6, and 5 cells measured in time periods 0–2 of experiment 2, respectively (Table 3, Fig. 5(B)).

The $^{13}C/^{12}C$ and $^{15}N/^{14}N$ of the UCYN-A and *C. watsonii*-like cells from the time 0 samples were not enriched and were similar to the natural abundance values of the parallel whole water (bulk) time 0 samples measured by the EA-IRMS (Table 3). The majority of UCYN-A cells (91%, 21 of 23) were enriched in ^{13}C above natural abundance (^{13}C atom % = 1.0662–1.0687) after the first and second time periods (Table 3, Fig. 5(A)). There was no significant difference between the measured $^{13}C/^{12}C$ of UCYN-A cells collected after time period 1 or time period 2 (Mann–Whitney, $p = 0.163$). On the other hand, the $^{13}C/^{12}C$ measured in the *C. watsonii*-like cells from time periods 1 and 2 were all highly enriched above natural abundance, and the cells incubated after time period 1 were significantly lower (^{13}C atom %, 2.2196 ± 0.0682) in ^{13}C than the cells incubated after time period 2 (^{13}C atom %, 2.7570 ± 0.1675) (*t*-test, $p < 0.001$) (Table 3, Fig. 5(B)). The C fixation rates for the *C. watsonii*-like cells were higher than the rates estimated for UCYN-A (Table 3).

After time period 2, all UCYN-A cells ($n = 23$) were also enriched in ^{15}N above natural abundance (atom % ^{15}N = 0.3664–0.3685) (Table 3, Fig. 5(A)). Similar to the ^{13}C enrichment, there was no significant difference in the ^{15}N enrichment measured in the UCYN-A cells after time period 1 or after time period 2 (*t*-test, $p = 0.114$). N_2 fixation rates for the UCYN-A cells were low and ranged from 6.35×10^{-5} to 5.14×10^{-3} fmol N cell^{-1} h^{-1} (Table 3). Not all *C. watsonii*-like cells (67%, 4 out of 6) were enriched above natural abundance after the first time period, while all five cells incubated after time period 2 had significantly higher cellular $^{15}N/^{14}N$ ratios (Table 3, Fig. 5(B)) (t-test, $p < 0.001$). The higher enrichment after time period 2 corresponded to higher N_2 fixation rates (0.49–0.63 fmol N cell^{-1} h^{-1}) for the *C. watsonii*-like cells (Table 3).

Discussion

The uncultivated unicellular cyanobacterium UCYN-A has recently been identified as an unusual cyanobacterium since it's genome lacks many of the key metabolic pathways (e.g. PSII, RuBisCo, TCA cycle) characteristic of cyanobacteria [58,68]. Furthermore, UCYN-A is considered an important diazotroph, as it is widespread and abundant (i.e. global geometric mean: $5.5 \times 10^6 \pm 4.5 \times 10^6$ *nifH* copies L^{-1}) in all major subtropical and

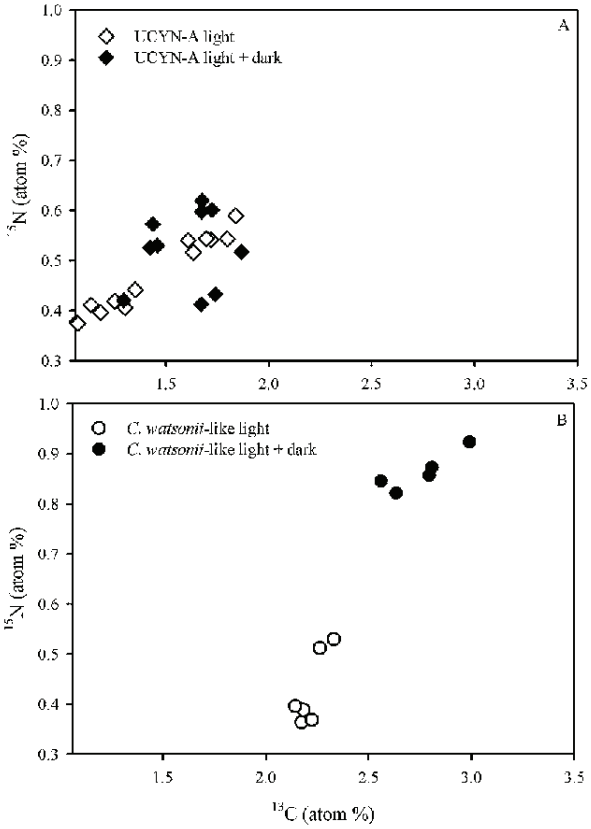

Fig. 5. Summary of nanoSIMS analysis of ^{15}N and ^{13}C measurements (atom %) for the unicellular populations: (A) UCYN-A and (B) C. watsonii-like cells. Open diamonds and circles (◇, ○) indicate measurements from cells incubated during the day; filled diamonds and circles (◆,●) indicate measurements from cells incubated overnight.

tropical oceanic provinces [32]. UCYN-A is difficult to isolate and identify microscopically in the field, and therefore is difficult to study. Direct rate measurements on individual cells have been hampered by a lack of appropriate methodological approaches. However, in the last few decades, various methodological breakthroughs in Fluorescence In Situ Hybridization (FISH) techniques [22,41,48], coupled to advancements in single-cell technology have provided a unique ability to simultaneously resolve identity and metabolic activity for the uncultured majority [2,13,44,62]. The primary objective of our study was to develop a highly specific assay that could identify and measure the C and N_2 fixation by UCYN-A cells.

Identifying UCYN-A in the environment

In the present study, we confirmed the identity, life style (free or attached cells), and metabolic activity of natural UCYN-A populations by developing and applying CARD-FISH assays with highly specific 16S rRNA oligonucleotide probes. In contrast to previous assays that targeted all unicellular diazotrophs (i.e. Nitro821)[4,31], the CARD-FISH assays and new probes (UCYN-A732 and UCYN-A159) presented here specifically target only UCYN-A cells. The combination of helpers (A and B), competitors (C. watsonii-732 and P. marinus-159), and stringent FA concentrations ensured a high specificity to UCYN-A cells, and, due to increased accessibility of the probe to the target site, increased the sensitivity of the assay.

In our various field samples collected during different seasons and locations in the subtropical North Atlantic, the optimized CARD-FISH assays with specific oligonucleotide probes showed that only UCYN-A cells were hybridized and no cross-hybridization to co-occurring non-target cells was observed. We observed UCYN-A living both freely or attached to a slightly larger eukaryotic cell. Similar observations have been recorded previously [4,17,31]. For example, in a Southwest Pacific Coral Lagoon, Biegala and Raimbault [4] used CARD-FISH and a general unicellular diazotrophic cyanobacterial probe (Nitro821) to show that small (<1.0 μm) unicellular cyanobacteria live freely, attached to inert particles or within the girdle of Dinophysoids (dinoflagellates). Le Moal et al. [31] also found similar results in the Mediterranean; however, in both studies, the Nitro821 probe was used which hybridizes all unicellular diazotrophs.

More recently, a study performed in the subtropical North Pacific at station ALOHA, applied the UCYN-A732 probe and a modified HISH-SIMS assay described here (without competitor) and found UCYN-A attached to slightly larger eukaryotic cell [57]. The partner eukaryotic cells described in the North Pacific study were similar in shape, chloroplast location, and cell diameter to the cells we identified in the samples collected earlier (2008, 2009) near the CV field site in the North East Atlantic, and in the samples collected in the North Atlantic (September 2006). Although the observations are limited by a low number of samples, the combined results suggest that the same symbiosis may be present in at least two ocean basins.

The primary purpose of the size-fractionation experiments was to concentrate UCYN-A cells to identify and quantify their abundance by microscopic cell counts, and then use the same cells in combination with single-cell activity measurements by HISH-SIMS. In an earlier size fractionation qPCR experiment from the North Pacific, Tripp et al. [58] recovered UCYN-A from multiple size fractions (0.2–25 μm) where the most UCYN-A gene copies were associated with the 0.2 and the 0.2–3.0 μm size fractions. Similarly, we found that UCYN-A gene copies were detected by qPCR on the 0.2 and 3.0 μm pore size filters. In parallel, we also observed free UCYN-A cells by CARD-FISH on both 0.2 and 3.0 μm size fractions. The attached UCYN-A cells were only recovered in the earlier field samples (2006, 2008, 2009), which had not been size fractionated or filtered with the peristaltic pump. Interestingly, free UCYN-A cells were also recovered in a previous study [57], which used flow cytometry to concentrate and collect cells. These authors concluded that the cells had fallen off from their partner cells during the procedure since the flow cytometric gate (1.0–3.0 μm) was larger than the UCYN-A cell diameter. Sample processing was different in 2010; a peristaltic pump was used with two inline size fractions, whereas in the earlier samplings (2006, 2008, 2009) there was much less handling and samples were collected by vacuum filtration. Therefore, the free UCYN-A cells we observed in the 2010 field expedition to CV could be a separate free-living population, or more likely, the cells became detached during sample processing, i.e. size fractionation, filtration and/or the CARD-FISH assay.

Diazotrophic abundance, distribution, and activity based on nifH and CARD-FISH at Cape Verde

In the waters at our CV study site, nutrient concentrations (e.g. DIN) are chronically low or below the detection limit in surface waters and thus favour the abundance and activity of N_2 fixers [61]. The highest UCYN-A nifH gene abundances presented here (3.69×10^6 nifH L^{-1}) were derived from surface water samples and were comparable with abundances reported by Langlois et al. [29] and recently by Rijkenberg et al. [51], who detected UCYN-A in surface waters close to our study site ranging 10^5–10^6 nifH gene copies L^{-1}. The abundance estimates for the UCYN-B nifH gene copies (10^3–10^4 L^{-1}) were similar to values previously reported in the eastern subtropical North Atlantic

(10^4 *nifH* gene copies L^{-1}) [29], and higher than other estimates from the western basin and further south in the eastern equatorial upwelling region (10^2–10^3 *nifH* gene copies L^{-1}) (Gulf of Guinea) [20,21]. A recent compilation of *nifH* qPCR abundance studies (1793 data periods) reports a range in average abundance for UCYN-A and UCYN-B of 4.5×10^6–6.8×10^6 *nifH* gene copies L^{-1} and 0.95×10^6–1.3×10^6 *nifH* gene copies L^{-1}, respectively [32]. Thus, the abundances for UCYN-A at the CV field site are in agreement with other studies from the same region and in other oceanic provinces suggesting UCYN-A (and UCYN-B) as a persistent population in the subtropical region.

In general, the cell abundances for UCYN-A by CARD-FISH were consistently one order of magnitude lower than the gene number estimates based on the *nifH* qPCRs. The discrepancies between the cell abundances given by the two methods can result from differences in the methodologies. Part of the discrepancy can be explained by the presence of multiple gene and/or genome copies in cyanobacteria cells [5,65]. However, permeability is not always 100% and due to multiple washing steps in the CARD-FISH assay, there is always a risk for cell loss, which could partially account for the lower UCYN-A cell abundances by CARD-FISH.

Here, we found similar temporal variation in *nifH* gene transcript abundance for both UCYN-A and UCYN-B, as has been reported previously [10,11,32,45]. Since many diazotrophs have evaded isolation, it is common practice to use *nifH* mRNA abundance as an indicator for N_2 fixation. For example, one study used *nifH* mRNA abundance as model input to predict the N_2 fixation rates attributed to certain populations, i.e. *Trichodesmium*, UCYN-A and UCYN-B [23]. However, as mentioned above, there are several caveats inherent with qPCR studies, and abundance of a particular target gene and its associated gene transcripts are not a direct measurement of enzyme activity. Therefore, direct measurements of substrate uptake, i.e. $^{15}N_2$, are a more appropriate and direct estimate of metabolic activity. Most recently, nanoSIMS has been used to determine rate measurements of single cells and results provide in addition insights into the variability of metabolic activity of cells [43], which cannot be resolved by standard molecular techniques (i.e. qPCR) or by mass spectrometry (i.e. analysis of bulk particulates like C and N).

N_2 and C fixation at Cape Verde

Our bulk estimates of N_2 fixation (0.11–1.72 nmol N L^{-1} h^{-1}) are elevated compared to previous reports from the subtropical North Atlantic, including areas near the Cape Verde study site (0.02–0.125 nmol N L^{-1} h^{-1}) [29,30,35]. However, our measurements were consistent with rates reported in other nutrient depleted sites (0.07–4.17 nmol N L^{-1} h^{-1}) [14,15,32,56]. Our estimated bulk C fixation rates (9.90–105 nmol C L^{-1} h^{-1}) were comparable with rates reported in the subtropical North Atlantic (41–83 nmol C L^{-1} h^{-1}) [35], and slightly higher than estimates made by Jardillier et al. [27] in the subtropical and tropical Northeast Atlantic Ocean (6.25–42.7 nmol C L^{-1} h^{-1}).

Average N_2 fixation rates were higher in the bottles filtered after time period 1 (daytime) in the first two experiments, suggesting that the phototrophic diazotrophic community may have been more active. Large, filamentous *Trichodesmium* cells and *Richelia* cells (the heterocystous symbionts of diatoms) were also observed at low densities (<5 cells L^{-1}) on the 3.0 μm nanoSIMS filters by epifluoresence microscopy. Larger diazotrophs can have significantly higher N_2 fixation rates compared to diazotrophs in the smaller size fraction (<10 μm). Thus, this larger size fraction may have contributed substantially to the daytime N_2 fixation [6,18,39,42,56,59]. NanoSIMS measurements on the larger diazotrophs were, however, outside the scope of our study and were therefore not included. Low wind velocities at the beginning of experiment 2 were recorded (3.37 ± 1.72 m s^{-1}) and may have resulted in less surface water mixing and a stratified water column. Low wind stress and a stable upper water column are conditions that favour *Trichodesmium* [9] and may help explain why we observed higher daytime N_2 fixation in the experiments 1 and 2. Whereas at the end of the expedition the wind increased (4.40 ± 0.86 m s^{-1}) and N_2 fixation rates were higher in the overnight bottles (experiment 3, time period 2). At the end of the expedition, we also detected UCYN-B *nifH* gene transcript abundance during the dark period of our diel experiment, and higher ^{15}N enrichment in *C. watsonii*-like cells based on nanoSIMS analysis than the cells measured after the daytime incubation. Combined our results suggest that the *C. watsonii*-like cells contributed to the night-time N_2 fixation activity measured in the whole water experiments.

N_2 fixation was likely underestimated in both the whole water uptake experiments and in the individual cells. In all our experiments, we assayed for N_2 fixation with the common standard $^{15}N_2$ method, which amends the isotope by a gas bubble [40]. Recent evidence shows that the bubble dissolution is slow (12–24 h), resulting in a lower isotope labelling percentage and underestimation of N_2 fixation [24,36,66]. The time of our amendments and incubation period is also an important factor to consider since the labelling percentage of $^{15}N_2$ in bottles incubated during the day was lower than the labelling percentage of $^{15}N_2$ in the bottles incubated overnight.

Single cell N_2 and C fixation rate measurements for unicellular cyanobacteria

Using HISH-SIMS, we identified, imaged and measured the enrichment of ^{13}C and ^{15}N in individual UCYN-A cells and used nanoSIMS for the *C. watsonii*-like cells. The UCYN-A cells were identified by epifluoresence microscopy and the ^{19}F signal resulting from the HISH assay. All UCYN-A cells were enriched in ^{15}N, which confirmed their N_2 fixation activity. Using the ^{15}N enrichment values determined by nanoSIMS, we estimated cell specific N_2 fixation rates for UCYN-A. The N_2 fixation rates were low (6.35×10^{-5}–5.14×10^{-3} fmol N $cell^{-1}$ h^{-1}), and also extremely reduced compared to those predicted by a diagnostic model based on growth and biomass for UCYN-A (0.4–8.3 fmol N $cell^{-1}$ h^{-1}) [23]. However, similar enrichment values were reported in UCYN-A cells attached to picoeukaryotes in the Thompson et al. [57] study. Using $^{15}N/^{14}N$ values in the latter study, the UCYN-A in the N. Pacific have similarly low N_2 fixation rates (i.e. 1.78×10^{-4}–2.39×10^{-3} fmol N $cell^{-1}$ h^{-1}) [57] to those reported here for the UCYN-A from the N. Atlantic.

Cell specific rates of N_2 fixation by the *C. watsonii*-like cells were higher, especially in the cells analysed from time period 2. The average N_2 fixation rate for the *C. watsonii*-like cells incubated after time period 1 (0.17 fmol N $cell^{-1}$ h^{-1}) and time period 2 (0.56 fmol N $cell^{-1}$ h^{-1}) were also similar to literature values reported for field (0.12–6.60 fmol N $cell^{-1}$ h^{-1}) and cultured (0.50–16.0 fmol N $cell^{-1}$ h^{-1}) *C. watsonii* populations [16,59,64,67,72].

Interestingly, the ^{13}C enrichment in the majority (21 of 23) of UCYN-A cells suggests that the cells were actively assimilating ^{13}C-bicarbonate, even though the genome of UCYN-A lacks the metabolic machinery for dissolved inorganic carbon (DIC) uptake [58,68]. However, we now know from the recent study in the subtropical N. Pacific that the UCYN-A cells associated with a picoeukaryote partner exchange fixed N_2 for fixed C and that the relationship is very fragile, i.e. UCYN-A cells will dislodge from the partnership when filtered [57]. If we assume that the UCYN-A cells in this study were initially associated and became dislodged during the sampling process, the ^{13}C enrichment of the UCYN-A populations from CV samples was most likely derived from the transfer of

^{13}C-labelled DOC from the photosynthetic host prior to detachment [57].

We used *nifH* gene abundance from qPCR assays for UCYN-A and UCYN-B (representative for *C. watsonii*-like cells) and their average N_2 fixation and C fixation rates (time 1 and time 2) from the nanoSIMS analyses in order to estimate each population's contribution to the total N_2 fixation and C fixation (measured in the parallel whole water bottles). This is a similar approach to previous work that utilized qPCR data and assumed rates based on diagnostic growth models or average published rates, to predict N_2 fixation by a particular population in the upper water column [20,23]; however, here, we have the advantage of direct estimates of individual C and N_2 fixation rates by the nanoSIMS measurements. We find that UCYN-A contributes little to time period 1 (0.16–0.50%) and time period 2 (0.33–0.64%) N_2 fixation while UCYN-B accounts for 3% of bulk N_2 fixation at time period 1 and 23% at time period 2. The daytime contribution by UCYN-B (time period 1) was surprising given that its preferred diazotrophic activity is at night [10,11,37,46,53,54,59,64,69]. Some of the daytime N_2 fixation activity can be attributed to activity during the filtration process, which started at the end of the light period, and continued into the dark. Combined, the UCYN-A and UCYN-B contribute little (2.7–3.6%) to C fixation with UCYN-A playing a minor role in this estimate ($\geq$0.04%).

Conclusion

We report an optimized CARD-FISH assay for identifying and quantifying UCYN-A abundance in the environment. A distinct advantage of the CARD-FISH assay compared to qPCR is that the life style of a cell (i.e. attached, living freely) can be visualized in addition to quantifying the cells' abundances. However, we found that sample collection can be disruptive since we only observed UCYN-A living in association with a small eukaryotic cell when the samples were not size-fractionated or filtered with a peristaltic pump. Interestingly though, a similar association between UCYN-A and a picoeukaryote which was reported in Pacific samples was detected in several samples from the North Atlantic. The observations in the North Atlantic cover distant locations and seasons, suggesting that the partnership between UCYN-A and a picoeukaryote is not geographically or seasonally isolated.

Our data also indicated that free UCYN-A contributed little to bulk N_2 and C fixation at our field site and much of the activity is derived from other co-occurring unidentified populations. However, it is likely that we underestimated N_2 fixation given the recent evidence about problems with bubble dissolution [24,36,66]. In addition, if UCYN-A was attached to another cell prior to our measurements likely some of the fixed N was transferred as has been observed previously [57]. The rates measured for UCYN-A therefore represent a minimum estimate, and would have been more underestimated relative to the rates of the *Crocsphaera*-like cells because of the start of the incubations coinciding with the most active N_2 fixation period for UCYN-A. Although few in number (<5 L^{-1}), the larger colonial diazotroph *Trichodesmium* spp. and the symbiotic *R. intracellularis* were also observed on the filters from the incubation samples. These species are known to have high N_2 fixation rates [7,18,33], and they also co-occur with a rich diversity of heterotrophic N_2 fixing populations [25,28,70,71]. The novel single cell approaches presented here are very promising and allow for the interrogation of the uncultivated majority, and emphasize the importance of quantifying the impact of various populations performing N_2 fixation.

Acknowledgments

The authors would like to thank Jörg Wulf, Daniela Franzke, Abdul Rahiman Sheik, Birgit Adam, Gaute Lavik, Thomas Max and Gabriele Klockgether for their technical assistance. We thank Jonathan P. Zehr, Brandon Carter, and Anne Thompson of the University of California for samples used to test our assays and many discussions on results presented herein. We thank two anonymous reviewers for their comments and helpful suggestions for improving our manuscript. We would also like to thank Hannah Halm and Philip Raab for their assistance and the captain and crew of the Synagoga and R/V Islandia for their help during sample collections in 2008 and 2010. A special acknowledgement to Oscar Melicio, Carlos Ferreira Santos, Pericles Silva, Ivanice Monteiro, and Nuno Vieira of the Insituto Nacional de Deesenvolvimento das Pescas (INDP), Cape Verde, for hosting and assisting our expedition. We thank the captain and crew of the R/V Maria S. Merian for help with sampling during the MSM 03/1 VISION from Island to the Azores expedition. AK also thanks Sara J. Bender for her helpful comments and discussions of the manuscript. This work was supported by the Max Planck Society and JL and WM thank the Bundesministerium für Bildung und Forschung (BMBF) for financial support through the SOPRAN II (Surface Ocean Processes in the Anthropocene) project, grant number.

Appendix A. Supplementary data

Supplementary data associated with this article can be found, in the online version, at http://dx.doi.org/10.1016/j.syapm.2013.02.002.

References

[1] Amann, R.I., Binder, B.J., Olson, R.J., Chisholm, S.W., Devereux, R., Stahl, D.A. (1990) Combination of 16S rRNA-targeted oligonucleotide probes with flow cytometry for analyzing mixed microbial populations. Appl. Environ. Microbiol. 56, 1919–1925.
[2] Behrens, S., Lösekann, T., Pett-Ridge, J., Weber, P.K., Ng, W.O., Stevenson, B.S., et al. (2008) Linking microbial phylogeny to metabolic activity at the single-cell level by using enhanced element labeling-catalyzed reporter deposition fluorescence in situ hybridization (EL-FISH) and NanoSIMS. Appl. Environ. Microbiol. 74, 3143–3150.
[3] Bench, S.R., Ilikchyan, I.N., Tripp, H.J., Zehr, J.P. (2011) Two strains of *Crocosphaera watsonii* with highly conserved genomes are distinguished by strain-specific features. Front. Aquat. Microbiol. 2, 1–13.
[4] Biegala, I.C., Raimbault, P. (2008) High abundance of diazotrophic picocyanobacteria (<3 μm) in a Southwest Pacific coral lagoon. Aquat. Microb. Ecol. 51, 45–53.
[5] Binder, B.J., Chisholm, S.W. (1990) Relationship between DNA cycle and growth rate in *Synechococcus* sp. strain PCC 6301. J. Bacteriol. 172, 2313–2319.
[6] Capone, D.G. (2001) Marine nitrogen fixation: what's the fuss? Curr. Opin. Microbiol. 4, 341–348.
[7] Capone, D.G., Burns, J.A., Montoya, J.P., Subramaniam, A., Mahaffey, C., Gunderson, T., et al. (2005) Nitrogen fixation by *Trichodesmium* spp.: an important source of new nitrogen to the tropical and subtropical North Atlantic Ocean. Glob. Biogeochem. Cycles 19, http://dx.doi.org/10.1029/2004GB002331.
[8] Capone, D.G., Zehr, J.P., Paerl, H.W., Bergman, B., Carpenter, E.J. (1997) *Trichodesmium*, a globally significant marine cyanobacterium. Science 276, 1221–1229.
[9] Carpenter, E.J., Price, C.C. (1976) Marine *Oscillatoria* (*Trichodesmium*): explanation for aerobic nitrogen fixation without heterocysts. Science 191, 1278–1280.
[10] Church, M.J., Jenkins, B.D., Karl, D.M., Zehr, J.P. (2005) Vertical distributions of nitrogen-fixing phylotypes at stn ALOHA in the oligotrophic North Pacific Ocean. Aquat. Microb. Ecol. 38, 3–14.
[11] Church, M.J., Short, C.M., Jenkins, B.D., Karl, D.M., Zehr, J.P. (2005) Temporal patterns of nitrogenase gene (*nifH*) expression in the oligotrophic North Pacific Ocean. Appl. Environ. Microbiol. 71, 5362–5370.
[12] Daims, H., Brühl, A., Amann, R., Schleifer, K.H., Wagner, M. (1999) The domain-specific probe EUB338 is insufficient for the detection of all bacteria: development and evaluation of a more comprehensive probe set. Syst. Appl. Microbiol. 22, 434–444.
[13] Dekas, A.E., Orphan, V.J. (2011) Identification of diazotrophic microorganisms in marine sediment via fluorescence in situ hybridization coupled to nanoscale secondary ion mass spectrometry (FISH-NanoSIMS). Methods Enzymol. 486, 281–305.

[14] Dore, J.E., Brum, J.R., Tupas, L.M., Karl, D.M. (2002) Seasonal and interannual variability in sources of nitrogen supporting export in the oligotrophic subtropical North Pacific Ocean. Limnol. Oceanogr. 47, 1595–1607.

[15] Falcón, L.I., Carpenter, E.J., Cipriano, F., Bergman, B., Capone, D.G. (2004) N_2 fixation by unicellular bacterioplankton from the Atlantic and Pacific Oceans: phylogeny and *in situ* rates. Appl. Environ. Microbiol. 70, 765–770.

[16] Falcón, L.I., Pluvinage, S., Carpenter, E.J. (2005) Growth kinetics of marine unicellular N_2-fixing cyanobacterial isolates in continuous culture in relation to phosphorus and temperature. Mar. Ecol. Prog. Ser. 285, 3–9.

[17] Foster, R.A., Carpenter, E.J., Bergman, B. (2006) Unicellular cyanobionts in open ocean dinoflagellates, radiolarians, and tintinnids: Ultrastructural characterization and immuno localization of phycoerythrin and nitrogenase. J. Phycol. 42, 453–463.

[18] Foster, R.A., Kuypers, M.M.M., Vagner, T., Paerl, R.W., Musat, N., Zehr, J.P. (2011) Nitrogen fixation and transfer in open ocean diatom–cyanobacterial symbioses. ISME J. 5, 1484–1493.

[19] Foster, R.A., O'Mullan, G.D. (2008) Nitrogen-fixing and nitrifying symbioses in the marine environment. In: Capone, D.G., Bronk, D.A., Mulholland, M.R., Carpenter, E.J., Burlington, M.A. (Eds.), Nitrogen in the marine environment, Elsevier Science, pp. 1197–1218.

[20] Foster, R.A., Subramaniam, A., Mahaffey, C., Carpenter, E.J., Capone, D.G., Zehr, J.P. (2007) Influence of the Amazon River plume on distributions of free-living and symbiotic cyanobacteria in the western tropical north Atlantic Ocean. Limnol. Oceanogr. 52, 517–532.

[21] Foster, R.A., Subramaniam, A., Zehr, J.P. (2009) Distribution and activity of diazotrophs in the Eastern Equatorial Atlantic. Environ. Microbiol. 11, 741–750.

[22] Fuchs, B.M., Glöckner, F.O., Wulf, J., Amann, R. (2000) Unlabeled helper oligonucleotides increase the in situ accessibility to 16S rRNA of fluorescently labeled oligonucleotide probes. Appl. Environ. Microbiol. 66, 3603–3607.

[23] Goebel, N.L., Edwards, C.A., Carter, B.J., Achilles, K.M., Zehr, J.P. (2008) Growth and carbon content of three different sized diazotrophic cyanobacteria observed in the subtropical North Pacific. J. Phycol. 44, 1212–1220.

[24] Großkopf, T., Mohr, W., Baustian, T., Schunck, H., Gill, D., Kuypers, M.M.M., et al. (2012) Doubling of marine dinitrogen-fixation rates based on direct measurements. Nature 488, 361–364.

[25] Halm, H., Lam, P., Ferdelman, T.G., Lavik, G., Dittmar, T., LaRoche, J., et al. (2012) Heterotrophic organisms dominate nitrogen fixation in the South Pacific Gyre. ISME J. 6, 1238–1249.

[26] Hecky, R.E., Kilham, P. (1988) Nutrient limitation of phytoplankton in freshwater and marine environments: a review of recent evidence on the effects of enrichment. Limnol. Oceanogr. 33, 796–822.

[27] Jardillier, L., Zubkov, M.V., Pearman, J., Scanlan, D.J. (2010) Significant CO_2 fixation by small prymnesiophytes in the subtropical and tropical northeast Atlantic Ocean. ISME J. 4, 1180–1192.

[28] Karl, D., Michaels, A., Bergman, B., Capone, D., Carpenter, E., Letelier, R., et al. (2002) Dinitrogen fixation in the world's oceans. Biogeochemistry 57, 47–98.

[29] Langlois, R.J., Hummer, D., LaRoche, J. (2008) Abundances and distributions of the dominant *nifH* phylotypes in the Northern Atlantic Ocean. Appl. Environ. Microbiol. 74, 1922–1931.

[30] LaRoche, J., Breitbarth, E. (2005) Importance of the diazotrophs as a source of new nitrogen in the ocean. J. Sea Res. 53, 67–91.

[31] Le Moal, M., Collin, H., Biegala, I.C. (2011) Intriguing diversity among diazotrophic picoplankton along a Mediterranean transect: a dominance of rhizobia. Biogeosciences 8, 827–840.

[32] Luo, Y.W., Doney, S.C., Anderson, L.A., Benavides, M., Bode, A., Bonnet, S., et al. (2012) Database of diazotrophs in global ocean: abundances, biomass and nitrogen fixation rates. Earth Syst. Sci. Data 5, 47–106.

[33] Mague, T.H., Weare, N.M., Holm-Hansen, O. (1974) Nitrogen fixation in the north Pacific Ocean. Mar. Biol. 24, 109–119.

[34] Mazard, S.L., Fuller, N.J., Orcutt, K.M., Bridle, O., Scanlan, D.J. (2004) PCR analysis of the distribution of unicellular cyanobacterial diazotrophs in the Arabian Sea. Appl. Environ. Microbiol. 70, 7355–7364.

[35] Mills, M.M., Ridame, C., Davey, M., La Roche, J., Geider, R.J. (2004) Iron and phosphorus co-limit nitrogen fixation in the eastern tropical North Atlantic. Nature 429, 292–294.

[36] Mohr, W., Großkopf, T., Wallace, D.W.R., LaRoche, J. (2010) Methodological underestimation of oceanic nitrogen fixation rates. PLoS ONE 5, e12583, doi: 12510.11371/journal.pone.0012583.

[37] Mohr, W., Intermaggio, M.P., LaRoche, J. (2010) Diel rhythm of nitrogen and carbon metabolism in the unicellular, diazotrophic cyanobacterium *Crocosphaera watsonii* WH8501. Environ. Microbiol. 12, 412–421.

[38] Moisander, P.H., Beinart, R.A., Hewson, I., White, A.E., Johnson, K.S., Carlson, C.A., et al. (2010) Unicellular cyanobacterial distributions broaden the oceanic N_2 fixation domain. Science 327, 1512–1514.

[39] Montoya, J.P., Holl, C.M., Zehr, J.P., Hansen, A., Villareal, T.A., Capone, D.G. (2004) High rates of N_2 fixation by unicellular diazotrophs in the oligotrophic Pacific Ocean. Nature 430, 1027–1032.

[40] Montoya, J.P., Voss, M., Kahler, P., Capone, D.G. (1996) A simple, high-precision. high-sensitivity tracer assay for N_2-fixation. Appl. Environ. Microbiol. 62, 986–993.

[41] Moraru, C., Lam, P., Fuchs, B.M., Kuypers, M.M.M., Amann, R. (2010) GeneFISH – an *in situ* technique for linking gene presence and cell identity in environmental microorganisms. Environ. Microbiol. 12, 3057–3073.

[42] Mulholland, M.R., Bronk, D.A., Capone, D.G. (2004) Dinitrogen fixation and release of ammonium and dissolved organic nitrogen by *Trichodesmium* IMS101. Aquat. Microb. Ecol. 37, 85–94.

[43] Musat, N., Foster, R.A., Vagner, T., Adam, B., Kuypers, M.M.M. (2012) Detecting metabolic activities in single cells, with emphasis on nanoSIMS. FEMS Microbiol. Rev. 36, 486–511.

[44] Musat, N., Halm, H., Winterholler, B., Hoppe, P., Peduzzi, S., Hillion, F., et al. (2008) A single-cell view on the ecophysiology of anaerobic phototrophic bacteria. Proc. Natl. Acad. Sci. U S A 105, 17861–17866.

[45] Needoba, J.A., Foster, R.A., Sakamoto, C., Zehr, J.P., Johnson, K.S. (2007) Nitrogen fixation by unicellular diazotrophic cyanobacteria in the temperate oligotrophic North Pacific Ocean. Limnol. Oceanogr. 52, 1317–1327.

[46] Pennebaker, K., Mackey, K.R.M., Smith, R.M., Williams, S.B., Zehr, J.P. (2010) Diel cycling of DNA staining and nifH gene regulation in the unicellular cyanobacterium *Crocosphaera watsonii* strain WH 8501 (*Cyanophyta*). Environ. Microbiol. 12, 1001–1010.

[47] Pernthaler, A., Amann, R. (2004) Simultaneous fluorescence in situ hybridization of mRNA and rRNA in environmental bacteria. Appl. Environ. Microbiol. 70, 5426–5433.

[48] Pernthaler, A., Pernthaler, J., Amann, R. (2004) Sensitive multi-color fluorescence in situ hybridization for the identification of environmental microorganisms. In: Kowalchuk, G.A., de Bruijn, F.J., Head, I.M., Akkermans, A.D.L., van Elsas, J.D. (Eds.), Molecular Microbial Ecology Manual, Kluwer Academic Publishers, pp. 711–726.

[49] Polerecky, L., Adam, B., Milucka, J., Musat, N., Vagner, T., Kuypers, M.M.M. (2012) Look@NanoSIMS – a tool for the analysis of nanoSIMS data in environmental microbiology. Environ. Microbiol. 4, 1009–1023.

[50] Rasband, W.S. 1997ndash2005 ImageJ, US National Institutes of Health, Bethesda, M. D.

[51] Rijkenberg, M.J.A., Langlois, R.J., Mills, M.M., Patey, M.D., Hill, P.G., Nielsdottir, M.C., et al. (2011) Environmental forcing of nitrogen fixation in the Eastern Tropical and Sub-Tropical North Atlantic Ocean. PLoS ONE 6, http://dx.doi.org/10.1371/journal.pone.0028989.

[52] Ryther, J.H., Dunstan, W.M. (1971) Nitrogen, phosphorus, and eutrophication in the coastal marine environment. Science 171, 1008–1013.

[53] Saito, M.A., Bertrand, E.M., Dutkiewicz, S., Bulygin, V.V., Moran, D.M., Monteiro, F.M., et al. (2011) Iron conservation by reduction of metalloenzyme inventories in the marine diazotroph *Crocosphaera watsonii*. Proc. Natl. Acad. Sci. U S A 108, 2184–2189.

[54] Shi, T., Ilikchyan, I., Rabouille, S., Zehr, J.P. (2010) Genome-wide analysis of diel gene expression in the unicellular N_2-fixing cyanobacterium *Crocosphaera watsonii* WH 8501. ISME J. 4, 621–632.

[55] Short, S.M., Jenkins, B.D., Zehr, J.P. (2004) Spatial and temporal distribution of two diazotrophic bacteria in the Chesapeake Bay. Appl. Environ. Microbiol. 70, 2186–2192.

[56] Sohm, J.A., Webb, E.A., Capone, D.G. (2011) Emerging patterns of marine nitrogen fixation. Nat. Rev. Microbiol. 9, 499–508.

[57] Thompson, A.W., Foster, R.A., Krupke, A., Carter, B.J., Musat, N., Vaulot, D., et al. (2012) Unicellular cyanobacterium symbiotic with a single-celled eukaryotic alga. Science 337, 1546–1550.

[58] Tripp, H.J., Bench, S.R., Turk, K.A., Foster, R.A., Desany, B.A., Niazi, F., et al. (2010) Metabolic streamlining in an open-ocean nitrogen-fixing cyanobacterium. Nature 464, 90–94.

[59] Tuit, C., Waterbury, J., Ravizza, G. (2004) Diel variation of molybdenum and iron in marine diazotrophic cyanobacteria. Limnol. Oceanogr. 49, 978–990.

[60] Turk, K.A., Rees, A.P., Zehr, J.P., Pereira, N., Swift, P., Shelley, R., et al. (2011) Nitrogen fixation and nitrogenase (*nifH*) expression in tropical waters of the eastern North Atlantic. ISME J. 5, 1201–1212.

[61] Voss, M., Croot, P., Lochte, K., Mills, M., Peeken, I. (2004) Patterns of nitrogen fixation along 10 N in the tropical Atlantic. Geophys. Res. Lett. 31, L23S09, http://dx.doi.org/10.1029/2004GL020127.

[62] Wagner, M. (2009) Single-cell ecophysiology of microbes as revealed by Raman microspectroscopy or secondary ion mass spectrometry imaging. Annu. Rev. Microbiol. 63, 411–429.

[63] Wallner, G., Amann, R., Beisker, W. (1993) Optimizing fluorescent *in situ* hybridization with rRNA targeted oligonucleotide probes for flow cytometric identification of microorganisms. Cytometry 14, 136–143.

[64] Webb, E.A., Ehrenreich, I.M., Brown, S.L., Valois, F.W., Waterbury, J.B. (2009) Phenotypic and genotypic characterization of multiple strains of the diazotrophic cyanobacterium, *Crocosphaera watsonii*, isolated from the open ocean. Environ. Microbiol. 11, 338–348.

[65] Whitton, B.A., Carr, N.G., Craig, I.W. (1971) A comparison of the fine structure and nucleic acid biochemistry of chloroplasts and blue-green algae. Protoplasma 72, 325–357.

[66] Wilson, S.T., Böttjer, D., Church, M.J., Karl, D.M. (2012) Comparative assessment of nitrogen fixation methodologies conductedin the oligotrophic North Pacific Ocean. Appl. Environ. Microbiol. 78, 6516–6523.

[67] Wilson, S.T., Tozzi, S., Foster, R.A., Ilikchyan, I., Kolber, Z.S., Zehr, J.P., et al. (2010) Hydrogen cycling by the unicellular marine diazotroph *Crocosphaera watsonii* strain WH8501. Appl. Environ. Microbiol. 76, 6797–6803.

[68] Zehr, J.P., Bench, S.R., Carter, B.J., Hewson, I., Niazi, F., Shi, T., et al. (2008) Globally distributed uncultivated oceanic N_2-fixing cyanobacteria lack oxygenic photosystem II. Science 322, 1110–1112.

[69] Zehr, J.P., Bench, S.R., Mondragon, E.A., McCarren, J., DeLong, E.F. (2007) Low genomic diversity in tropical oceanic N_2-fixing cyanobacteria. Proc. Natl. Acad. Sci. USA 104, 17807–17812.

[70] Zehr, J.P., Jenkins, B.D., Short, S.M., Steward, G.F. (2003) Nitrogenase gene diversity and microbial community structure: a cross system comparison. Environ. Microbiol. 5, 539–554.
[71] Zehr, J.P., Mellon, M.T., Zani, S. (1998) New nitrogen-fixing microorganisms detected in oligotrophic oceans by amplification of nitrogenase (*nifH*) genes. Appl. Environ. Microbiol. 64, 3444–3450.
[72] Zehr, J.P., Montoya, J.P., Jenkins, B.D., Hewson, I., Mondragon, E., Short, C.M., et al. (2007) Experiments linking nitrogenase gene expression to nitrogen fixation in the North Pacific subtropical gyre. Limnol. Oceanogr. 52, 169–183.
[73] Zehr, J.P., Waterbury, J.B., Turner, P.J., Montoya, J.P., Omoregie, E., Steward, G.F., et al. (2001) Unicellular cyanobacteria fix N_2 in the subtropical North Pacific Ocean. Nature 412, 635–637.

2.2.1 Manuscript II: Supplementary Information

Probe design and optimizations

The UCYN-A specific probes, UCYN-A732 and UCYN-A159, and the corresponding helpers and competitor oligonucleotides (Table 1) were designed with the PROBE DESIGN tool of the ARB software [1]. The 16S rRNA sequences used for the probe design were obtained from GENBANK (Accession numbers: JQ246083-JQ246089; EU188119, EU1188123, EU188133, EU1188142, EU188278, EU188382, CP001842). 16S rRNA sequences were also obtained by cloning and sequencing DNA amplicons derived from PCRs on samples collected from stations in the vicinity of the Cape Verde (CV) Islands (including the field site reported here)(GENBANK accession numbers JQ246081, JQ246082, JQ246089) and from PCRs of cells collected by flow cytometry from the subtropical North Pacific (GENBANK, accession numbers JQ246083-246088) courtesy of Dr. Jonathan P. Zehr laboratory (University of California, Santa Cruz).

Probe specificities were checked against the ARB and SILVA databases [3] and the Ribosomal Database Project [2]. Only the UCYN-A 16S rRNA sequence showed 100 % identity with the UCYN-A732 and UCYN-A159 probes. The stringent formamide (FA) concentration for each probe was determined in hybridization assays with increasing FA concentrations from 0 to 70 % at 5 % increments. After incubation with each FA concentration, the hybridized filters were visually inspected and evaluated using fluorescence microscopy.

We used flow cytometric sorted cells (1.0 - 3.0 µm cell diameter gate), pre-screened for UCYN-A by *nifH* qPCR assays, as representative positive controls to verify the UCYN-A732 probe specificity and the hybridization conditions (e.g. 50 % FA concentration, the use of helper oligonucleotides, hybridization temperature of 35 ^{o}C). A second sample and negative control comprised of flow cytometric sorted pico-cyanobacteria identified by forward scatter (FSC) and red fluorescence (488 nm laser) as *Synechococcus* cells, was also tested with the UCYN-A732 probe (both samples courtesy of Zehr laboratory, University of California). In both assays, the competitor oligonucleotide was omitted, but the helper oligonucleotides were used; the hybridization was positive for the UCYN-A enriched sample and no hybridization was observed in the

Synechococcus sample. However, in order to ensure probe specificity in our field samples, a competitor oligonucleotide *C. watsonii*-732 was designed and used in combination with the specific probe UCYN-A732 and the two helpers in an improved hybridization assay.

Formamide concentration

For the UCYN-A732 probe, evaluation of stringent FA concentration was done using field samples from CV (December 2010), as well as filters containing cells of *C. watsonii* WH8501. *Crocosphaera watsonii* contains 1 mismatch on the target site to the UCYN-A732 probe. The least cross-hybridization to *C. watsonii* WH8501 cells occurred at 50 % and 55 % FA; no cross-hybridization with *C.watsonii* WH8501 cells occurred above 55 % FA. However, when field samples were tested, a decrease in signal intensity of the hybridized target cells was observed at 55 % and 60 % FA. Above 60 % FA, no hybridized cells could be detected on the filters. As such, we determined that the optimal FA concentration that ensures high signal detection of the UCYN-A target cells with minimum cross-hybridization was 50 % FA for UCYN-A732 probe. Moreover, the probe accessibility to the UCYN-A 16S rRNA was enhanced by using the probe in combination with two unlabeled oligonucleotides called helpers A and B located up and downstream of the probe (Table 1).

For UCYN-A159, the evaluation of stringent FA concentrations was done only on CV field samples (2010) in the same way as described for UCYN-A732. The highest FA concentration that showed optimal signal intensity of the hybridized cells was 60 % FA. We tested the specificity of UCYN-A159 at 60 % FA concentration in a double hybridization approach with the UCYN-A732 probe in combination with the corresponding helpers and competitor oligonucleotides *C.watsonii*-732 and *P.marinus*-159 (Table 1) and two different tyramides dyes (Alexa488 and Alexa594)(see below)(Fig. 2C). At higher FA concentrations (i.e 65 % and 70 %), the signal intensity of UCYN-A159 decreased considerably. At lower FA concentrations (i.e. 45, 50 and 55 %), probe signal intensity was as high as observed in the 60 % FA. However, these lower FA concentrations need to be further tested for probe specificity, either against the 1 mismatch control *P. marinus* or in combination with UCYN-A732 probe.

Dual Hybridizations

Two dual hybridizations were performed using a combination of HRP-UCYN-A732 and HRP-UCYN-A159 in the first assay and HRP-UCYN-A732 and HRP-*C. watsonii*-732 competitor oligonucleotide in the second assay. In both dual hybridizations, Alexa488 tyramide was used for the first hybridization, whereas Alexa594 tyramide was used in the second hybridization. The procedures are similar to those described above for a single hybridization: cell permeabilization, followed by the first hybridization and detection of the probe. Subsequently, the HRP introduced in the first hybridization is inactivated using 30 % H_2O_2 for 10 min at room teperature, followed by an ultrapure water wash step and a second hybridization with no second permeabilization. Standard mounting and epifluoresence microscopy is used for visualization.

It should be noted that due to a sequence error, CARD-FISH counts and HISH-SIMS analyses were initially performed with a helper B probe that lacked the 3rd base on the 5' end. The error was corrected, tested, and we concluded that the sequence error did not influence the binding ability of the helper or the probe specificity.

Calculations. The biovolume (V) was calculated for each individual cell according to Sun and Liu [4]:

$$V = (\pi/6) \times Ø^3 \quad (1)$$

where Ø is the cell diameter. Estimates of carbon (C) content per cell used the relationship described by Verity et al. [6]:

$$\text{Log}\,[C] = -0.363 + (0.863 \times (\text{Log}\,(V)) \quad (2)$$

The C content per cell (C_{con}) was converted into N content per cell (N_{con}) based on conversion factors provided by Tuit et al. [5] assuming a modified Redfield ratio (C:N) of 8.6.

The isotopic ratios ($R_C = {}^{13}C/{}^{12}C$ and $R_N = {}^{15}N/{}^{14}N$) based on ROI selections and SIMS analysis were used to calculate atom percent (AT %) enrichment of ^{13}C or ^{15}N by:

$$A_C = R_C/(R_C + 1) \quad (3)$$

$$A_N = R_N/(R_N + 1) \quad (4)$$

where A_C represents AT % enrichment of ^{13}C and A_N represents the AT % enrichment of ^{15}N. The cell specific C and N_2 assimilation (F_C or F_N) was calculated for each time point by:

$$F_C = ({}^{13}C_{ex} \times C_{con})/C_{SR} \quad (5)$$

$$F_N = ({}^{15}N_{ex} \times N_{con})/N_{SR} \quad (6)$$

where ${}^{13}C_{ex}$ and ${}^{15}N_{ex}$ represent the atom % enrichment of ${}^{13}C$ and ${}^{15}N$ of the individual ROIs from which we subtracted the mean atom % ${}^{13}C$ and ${}^{15}N$ of the time 0 samples of bulk particulate pools measured by the EA-IRMS. We also measured the atom % ${}^{13}C$ and ${}^{15}N$ for individual UCYN-A and *C. watsonii*-like cells from the time 0 samples using nanoSIMS in order to use these as the natural abundance values of C and N isotopes for each cell population. However, the nanoSIMS at our institute is optimized to measure isotopic ratios for enriched cells and therefore the measurements of natural abundance are not well calibrated. The EA-IRMS, which is calibrated for both non-enriched and enriched samples with high instrument accuracy and precision (e.g. 0.3651 ± 0.0000 ${}^{15}N$ atom % and 1.0658 ± 0.0004 ${}^{13}C$ atom % based on the mean and standard deviation of caffeine standards measured in conjunction with the samples) was used to measure natural abundances of C and N isotopes in the particulate fraction. These latter values were used for normalization of ${}^{13}C_{ex}$ and ${}^{15}N_{ex}$. The C_{SR} and N_{SR} is the estimated labelling percentage of C and N in the experimental bottle.

References

[1] Ludwig, W., Strunk, O., Westram, R., Richter, L., Meier, H. (2004) ARB: A software environment for sequence data. Nucleic Acids Res. 32, 1363□1371.
[2] Maidak, B.L., Cole, J.R., Lilburn, T.G., Parker Jr, C.T., Saxman, P.R., Stredwick, J.M., et al. (2000) The RDP (ribosomal database project) continues. Nucleic Acids Res. 28, 173□174.
[3] Pruesse, E., Quast, C., Knittel, K., Fuchs, B.M., Ludwig, W., Peplies, J., et al. (2007) SILVA: A comprehensive online resource for quality checked and aligned ribosomal RNA sequence data compatible with ARB. Nucleic Acids Res. 35, 7188□7196.
[4] Sun, J., Liu, D. (2003) Geometric models for calculating cell biovolume and surface area for phytoplankton. J. Plank. Res. 25, 1331□1346.
[5] Tuit, C., Waterbury, J., Ravizza, G. (2004) Diel variation of molybdenum and iron in marine diazotrophic cyanobacteria. Limnol. Oceanogr. 49, 978□990.
[6] Verity, P.G., Robertson, C.Y., Tronzo, C.R., Andrews, M.G., Nelson, J.R., Sieracki, M.E. (1992) Relationships between cell volume and the carbon and nitrogen content of marine photosynthetic nanoplankton. Limnol. Oceanogr. 37, 1434□1446.

Supplementary Fig. 1. Epifluorescent images of the UCYN-A732 probe used in assays with and without helpers A and B. (A-B) UCYN-A cell hybridized without helpers required a longer exposure time (935 ms) to visualize and resulted in higher background signal (arrows). (C-D) A UCYN-A cell hybridized with helpers required a shorter exposure time (211 ms) and results in lower background signals. The overlay of the UCYN-A cell hybridized with the UCYN-A probe (green), natural auto-fluorescence (red) of the partner cell and DAPI (blue) are shown in A and C. Scale bar is 2.0 µm.

Supplementary Fig. 2. An overlay of epifluorescent images of *C. watsonii* WH8501 cells hybridized with UCYN-A732, helpers at two different FA concentrations: (A) 45% and (B) 50%. The probe signal emits green while natural auto-fluorescence of *C. watsonii* WH8501 phycoerythrin is red. Note the increased stringency of UCYN-732A probe at 50% FA. Scale bar is 2.0 □m.

Supplementary Table 1. Summary of types of samples collected and locations in the North Atlantic Ocean reported here. The cross indicates that samples have been collected for the designated type of analysis.

Supplementary Table 2. Summary of the cell diameter measured microscopically on field populations of attached and free UCYN-A (free) cells and their partner cells collected in various locations of the subtropical North Atlantic Ocean. Locations of collections are shown in Fig. 1.

Supplementary Fig. 1

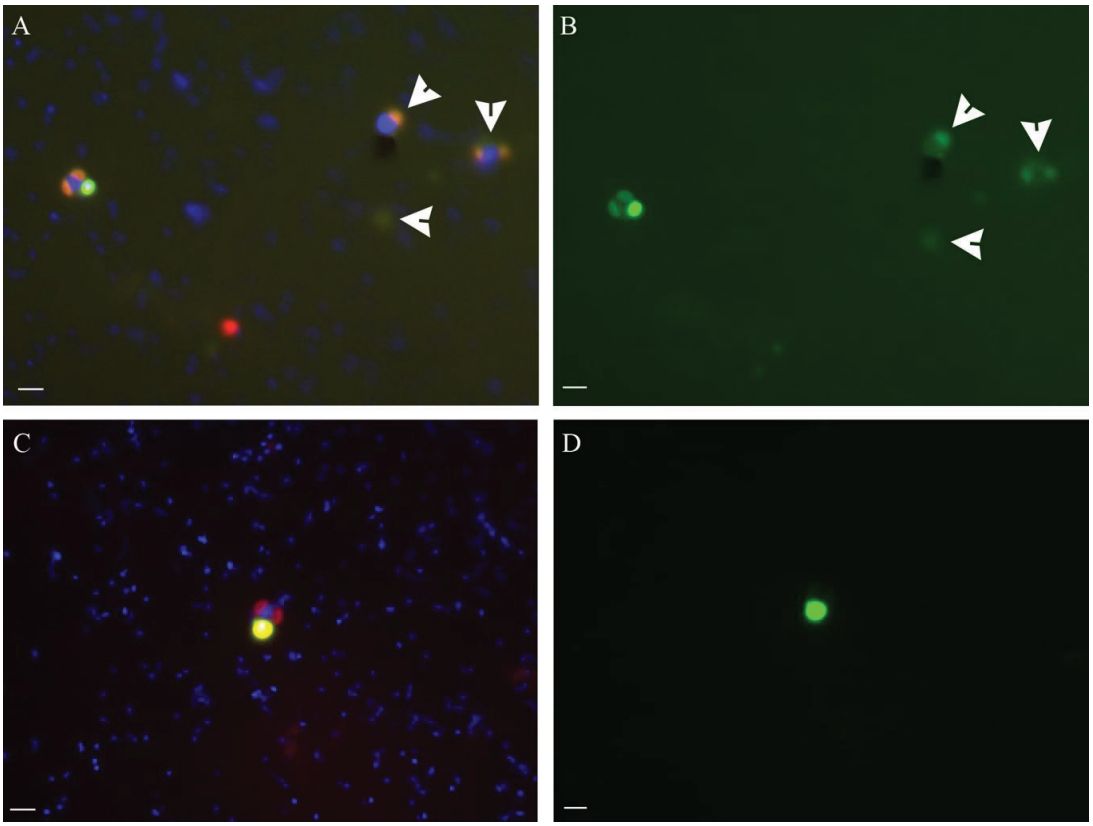

Supplementary Fig. 2

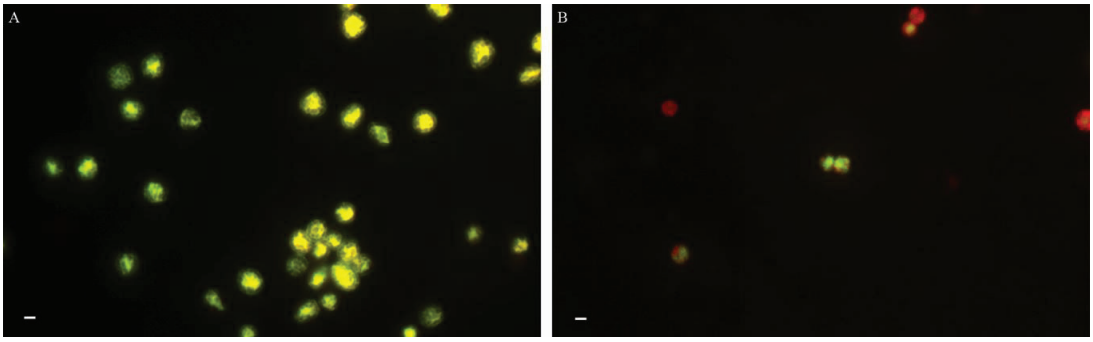

Supplementary Table 1

Expedition	Latitude	Longitude	Date	Experiment	Depth [m]	sample type			
						EA-IRMS	DNA/RNA	FISH	nanoSIMS
Cape Verde 2010	16.76 N	25.12 W	12/03/10	1	0	X	X	X	X
			12/05/10	2	0	X	X	X	X
			12/08/10	3	0	X	X	X	X
			12/08/10	Depth profile	1, 30, 60	-	X	X	-
			12/10/10	Diel	0	-	X	-	-
			12/5/10	Size fractionation	0		X	X	
Cape Verde 2009	17.03 N	24.78 W	5/25/09	-	10	-	-	X	-
MSM 08/1	17.08 N	23.00 W	4/23/08	-	10	-	-	X	-
VISION 2006	34.07 N	30.00 W	9/30/06	-	30	-	-	X	-

Supplementary Table 2.

Sample location and date	UCYN-A cell diameter (□m)	Partner cell diameter (□m)
North Atlantic September 2006	2.09	4.28
North Atlantic September 2006	1.26	2.09
North Atlantic September 2006	1.44	2.39
CV April 2008	2.94	5.57
CV April 2008	2.96	4.68
CV April 2008	2.19	4.06
CV May 2009	1.15	1.99
CV December 2010	1.52	free
CV December 2010	1.74	free
CV December 2010	1.31	free
CV December 2010	1.31	free
CV December 2010	1.38	free
CV December 2010	1.17	free
CV December 2010	1.03	free
CV December 2010	1.27	free
CV December 2010	1.31	free
CV December 2010	1.25	free
CV December 2010	1.06	free
CV December 2010	1.06	free
CV December 2010	0.97	free
CV December 2010	1.52	free
CV December 2010	1.64	free
CV December 2010	1.32	free
CV December 2010	1.54	free
CV December 2010	1.36	free
CV December 2010	1.10	free
CV December 2010	1.37	free
CV December 2010	1.51	free
CV December 2010	1.52	free
CV December 2010	1.19	free
CV December 2010	1.50	free
CV December 2010	1.02	free
CV December 2010	1.05	free
CV December 2010	0.99	free
CV December 2010	1.16	free
CV December 2010	0.69	free
CV December 2010	1.10	free
CV December 2010	0.90	free
CV December 2010	1.06	free
CV December 2010	1.31	free
CV December 2010	1.06	free
CV December 2010	1.13	free
CV December 2010	0.98	free
CV December 2010	1.28	free

2.3 Manuscript III: Distribution of the association between unicellular algae and the dinitrogen (N_2) fixing cyanobacterium UCYN–A in the North Atlantic Ocean

Andreas Krupke[1]*, Gaute Lavik[1], Hannah Halm[1,2], Bernhard M Fuchs[1] Rudolf I Amann[1], Marcel MM Kuypers[1]

[1]Max Planck Institute for Marine Microbiology, 28359 Bremen, Germany
[2]Current address: Helmholtz–Zentrum Potsdam Deutsches GeoForschungsZentrum GFZ Mikrobielles GeoEngineering, 14473 Potsdam, Germany

*Corresponding author: Andreas Krupke, Department of Biogeochemistry, Max Planck Institute for Marine Microbiology, Celsiusstr. 1, 28359 Bremen, Germany.
Email: akrupke@mpi–bremen.de

Key words: Diazotrophss, *Haptophyta*, double CARD–FISH, symbiosis

Abstract

Dinitrogen (N_2) fixing microorganisms are important for marine ecosystems because they convert atmospheric N_2 gas into bioavailable nitrogen compounds, which affects marine productivity and carbon sequestration. The globally abundant, uncultured unicellular cyanobacteria UCYN–A was recently discovered living in association with a eukaryote. Here, we established a double CARD–FISH approach that identified both partners (i.e. UCYN–A and its associated eukaryote (e.g. *Haptophyta*) and provided quantitative information on their distribution and abundance across distinct water masses along a transect in the North Atlantic Ocean. The fixation of N_2 activity coincided with the detection of UCYN–A cells and was only observed in oligotrophic (<0.067 NO_3^- µM and <0.04 PO_4^{3-} µM), warm (>18 °C) surface waters. Parallel genomic analysis from these waters targeted unicellular diazotrophs; findings indicated that only UCYN–A cells were present, and when coupled to the N_2 fixation data, indicated that this group of microorganisms was partially responsible for N_2 fixation in this region. UCYN–A cells were enumerated in association with an algal partner or as free–living using the double CARD–FISH approach. We demonstrated that UCYN–A cells living in association with a *Haptophyta* were the dominant form (87.0±6.1%), whereas free–living UCYN–A cells represented only a minor fraction (5.2±3.9%). Interestingly, we also detected UCYN–A cells living in association with an unknown eukaryote (7.8±5.2%). This study provides useful information on the environmental factors that select for the distribution of the UCYN–A association and raises questions about the host specificity in the North Atlantic Ocean.

Introduction

Dinitrogen (N_2) fixation provides the main source of fixed nitrogen (N), the limiting nutrient for primary production, in open ocean ecosystems (Karl et al., 2002). A small and diverse group of microorganisms, commonly referred to as diazotrophs, perform the biologically mediated process of converting atmospheric N_2 gas into ammonia (NH_3), which is catalyzed by the nitrogenase enzyme complex (Zehr et al., 1998). These microorganisms are particularly favored in oligotrophic systems because of their ability to overcome N limitation (Zehr et al., 1998; Karl et al., 2002; Voss et al., 2004).

Cyanobacteria constitute the dominant diazotrophs in open ocean waters and their impact on the marine carbon (C) and N cycles is significant (Karl et al., 1997; Mahaffey et al., 2005; Capone and Knapp, 2007). The widely abundant filamentous non–heterocystous *Trichodesmium* sp. and diatom symbionts, such as *Richelia intracellularis*, are considered major contributors to N_2 fixation activity in the oceans (Mague et al., 1974; Capone et al., 1997; Carpenter et al., 1999). Foster et al. (2011) showed that substantial amounts of fixed N are transferred from the diazotroph to the host cell, leading to enhanced growth rates. These findings highlight the importance of eukaryotic–diazotrophic associations in the world's oceans and their influence on the marine C and N cycles.

The discovery of widely distributed new diazotrophic microorganisms (i.e. unicellular diazotrophs) in concert with elevated N_2 fixation activity indicated that these microorganisms constitute important members of the diazotrophic community (Zehr et al., 2001; LaRoche and Breitbarth, 2005; Langlois et al., 2008). In particular, the ubiquitous unicellular cyanobacteria UCYN–A, discovered more than one decade ago (Zehr et al., 1998), likely plays an important role in N_2 fixation (Zehr et al., 2008). Currently, our knowledge about these microorganisms is very limited because they have not been obtained in culture. The genome of UCYN–A lacks certain metabolic pathways characteristic for cyanobacteria (e.g. PSII, RuBisCo, TCA cycle), raising questions how these microbes thrive in the environment (Bothe et al., 2010; DeLong, 2010; Tripp et al., 2010). These remarkable findings in combination with a reduced genome size compared to other unicellular cyanobacteria suggests that UCYN–A depends on other microorganisms for organic carbon compounds to sustain growth requirements (Tripp et al., 2010).

The widely distributed UCYN–A population has recently been detected in association with an eukaryotic algae (Thompson et al., 2012). The authors observed the exchange of carbon and nitrogen based on stable isotope tracer incubation experiments in the North Pacific. This nutrient exchange may provide an explanation for how UCYN–A can thrive in oligotrophic environments despite lacking the genes for photosynthesis and other important biosynthetic pathways (Tripp et al., 2010). Our understanding of the ecophysiological interaction between UCYN–A and its partner cell is still limited. Whether or not this association is obligatory for UCYN–A survival remains to be answered since UCYN–A cells have also been observed as free–living (Thompson et al., 2012; Krupke et al., 2013). This association warrants further investigation in order to accurately quantify the distribution of UCYN–A as associated versus free–living, and to determine the biogeochemical importance of this association in oligotrophic surface waters.

In this study, the primary objective was to target both partners of the association described by Thompson et al. (2012) and to quantify their cellular abundance and distribution in the North Atlantic. We developed a double Catalyzed Reporter Deposition–Fluorescence *In Situ* Hybridization (double CARD–FISH) assay using a specific oligonucleotide probe for UCYN–A (Krupke et al., 2013) in combination with different oligonucleotides targeting various eukaryotic partners. This method was applied on samples collected along the 30° W meridian in the North Atlantic Ocean, crossing different biogeographical provinces (Longhurst, 1998). We provide quantitative information on the association between UCYN–A and the eukaryotic partner cell in the marine environment based on the double CARD–FISH approach. This study forms the foundation for future ecophysiological studies on this important group of diazotrophic cyanobacteria.

Material and methods

The VISION cruise MSM03/01 was conducted in September 2006 on board the German R/V Maria S. Merian. Seawater was collected in the North Atlantic from the Arctic Circle (66°39,27`N; 29°36,65`W) along the 30° W meridian towards the Azores (34°24,87`N; 28°28,90`W). This expedition covered 18 different stations (Supplementary Fig. 1) and water samples were retrieved using a rosette of 20 L Niskin bottles mounted on a conductivity–temperature–density profiler (CTD). In this study we mainly focus on samples collected within the upper water body (0–200 m depth).

Nutrient measurements. Seawater samples were collected and filtered immediately through 0.45 µm in–line filters attached to a 60 mL clean syringe and transferred into two Falcon™ tubes (Franklin Lakes, USA). Samples for the analysis of phosphate (PO_4^{3-}), nitrate (NO_3^-) and nitrite (NO_2^-) were stored at –80 °C and measured spectrophotometrically using a continuous–flow analyzer and standard AA3 methods (Seal Analytical, Norderstedt, Germany).

Stable isotope incubation experiments. Seawater from the upper water column (0–80 m) was collected in the morning (8–9 AM) or evening (5–6 PM) and transferred into light transparent 1.0 L incubation bottles and closed without air bubbles. Bottles were amended immediately with 4 mL $^{15}N_2$ gas (18.2–25.7% labeling) (98% + $^{15}N_2$, Sigma–Aldrich, St. Louis, MO, USA) and 200 µM ^{13}C bicarbonate solution ($H^{13}CO_3^-$) (6.7–8.0% labeling) (98% + $^{13}CO_2$, Sigma–Aldrich, St. Louis, MO, USA) with a gas tight syringe. After injection, bottles were shaken for 5 minutes and incubated in one replicate for several hours (1.2–12.7 h). For each experimental series, parallel dark incubation was also carried out by covering bottles with aluminum foil. Bottles from >40 m depth were covered using a black gauze material (mesh size 1 mm^2) to reduce light intensity. Samples obtained in the morning were incubated on deck in a water bath with continuously flowing surface seawater. Seawater samples collected in the evening were incubated in the lab placed in a chamber with continuously flowing surface seawater and *in situ* light conditions simulated with light bulbs.

EA–IRMS analysis. For the stable isotope incubation experiments, one 1.0 L incubation bottle per treatment was vacuum filtered onto pre–combusted 25 mm diameter Glass Fiber filters (Whatman GF/F; Sigma–Aldrich, St. Louis, MO, USA) held in a rosette filtration system (Millipore, Eschborn, Germany). The GF/F filters were freeze–dried

over night, acid–fumed (37% HCl) for 24 hours in a desiccator, and packaged for combustion analysis. We used an automated elemental analyzer (Thermo Flash EA, 1112 Series) coupled to a Delta Plus Advantage mass spectrometer (Thermo Finnigan, Dreieich, Germany) in order to measure the C and N content. CO_2 and N_2 fixation rates were calculated as a function of the change in the tracer concentration of the particulate organic pool over the incubation time, as described in detail in Montoya et al. (1996).

CARD–FISH sampling. Additional seawater (500 mL) was collected from each station throughout the water column (0–200 m depth) and used for CARD–FISH assays. Seawater was immediately fixed with formaldehyde solution (Fluka, Sigma–Aldrich, Germany) for 2 hours at room temperature (RT) (final concentration 1% v/v). After the fixative step seawater was vacuum–filtered at 100 mbar onto 0.2 µm pore size polycarbonate filters (Millipore, Eschborn, Germany) (Gómez–Pereira et al., 2010). Subsequently, filters were washed twice with 10 mL sterile MilliQ (MQ) water and stored frozen at –20° C until further processing.

Double CARD–FISH assay. In the first round of hybridization, specific oligonucleotide probes, including: PRAS04 (Not et al., 2004), COCCO01 (Eller et al., 2007) and PRYM02 (Simon et al., 2000), were applied following standard protocols (Pernthaler and Amann, 2004; Pernthaler et al., 2004) in order to target the 18S rRNA of eukaryotic cells that potentially live in association with UCYN–A cells (Table 1). In the second round of hybridization, the oligonucleotide probe UCYN–A732 targeting the 16S rRNA specific for UCYN–A cells and its corresponding helper probes Helper A–732 and Helper B–732 were applied according to Krupke et al. (2013) (Table 1). At each hybridization step the used HRP–oligonucleotide probes were at working solutions of 8.42 pmol μL^{-1} diluted in the hybridization buffer (1:300; v:v). During the double CARD–FISH approach, the oligonucleotides EUB I–III (Amann et al., 1990) or EUK516 (Amann et al., 1990) were used as positive controls and the oligonucleotide NON338 (Wallner et al., 1993) as a negative control (Table 1). All hybridizations were performed at optimal formamide (FA) concentrations to ensure maximal stringency (Table 1).

Phylogenetic identification and cell counts were performed on filter sections using standard protocols (Pernthaler et al., 2004; Pernthaler and Pernthaler, 2007) with some changes for the double CARD–FISH assays. The cell wall was permeabilized by treatment with lysozyme solution (10 mg mL^{-1} in 0.05 M EDTA, pH 8.0; 0.1 M TrisHCl;

Fluka, Taufkirchen, Germany) for 1 h at 37 °C, followed by the inactivation of endogenous peroxidases using 0.01 M HCl for 10 min at RT. During the first CARD–FISH, eukaryotic cells were hybridized for 3 h at 46 °C and washed in washing buffer for 15 min at 48 °C. The first CARD was performed for 20 min at 46 °C using Alexa594 tyramides (Molecular probes, Leiden, The Netherlands) (Pernthaler et al., 2004). Afterwards, filter sections were washed in 1 x PBS for 10–20 minutes in the dark and placed in 3% H_2O_2 solution for 20 min at RT in order to inactivate the HRP for the second CARD–FISH. Therefore, UCYN–A cells were hybridized for 8 h at 35 °C and washed in washing buffer for 15 min at 37 °C. The second CARD was performed for 20 min at 46 °C using Oregon Green 488 tyramides (Molecular probes, Leiden, The Netherlands). The cells were counterstained with 1 µg mL^{-1} 4',6–diamidino–2–phenylindol (DAPI) for 10 min at RT in the dark. For microscopy counts, filter sections were embedded in a mixture of low fluorescence glycerol mountant (Citifluor AF1, Citifluor Ldt London, United Kingdom) and mounting fluid Vecta Shield (Vecta Laboratories, Burlingame, CA USA) in a 4:1 ratio.

Microscopy and cell abundances. Microscopic evaluation and counting was performed with a Zeiss Axioskop II fluorescence microscope (Zeiss, Berlin, Germany). Initial counting attempts were conducted under 1000x magnification in a given grid area, but counts of positively hybridized UCYN–A cells varied between each field of view. Counting reliability was improved by using a 630x magnification in order to cover a bigger area of each filter section. A distinct number of grids were counted in order to improve the comparison between each filter section. Filter sections within the upper water column (10–200 m depth) from every station were counted on 155 grids (grid area = 9843.75 μm^2) separately in duplicates or triplicates. Positively hybridized UCYN–A cells were quantified according to three different categories: (1) UCYN–A cells in association with a positively hybridized *Haptophyta*, (2) UCYN–A cells with an unknown eukaryote, (3) UCYN–A cells appearing as free–living.

Scanning electron microscopy. Filter sections that revealed high abundances of UCYN–A associations were selected for further analysis using a Quanta FEG 250 Scanning Electron Microscope (FEI, Eindhoven, NL). Targeted cells were measured in high vacuum mode and an accelerating voltage of 2.0 kV.

DNA extraction and amplicon pyrosequencing. DNA samples from 20 m depth and stations 14–18 were used for 454 pyrosequencing technology applying 16S and 18S rRNA primer sets. At each station, approximately 100 L seawater were pooled from 5 L Niskin bottles and pre–filtered through a 10 µm steel mesh cartridge (Wolftechnik, Weil der Stadt, Germany) onto cellulose acetate filters (142 mm diameter, 0.2 µm pore size; Sartorius, Goettingen, Germany). Samples were stored at –80 °C until further processing. DNA was extracted and purified following the DNeasy plant mini kit (Qiagen, Hilden, Germany) protocol with minor modifications (Turk et al., 2011). The bacterial 16S rRNA and the eukaryotic 18S rRNA genes were amplified and sequenced using the amplicon pyrosequencing facility at the Research and Testing Laboratories (Lubbock, Texas). The 16S rRNA primer NITRO821R (Mazard et al., 2004) and CYA359F (Nübel et al., 1997) targeting unicellular diazotrophic microorganisms were used to verify the presence of UCYN–A. The universal 18S rRNA primer Ek1269R and Ek555F (López–García et al., 2003) were used to assess the diversity of the entire picoeukaryote population. The generated sequence data from amplicon pyrosequencing was quality–controled by Research and Testing Laboratories, following standard procedure (Sun et al., 2011). Subsequently, sequences were processed by the NGS (Next Generation Sequencing) analysis pipeline of the SILVA rRNA gene database project (SILVAngs) (Quast et al., 2013). Each sequence read was aligned using the SILVA Incremental Aligner (SINA) (Pruesse et al., 2012) against the SILVA SSU rRNA SEED (A vector sequence database and a collection of non–chimeric sequences). Quality control was performed after Quast et al. (2013) and unique sequence reads were clustered into Operational Taxonomic Unit`s (OTUs) after dereplication (removal of identical reads) using cd–hit–est (version 3.1.2; http://www.bioinformatics.org/cd–hit) (Li and Godzik, 2006). Clustering was run in accurate mode, ignoring overhangs, and applying identity criteria of 1.00 and 0.98, respectively. The classification was performed by a local nucleotide BLAST search against the non–redundant version of the SILVA SSU Ref dataset (release 111; http://www.arb–silva.de) using BLASTN (version 2.2.22+; http://blast.ncbi.nlm.nih.gov/Blast.cgi) with standard settings (Camacho et al., 2009). Reads without any BLAST hits or reads with weak BLAST hits, where the function “(% sequence identity +% alignment coverage)/2" did not exceed the value of 93, remain unclassified. These reads were assigned to the meta group “No Relative" in the

SILVAngs fingerprint and Krona charts (Ondov et al., 2011). In addition, unique 16S rRNA sequences that have been clustered in OTUs and subsequently classified have been selected for phylogenetic reconstruction using the ARB software (Ludwig et al., 2004). This procedure yields quantitative information (number of individual reads per taxonomic path), within the limitations of PCR, sequencing technique biases, and multiple rRNA operons.

Results and discussion

Symbiotic associations play an important ecological role in marine ecosystems and are considered a major source of evolutionary innovation (Margulis and Fester, 1991). The recent discovery of UCYN–A living in association with eukaryotic algae represents an intriguing model for symbiosis and may provide evolutionary insight about the development of plastids (Thompson et al., 2012; Krupke et al., 2013). UCYN–A was originally detected using distinct *nifH* gene sequences by Zehr et al. (1998); subsequent studies have shown that these cyanobacteria are widely abundant in all major ocean basins (Zehr et al., 2008; Moisander et al., 2010). Further, UCYN–A genome analysis revealed an unusual physiology within cyanobacteria because fundamental metabolic systems including the photosystem II are absent (Tripp et al., 2010).

Previous investigations estimated the specific *nifH* gene abundance of UCYN–A without taking into account different associations, e.g. in association with a unicellular alga (Thompson et al., 2012; Krupke et al., 2013). Here, we applied a double CARD–FISH approach to visualize both partners simultaneously. Using this method, we identified the eukaryotic partner of UCYN–A, and quantified the cellular abundance and distribution of this association along the VISION cruise (Supplementary Fig. 1).

Environmental Parameters. The cruise transect crossed four different oceanic provinces as defined by Longhurst (1998); further analysis of physico–chemical properties revealed nine distinct water masses (Oliver and Irwin, 2008; Gómez–Pereira et al., 2010). The study site has previously been characterized in detail by Gómez–Pereira et al. (2010). Briefly, surface water temperatures gradually increased from the coast of Greenland towards the Azores, whereas nutrient concentrations decreased with increasing temperature. Nutrient concentrations (e.g. PO_4^{3-} or NO_3^-) in the Boreal Polar (BPLR) and Arctic (ARCT) provinces are similar to values reported by Williams and Follows (1998), describing cold and nutrient–rich water masses in the North Atlantic. Along the North Atlantic Drift (NADR) province towards the North Atlantic Subtropical Gyre (NAST) province close to the Azores, nutrient concentrations in surface waters (0–50 m depth) further declined and concentrations for PO_4^{3-} (0.0–0.043 µM) were similar to values measured by others (Michaels et al., 1996; Jardillier et al., 2010), but elevated compared to values documented by Wu et al. (2000). These findings show a clear transition from

cold and nutrient–rich waters into warm and nutrient–depleted (oligotrophic) environments along the VISION transect. The transition towards oligotrophic conditions in the NAST province point out the potential for nitrogen limitation as indicated by the relationship of nitrogen (N) to phosphorus (P) in surface waters (0–50 m depth), which differ substantially from a 16:1 Redfield ratio (Fig. 1A). Along the transect, N/P ratios within the top 50 m depth between station 2–11 were substantially higher (N/P = 6.9–15.7) compared to ratios between station 12–19 (N/P = 0.7–10.3) (Fig. 1A). The transition toward an N–limited environment indicates favorable conditions for diazotrophs (Karl et al., 2002; LaRoche and Breitbarth, 2005). This is further supported by increasing N/P ratios below 100 m water depth within the NAST province (Fig. 1A); N_2 fixation activity is known to support new and export production in marine systems, generally leading to elevated N/P ratios in deeper water zones (Karl et al., 1997).

Bulk CO_2 and N_2 fixation rates. We measured bulk CO_2 and N_2 fixation activity and calculated volumetric rates, as well as areal rates (Fig. 1 B,C; Supplementary Table 1). Volumetric CO_2 fixation rates under light conditions tended to be lower compared to previous investigations in the North Atlantic (Mills et al., 2004; Jardillier et al., 2010). In parallel, areal CO_2 fixation rates varied more than ten–fold between each station (Fig. 1B; Supplementary Table 1), but were not significantly different between the ocean provinces (One Way ANOVA, p = 0.876). The small cyanobacteria *Prochlorococccus* and *Synechococcus* have been detected and quantified along the VISION transect (Gómez–Pereira et al., 2010), and the measured CO_2 fixation activity can be partially assigned to the presence of these populations given their substantial role as primary producers (Goericke and Welschmeyer, 1993; Liu et al., 1997; Veldhuis et al., 1997).

N_2 fixation was not detected in the BPLR, ARCT or NADR provinces; N_2 fixation was detected in the NAST province, indicating the presence of diazotrophs (Fig. 1C; Supplementary Table 1). The subtropical and tropical North Atlantic is characterized by elevated iron supply due to Saharan dust input (Stuut et al., 2005) that might stimulate N_2 fixation activity given the high iron demand of diazotrophs (Carpenter and Romans, 1991; Falkowski, 1997; Capone et al., 2005; Jickells et al., 2005). Our observations in the NAST province clearly underline the spatial occurrence of N_2 fixation activity with surface water temperatures and depleted nutrient concentrations (e.g. low N/P ratios; Fig.

1A), as suggested by previous studies (Carpenter and Romans, 1991; Capone et al., 1997; LaRoche and Breitbarth, 2005).

Generally, N_2 fixation activity tended to be higher under light conditions compared to dark conditions, except at station 17 (Fig. 1C). However, areal estimates of N_2 fixation activity between light (2.4–5.1 µmol m^{-2} h^{-1}) and dark conditions (1.9–5.4 µmol m^{-2} h^{-1}) were not significantly different (ANOVA on Ranks, P = 0.486; Supplementary Table 1). The observed N_2 fixation rates in both treatments indicate that a mixed diazotrophic community was present containing diazotrophic populations with different temporal activity pattern, e.g. *Crocosphaera* sp. fix N_2 in the dark, whereas UCYN–A fix N_2 in the light (Church et al., 2005b). The measured volumetric and areal rates (Supplementary Table 1) have to be considered cautiously since the incubation experiments were rather short in time length (~5 hours) and we applied the common $^{15}N_2$ gas tracer addition method ("bubble method"), which has been demonstrated to underestimate N_2 fixation activity substantially (Mohr et al., 2010b; Großkopf et al., 2012). Our volumetric rate measurements (Supplementary Table 1) are comparable with previously reported rates from the North Atlantic (Mills et al., 2004; LaRoche and Breitbarth, 2005; Langlois et al., 2008; Krupke et al., 2013), and they are consistent with literature values from other oligotrophic regions using the $^{15}N_2$ gas bubble tracer method (0.07–4.17 nmol N L^{-1} h^{-1}) (Dore et al., 2002; Falcón et al., 2004a; Sohm et al., 2011; Luo et al., 2012).

Visualization of UCYN–A association. A study in the North Pacific by Thompson et al. (2012) revealed that 18S rRNA host sequences of UCYN–A clustered together with calcareous nanoplankton within the *prymnesiophyceae* (i.e. *Braarudosphaera bigelowii*) and coccolithophores (i.e. *Chrysochromulina parkeae*). The double CARD–FISH approach was established to target both partners by applying the UCYN–A732 oligonucleotide probe (Krupke et al., 2013) in combination with different oligonucleotide probes targeting groups of prasinophytes (PRAS04) (Not et al., 2004), coccolithophores (COCCO01) (Eller et al., 2007) and *Haptophyta* (PRYM02) (Simon et al., 2000) (Table 1). These groups of organisms have been shown to be of ecological significance in marine systems due to their extensive role in carbon sequestration and are widely distributed and abundant in the oceans (Unrein et al., 2007; Zubkov and Tarran, 2008; Cuvelier et al., 2010; Jardillier et al., 2010). We detected positively hybridized UCYN–A

cells associated with positively hybridized *Haptophyta* cells (Fig. 2A,B). In contrast, positively hybridized UCYN–A cells were not found in association with members of the coccolithophores or prasinophytes *(*data not shown).

The cell diameters for UCYN–A (1.16 ± 0.24; n = 52) and the *Haptophyta* partner (2.26 ± 0.75; n = 52) were determined based on epi–fluorescence microscopy, and they were consistent with previous investigations (Thompson et al., 2012; Krupke et al., 2013). Smaller UCYN–A cells were associated with smaller *Haptophyta* cells and vise versa (R^2 = 0.8058; n = 52), indicative of different growth stages. Further evaluation of attached UCYN–A cells showed them located on the polar end of the eukaryote or slightly shifted to the side (Fig. 2A–C). It appears that UCYN–A cells live attached to the eukaryotic partner within a cell–surface association as observed in the North Pacific (Thompson et al., 2012). Epi–fluorescence and scanning electron microscopic observations indicate that UCYN–A cells are slightly engulfed by the eukaryote and embedded in a preformed slot (Fig. 2B,E,F). The latter analysis provide the first scanning electron images of the UCYN–A association. Additionally, calcium carbonate plates (i.e. coccoliths) were not detected on the associated eukaryotic partner cell, indicating that UCYN–A may also associate with non–calcifying nanoplankton.

In this study we did not observe two UCYN–A cells associated with one eukaryote as observed in the North Pacific (Thompson et al., 2012). Thus far, the mechanisms determining the number of UCYN–A cells associating with a eukaryote are not clear. Other eukaryotes are able to regulate the number of their symbionts to enhance growth conditions (Reisser, 1986, 1992; Johnson, 2011). A recent study by Van Mooy et al. (2012) documented that multiple bacterial cells living epibiotically on the diazotroph *Trichodesmium* sp. enhance the uptake of phosphorus, implying a specific ecophysiological advantage for maintain numerous symbionts.

Diversity of unicellular cyanobacteria and picoeukaryotes. The stations that revealed positively hybridized UCYN–A cells were selected for 16S rRNA gene pyrosequencing using a specific primer set to target unicellular cyanobacteria. Subsequent phylogenetic reconstruction analysis showed that 96.73% of the generated OTUs clustered next to UCYN–A phylotypes, thus, confirming the presence of this cyanobacterium (Supplementary Fig. 2). Parallel 18S rRNA gene pyrosequencing was performed on the

same stations in order to gather more insights into the phylogeny of the potential eukaryotic partner cell.

The generated dataset showed a high diversity within picoeukaryotes at stations 14–18 (Fig. 3A). Among *Prymnesiophyceae*, we confirmed the presence of the taxa *Braarudosphaera* and *Chrysochrymulina*. These groups have been shown to harbor phylotype sequences of the eukaryotic partner cell of UCYN–A (Thompson et al., 2012). Here, we observed large differences in the relative abundances of distinct taxa within *Prymnesiophyceae* between stations 14 until 18. For instance, generated OTUs of *Braarudosphaera* ranged between 5–50% in relative abundances, whereas this taxa was absent at station 17 and 18 (Fig. 3E,F). The relative abundances of the taxa *Chrysochrumulina* also varied between the respective stations (Fig. 3E,F). These results indicate that the partner cells of UCYN–A fall into various taxa within *Prymnesiophyceae*, and that their distribution varies spatially. Furthermore, we encountered UCYN–A cells associated with eukaryotes other than *Haptophyta* in the double CARD–FISH assays (section below). These eukaryotes might belong to the groups *Syndiniales* and *Dinophyceae* of the phylum *Alveolata*; both groups had the highest sequence representation within the eukaryotic community, comprising on average 48.8 % of the relative abundances (Fig. 3A). But, it is possible that the relative abundances of these groups could be overrepresented due to multiple 18S rDNA gene copies in their genome (Zhu et al., 2005; Koid et al., 2012). We identified the eukaryotic partner cell for UCYN–A as a *Haptophyta* based on CARD–FISH assays (section below), and measured a large degree of eukaryotic diversity and varying relative abundances within *Haptophyta* (genomic data), as well as among other groups (e.g. *Alveolata*). From these findings, we hypothesize that UCYN–A might associate with a wide range of eukaryotic partners, raising questions about the specificity of this form of association. The possibility to associate with a variety of hosts indicate diverse metabolic capabilities to thrive in the environment and might be the reason why UCYN–A is found in contrasting water regimes based on *nifH* gene sequence abundances (Short and Zehr, 2007; Rees et al., 2009; Moisander et al., 2010).

Quantification and distribution of the UCYN–A association. The appearance of UCYN–A was enumerated into three different categories using the CARD–FISH approach: (1) in association with a *Haptophyta*, (2) in association with an unknown eukaryote and (3) as

free–living cells (Fig. 4A–F). The abundance of the UCYN–A association was also quantified for the first time, and their distribution patterns were determined based on cell counts (Fig. 4A–C). Along the VISION transect in the North Atlantic within the upper water column (≤ 200 m depth), UCYN–A cells were completely absent within the BPLR, ARCT and NADR provinces and only appeared in the NAST province (Fig. 4A–C). These observations clearly demonstrate that these microbes thrive best (~10^3–10^4 cells mL^{-1}) in oligotrophic environments where nutrient concentrations are low (<0.8 NOx µM and <0.04 PO_4^{3-}) and water temperatures are above 18 °C. UCYN–A cells were usually observed in surface waters with low N/P ratios (~2.0), and only when N_2 fixation activity was measured, indicating that the UCYN–A population partially contributed to observed N_2 fixation rates (Fig. 1C and Fig. 3A–C).

Quantitative information on the UCYN–A population shows that UCYN–A cells mainly live in association with eukaryotes (Fig. 4A–C). Highest abundances were measured at station 14 with UCYN–A cells associated with a *Haptophyta* (1.8–2.6 x 10^4 ml^{-1}) and an unknown eukaryote (1.5–4.7 x 10^3 mL^{-1}) (Fig. 4A,B). Most UCYN–A cells within the NAST province (≤ 50 m depth) appear in association with a *Haptophyta* (87.0±6.1%) whereas a smaller fraction is associated with an unknown eukaryote (7.8±5.2%). Other UCYN–A cells in that region were detected as free–living and only represented a minor fraction (5.2 ± 3.9%). The total UCYN–A population below 50 m depth becomes patchy and irregular; the fraction of free–living UCYN–A cells increases (32.9±45.4%), and the fraction of UCYN–A cells in association decreases (67.1±45.4%) (Fig. 4A–C). With the exception of station 16 and 17, the UCYN–A association was absent below 100 m water depth (Fig. 3A–C). This absence is typical for cyanobacteria and photosynthetically active microorganisms in general due to the lack of light energy (Zehr et al., 2001; Karl et al., 2002; Uitz et al., 2006). Interestingly, UCYN–A cells in association with an unknown eukaryote were higher than UCYN–A cells in association with a *Haptophyta* at depths below 50 m at station 16 and 17 (Supplementary Fig. 3A,B). These results imply a potential host–depth differentiation along the water column and might disclose a niche partitioning among UCYN–A.

Conclusions and outlook. In general, associations and cell–to–cell interactions between diazotrophs and eukaryotes have been overlooked in open ocean systems and little is known about the abundances, distribution and ecological significance of these couplings.

Here, we identified UCYN–A and their partner cell as a *Haptophyta* using a double CARD–FISH approach, and provided quantitative information on the cellular abundance and distribution of this association in the North Atlantic. This information improves our understanding on the environmental parameters that select for UCYN–A associations. Further investigations targeting the unknown eukaryotes associating with UCYN–A and subgroups of *Haptophyta* would provide insights on potential physiological interactions and host specificity, refining our understanding how these interactions affect marine ecosystems and shape biogeochemical cycles.

Acknowledgements

We thank the Captain, officers and crew of the FS Maria S. Merian (cruise MSM03/01) for their help during the cruise. We also thank Gabriele Klockgether, Daniela Nini and Sten Littman for their technical assistance. AK also thanks Timothy G. Ferdelman and Sara J. Bender for their helpful comments and discussion on the manuscript. This study was funded by the Max Planck Society.

Tables and Figures

Table 1: Summary of 16S (*) and 18S (**) rRNA targeted oligonucleotide probes with correlating formamide (FA) concentrations and specificities used in the double CARD–FISH assays. The corresponding target microorganisms and references are listed.

Fig. 1: Overview of (A) the ratio of nitrogen species (NO_x = NO_3^- and NO_2^-) over phosphate (PO_4^{3-}) expressed as N/P, (B) bulk CO_2 and (C) N_2 fixation rates along the VISION transect. Bulk fixation rates were integrated between 0–80 m depth and the white bars represent bulk rates under light conditions and the black bars refer to bulk rates determined under dark conditions. Bulk activity was not measured at stations 7, 13, 15, and 19 as indicated by the symbol "X"; not detectable N_2 fixation activity is indicated by "nd". Panel (A) was generated using Ocean Data View software and the automatic scaling feature. The ocean provinces are separated by dashed lines from left to right: BPLR = Boreal Polar Province, ARCT = Arctic Province, NADR = North Atlantic Drift Province, NAST = North Atlantic Subtropical Gyre Province.

Fig. 2: Double *in situ* hybridization using specific HRP–labelled oligonucleotide probes targeting UCYN–A and the associated eukaryote. The green fluorescence signals refer to the deposition of Oregon Green 488 tyramides and the red fluorescence signals refer to Alexa 594 tyramides. The blue fluorescence signals refer to DAPI staining. The UCYN–A cell has been targeted by the UCYN–A732 probe and the eukaryote has been targeted by the PRYM02 probe. (A,B) The successful double hybridization of UCYN–A (red) located either (A) at the polar end or (B) slightly shifted to the side of a prymnesiophyte (green). Two chloroplasts are located on each side of the prymnesiophyte (A) and reveal light autofluorescence. (C) A positively hybridized UCYN–A cell associated with a eukaryote that has not been targeted by the applied PRYM02 probe. (D) A free–living UCYN–A cell, positively hybridized by the UCYN–A732 probe. (E) The successful double hybridization of UCYN–A (green) and a prymnesiophyte (red), and the (F) complementary electron microscopy analysis displaying the slightly engulfed UCYN–A cell indicated by the dashed line, where no coccolith structure was visible. Scale bar, 5 µm (A–D) and 1 µm (E,F).

Fig. 3: Overview of the diversity and the relative abundance of taxonomic groups within the picoeukaryote population visualized in a hierarchical structure by using the interactive metagenomic visualization tool *Krona*. (A) The picoeukaryote community composition pooled together from station 14–18, and (B–F) *Haptophyta* phylum diversity down to the family level for each station.

Fig. 4: Vertical distribution of UCYN–A throughout the upper 200 m depth along the VISION transect based on cell enumeration using double in situ hybridization of the UCYN–A732 and PRYM02 oligonucleotide probes. Positively hybridized (A) UCYN–A cells in association with eukaryotes that were hybridized by PRYM02, (B) in association with an unknown eukaryote that was not hybridized by the PRYM02 probe, and (C) as free–living. The ocean provinces are separated by dashed lines from left to right: BPLR = Boreal Polar Province, ARCT = Arctic Province, NADR = North Atlantic Drift Province, NAST = North Atlantic Subtropical Gyre Province.

Table 1

Probe name	Target	Sequence (5’ → 3’)	% FA	Reference
UCYN–A 732*	Unicellular cyanobacteria Group A	GTTACGGTCCAGTAGCAC	50	Krupke et al. (2013)
Helper A–732*	Unicellular cyanobacteria Group A	GCCTTCGCCACCGATGTTCTT	50	Krupke et al. (2013)
Helper B–732*	Unicellular cyanobacteria Group A	AGCTTTCGTCCCTGAGTGTCA	50	Krupke et al. (2013)
PRYM02**	*Haptophyta*	GGAATACGAGTGCCCCTGAC	40	Simon et al. (2000)
PRAS04**	*Mamiellales* (except the genus Dolichomatix)	CGTAAGCCCGCTTTGAAC	40	Not et al. (2004)
COCOO01**	*Coccolithales*	TTTCCCGAAAGGTGCTGA	5	Eller et al. (2007)
EUK516**	*Eukarya*	ACCAGACTTGCCCTCC	35	Amann et al. (1990)
EUB338 I*	Most *Bacteria*	GCTGCCTCCCGTAGGAGT	35	Amann et al. (1990)
EUB338–II*	supplement to EUB 338: *Planctomycetales*	GCAGCCACCCGTAGGTGT	35	Daims et al. (1999)
EUB338–III*	supplement to EUB 338: *Verrucomicrobiales*	GCTGCCACCCGTAGGTGT	35	Daims et al. (1999)
NON338*	Antisense of EUB338	ACTCCTACGGGAGGCAGC	35	Wallner et al. (1993)

Fig. 1

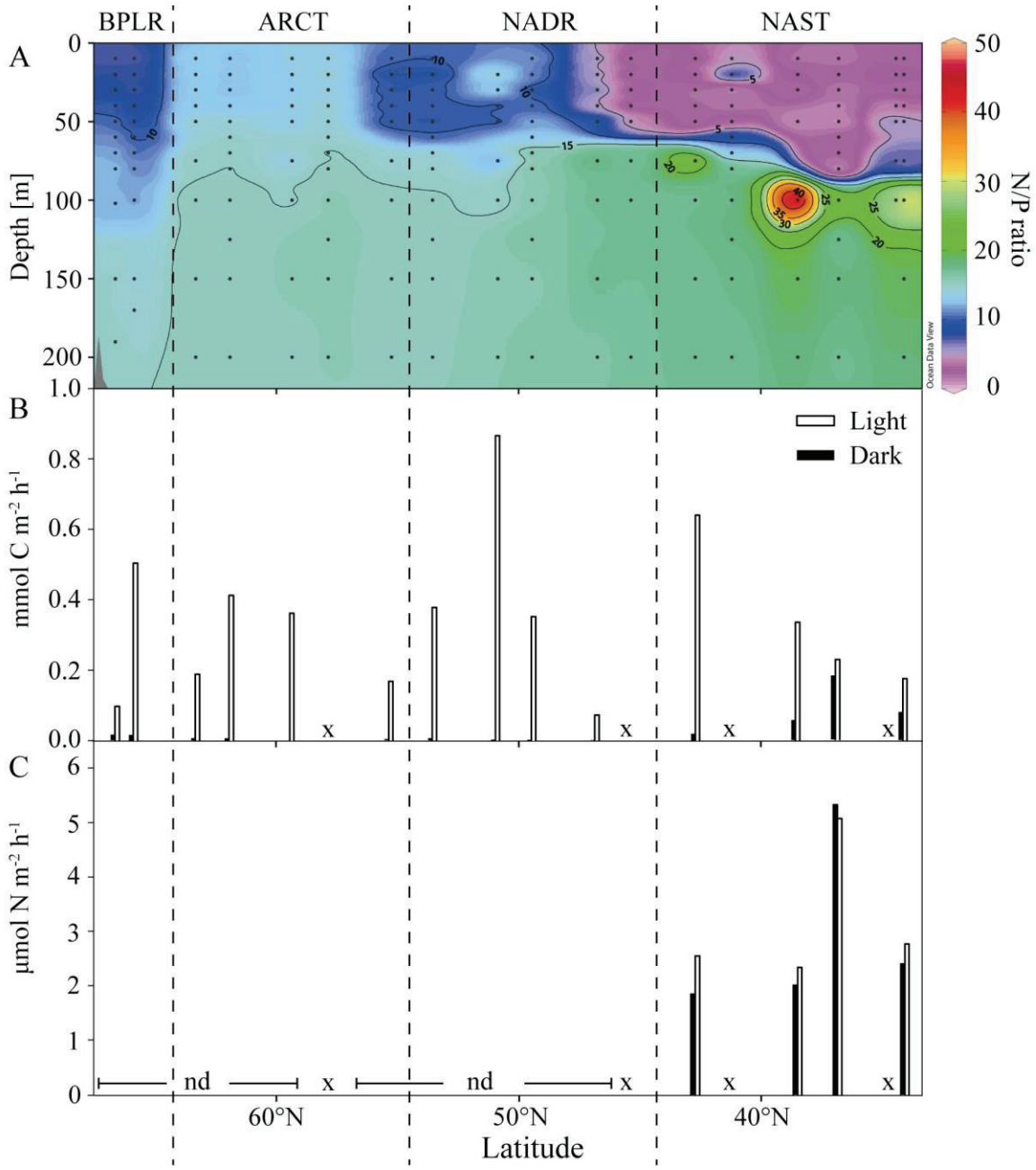
BPLR
ARCT
NADR
NAST
A
Depth [m]
N/P ratio
Ocean Data View
B
mmol C m-2 h-1
Light
Dark
C
µmol N m-2 h-1
nd
x
60°N
50°N
40°N
Latitude

Fig. 2

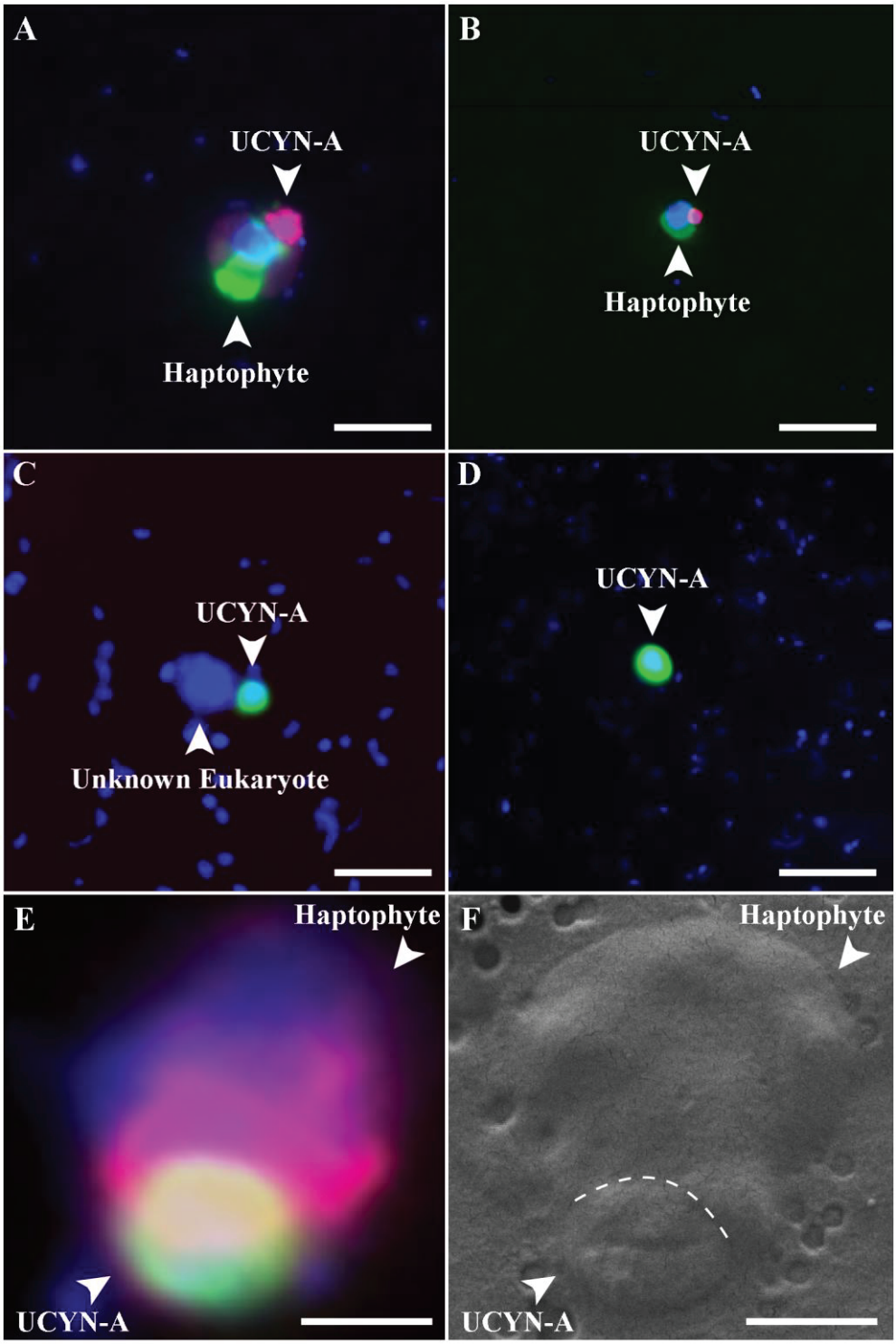
A
UCYN-A
Haptophyte
B
UCYN-A
Haptophyte
C
UCYN-A
Unknown Eukaryote
D
UCYN-A
E
Haptophyte
UCYN-A
F
Haptophyte
UCYN-A

Fig. 3

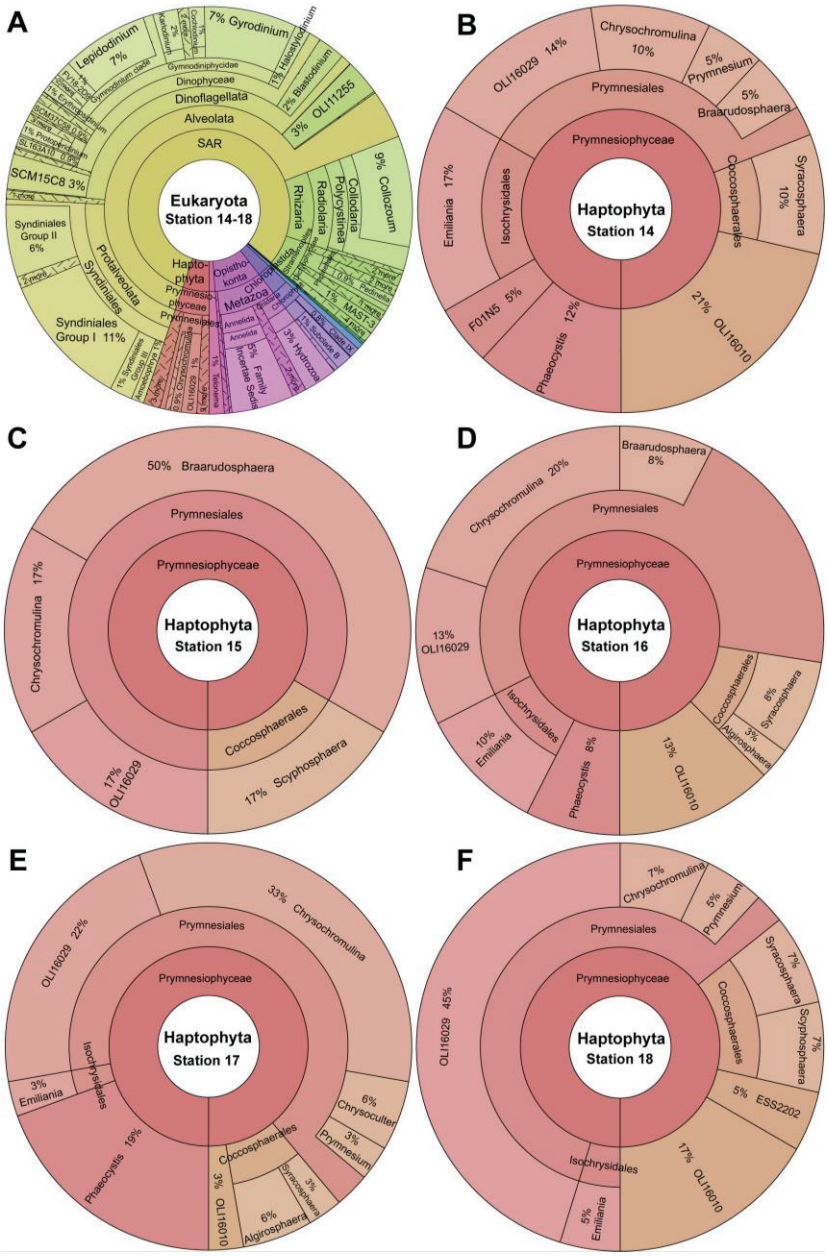
A
Eukaryota
Station 14-18
SAR
Alveolata
Dinoflagellata
Dinophyceae
Gymnodiniphycidae
Lepidodinium 7%
7% Gyrodinium
Biastodinium
3% OLI11255
9% Collozoum
Collodaria
Polycystinea
Radiolaria
Rhizaria
SCM15C8 3%
Syndiniales Group II 6%
Syndiniales Group I 11%
Syndiniales
Protalveolata
Haptophyta
Prymnesiophyceae
Prymnesiales
Opisthokonta
Metazoa
Annelida
Chrysophyceae
MAST-3
B
Haptophyta
Station 14
Prymnesiophyceae
Prymnesiales
Isochrysidales
Coccosphaerales
OLI16029 14%
Chrysochromulina 10%
5% Prymnesium
5% Braarudosphaera
Syracosphaera 10%
21% OLI16010
Phaeocystis 12%
F01N5 5%
Emiliania 17%
C
Haptophyta
Station 15
Prymnesiophyceae
Prymnesiales
Coccosphaerales
50% Braarudosphaera
Chrysochromulina 17%
17% OLI16029
17% Scyphosphaera
D
Haptophyta
Station 16
Prymnesiophyceae
Prymnesiales
Isochrysidales
Coccosphaerales
Braarudosphaera 8%
Chrysochromulina 20%
13% OLI16029
10% Emiliania
Phaeocystis 8%
13% OLI16010
8% Syracosphaera
3% Algirosphaera
E
Haptophyta
Station 17
Prymnesiophyceae
Prymnesiales
Isochrysidales
Coccosphaerales
33% Chrysochromulina
OLI16029 22%
3% Emiliania
Phaeocystis 19%
3% OLI16010
6% Algirosphaera
3% Syracosphaera
3% Prymnesium
6% Chrysoculter
F
Haptophyta
Station 18
Prymnesiophyceae
Prymnesiales
Isochrysidales
Coccosphaerales
7% Chrysochromulina
5% Prymnesium
7% Syracosphaera
7% Scyphosphaera
5% ESS2202
17% OLI16010
5% Emiliania
OLI16029 45%

Fig. 4

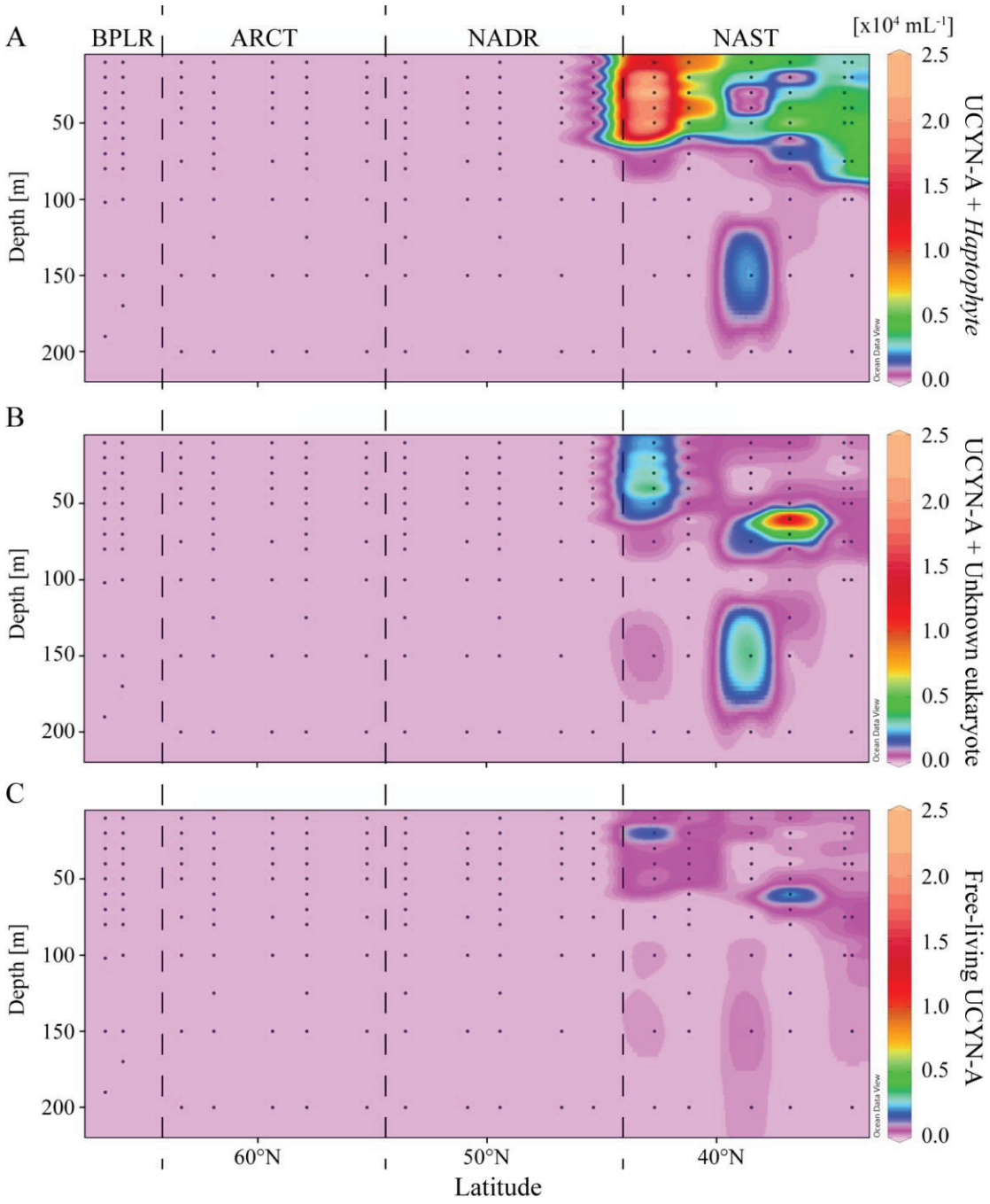
A
B
C
BPLR
ARCT
NADR
NAST
[x10⁴ mL⁻¹]
Depth [m]
50
100
150
200
2.5
2.0
1.5
1.0
0.5
0.0
UCYN-A + Haptophyte
UCYN-A + Unknown eukaryote
Free-living UCYN-A
Ocean Data View
60°N
50°N
40°N
Latitude

References

Amann, R.I., Binder, B.J., Olson, R.J., Chisholm, S.W., Devereux, R., and Stahl, D.A. (1990) Combination of 16S rRNA-targeted oligonucleotide probes with flow cytometry for analyzing mixed microbial populations. *Appl Environ Microbiol* **56**: 1919-1925.

Bothe, H., Tripp, H.J., and Zehr, J.P. (2010) Unicellular cyanobacteria with a new mode of life: The lack of photosynthetic oxygen evolution allows nitrogen fixation to proceed. *Arch Microbiol* **192**: 783-790.

Camacho, C., Coulouris, G., Avagyan, V., Ma, N., Papadopoulos, J., Bealer, K., and Madden, T. (2009) BLAST+: architecture and applications. *BMC Bioinformatics* **10**: 1-9.

Capone, D.G., and Knapp, A.N. (2007) Oceanography: A marine nitrogen cycle fix? *Nature* **445**: 159-160.

Capone, D.G., Zehr, J.P., Paerl, H.W., Bergman, B., and Carpenter, E.J. (1997) *Trichodesmium*, a globally significant marine cyanobacterium. *Science* **276**: 1221-1229.

Capone, D.G., Burns, J.A., Montoya, J.P., Subramaniam, A., Mahaffey, C., Gunderson, T. et al. (2005) Nitrogen fixation by *Trichodesmium* spp.: An important source of new nitrogen to the tropical and subtropical North Atlantic Ocean. *Glob Biogeochem Cycles* **19**: 1-17.

Carpenter, E.J., and Romans, K. (1991) Major role of the cyanobacterium *Trichodesmium* in nutrient cycling in the North Atlantic Ocean. *Science* **254**: 1356-1358.

Carpenter, E.J., Montoya, J.P., Burns, J., Mulholland, M.R., Subramaniam, A., and Capone, D.G. (1999) Extensive bloom of a N_2-fixing diatom/cyanobacterial association in the tropical Atlantic Ocean. *Mar Ecol Prog Ser* **185**: 273-283.

Church, M.J., Short, C.M., Jenkins, B.D., Karl, D.M., and Zehr, J.P. (2005) Temporal patterns of nitrogenase gene (*nifH*) expression in the oligotrophic North Pacific Ocean. *Appl Environ Microbiol* **71**: 5362-5370.

Cuvelier, M.L., Allen, A.E., Monier, A., McCrow, J.P., Messié, M., Tringe, S.G. et al. (2010) Targeted metagenomics and ecology of globally important uncultured eukaryotic phytoplankton. *Proceedings of the National Academy of Sciences* **107**: 14679-14684.

Daims, H., Brühl, A., Amann, R., Schleifer, K.H., and Wagner, M. (1999) The domain-specific probe EUB338 is insufficient for the detection of all Bacteria: Development and evaluation of a more comprehensive probe set. *Syst Appl Microbiol* **22**: 434-444.

DeLong, E.F. (2010) Interesting things come in small packages. *Genome Biol* **11**: 118.

Dore, J.E., Brum, J.R., Tupas, L.M., and Karl, D.M. (2002) Seasonal and interannual variability in sources of nitrogen supporting export in the oligotrophic subtropical North Pacific Ocean. *Limnol Oceanogr* **47**: 1595-1607.

Eller, G., Töbe, K., and Medlin, L.K. (2007) Hierarchical probes at various taxonomic levels in the Haptophyta and a new division level probe for the Heterokonta. *J Plank Res* **29**: 629-640.

Falcón, L.I., Carpenter, E.J., Cipriano, F., Bergman, B., and Capone, D.G. (2004) N_2 fixation by unicellular bacterioplankton from the Atlantic and Pacific Oceans: Phylogeny and *in situ* rates. *Appl Environ Microbiol* **70**: 765-770.

Falkowski, P.G. (1997) Evolution of the nitrogen cycle and its influence on the biological sequestration of CO_2 in the ocean. *Nature* **387**: 272-275.

Foster, R.A., Kuypers, M.M.M., Vagner, T., Paerl, R.W., Musat, N., and Zehr, J.P. (2011) Nitrogen fixation and transfer in open ocean diatom–cyanobacterial symbioses. *ISME J* **5**: 1484-1493.

Goericke, R., and Welschmeyer, N.A. (1993) The marine prochlorophyte *Prochlorococcus* contributes significantly to phytoplankton biomass and primary production in the Sargasso Sea. *Deep-Sea Res Pt I* **40**: 2283-2294.

Gómez-Pereira, P.R., Fuchs, B.M., Alonso, C., Oliver, M.J., van Beusekom, J.E.E., and Amann, R. (2010) Distinct flavobacterial communities in contrasting water masses of the North Atlantic Ocean. *The ISME journal* **4**: 472-487.

Großkopf, T., Mohr, W., Baustian, T., Schunck, H., Gill, D., Kuypers, M.M.M. et al. (2012) Doubling of marine dinitrogen-fixation rates based on direct measurements. *Nature* **488**: 361-364.

Jardillier, L., Zubkov, M.V., Pearman, J., and Scanlan, D.J. (2010) Significant CO_2 fixation by small prymnesiophytes in the subtropical and tropical northeast Atlantic Ocean. *ISME J* **4**: 1180-1192.

Jickells, T.D., An, Z.S., Andersen, K.K., Baker, A.R., Bergametti, G., Brooks, N. et al. (2005) Global iron connections between desert dust, ocean biogeochemistry, and climate. *Science* **308**: 67-71.

Johnson, M.D. (2011) Acquired phototrophy in ciliates: a review of cellular interactions and structural adaptations. *J Eukaryot Microbiol* **58**: 185-195.

Karl, D., Letelier, R., Tupas, L., Dore, J., Christian, J., and Hebel, D. (1997) The role of nitrogen fixation in biogeochemical cycling in the subtropical North Pacific Ocean. *Nature* **388**: 533-538.

Karl, D., Michaels, A., Bergman, B., Capone, D., Carpenter, E., Letelier, R. et al. (2002) Dinitrogen fixation in the world's oceans. *Biogeochemistry* **57**: 47-98.

Koid, A., Nelson, W.C., Mraz, A., and Heidelberg, K.B. (2012) Comparative analysis of eukaryotic marine microbial assemblages from 18S rRNA gene and gene transcript clone libraries by using different methods of extraction. *Appl Environ Microbiol* **78**: 3958-3965.

Krupke, A., Musat, N., LaRoche, J., Mohr, W., Fuchs, B.M., Amann, R.I. et al. (2013) *In situ* identification and N_2 and C fixation rates of uncultivated cyanobacteria populations. *Syst Appl Microbiol* **36**: 259-271.

Langlois, R.J., Hummer, D., and LaRoche, J. (2008) Abundances and distributions of the dominant *nifH* phylotypes in the Northern Atlantic Ocean. *Appl Environ Microbiol* **74**: 1922-1931.

LaRoche, J., and Breitbarth, E. (2005) Importance of the diazotrophs as a source of new nitrogen in the ocean. *J Sea Res* **53**: 67-91.

Li, W., and Godzik, A. (2006) Cd-hit: a fast program for clustering and comparing large sets of protein or nucleotide sequences. *Bioinformatics* **22**: 1658-1659.

Liu, H., Nolla, H.A., and Campbell, L. (1997) *Prochlorococcus* growth rate and contribution to primary production in the equatorial and subtropical North Pacific Ocean. *Aquat Microb Ecol* **12**: 39-47.

Longhurst, A. (1998) Ecological geography of the seaAcademic. *San Diego*.

López-García, P., Philippe, H., Gail, F., and Moreira, D. (2003) Autochthonous eukaryotic diversity in hydrothermal sediment and experimental microcolonizers at the Mid-Atlantic Ridge. *Proceedings of the National Academy of Sciences* **100**: 697-702.

Ludwig, W., Strunk, O., Westram, R., Richter, L., and Meier, H. (2004) ARB: A software environment for sequence data. *Nucleic Acids Res* **32**: 1363-1371.

Luo, Y.W., Doney, S.C., Anderson, L.A., Benavides, M., Bode, A., Bonnet, S. et al. (2012) Database of diazotrophs in global ocean: Abundances, biomass and nitrogen fixation rates. *Earth Syst Sci Data* **5**: 47-106.

Mague, T.H., Weare, N.M., and Holm-Hansen, O. (1974) Nitrogen fixation in the north Pacific Ocean. *Mar Biol* **24**: 109-119.

Mahaffey, C., Michaels, A.F., and Capone, D.G. (2005) The conundrum of marine N_2 fixation. *Am J Sci* **305**: 546-595.

Margulis, L., and Fester, R. (1991) *Symbiosis as a source of evolutionary innovation: Speciation and morphogenesis*: MIT Press.

Mazard, S.L., Fuller, N.J., Orcutt, K.M., Bridle, O., and Scanlan, D.J. (2004) PCR analysis of the distribution of unicellular cyanobacterial diazotrophs in the Arabian Sea. *Appl Environ Microbiol* **70**: 7355-7364.

Michaels, A.F., Olson, D., Sarmiento, J.L., Ammerman, J.W., Fanning, K., Jahnke, R. et al. (1996) Inputs, losses and transformations of nitrogen and phosphorus in the pelagic North Atlantic Ocean. *Biogeochemistry* **35**: 181-226.

Mills, M.M., Ridame, C., Davey, M., La Roche, J., and Geider, R.J. (2004) Iron and phosphorus co-limit nitrogen fixation in the eastern tropical North Atlantic. *Nature* **429**: 292-294.

Mohr, W., Großkopf, T., Wallace, D.W.R., and LaRoche, J. (2010) Methodological underestimation of oceanic nitrogen fixation rates. *PLoS ONE* **5**: e12583.

Moisander, P.H., Beinart, R.A., Hewson, I., White, A.E., Johnson, K.S., Carlson, C.A. et al. (2010) Unicellular cyanobacterial distributions broaden the oceanic N_2 fixation domain. *Science* **327**: 1512-1514.

Montoya, J.P., Voss, M., Kahler, P., and Capone, D.G. (1996) A Simple, High-Precision, High-Sensitivity Tracer Assay for N_2-Fixation. *Appl Environ Microbiol* **62**: 986-993.

Not, F., Latasa, M., Marie, D., Cariou, T., Vaulot, D., and Simon, N. (2004) A single species, *Micromonas pusilla* (Prasinophyceae), dominates the eukaryotic picoplankton in the western English Channel. *Appl Environ Microbiol* **70**: 4064-4072.

Nübel, U., Garcia-Pichel, F., and Muyzer, G. (1997) PCR primers to amplify 16S rRNA genes from cyanobacteria. *Appl Environ Microbiol* **63**: 3327-3332.

Oliver, M.J., and Irwin, A.J. (2008) Objective global ocean biogeographic provinces. *Geophys Res Lett* **35**: 1-6.

Ondov, B., Bergman, N., and Phillippy, A. (2011) Interactive metagenomic visualization in a Web browser. *BMC Bioinformatics* **12**: 385.

Pernthaler, A., and Amann, R. (2004) Simultaneous fluorescence in situ hybridization of mRNA and rRNA in environmental bacteria. *Appl Environ Microbiol* **70**: 5426-5433.

Pernthaler, A., and Pernthaler, J. (2007) Fluorescence *In Situ* Hybridization for the Identification of Environmental Microbes. In *Protocols for Nucleic Acid Analysis by Nonradioactive Probes* pp. 153-164.

Pernthaler, A., Pernthaler, J., and Amann, R. (2004) Sensitive multi-color fluorescence in situ hybridization for the identification of environmental microorganisms. *Mol Microb Ecol Man* **3**: 711-726.

Pruesse, E., Peplies, J., and Glöckner, F.O. (2012) SINA: Accurate high-throughput multiple sequence alignment of ribosomal RNA genes. *Bioinformatics* **28**: 1823-1829.

Quast, C., Pruesse, E., Yilmaz, P., Gerken, J., Schweer, T., Yarza, P. et al. (2013) The SILVA ribosomal RNA gene database project: Improved data processing and web-based tools. *Nucleic Acids Res* **41**: 590-596.

Rees, A.P., Gilbert, J.A., and Kelly-Gerreyn, B.A. (2009) Nitrogen fixation in the western English Channel (NE Atlantic ocean). *Mar Ecol Prog Ser* **374**: 7-12.

Reisser, W. (1986) Endosymbiotic associations of freshwater protozoa and algae. *Prog Protist* **1**: 195-214.

Reisser, W. (1992) Endosymbiotic associations of algae with freshwater protozoa and invertebrates. *Algae and symbioses: plants, animals, fungi, viruses, interactions explored* **1**: 1-19.

Short, S.M., and Zehr, J.P. (2007) Nitrogenase gene expression in the Chesapeake Bay Estuary. *Environ Microbiol* **9**: 1591-1596.

Simon, N., Campbell, L., Örno lfsdo ttir, E., Groben, R., Guillou, L., Lange, M., and Medlin, L.K. (2000) Oligonucleotide probes for the identification of three algal groups by dot blot and fluorescent whole-cell hybridization. *J Eukaryot Microbiol* **47**: 76-84.

Sohm, J.A., Webb, E.A., and Capone, D.G. (2011) Emerging patterns of marine nitrogen fixation. *Nat Rev Microbiol* **9**: 499-508.

Stuut, J.-B., Zabel, M., Ratmeyer, V., Helmke, P., Schefuß, E., Lavik, G., and Schneider, R. (2005) Provenance of present-day eolian dust collected off NW Africa. *J Geophys Res* **110**: 1-14.

Sun, Y., Wolcott, R.D., and Dowd, S.E. (2011) Tag-encoded FLX amplicon pyrosequencing for the elucidation of microbial and functional gene diversity in any environment. In *High-Throughput Next Generation Sequencing*: Springer, pp. 129-141.

Thompson, A.W., Foster, R.A., Krupke, A., Carter, B.J., Musat, N., Vaulot, D. et al. (2012) Unicellular cyanobacterium symbiotic with a single-celled eukaryotic alga. *Science* **337**: 1546-1550.

Tripp, H.J., Bench, S.R., Turk, K.A., Foster, R.A., Desany, B.A., Niazi, F. et al. (2010) Metabolic streamlining in an open-ocean nitrogen-fixing cyanobacterium. *Nature* **464**: 90-94.

Turk, K.A., Rees, A.P., Zehr, J.P., Pereira, N., Swift, P., Shelley, R. et al. (2011) Nitrogen fixation and nitrogenase (*nifH*) expression in tropical waters of the eastern North Atlantic. *ISME J* **5**: 1201-1212.

Uitz, J., Claustre, H., Morel, A., and Hooker, S.B. (2006) Vertical distribution of phytoplankton communities in open ocean: An assessment based on surface chlorophyll. *J Geophys Res* **111**: 1-23.

Unrein, F., Massana, R., Alonso-Sáez, L., and Gasol, J.M. (2007) Significant year-round effect of small mixotrophic flagellates on bacterioplankton in an oligotrophic coastal system. *Limnol Oceanogr* **52**: 456-469.

Van Mooy, B.A.S., Hmelo, L.R., Sofen, L.E., Campagna, S.R., May, A.L., Dyhrman, S.T. et al. (2012) Quorum sensing control of phosphorus acquisition in *Trichodesmium* consortia. *The ISME journal* **6**: 422-429.

Veldhuis, M.J.W., Kraay, G.W., Van Bleijswijk, J.D.L., and Baars, M.A. (1997) Seasonal and spatial variability in phytoplankton biomass, productivity and growth in the northwestern Indian Ocean: The southwest and northeast monsoon, 1992-1993. *Deep-Sea Res Pt I* **44**: 425-449.

Voss, M., Croot, P., Lochte, K., Mills, M., and Peeken, I. (2004) Patterns of nitrogen fixation along 10 °N in the tropical Atlantic. *Geophys Res Lett* **31**: 1-4.

Wallner, G., Amann, R., and Beisker, W. (1993) Optimizing fluorescent *in situ* hybridization with rRNA targeted oligonucleotide probes for flow cytometric identification of microorganisms. *Cytometry* **14**: 136-143.

Williams, R.G., and Follows, M.J. (1998) The Ekman transfer of nutrients and maintenance of new production over the North Atlantic. *Deep-Sea Res Pt I* **45**: 461-490.

Wu, J., Sunda, W., Boyle, E.A., and Karl, D.M. (2000) Phosphate depletion in the western North Atlantic Ocean. *Science* **289**: 759-762.

Zehr, J.P., Mellon, M.T., and Zani, S. (1998) New nitrogen-fixing microorganisms detected in oligotrophic oceans by amplification of nitrogenase (*nifH*) genes. *Appl Environ Microbiol* **64**: 3444-3450.

Zehr, J.P., Waterbury, J.B., Turner, P.J., Montoya, J.P., Omoregie, E., Steward, G.F. et al. (2001) Unicellular cyanobacteria fix N_2 in the subtropical North Pacific Ocean. *Nature* **412**: 635-637.

Zehr, J.P., Bench, S.R., Carter, B.J., Hewson, I., Niazi, F., Shi, T. et al. (2008) Globally distributed uncultivated oceanic N_2-fixing cyanobacteria lack oxygenic photosystem II. *Science* **322**: 1110-1112.

Zhu, F., Massana, R., Not, F., Marie, D., and Vaulot, D. (2005) Mapping of picoeucaryotes in marine ecosystems with quantitative PCR of the 18S rRNA gene. *FEMS Microbiol Ecol* **52**: 79-92.

Zubkov, M.V., and Tarran, G.A. (2008) High bacterivory by the smallest phytoplankton in the North Atlantic Ocean. *Nature* **455**: 224-226.

2.3.1 Manuscript III: Supplementary Information

Supplementary Fig. 1: The VISION cruise track in the North Atlantic covering 18 stations (S2–S19) represented by the black dots. The dashed lines indicate different biogeographical provinces defined after Longhurst (1998): Boreal Polar Province (BPLR), Arctic Province (ARCT), North Atlantic Drift Province (NADR) and North Atlantic Subtropical Gyre Province (NAST).

Supplementary Fig. 2: Maximum–Likelihood phylogenetic reconstruction inferred from unique sequences clustered into classified OTUs. Almost all OTUs (426 = 92.8%) clustered next to UCYN–A sequences indicated by "UCYN–A cluster". Other sequences were selected and used for comparison, labeled with genus and species names, and the values indicated at the nodes represent the percentage from 1,000 bootstrap replicates. The other OTUs (7.2%) clustered amongst the Sva0996 marine group (14 x OTUs), chloroplast (1 x OTU), *Prochlorococccus* (2 x OTU) and *Synechococcus* (1 x OTU).

Supplementary Fig. 3: The vertical distribution of UCYN–A in association with (A) a *Haptophyta* cell positively hybridized by the PRYM02 oligonucleotide probe and (B) an unknown eukaryote that was not hybridized by PRYM02, in the upper 200 m at station 16 and 17 along the VISION transect. Cell enumeration was based on double in situ hybridization by applying the UCYN–A732 and PRYM02 oligonucleotide probes.

Supplementary Table 1: Overview of bulk CO_2 and N_2 fixation activity expressed in volumetric and areal rates (integrated between 0–80 m depth).

Supplementary Fig. 1

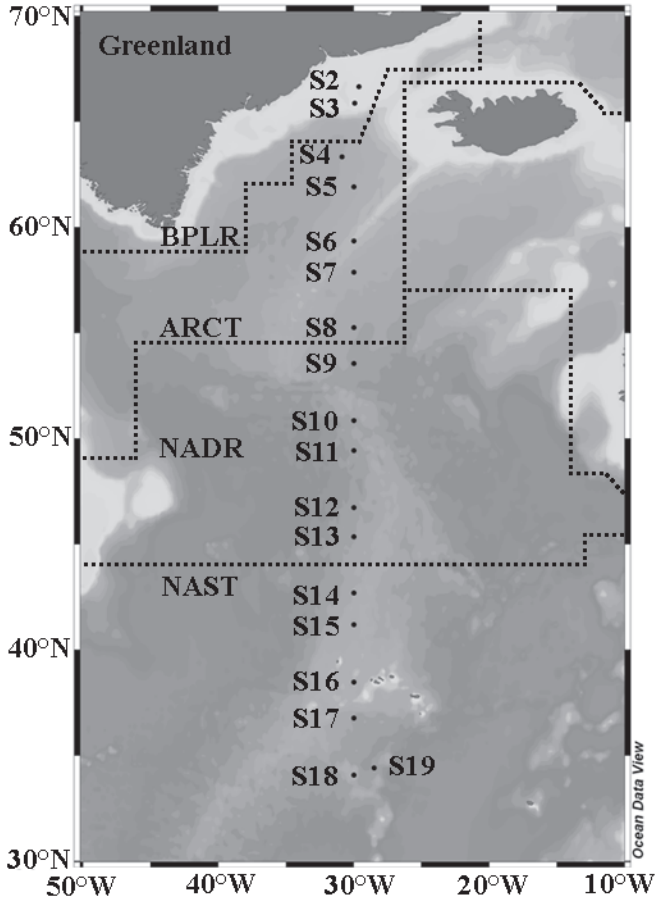

Supplementary Fig. 2

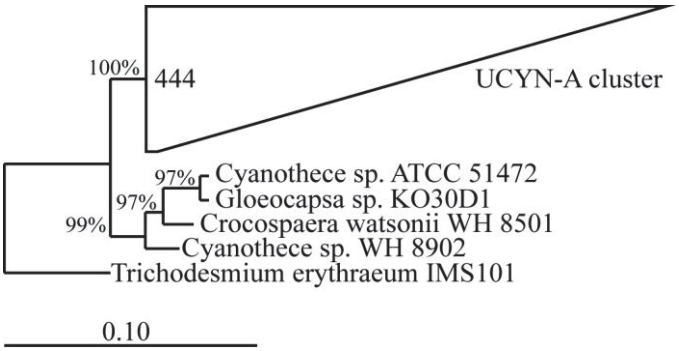

Supplementary Fig. 3

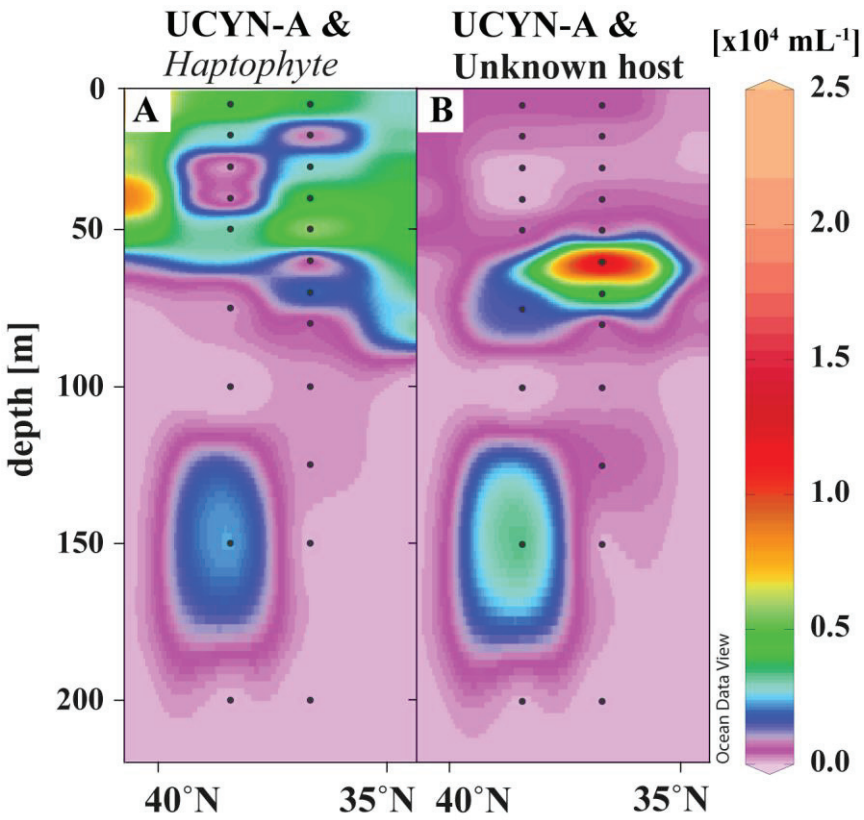

Supplementary Table 1:

			Volumetric rates		Areal rates		Volumetric rates		Areal rates	
			CO_2 fixation [nmol L^{-1} h^{-1}]		CO_2 fixation [mmol m^{-2} h^{-1}]		N_2 fixation [nmol L^{-1} h^{-1}]		N_2 fixation [µmol m^{-2} h^{-1}]	
Station	Latitude [°N]	Depth [m]	Light	Dark	Light	Dark	Light	Dark	Light	Dark
2	66.39	0	3.68	1.38	0.10	0.02	nd*	nd*	nd*	nd*
		20	0.32	0.03			nd*	nd*		
		60	1.31	0.10			nd*	nd*		
3	65.53	0	6.34	0.25	0.51	0.02	nd*	nd*	nd*	nd*
4	63.20	0	0.22	0.25	0.19	0.01	nd*	nd*	nd*	nd*
		20	4.32	0.08			nd*	nd*		
		40	4.95	0.22			nd*	nd*		
		75	0.09	nd*			nd*	nd*		
5	61.55	0	2350	0.30	0.42	0.01	nd*	nd*	nd*	nd*
		20	7.86	0.29			nd*	nd*		
		60	0.46	0.03			nd*	nd*		
6	59.21	0	24.02	X**	0.36	0.00	nd*	nd*	nd*	nd*
		20	4.50	0.03			nd*	nd*		
		75	0.70	nd*			nd*	nd*		
8	55.15	0	6.17	0.02	0.17	0.01	nd*	nd*	nd*	nd*
		20	2.50	0.15			nd*	nd*		
		40	2.04	0.11			nd*	nd*		
		75	0.59	0.04			nd*	nd*		
9	53.33	0	8.01	0.06	0.38	0.01	nd*	nd*	nd*	nd*

		20	2.68	0.11			nd*	nd*		
		40	4.92	0.13			nd*	nd*		
10	50.51	0	36.56	0.04	0.87	0.01	nd*	nd*	nd*	nd*
		40	7.18	0.07			nd*	nd*		
11	49.26	0	10.34	nd*	0.35	0.01	nd*	nd*	nd*	nd*
		20	X**	nd*			nd*	nd*		
		40	5.02	0.11			nd*	nd*		
12	46.44	0	5.93	nd*	0.07	0.00	nd*	nd*	nd*	nd*
		20	0.26	nd*			nd*	nd*		
		40	0.28	0.13			nd*	nd*		
		75	0.11	nd*			nd*	nd*		
14	42.42	0	4.35	0.42	0.64	0.02	0.0238	0.0320	2.6	1.9
		20	8.56	0.26			0.0333	0.0221		
16	38.29	0	4.97	0.75	0.34	0.06	0.0437	0.0292	2.4	2.0
		20	4.01	0.71			0.0334	0.0278		
		40	4.14	0.76			0.0250	0.0236		
		60	2.60	0.52			0.0195	0.0168		
17	36.47	0	2.04	2.38	0.23	0.18	0.0502	0.0675	5.1	5.4
		20	3.65	2.59			0.0728	0.0686		
		40	2.71	2.16			0.0628	0.0661		
18	34.44	0	1.47	1.13	0.18	0.08	0.0328	0.0316	2.8	2.4
		20	1.94	1.18			0.0371	0.0381		
		60	2.48	0.95			0.0343	0.0270		

* not detected
** not performed

2.4 Manuscript IV: The effect of nutrients on carbon and nitrogen fixation by the UCYN–A–*Haptophyta* symbiosis

Andreas Krupke[1*], Bernhard M Fuchs[1] and Marcel M.M. Kuypers[1]

[1]Max Planck Institute for Marine Microbiology, Bremen, Germany D–28359
[*]Corresponding author: Andreas Krupke, Department of Biogeochemistry, Max Planck Institute for Marine Microbiology, Celsiusstr. 1, D–28359 Bremen, Germany.
Email: akrupke@mpi–bremen.de

Potential co–authors: Wiebke Mohr[2,3], Julie LaRoche[2,4], Rudolf I Amann[1]
[1]Max Planck Institute for Marine Microbiology, Bremen, Germany
[2]Leibniz–Institut für Meereswissenschaften, Kiel, Germany
[3]current address: Harvard University, Cambridge, USA.
[4]current address: Dalhousie University, Halifax, Canada

Contribution: WM and JLR were organizing the field expedition, leading the experimental design and involved in sample collection. RIA provided scientific feedback and comments.

In Preparation for: *Environmental Microbiology*

Key words: N_2 fixation, Saharan Dust, nutrient transfer, nanoSIMS

Abstract

Biological N_2 fixation constitutes the major source of nitrogen in open ocean systems, regulating the marine nitrogen inventory and primary productivity. Symbiotic relationships between phytoplankton and N_2 fixing microorganisms (diazotrophs) have been suggested to play a significant role in the ecology and biogeochemistry in these oceanic regions. In the subtropical North Atlantic Ocean we identified field populations of uncultured unicellular cyanobacteria group A (UCYN–A) associated with photosynthetic *Haptophyta* partner cells using double Catalyzed Reporter Deposition–Fluorescence *In Situ* Hybridization (CARD–FISH) assays. Stable isotope incubation experiments with the addition of ^{13}C–Bicarbonate and dissolved $^{15}N_2$ gas in combination with various nutrient amendments (including iron, phosphorus, ammonium–nitrate and Saharan Dust) were performed to examine physiological interactions between individual UCYN–A and *Haptophyta* cells. NanoSIMS imaging revealed a tight physiological coupling in the transfer of carbon (R^2 = 0.6232; n = 44) and nitrogen (R^2 = 0.9659; n = 44) between host and symbiont. Generally, inorganic carbon fixation was enhanced in all nutrient incubations. In contrast, N_2 fixation was only stimulated when iron, Saharan Dust and/or phosphorus were added, emphasizing on aeolian dust deposition as a major parameter in constraining N_2 fixation of UCYN–A. Interestingly, the addition of ammonium–nitrate did not inhibit N_2 fixation by UCYN–A, but resulted in enhanced growth and decreased $^{15}N_2$ derived ^{15}N uptake by the associated *Haptophyta*. Moreover, after fixed nitrogen additions, a third unknown microbial partner was observed within individual UCYN–A associations. Our single cell measurements demonstrate the physiological complexity of the UCYN–A association and highlight the importance of aeolian dust on ocean productivity in this region.

Introduction

Open ocean environments are generally characterized by the scarcity of nutrients, particularly bioavailable nitrogen (N), which limits primary productivity (Karl et al., 2002). In such oligotrophic environments, the activity of diazotrophs, prokaryotic microorganisms that mediate the fixation of atmospheric N_2, (Zehr et al., 1998; LaRoche and Breitbarth, 2005) are favored since they can overcome N limitation. N_2 fixation constitutes the main source of fixed N in these waters, supplying fixed N to open ocean ecosystems.

Since the 1960´s (Dugdale et al., 1961), the most studied diazotroph has been the non–heterocystous cyanobacterium *Trichodesmium* spp., which contributes significantly to N_2 fixation in tropical and subtropical oceans (Capone et al., 2005). Other abundant diazotrophs in the open ocean are the nitrogen fixing cyanobacterium *Richelia* sp. found in association with diatoms (Mague et al., 1974; Villareal, 1991; Carpenter et al., 1999; Foster et al., 2011). N_2 fixation via these symbioses can fuel primary production and result in an enhanced sinking flux of organic carbon, which could play a mayor role in regulating the efficiency and amount of carbon (C) sequestered in the ocean (Subramaniam et al., 2008; Karl et al., 2012).

More recently, the importance of N_2 fixing unicellular cyanobacteria populations (UCYN–A, UCYN–B, UCYN–C) has been recognized (Zehr et al., 1998; Zehr et al., 2001; Montoya et al., 2004). Surveys based on quantitative PCR (qPCR) assays that target diazotroph abundance using the marker nitrogen fixation gene *nifH* (which encodes nitrogenase, the key enzyme for N_2 fixation) have revealed their widespread distribution throughout the oceans (Short et al., 2004; Church et al., 2005a; Langlois et al., 2008; Moisander et al., 2010).

The *nifH* gene phylotypes of UCYN–A often outnumber other diazotrophs (Moisander et al., 2010; Luo et al., 2012) and can be found in more diverse environments than most other diazotrophs (Short and Zehr, 2007; Rees et al., 2009; Moisander et al., 2010). UCYN–A *nifH* gene expression as mRNA is usually highest during the day, unlike other UCYN groups that express *nifH* and fix N_2 mainly during the night (Foster et al., 2013) to protect nitrogenase from oxygen produced during photosynthesis (Colon-Lopez and Sherman, 1998; Church et al., 2005b; Mohr et al., 2010a; Turk et al., 2011). Recent investigations report that the genome of UCYN–A lack genes for certain metabolic pathways characteristic for the oxygen evolving photosystem, which explains why UCYN–A expresses the oxygen sensitive nitrogenase during the day. The unusual metabolism of UCYN–A raises questions how these microorganisms thrive in open ocean systems (Zehr et al., 2008; DeLong, 2010; Tripp et al., 2010).

UCYN–A has recently been found living in association with unicellular photosynthetic eukaryotes belonging to the *Prymnesiophytes* (Thompson et al., 2012; Krupke et al., 2013). It has been hypothesized that the eukaryotic photosynthetic partner provides carbohydrates for UCYN–A and in return, obtains nitrogen compounds from UCYN–A (Thompson et al., 2012). Cultures of UCYN–A, unfortunately, do not exist, and therefore, environmental observations and field experiments are necessary for acquiring information concerning UCYN–A metabolism, and for quantifying the contribution of UCYN–A to the marine C and N cycles. Moreover, understanding the nutrient requirements and environmental parameters that regulate the physiological interactions between UCYN–A cells and their eukaryotic partner are still missing.

The primary nutrient that limits N_2 fixation in the world's oceans is an ongoing debate. Previous studies showed that the availability of phosphorus (P) (Sañudo–Wilhelmy et al., 2001) or iron (Fe) (Shi et al., 2007; Fu et al., 2008) can limit N_2 fixation activity, and Mills et al. (2004) demonstrated co–limitation of P and Fe in the North Atlantic. The effects of nutrient limitation on cellular growth and N_2 fixation has been investigated for cultured representatives such as *Trichodesmium* sp. or *Crocosphaera watsonii* (Berman–Frank et al., 2001a; Webb et al., 2001; Kustka et al., 2003; Hewson et al., 2009). Presently, no studies on the effect of P or Fe limitation on N_2 fixation and growth in the UCYN–A association exist. To address this issue, we conducted a wide range of nutrient amendment experiments to investigate the effect of nutrient additions on cellular CO_2 and N_2 fixation rates, adding inorganic nitrogen, phosphorus, and iron, as well as dust in varying combinations. Water samples were collected in the vicinity of the Cape Verdean Islands where UCYN–A is present throughout the year (LaRoche, unpublished results); this area is also characterized by elevated iron inputs due to Saharan Dust deposition (Guieu et al., 2002; Jickells et al., 2005; Stuut et al., 2005). Double CARD–FISH assays targeted UCYN–A cells, as well as their partner cells, and allowed us to visualize the cells' metabolic activity on a single cell level using nanometer scale secondary ion mass spectrometry (nanoSIMS). The aim was to investigate the effect of nutrients on C and N_2 fixation by the UCYN–A–eukaryote symbiosis.

Material and methods

Nutrient and stable isotope incubation experiments. Seawater for experiments was collected near the Cape Verdean Islands (located in the eastern tropical North Atlantic at 16.59° N, 24.52° W) on board the R/V *Islandia* in May 2009. Sample water from the upper water zone (10–20 m) was collected in the morning using a rosette of 12 x 5 L Niskin bottles mounted on a conductivity–temperature–density profiler (CTD).

Seawater from the Nisken bottles was transferred into acid cleaned 4.5 L polycarbonate bottles, which were subsequently used for incubation experiments that measured CO_2 and N_2 fixation. These incubation bottles were filled without air bubbles, closed with Teflon lined butyl septum caps and amended with nutrients yielding ten different treatments: (1) C = control, no nutrients added, (2) N = NH_4^+ (ammonium) + NO_3^- (nitrate), (3) P = PO_4^{3-} (phosphate) (4) Fe =Fe^{2+} (iron), (5) NP = NH_4^+ + NO_3^- + PO_4^{3-}, (6) NFe = NH_4^+ + NO_3^- + Fe^{2+}, (7) PFe = PO_4^{3-} + Fe^{2+}, (8) NPFe = NH_4^+ + NO_3^- + PO_4^{3-} + Fe^{2+}, (9) DI = Saharan Dust I, and (10) DII = Saharan Dust II. The following concentrations were added for N [2 µM], Fe [2 nM], P [0.2 µM], DI [2 mg L^{-1}] and DII [4 mg L^{-1}]. The utilized Saharan Dust represents surface soil collected under clean conditions from various locations in southern Algeria (Guieu and Thomas, 1996). The dust amendment contained P (0.14% ± 0.01%), Fe (4.97% ± 0.49%) and total nitrogen (0.12%± 0.003%) (Mills et al., 2004). Each treatment was prepared in triplicate.

Incubation bottles for each treatment were placed in an incubator with continuously flowing surface seawater and shaded to 25% surface irradiance. After 24 h of incubation, all bottles were amended with $^{15}N_2$ enriched liquid (~13 % labeling) (98% + $^{15}N_2$, Sigma–Aldrich, St. Louis, MO, USA) following the improved $^{15}N_2$ tracer technique (Mohr et al., 2010b; Großkopf et al., 2012) and 240 µM ^{13}C bicarbonate solution ($H^{13}CO_3^-$) (~10 %) (98% + $^{13}CO_2$, Sigma–Aldrich, St. Louis, MO, USA) using a gas tight syringe. Incubation bottles were incubated for an additional 24 h period. Bulk CO_2 and N_2 fixation rates were determined and will be reported in a separate study on total CO_2 and N_2 fixation rates (Mohr et al., unpublished).

Double CARD–FISH assay. At the end of the incubation period, triplicate 20 mL aliquots of water were preserved in 1% paraformaldehyde (PFA) for approximately 1 h at room temperature (RT). Subsequently, these samples were individually filtered through 0.2 µm pore size filters (GTTP, 25 mm diameter), and pre–sputtered with gold (Au) and palladium (Pd) using a vacuum filtration manifold (Merck Millipore, Billerica, USA). After filtration,

filters were washed in 1 x phosphate buffered saline (PBS) solution (130 mM NaCl; 10 mM Na_2HPO_4; pH 7.6) and stored at –20 °C until further processing.

In the first CARD–FISH (Catalyzed Reporter Deposition–Fluorescence *In Situ* Hybridization) application, we used the 18S rRNA oligonucleotide probe PRYM02 targeting *Haptophyta* (Simon et al., 2000) following standard protocols (Pernthaler and Amann, 2004; Pernthaler et al., 2004). In the second CARD–FISH the oligonucleotide probe UCYN–A732, targeting the 16S rRNA specific for UCYN–A cells, and its corresponding helper probes Helper A–732 and Helper B–732 were applied to increase the probes' access to 16S rRNA target regions according to Krupke et al. (2013). Horseradish peroxidase (HRP) labeled oligonucleotide probes were at working solutions of 8.42 pmol μL^{-1} following dilution in the hybridization buffer (1:300; v:v). All hybridizations were performed at optimal formamide (FA) concentrations to ensure maximal stringency (Krupke et al., 2013); the oligonucleotides EUB338 (Amann et al., 1990) or EUK516 (Amann et al., 1990) were used as positive controls and the oligonucleotide NON338 (Wallner et al., 1993) was used as a negative control.

Phylogenetic identification was performed on filter sections using standard protocols (Pernthaler et al., 2004; Pernthaler and Pernthaler, 2007) with some changes for the double CARD–FISH assays. Changes include permeabilization of the cell wall with lysozyme solution (10 mg mL^{-1} in 0.05 M EDTA, pH 8.0; 0.1 M TrisHCl; Fluka, Taufkirchen, Germany) for 1 h at 37 °C, followed by the inactivation of endogenous peroxidases using 0.01 M HCl for 10 min at RT. In the first CARD–FISH application, eukaryotic cells were hybridized for 3 h at 46 °C and washed in washing buffer for 15 min at 48 °C. The first CARD was performed for 20 min at 46 °C using Alexa594 tyramides (Molecular probes, Leiden, The Netherlands) (Pernthaler et al., 2004). Afterwards, filter sections were washed in 1 x PBS for 10–20 min in the dark and placed in 3% H_2O_2 solution for 20 min at RT in order to inactivate the HRP for the second round of hybridization. UCYN–A cells were hybridized for 8 h at 35 °C and washed in washing buffer for 15 min at 37 °C. The second CARD was performed for 20 min at 46 °C using fluorine (^{19}F) labeled tyramides (i.e. Oregon Green 488, Molecular probes, Leiden, The Netherlands). The cells were counterstained with 1 µg mL^{-1} 4',6–diamidino–2–phenylindol (DAPI) for 10 min at RT in the dark.

Marking, microscopy and mapping for nanoSIMS. Laser markings were made near positively hybridized UCYN–A cells associated with a positively hybridized *Haptophyta* with a Laser Micro–dissection (LMD) Microscope 6500 (Leica, Berlin, Germany). We used optical filter sets suitable for the Oregon Green 488 tyramides to reveal positively hybridized UCYN–A cells (excitation Maximum: 498 nm; emission Maximum: 526 nm) and the Alexa

594 tyramides to reveal positively hybridized *Haptophyta* (excitation Maximum: 550 nm; emission Maximum: 570 nm). Filter pieces were then embedded in a mixture of low fluorescence glycerol mountant (Citifluor AF1, Citifluor Ldt London, United Kingdom) and mounting fluid Vecta Shield (Vecta Laboratories, Burlingame, CA USA) in a 4:1 ratio in order to take microscopic pictures using a Zeiss Axioskop II fluorescence microscope (Zeiss, Berlin, Germany). These pictures were used for orientation purposes during subsequent nanoSIMS analysis and for post–processing using look@nanoSIMS software (Polerecky et al., 2012). Prior to nanoSIMS analysis, filter pieces were washed with ultra pure water and air–dried.

NanoSIMS measurements. Single cell activity was visualized using a Cameca NanoSIMS 50L instrument (Cameca, Gennevilliers France). Prior to analysis, the area was pre–sputtered for 1–2 min with a rastered high–current Cs^- beam to implant Cs and remove surface contaminants. Then, sample surfaces were rastered with a 16 keV Cesium (Cs^+) beam and a current between 25–35 pA. Primary ions were focused into a nominal ~100–120 nm spot diameter. The primary ion beam was used to raster the analyzed area with an image size of 256 x 256 pixels and a dwelling time of 1 or 3 ms per pixel. Raster areas were usually 10 x 10 µm. Negatively charged secondary ions of carbon (C), fluorine (F), nitrogen (as CN) and sulfur (S) (i.e. $^{12}C^-$, $^{13}C^-$, $^{19}F^-$, $^{12}C^{14}N^-$, $^{12}C^{15}N^-$ and $^{32}S^-$) were measured simultaneously in raster imaging mode by electron multiplier detectors.

All scans (40–50 planes) were corrected for drift of the beam and sample stage after acquisition. Isotope ratio images were created as the ratio of a sum of total counts for each pixel over all recorded planes in respect to the investigated isotope. Regions of interest (ROIs) around cell structures were circled and calculated using the automated threshold feature based on the *look@nanosims* software (Polerecky et al., 2012). Cell dimensions were estimated from the ROIs and the *look@nanosims* software.

Calculations. Carbon and nitrogen uptake for individual cells was estimated using the equations listed below. The biovolume (V) was calculated according to Sun and Liu (2003):

$$V = (\pi/6) \times Ø^3 \quad (1)$$

where Ø is the cell diameter. Estimates of C content per individual UCYN–A cell was followed by the Verity et al. (1992):

$$\text{Log [C]} = -0.363 + (0.863 \times (\text{Log (V)})) \quad (2)$$

Estimates of C content per individual *Haptophyta* cell was followed by Strathmann (1967):

$$\text{Log [C]} = -0.422 + (0.758 \times (\text{Log (V)})) \quad (3)$$

The C content per cell (C_{con}) was converted into N content per cell (N_{con}) based on conversion factors provided by Tuit et al. (2004) assuming a modified Redfield ratio (C:N) of 8.6. The isotopic ratios (R_C = $^{13}C/^{12}C$ and R_N = $^{15}N/^{14}N$) based on ROI selections and nanoSIMS analysis were used to calculate atom percent (AT%) enrichment of ^{13}C or ^{15}N by:

$$A_C = R_C/(R_C + 1) \quad (4)$$

$$A_N = R_N/(R_N + 1) \quad (5)$$

where A_C represents AT% enrichment of ^{13}C and A_N represents the AT% enrichment of ^{15}N. The cell specific C and N uptake (F_C or F_N) was calculated according to the length of incubation time under stable isotope amendments (i.e. 24 hours) by:

$$F_C = (^{13}C_{ex} \text{ x } C_{con})/C_{SR} \quad (6)$$

$$F_N = (^{15}N_{ex} \text{ x } N_{con})/N_{SR} \quad (7)$$

where $^{13}C_{ex}$ and $^{15}N_{ex}$ represent the AT% enrichment of ^{13}C and ^{15}N of the individual ROIs corrected for by the mean AT% ^{13}C and AT% ^{15}N at time–zero. Time–zero AT% were determined on bulk samples using elemental analyzer–isotope ratio mass spectrometry (EA–IRMS). The EA–IRMS is well calibrated for both non–enriched and enriched samples with high instrument accuracy and precision (e.g. 0.3651 ± 0.0000 ^{15}N atom % and 1.0658 ± 0.0004 ^{13}C atom % based on the mean and standard deviation of caffeine standards). The C_{SR} and N_{SR} is the estimated labelling percentage of C and N in the experimental bottle.

Statistical evaluations. Single cell C and N uptake results (i.e. AT% ^{13}C and ^{15}N as well as CO_2 and N_2 fixation rates) were statistically evaluated using SigmaStat 3.5 software. We applied the t–test to compare measurements between two individual treatments. In case of a failure in normalizing individual treatment datasets we applied either Mann–Whitney Rank Sum Test (MW–test) or Equal Variance Test (EV–test).

Results

Visualization of UCYN–A–Haptophyta associations. UCYN–A cells and their *Haptophyta* partner cells were simultaneously identified via the double labeling CARD–FISH approach (Fig. 1A,D,G small inserts). The application of the UCYN–A specific oligonucleotide probe (Krupke et al., 2013) in concert with the deposition of halogenated tyramides and subsequent nanoSIMS measurements allowed us to further verify the phylogenetic identification of UCYN–A cells based on ^{19}F signals (Fig. 1A,D,G). We imaged the single cell C and N uptake by UCYN–A and the associated *Haptophyta* cells. Examples are shown for individual associations in the treatment with no nutrient addition (control), N treatment (NO_3^- and NH_4^+ addition), and one of the two sets of Saharan Dust addition (DII treatment) (Fig. 1A–I).

NanoSIMS measurements of all examined cells gave average cell diameters of 0.83±0.15 µm for UCYN–A, and 1.66±0.23 µm for *Haptophyta* cells. Individual values, however, were used to estimate biovolumes at the end of each treatment (Fig. 2A,B, Supplementary Fig. 1A–D). The largest biovolumes of UCYN–A cells were detected when N species (NO_3^- and NH_4^+) in combination with P or Fe were added in the NP and NPFe treatment (0.51±0.11 μm^3, 0.43±0.09 μm^3, respectively) (Fig. 2A). Overall, the nutrient additions yielded biovolumes of UCYN–A cells that were not significantly different from the unamended control (MW–test, $p = 0.065$ and t–test, $p \geq 0.064$).

In contrast, nutrient additions led to strikingly increased biovolumes for *Haptophyta* cells. Except for the Fe and DII treatments, all measured biovolumes were significantly larger (on average 3.05±0.16 μm^3) than the control (1.56±0.21 μm^3) (MW–test, $p \leq 0.019$ and t–test, $p \leq 0.03$) (Fig. 2B). The strongest response was observed during the NP treatment (3.60±0.20 μm^3). The obtained biovolume observed in the PFe treatment was twice as large as in the control (Fig. 2B). Overall, estimated biovolumes for the associated *Haptophyta* cells were ~3–10 times greater than values for UCYN–A cells (Fig. 3B).

Carbon uptake in UCYN–A and associated Haptophyta cells. All nutrient additions resulted in greater ^{13}C enrichment, as well as elevated C fixation rates for UCYN–A and their associated *Haptophyta* cell compared to control measurements (Fig. 4A–D). On average, UCYN–A cells were about one third more enriched in ^{13}C in the nutrient addition experiments than cells under control conditions (AT% ^{13}C 2.39±0.19). However, this ^{13}C enrichment was only significant in the following treatments, (1) Fe = AT% ^{13}C 3.91±0.19, (2) NP = AT% ^{13}C 3.31±0.38, (3) NPFe = AT% ^{13}C 3.36±0.20 and (4) DII = (AT% ^{13}C 3.31±0.28) (MW–test, $p \leq 0.036$ and EV–test, $p = 0.008$) (Fig. 4A and Supplementary Fig. 2A,B). Calculated C fixation rates of UCYN–A were up to 3 times higher after nutrient

addition than in the control treatment (0.06±0.01 fmol C $cell^{-1}$ h^{-1}) and differed significantly from the control in the Fe treatment (0.15±0.02 fmol C $cell^{-1}$ h^{-1}, MW–test, p = 0.03), NP treatment (0.19±0.04 fmol C $cell^{-1}$ h^{-1}, t–test, p = 0.004), and the NPFe treatment (0.15±0.01 fmol C $cell^{-1}$ h^{-1}, t–test, p < 0.002) (Fig. 4B). Elevated C uptake was observed in the experiment where P and Fe were added (PFe treatment), but the available dataset for this treatment is limited since only one measurement could be performed. No data is available from the P only treatment because no double–hybridized UCYN–A–eukaryote associations were detected in the samples.

In associated *Haptophyta* cells ^{13}C enrichments were up to 2 times as large as the ^{13}C enrichment of the associated UCYN–A cells. C fixation rates for *Haptophyta* were up to 7 times greater than for UCYN–A (Fig. 4A–D, Supplementary Fig. 3A–I). Generally, ^{13}C enrichments within *Haptophyta* cells increased during all treatments (AT% ^{13}C 4.02±0.11) compared to the control (AT% ^{13}C 3.49±0.27), but were not significantly different between treatments (MW–test, p > 0.121) (Fig. 4C). C fixation rates for *Haptophyta* cells were elevated after nutrient additions and were on average about twice as high (0.62±0.03 fmol C $cell^{-1}$ h^{-1}) as in the control treatment (0.31±0.3 fmol C $cell^{-1}$ h^{-1}) (Fig. 4D). The highest C fixation rates were encountered in the NP treatment with 0.84±0.09 fmol C $cell^{-1}$ h^{-1}. Measured C fixation rates increased significantly in all nutrient treatments compared to the control (MW–test, p = 0.028 and t–test, $p \leq 0.007$), except in one of the treatments with Saharan Dust addition (DII treatment) (Fig. 4D).

Nitrogen uptake in UCYN–A and associated Haptophyta cells. ^{15}N enrichment of UCYN–A cells in treatments where additional nitrogen species were available did not differ significantly from the control (MW–test, $p \geq 0.214$ and EV–test, p > 0.064) (Fig. 4E). ^{15}N enrichments were either slightly greater (NP and NFe treatments) or up to one third lower (N and NPFe treatments) compared to control values with AT% ^{15}N 1.08±0.10 (Fig. 4E).

In contrast, UCYN–A cells were significantly enriched in ^{15}N (2–3 fold) when iron and Saharan Dust was added compared to control (AT% ^{15}N values of 1.89±0.11, 1.95±0.17 and 2.97±0.43 for Fe, DI and DII treatments, respectively; MW–test, $p \leq 0.043$) (Fig. 4E, Supplementary Fig. 2A,B). Corresponding N_2 fixation rates for UCYN–A cells were also significantly higher in the Fe, DI and DII treatments (0.0072±0.0014, 0.0069±0.0021 and 0.0134±0.0042 fmol N $cell^{-1}$ h^{-1}, respectively; MW–test, p < 0.03 and t–test, p < 0.043) than in the control (0.0031±0.0005 fmol N $cell^{-1}$ h^{-1}; t–test, p = 0.24) (Fig. 4F). N_2 fixation rates were not significantly different from the control (0.0031±0.0005 fmol N $cell^{-1}$ h^{-1}) when inorganic nitrogen (i.e. NO_3^- and NH_4^+) was available (Fig. 4F).

The ^{15}N enrichment of the *Haptophyta* cells remained mostly unaltered compared to the control when nitrogen compounds (i.e. NH_4^+ and NO_3^-) were added in combination with phosphorus or iron (AT% ^{15}N 1.43±0.15) (Fig. 4G). However, ^{15}N–enrichment within *Haptophyta* cells dropped significantly in the N treatment (AT% ^{15}N 0.89±0.14) and the NPFe treatment (AT% ^{15}N 1.25±0.08) (EV–test, p = 0.021 and MW–test, p = 0.045) (Fig. 4G). In contrast, *Haptophyta* cells ^{15}N enrichments were significantly enhanced (2–3 fold) upon Fe, and dust (experiments DI and DII) additions (AT% ^{15}N values of 2.23±0.13, 2.36±0.22 and 3.54±0.52, respectively; EV–test, p = 0.017 and MW–test, p = 0.004) (Fig. 4G). The PFe treatment also yielded elevated ^{15}N enrichment (AT% ^{15}N 3.29) nearly twice as high as the control values (AT% ^{15}N 1.43±0.15) (Fig. 4).

Assimilation rates of N_2 derived N within *Haptophyta* cells increased upon all nutrient additions compared to the control experiment (0.0158±0.0024 fmol N cell^{-1} h^{-1}), except after the addition of NO_3^- and NH_4^+, when rates declined (0.0127±0.0034 fmol N cell^{-1} h^{-1}) (Fig. 4H). The assimilation rates of N_2 derived N by *Haptophyta* cells were significantly enhanced in the Fe, DI and DII treatment (0.0326±0.0034, 0.0475±0.0023 and 0.0580±0.0144 fmol N cell^{-1} h^{-1}) relative to the control (MW–test, $p \leq 0.004$) (Fig. 4H). An even higher rate of 0.0789 fmol N cell^{-1} h^{-1}was observed for the *Haptophyta* cell in the PFe treatment (ca. 5 times the rate of the control; see Fig. 4H).

Observation of unknown structures within the UCYN–A–Haptophyta association. When NO_3^- and NH_4^+ were added a third structure in the UCYN–A–*Haptophyta* associations was sometimes observed (Fig. 3A–F). This enigmatic structure was slightly smaller than UCYN–A cells with a cell diameter of 0.70±0.06 and a cell biovolume of 0.21±0.06. These structures were highly enriched in ^{13}C (AT% ^{13}C 5.16 ± 0.44), but low in ^{15}N (AT% ^{15}N 0.54 ± 0.06). On average, these structures were about two–thirds more enriched in ^{13}C than UCYN–A cells and about one–third more than *Haptophyta* cells (Fig. 3B and Fig. 4A,C). These structures were approximately one–third lower enriched in ^{15}N than UCYN–A cells, and two–thirds lower than *Haptophyta* cells across all treatments (Fig. 2C and Fig. 4E,G).

Discussion

Nutrients limiting N_2 fixation by UCYN–A. Our experiments demonstrate that Saharan Dust additions stimulate UCYN–A N_2 fixation activity and can be further enhanced when the amount of Saharan Dust is doubled, as in the DII treatment (Fig. 4E,F). The uptake of Fe from the iron–rich Saharan Dust could explain why dust additions enhanced N_2 fixation, which is supported by the fact that Fe additions also significantly stimulate N_2 fixation by UCYN–A. Aeolian dust might also provide molybdenum (Mo), another component that is suggested to limit N_2 fixation (Howarth and Cole, 1985). The genome of UCYN–A revealed the capacity to take up Mo as well as Fe, both trace metals are required for electron carrier proteins and serve as cofactors for the nitrogenase enzyme (Postgate, 1982; Kustka et al., 2003).

Previous studies also showed that dust deposition in the marine environment releases P (Ridame and Guieu, 2002; Bonnet and Guieu, 2004). Unfortunately, we could not determine the effect of phosphorus addition only (P treatment) on the N_2–fixation rates by UCYN–A, but our results from the PFe treatment revealed elevated CO_2 and N_2 fixation activity (Fig. 4A–H). Both nutrients (i.e P and Fe) have been shown to co–limit N_2 fixation in oligotrophic waters (Mills et al., 2004). Overall, our combined results indicate that the diazotrophic partner is limited by P and Fe near the Cape Verdean Islands.

Nutrients limiting CO_2 fixation by the Haptophyta partner. All nutrient additions resulted in enhanced photosynthetic activity of the *Haptophyta* partner, which concomitantly led to increased biovolumes (Fig. 2B) (Falkowski and Owens, 1980; Gallagher and Alberte, 1985; Coles et al., 2004). Our combined results indicate that the *Haptophyta* partner growth is N, P and Fe limited in the vicinity of the Cape Verde islands.

Carbon and nitrogen transfer between UCYN–A and Haptophyta cells. The genome of UCYN–A lacks genes for any known CO_2 fixation pathway, but has the genetic repertoire to perform N_2 fixation (Zehr et al., 2001; Tripp et al., 2010). Therefore, we hypothesize that the observed ^{13}C enrichment in the UCYN–A originates from C transfer from the photosynthetic *Haptophyta*, whereas the ^{15}N enrichment within the *Haptophyta* results from a transfer of $^{15}N_2$ derived fixed ^{15}N from UCYN–A (Fig. 1A–I and Fig. 4A–H). In all treatments, we observe a significant correlation between the carbon enrichment and uptake rates ($R^2 = 0.6232$; n = 44, two–tailed probability, $p < 0.001$), as well as the nitrogen enrichment and uptake rates ($R^2 = 0.9659$; n = 44, two–tailed probability, $p < 0.001$) of UCYN–A and the associated *Haptophyta* cells (Fig. 5A–D). Based on the determined ^{13}C and ^{15}N enrichment within individual associations, we estimate that on average UCYN–A cells assimilated 16.4±7.1% of all C fixed by the *Haptophyta* and the *Haptophyta* cells assimilated 85.4±5.1% of nitrogen fixed by

UCYN–A. These values are similar to recent findings that show that UCYN–A transfers up to 95% of its fixed N to the host, and in turn receives approximately 17% of the inorganic C fixed by the host (Thompson et al., 2012). A similar transfer of C and N has also been reported for symbiotic relationships between diatoms and N_2 fixing cyanobacteria (Foster et al., 2011). Thus far, it is not clear which organic C compound is transferred from the *Haptophyta* to the UCYN–A. Insight my be obtained from cultured representatives closely related to UCYN–A, such as *Cyanothece* sp. ATCC 51142 that can grow in the presence of 3–(3,4–dichlorophenyl)–1,1–dimethylurea and glycerol (Reddy et al., 1993; Vu et al., 2012).

Our results show a very tight coupling between ^{15}N enrichments of symbiont and host, indicating that the amount of N_2 derived N that is taken up by the *Haptophyta* depends mainly on the UCYN–A N_2 fixation activity. The addition of NH_4^+ and NO_3^- does not cause N_2 fixation inhibition; these findings are similar to the observations for other cultivated members of the UCYN group (Dekaezemacker and Bonnet, 2011; Großkopf and LaRoche, 2012). The addition of inorganic N does enhance *Haptophyta* C–based growth (Fig. 2A,B and Fig. 4C). The high rate of ^{13}C uptake, but low rate of ^{15}N uptake within *Haptophyta* cells upon NH_4^+ and NO_3^- addition, suggests that the eukaryote can switch to fixed N uptake from external sources other than UCYN–A. However, under typical oligotrophic conditions in the open ocean, N_2 fixation by UCYN–A would be the main source of fixed N for the partner *Haptophyta* cells.

Formation of unknown structures within the UCYN–A–Haptophyta association. Intriguingly, an unknown structure within the association occurred in all treatments with ammonium and nitrate additions (Fig. 3A–F). This enigmatic structure is characterized by high ^{13}C enrichment, but low ^{15}N enrichment. In comparison to *Haptophyta* cells, these structures were approximately 2–fold more enriched in ^{13}C, Presently, it is unclear what this structure might represent: it could be a C–storage compartment for (e.g.) carbohydrates or it could represent an early stage of coccoliths formation. The latter would likely play a role in estimates of carbon sedimentation rates and overall carbon flux to the deep ocean (Bramlette, 1958; Honjo, 1976; Fritz, 1999). The application of scanning electron microscopy would help to verify the presence of $CaCO_3$ attached plates.

This enigmatic structure may also represent an attached unidentified microorganism since it contains C, N and sulfur (S), even though no strong DAPI signal could be observed (Fig. 1B–F). Diffuse or very weak DAPI signals are common for small cells as was observed for the co–occurring UCYN–A cells. Because this “unknown” microorganism is more enriched in ^{13}C than the photosynthetic partner algae of UCYN–A, it may represent a photosynthetic or chemoautotrophic organism.

Concluding remarks. This study provides the first insight into the physiological responses of field populations of the UCYN–A–*Haptophyta* association to nutrient addition. We observed that the addition of Fe and dust stimulate UCYN–A N_2 fixation activity. These results emphasize the role of Saharan aeolian dust inputs as the main substrate constraining N_2 fixation activity by UCYN–A in the vicinity of the Cape Verdean Islands. The *Haptophyta* appears to benefit directly from the close association with the UCYN–A due to fixed N transfer, especially under dust supply. The discovery of a third microstructure within the UCYN–A–*Haptopyhte* association, most likely an unknown cell, underlines the complexity of interactions among microorganisms in oligotrophic surface waters. The determined cell diameter and biovolumes of these two partner cells can be helpful in refining estimates of single cell C contents and growth rate of this widely, but uncultivated association (Goebel et al., 2008). Furthermore, insights gained from this study may provide helpful information for isolation attempts of both partner cells. This can further be supported by future efforts gathering genetic information on the metabolic repertoire of the associated *Haptophyta* to unravel mechanisms and potential pathways regulating the C and N exchange within this association. Thus far, we do not know anything about grazing, recycling or export of UCYN–A in open ocean systems. Hence, quantitative information on the mechanisms involved in CO_2 and N_2 fixation, release of fixed N and sinking rates of UCYN–A–*Haptophyta* associations will deepen our understanding of their impact on global C and N cycle.

Figures

Fig. 1: Visualization of the UCYN–A association linking the phylogenetic identity of UCYN–A according to the ^{19}F signal (A, D, G) and its single cell activity (including the *Haptophyta* partner cell) based on isotopic ratios for C ($^{13}C/^{12}C$ = middle panels B,E,H) and N ($^{15}N/^{14}N$ = right panels C,F,I) within different nutrient amendment incubation experiments. Inset panels on the left side show the corresponding epi–fluorescent images of the UCYN–A cells (green signal) and its associated *Haptophyta* cell (red signal), as well as DAPI staining (blue signal) based on double CARD–FISH approach taken prior to nanoSIMS analysis. NanoSIMS images refer to different nutrient amendment incubation experiments: (A–C) Control = no nutrient added, (D–F) N = NH_4^+ + NO_3^- addition, (G–I) DII = 4 mg/L Saharan Dust. Warmer colors represent higher abundance of the respective isotopes.

Fig. 2: Overview of average biovolumes with standard error for (A) UCYN–A and (B) the associated *Haptophyta* cells with respect to all treatments from left to right: (1) Ctr = control, no nutrients added, (2) N = NH_4^+ (ammonium) + NO_3^- (nitrate), (3) Fe =Fe^{2+} (iron), (4) NP = NH_4^+ + NO_3^- + PO_4^{3-}, (5) NFe = NH_4^+ + NO_3^- + Fe^{2+}, (6) PFe = PO_4^{3-} + Fe^{2+}, (7) NPFe = NH_4^+ + NO_3^- + PO_4^{3-} + Fe^{2+}, (8) DI = Saharan Dust I, and (9) DII = Saharan Dust II. The asterisks indicate statistically different compared to the control. No statistics were performed on the PFe treatment and single cell rates. Dashed line indicates average values of control measurements.

Fig. 3: Visualization of the UCYN–A association within the NP treatment linking the phylogenetic identity of UCYN–A and its single cell activity (including the *Haptophyta* partner cell). Panels show (A) deposited fluorine labeled tyramides according to the ^{19}F signals, (B) ^{13}C enrichment = $^{13}C/^{12}C$, (C) ^{15}N enrichment = $^{15}N/^{14}N$, (D) DAPI signal shown in black–white, (E) carbon and nitrogen distribution = $^{12}C/^{14}N$ * 1000 and (F) sulfur = ^{32}S. Inset panel on the left side show the corresponding epi–fluorescent images of the UCYN–A cells (green signal) and it's associated *Haptophyta* cell (red signal), as well as DAPI staining (blue signal) based on double CARD–FISH approach taken prior to nanoSIMS analysis. An unknown structure attached to the UCYN–A association that has (D) a weak DAPI signal but enriched in C and depleted in N (B,C). Next to C and N signals (B,C,E) it also contains (S) sulfur. Such a structure was only found when fixed nitrogen was added. Warmer colors represent higher abundance of the respective isotopes. Brighter white DAPI signals indicate stronger staining due to more DNA.

Fig. 4: Overview of nanoSIMS measurements for the association between UCYN–A and a *Haptophyta* from the nutrient amendment incubation experiments. The panels on the left side represent the isotopic enrichment in AT% for individual cells for ^{13}C (A = UCYN–A; C = *Haptophyta*) and ^{15}N (E = UCYN–A; G = *Haptophyta*). The panels on the right side (B,D,F,H) show the corresponding single cell activity in fmol cell^{-1} h^{-1} for C and N fixation, estimated based on obtained nanoSIMS values (AT%) and cell dimension analysis. Abbreviations for listed treatments follow Fig. 2. The asterisk symbol indicates statistical significance compared to control. No statistics were performed on the PFe treatment and single cell rates. Dashed line indicates average values of control measurements.

Fig. 5: Single cell enrichments and rates for (A,B) carbon in AT% ^{13}C and fmol C cell^{-1} h^{-1} as well as for (C,D) nitrogen in AT% ^{15}N and fmol N cell^{-1} h^{-1} within individual associations between UCYN–A and its corresponding *Haptophyta* partner cell across all treatments. Abbreviations of treatments follow Fig. 2.

Fig. 1

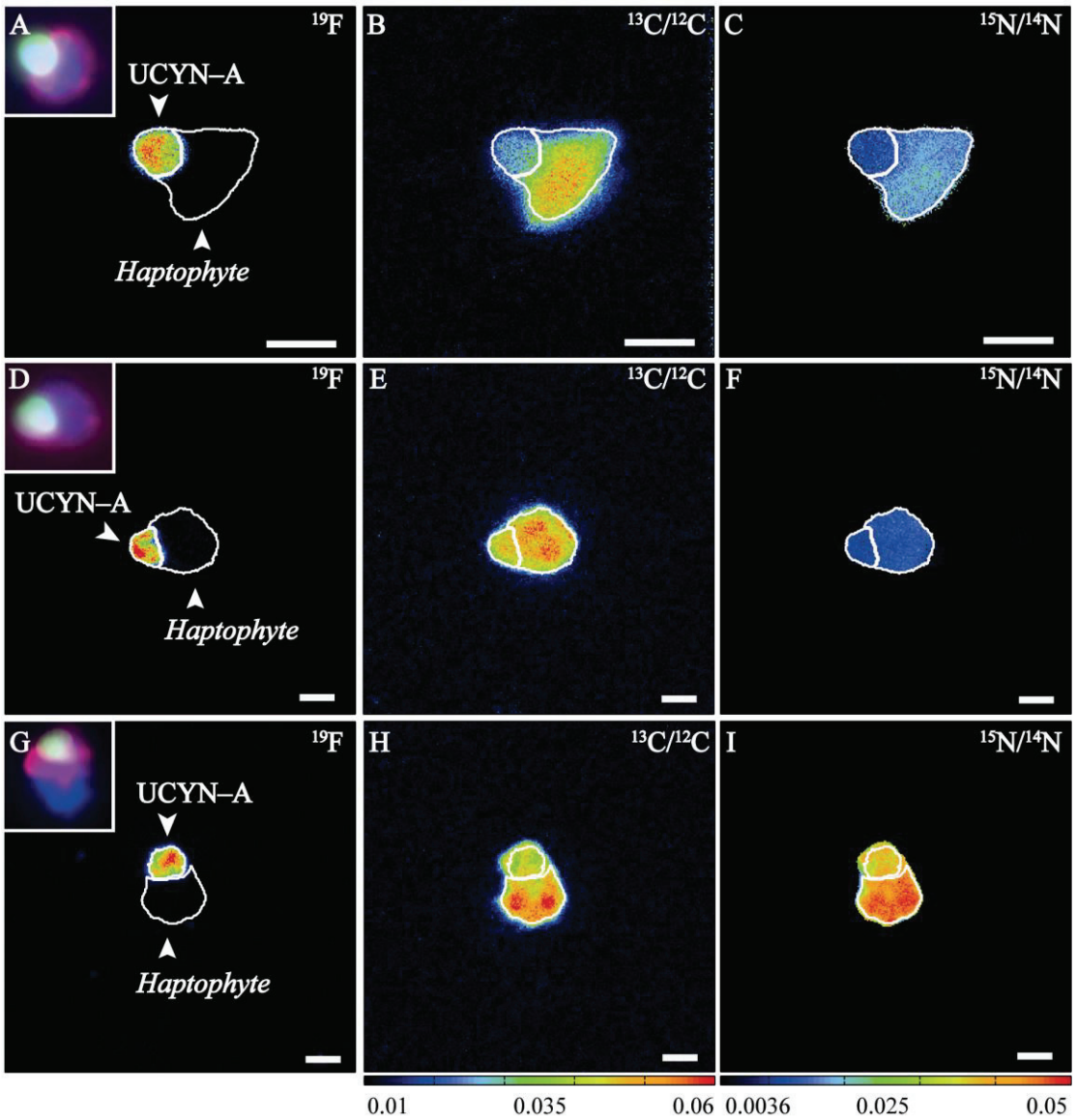
A
19F
UCYN–A
Haptophyte
B
13C/12C
C
15N/14N
D
19F
UCYN–A
Haptophyte
E
13C/12C
F
15N/14N
G
19F
UCYN–A
Haptophyte
H
13C/12C
I
15N/14N
0.01
0.035
0.06
0.0036
0.025
0.05

Fig. 2

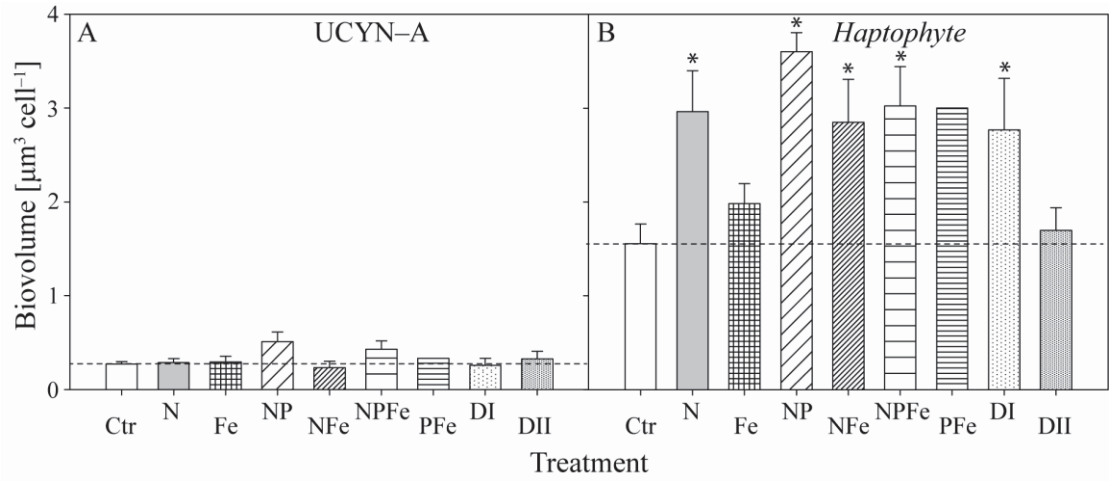
A
UCYN–A
B
Haptophyte
Biovolume [µm³ cell⁻¹]
0
1
2
3
4
Ctr
N
Fe
NP
NFe
NPFe
PFe
DI
DII
Treatment

Fig. 3

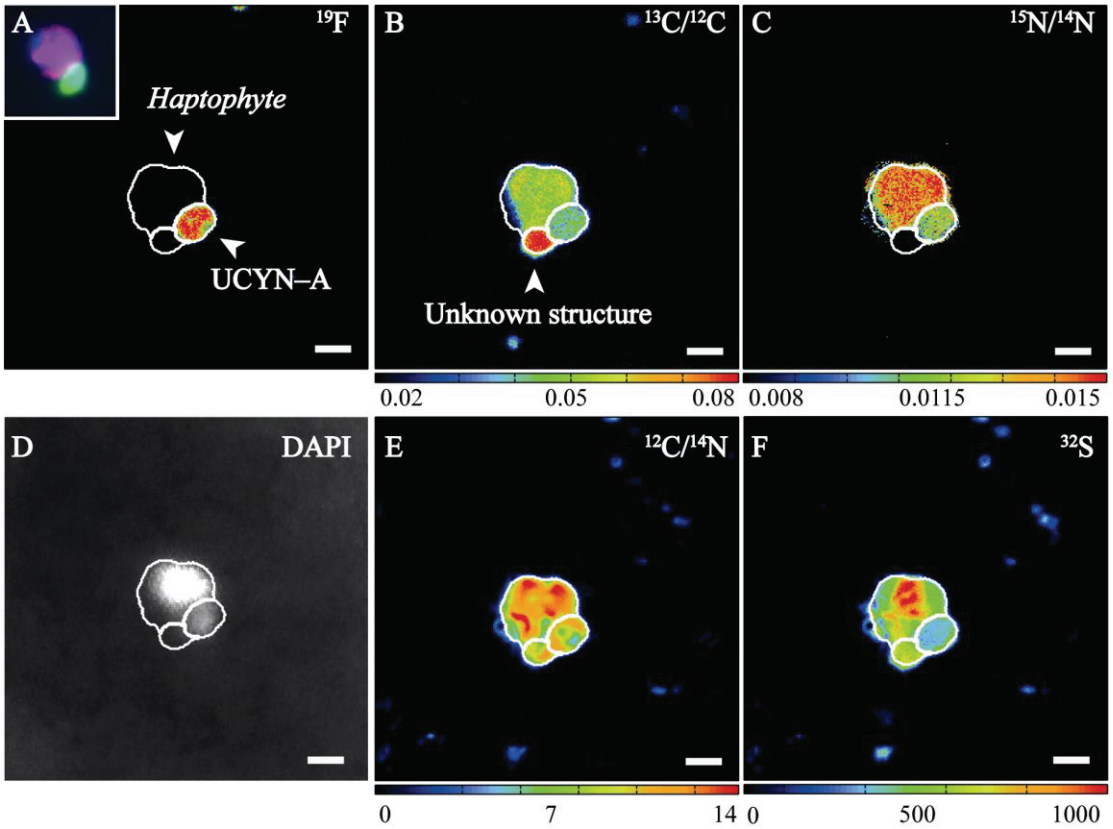
A
19F
Haptophyte
UCYN–A
B
13C/12C
Unknown structure
0.02
0.05
0.08
C
15N/14N
0.008
0.0115
0.015
D
DAPI
E
12C/14N
0
7
14
F
32S
0
500
1000

Fig. 4

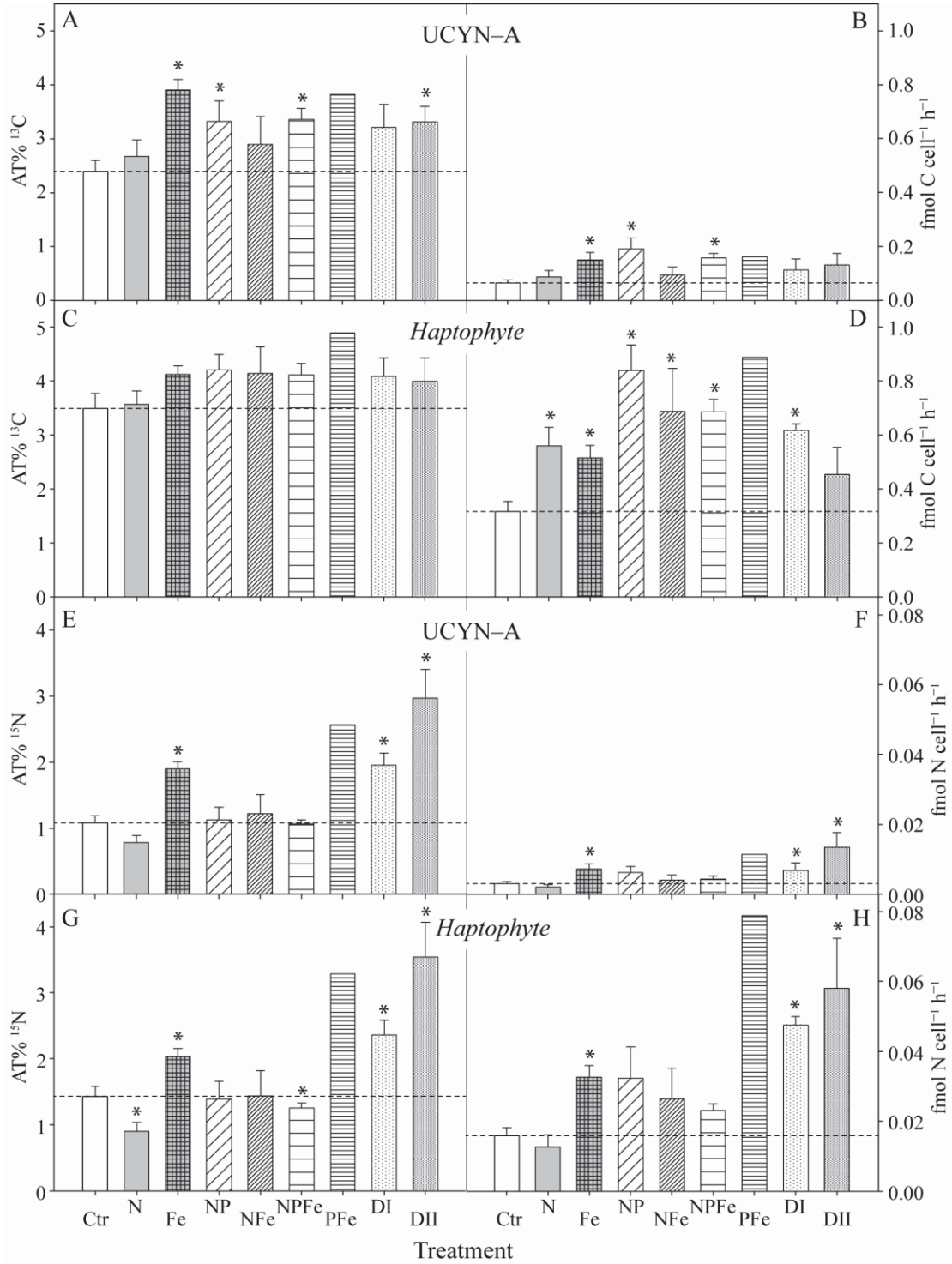
A
UCYN–A
B
AT% 13C
fmol C cell−1 h−1
C
Haptophyte
D
E
UCYN–A
F
AT% 15N
fmol N cell−1 h−1
G
Haptophyte
H
Ctr
N
Fe
NP
NFe
NPFe
PFe
DI
DII
Treatment

Fig. 5

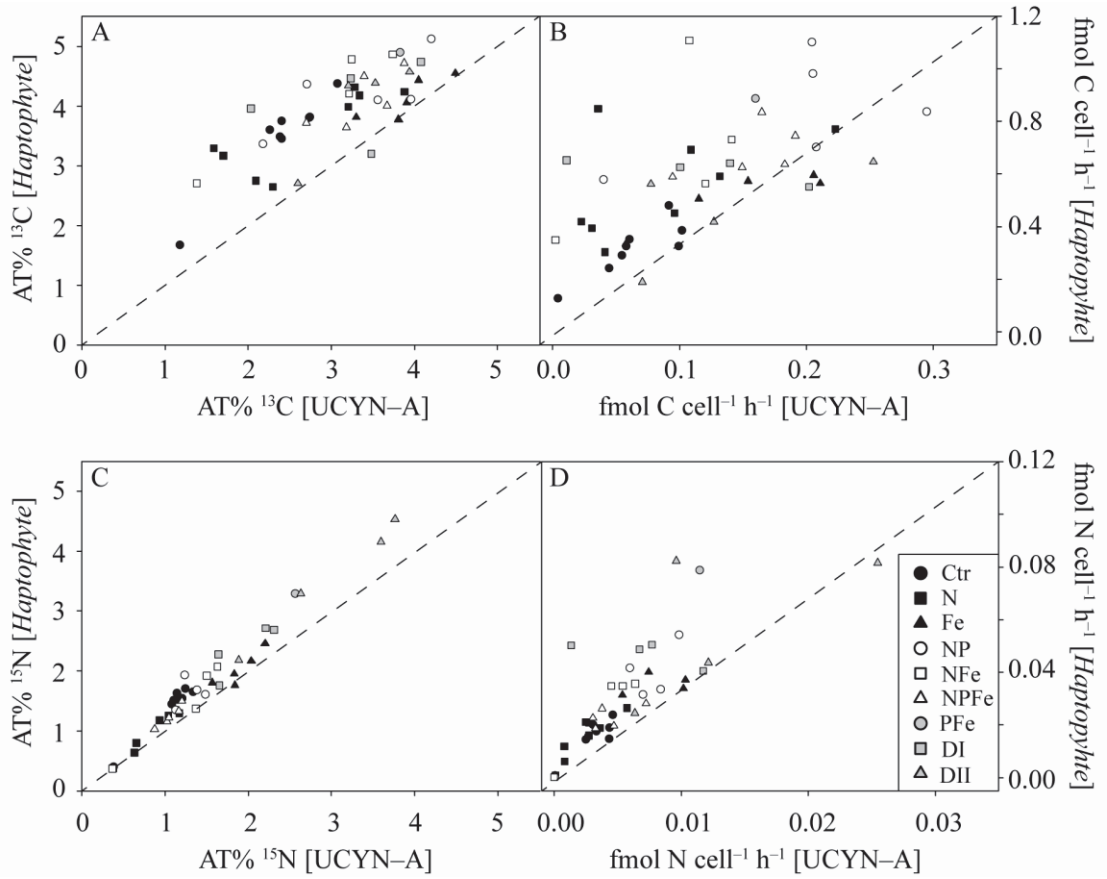
A
B
C
D
AT% 13C [Haptophyte]
AT% 13C [UCYN–A]
fmol C cell−1 h−1 [Haptopyhte]
fmol C cell−1 h−1 [UCYN–A]
AT% 15N [Haptophyte]
AT% 15N [UCYN–A]
fmol N cell−1 h−1 [Haptopyhte]
fmol N cell−1 h−1 [UCYN–A]
Ctr
N
Fe
NP
NFe
NPFe
PFe
DI
DII

Acknowledgements

The authors would like to thank the captain and crew of the R/V *Islandia* and Philip Raab for their assistance during sample collection. We also want to thank Oscar Melicio, Carlos Ferreira Santos, Pericles Silva, Ivanice Monteiro, and Nuno Vieira of the Insituto Nacional de Deesenvolvimento das Pescas (INDP), Cape Verde, for hosting and assisting during this expedition. AK also wants to thank Timothy G. Ferdelman and Sara J. Bender for constructive and important feedback to the manuscript. This study was funded by the Max Planck Society.

References

Amann, R.I., Binder, B.J., Olson, R.J., Chisholm, S.W., Devereux, R., and Stahl, D.A. (1990) Combination of 16S rRNA–targeted oligonucleotide probes with flow cytometry for analyzing mixed microbial populations. *Appl Environ Microbiol* **56**: 1919–1925.

Berman–Frank, I., Cullen, J.T., Shaked, Y., Sherrell, R.M., and Falkowski, P.G. (2001) Iron availability, cellular iron quotas, and nitrogen fixation in *Trichodesmium*. *Limnol Oceanogr* **46**: 1249–1260.

Bonnet, S., and Guieu, C. (2004) Dissolution of atmospheric iron in seawater. *Geophys Res Lett* **31**: 1–4.

Bramlette, M.N. (1958) Significance of coccolithophorids in calcium–carbonate deposition. *Geol Soc Am Bull* **69**: 121–126.

Capone, D.G., Burns, J.A., Montoya, J.P., Subramaniam, A., Mahaffey, C., Gunderson, T. et al. (2005) Nitrogen fixation by *Trichodesmium* spp.: An important source of new nitrogen to the tropical and subtropical North Atlantic Ocean. *Glob Biogeochem Cycles* **19**: 1–17.

Carpenter, E.J., Montoya, J.P., Burns, J., Mulholland, M.R., Subramaniam, A., and Capone, D.G. (1999) Extensive bloom of a N_2–fixing diatom/cyanobacterial association in the tropical Atlantic Ocean. *Mar Ecol Prog Ser* **185**: 273–283.

Church, M.J., Jenkins, B.D., Karl, D.M., and Zehr, J.P. (2005a) Vertical distributions of nitrogen-fixing phylotypes at stn ALOHA in the oligotrophic North Pacific Ocean. *Aquat Microb Ecol* **38**: 3–14.

Church, M.J., Short, C.M., Jenkins, B.D., Karl, D.M., and Zehr, J.P. (2005b) Temporal patterns of nitrogenase gene (*nifH*) expression in the oligotrophic North Pacific Ocean. *Appl Environ Microbiol* **71**: 5362–5370.

Coles, V.J., Hood, R.R., Pascual, M., and Capone, D.G. (2004) Modeling the impact of *Trichodesmium* and nitrogen fixation in the Atlantic Ocean. *J Geophys Res* **109**: 1–17.

Colon-Lopez, M.S., and Sherman, L.A. (1998) Transcriptional and translational regulation of photosystem I and II genes in light-dark- and continuous-light-grown cultures of the unicellular cyanobacterium *Cyanothece* sp. strain ATCC 51142. *J Bacteriol* **180**: 519–526.

Dekaezemacker, J., and Bonnet, S. (2011) Sensitivity of N_2 fixation to combined nitrogen forms ($NO_3^-$and NH_4^+) in two strains of the marine diazotroph *Crocosphaera watsonii* (Cyanobacteria). *Mar Ecol Prog Ser* **438**: 33–46.

DeLong, E.F. (2010) Interesting things come in small packages. *Genome Biol* **11**: 118.

Dugdale, R.C., Menzel, D.W., and Ryther, J.H. (1961) Nitrogen fixation in the Sargasso Sea. *Deep Sea Res* **7**: 297–300.

Falkowski, P.G., and Owens, T.G. (1980) Light–Shade Adaptation: Two strategies in marine phytoplankton. *Plant Physiol* **66**: 592–595.

Foster, R.A., Sztejrenszus, S., and Kuypers, M.M. (2013) Measuring carbon and N_2 fixation in field populations of colonial and free–living unicellular cyanobacteria using nanometer-scale secondary ion mass spectrometry. *J Phycol*: 1–15.

Foster, R.A., Kuypers, M.M.M., Vagner, T., Paerl, R.W., Musat, N., and Zehr, J.P. (2011) Nitrogen fixation and transfer in open ocean diatom–cyanobacterial symbioses. *ISME J* **5**: 1484–1493.

Fritz, J.J. (1999) Carbon fixation and coccolith detachment in the coccolithophore *Emiliania huxleyi* in nitrate–limited cyclostats. *Mar Biol* **133**: 509–518.

Fu, F.–X., Mulholland, M.R., Garcia, N.S., Beck, A., Bernhardt, P.W., Warner, M.E. et al. (2008) Interactions between changing pCO_2, N_2 fixation, and Fe limitation in the marine unicellular cyanobacterium *Crocosphaera*. *Limnol Oceanogr* **53**: 2472–2484.

Gallagher, J.C., and Alberte, R.S. (1985) Photosynthetic and cellular photoadaptive characteristics of three ecotypes of the marine diatom, *Skeletonema costatum* (Grev.) Cleve. *J exp mar Biol Ecol* **94**: 233–250.

Goebel, N.L., Edwards, C.A., Carter, B.J., Achilles, K.M., and Zehr, J.P. (2008) Growth and carbon content of three different sized diazotrophic cyanobacteria observed in the subtropical North Pacific. *J Phycol* **44**: 1212–1220.

Großkopf, T., and LaRoche, J. (2012) Direct and indirect costs of dinitrogen fixation in *Crocosphaera watsonii* WH8501 and possible implications for the nitrogen cycle. *Front Aquat Microbiol* **3**: 1–10.

Großkopf, T., Mohr, W., Baustian, T., Schunck, H., Gill, D., Kuypers, M.M.M. et al. (2012) Doubling of marine dinitrogen-fixation rates based on direct measurements. *Nature* **488**: 361–364.

Guieu, C., and Thomas, A.J. (1996) Saharan aerosols: From the soil to the ocean. In *The impact of desert dust across the Mediterranean*: Springer, pp. 207–216.

Guieu, C., Loÿe-Pilot, M.D., Ridame, C., and Thomas, C. (2002) Chemical characterization of the Saharan dust end–member: Some biogeochemical implications for the western Mediterranean Sea. *J Geophys Res* **107**: 1–11.

Hewson, I., Poretsky, R.S., Beinart, R.A., White, A.E., Shi, T., Bench, S.R. et al. (2009) *In situ* transcriptomic analysis of the globally important keystone N_2–fixing taxon *Crocosphaera watsonii*. *ISME J* **3**: 618–631.

Honjo, S. (1976) Coccoliths: production, transportation and sedimentation. *Mar Micropaleontol* **1**: 65–79.

Howarth, R.W., and Cole, J.J. (1985) Molybdenum availability, nitrogen limitation, and phytoplankton growth in natural waters. *Science* **229**: 653–655.

Jickells, T.D., An, Z.S., Andersen, K.K., Baker, A.R., Bergametti, G., Brooks, N. et al. (2005) Global iron connections between desert dust, ocean biogeochemistry, and climate. *Science* **308**: 67–71.

Karl, D., Michaels, A., Bergman, B., Capone, D., Carpenter, E., Letelier, R. et al. (2002) Dinitrogen fixation in the world's oceans. *Biogeochemistry* **57**: 47–98.

Karl, D.M., Church, M.J., Dore, J.E., Letelier, R.M., and Mahaffey, C. (2012) Predictable and efficient carbon sequestration in the North Pacific Ocean supported by symbiotic nitrogen fixation. *P Natl Acad Sci USA* **109**: 1842–1849.

Krupke, A., Musat, N., LaRoche, J., Mohr, W., Fuchs, B.M., Amann, R.I. et al. (2013) *In situ* identification and N_2 and C fixation rates of uncultivated cyanobacteria populations. *Syst Appl Microbiol* **36**: 259–271.

Kustka, A.B., Sanudo–Wilhelmy, S.A., Carpenter, E.J., Capone, D., Burns, J., and Sunda, W.G. (2003) Iron requirements for dinitrogen–and ammonium–supported growth in cultures of *Trichodesmium* (IMS 101): Comparison with nitrogen fixation rates and iron: carbon ratios of field populations. *Limnol Oceanogr* **48**: 1869–1884.

Langlois, R.J., Hummer, D., and LaRoche, J. (2008) Abundances and distributions of the dominant *nifH* phylotypes in the Northern Atlantic Ocean. *Appl Environ Microbiol* **74**: 1922–1931.

LaRoche, J., and Breitbarth, E. (2005) Importance of the diazotrophs as a source of new nitrogen in the ocean. *J Sea Res* **53**: 67–91.

Luo, Y.W., Doney, S.C., Anderson, L.A., Benavides, M., Bode, A., Bonnet, S. et al. (2012) Database of diazotrophs in global ocean: Abundances, biomass and nitrogen fixation rates. *Earth Syst Sci Data* **5**: 47–106.

Mague, T.H., Weare, N.M., and Holm–Hansen, O. (1974) Nitrogen fixation in the north Pacific Ocean. *Mar Biol* **24**: 109–119.

Mills, M.M., Ridame, C., Davey, M., La Roche, J., and Geider, R.J. (2004) Iron and phosphorus co–limit nitrogen fixation in the eastern tropical North Atlantic. *Nature* **429**: 292–294.

Mohr, W., Intermaggio, M.P., and LaRoche, J. (2010a) Diel rhythm of nitrogen and carbon metabolism in the unicellular, diazotrophic cyanobacterium *Crocosphaera watsonii* WH8501. *Environ Microbiol* **12**: 412–421.

Mohr, W., Großkopf, T., Wallace, D.W.R., and LaRoche, J. (2010b) Methodological underestimation of oceanic nitrogen fixation rates. *PLoS ONE* **5**: e12583.

Moisander, P.H., Beinart, R.A., Hewson, I., White, A.E., Johnson, K.S., Carlson, C.A. et al. (2010) Unicellular cyanobacterial distributions broaden the oceanic N_2 fixation domain. *Science* **327**: 1512–1514.

Montoya, J.P., Holl, C.M., Zehr, J.P., Hansen, A., Villareal, T.A., and Capone, D.G. (2004) High rates of N_2 fixation by unicellular diazotrophs in the oligotrophic Pacific Ocean. *Nature* **430**: 1027–1032.

Pernthaler, A., and Amann, R. (2004) Simultaneous fluorescence in situ hybridization of mRNA and rRNA in environmental bacteria. *Appl Environ Microbiol* **70**: 5426–5433.

Pernthaler, A., and Pernthaler, J. (2007) Fluorescence *In Situ* Hybridization for the Identification of Environmental Microbes. In *Protocols for Nucleic Acid Analysis by Nonradioactive Probes* pp. 153–164.

Pernthaler, A., Pernthaler, J., and Amann, R. (2004) Sensitive multi–color fluorescence in situ hybridization for the identification of environmental microorganisms. *Mol Microb Ecol Man* **3**: 711–726.

Polerecky, L., Adam, B., Milucka, J., Musat, N., Vagner, T., and Kuypers, M.M.M. (2012) Look@NanoSIMS – A tool for the analysis of nanoSIMS data in environmental microbiology. . *Environ Microbiol* **4**: 1009–1023.

Postgate, J.R. (1982) *The fundamentals of nitrogen fixation*. Cambridge University Press.

Reddy, K.J., Haskell, J.B., Sherman, D.M., and Sherman, L.A. (1993) Unicellular, aerobic nitrogen–fixing cyanobacteria of the genus *Cyanothece*. *J Bacteriol* **175**: 1284–1292.

Rees, A.P., Gilbert, J.A., and Kelly–Gerreyn, B.A. (2009) Nitrogen fixation in the western English Channel (NE Atlantic ocean). *Mar Ecol Prog Ser* **374**: 7–12.

Ridame, C., and Guieu, C. (2002) Saharan input of phosphate to the oligotrophic water of the open western Mediterranean Sea. *Limnol Oceanogr* **47**: 856–869.

Sañudo–Wilhelmy, S.A., Kustka, A.B., Gobler, C.J., Hutchins, D.A., Yang, M., Lwiza, K. et al. (2001) Phosphorus limitation of nitrogen fixation by *Trichodesmium* in the central Atlantic Ocean. *Nature* **411**: 66–69.

Shi, T., Sun, Y., and Falkowski, P.G. (2007) Effects of iron limitation on the expression of metabolic genes in the marine cyanobacterium *Trichodesmium erythraeum* IMS101. *Environ Microbiol* **9**: 2945–2956.

Short, S.M., and Zehr, J.P. (2007) Nitrogenase gene expression in the Chesapeake Bay Estuary. *Environ Microbiol* **9**: 1591–1596.

Short, S.M., Jenkins, B.D., and Zehr, J.P. (2004) Spatial and temporal distribution of two diazotrophic bacteria in the Chesapeake Bay. *Appl Environ Microbiol* **70**: 2186–2192.

Simon, N., Campbell, L., Örno lfsdo ttir, E., Groben, R., Guillou, L., Lange, M., and Medlin, L.K. (2000) Oligonucleotide probes for the identification of three algal groups by dot blot and fluorescent whole–cell hybridization. *J Eukaryot Microbiol* **47**: 76–84.

Strathmann, R.R. (1967) Estimating the organic carbon content of phytoplankton from cell volume or plasma volume. *Limnol Oceanogr* **12**: 411–418.

Stuut, J.–B., Zabel, M., Ratmeyer, V., Helmke, P., Schefuß, E., Lavik, G., and Schneider, R. (2005) Provenance of present–day eolian dust collected off NW Africa. *J Geophys Res* **110**: 1–14.

Subramaniam, A., Yager, P.L., Carpenter, E.J., Mahaffey, C., Björkman, K., Cooley, S. et al. (2008) Amazon River enhances diazotrophy and carbon sequestration in the tropical North Atlantic Ocean. *P Natl Acad Sci USA* **105**: 10460–10465.

Sun, J., and Liu, D. (2003) Geometric models for calculating cell biovolume and surface area for phytoplankton. *J Plank Res* **25**: 1331–1346.

Thompson, A.W., Foster, R.A., Krupke, A., Carter, B.J., Musat, N., Vaulot, D. et al. (2012) Unicellular cyanobacterium symbiotic with a single–celled eukaryotic alga. *Science* **337**: 1546–1550.

Tripp, H.J., Bench, S.R., Turk, K.A., Foster, R.A., Desany, B.A., Niazi, F. et al. (2010) Metabolic streamlining in an open–ocean nitrogen–fixing cyanobacterium. *Nature* **464**: 90–94.

Tuit, C., Waterbury, J., and Ravizza, G. (2004) Diel variation of molybdenum and iron in marine diazotrophic cyanobacteria. *Limnol Oceanogr* **49**: 978–990.

Turk, K.A., Rees, A.P., Zehr, J.P., Pereira, N., Swift, P., Shelley, R. et al. (2011) Nitrogen fixation and nitrogenase (*nifH*) expression in tropical waters of the eastern North Atlantic. *ISME J* **5**: 1201–1212.

Verity, P.G., Robertson, C.Y., Tronzo, C.R., Andrews, M.G., Nelson, J.R., and Sieracki, M.E. (1992) Relationships between cell volume and the carbon and nitrogen content of marine photosynthetic nanoplankton. *Limnol Oceanogr* **37**: 1434–1446.

Villareal, T.A. (1991) Nitrogen-fixation by the cyanobacterial symbiont of the diatom genus *Hemiaulus*. *Mar Ecol Prog Ser* **76**: 201–204.

Vu, T.T., Stolyar, S.M., Pinchuk, G.E., Hill, E.A., Kucek, L.A., Brown, R.N. et al. (2012) Genome–scale modeling of light–driven reductant partitioning and carbon fluxes in diazotrophic unicellular cyanobacterium *Cyanothece* sp. ATCC 51142. *PLoS Comput Biol* **8**: e1002460.

Wallner, G., Amann, R., and Beisker, W. (1993) Optimizing fluorescent *in situ* hybridization with rRNA targeted oligonucleotide probes for flow cytometric identification of microorganisms. *Cytometry* **14**: 136–143.

Webb, E.A., Moffett, J.W., and Waterbury, J.B. (2001) Iron stress in open–ocean cyanobacteria (*Synechococcus*, *Trichodesmium*, and *Crocosphaera* spp.): Identification of the IdiA protein. *Appl Environ Microbiol* **67**: 5444–5452.

Zehr, J.P., Mellon, M.T., and Zani, S. (1998) New nitrogen–fixing microorganisms detected in oligotrophic oceans by amplification of nitrogenase (*nifH*) genes. *Appl Environ Microbiol* **64**: 3444–3450.

Zehr, J.P., Waterbury, J.B., Turner, P.J., Montoya, J.P., Omoregie, E., Steward, G.F. et al. (2001) Unicellular cyanobacteria fix N_2 in the subtropical North Pacific Ocean. *Nature* **412**: 635–637.

Zehr, J.P., Bench, S.R., Carter, B.J., Hewson, I., Niazi, F., Shi, T. et al. (2008) Globally distributed uncultivated oceanic N_2–fixing cyanobacteria lack oxygenic photosystem II. *Science* **322**: 1110–1112.

2.4.1 Manuscript IV: Supplementary Information

Supplementary Fig. 1: Summary of AT% ^{13}C and ^{15}N isotopic signal for (A,C) UCYN–A and (B,D) *Haptophyta* cells correlating to the respective cell diameters. Listed treatments from top to bottom: Ctr = control; N = NH_4^+ + NO_3^-; F = Fe^{2+}; NP = NH_4^+ + NO_3^- + PO_4^{3-}; NF = NH_4^+ + NO_3^- + Fe^{2+}; NPFe = NH_4^+ + NO_3^- + PO_4^{3-} + Fe^{2+}; DI = 2 mg/L Saharan dust; DII = 4 mg/L Saharan Dust.

Supplementary Fig. 2: Summary of nanoSIMS measurements showing the ^{13}C and ^{15}N isotopic signal in AT% for association between (A) UCYN–A and (B) *Haptophyta* according to different nutrient amendment incubation experiments. Listed treatments from top to bottom: Ctr = control; N = NH_4^+ + NO_3^-; F = Fe^{2+}; NP = NH_4^+ + NO_3^- + PO_4^{3-}; NF = NH_4^+ + NO_3^- + Fe^{2+}; NPFe = NH_4^+ + NO_3^- + PO_4^{3-} + Fe^{2+}; DI = 2 mg/L Saharan dust; DII = 4 mg/L Saharan Dust.

Supplementary Fig. 3: Summary of nanoSIMS measurements showing the ^{13}C and ^{15}N isotopic signal (AT%) within individual UCYN–A cells and their corresponding partner cell (*Haptophyta*) according to various nutrient amendment incubation experiments. Circles (open and filled) represent UCYN–A cells and squares (open and filled) represent *Haptophyta* cells. The color coding refers to the respective partner cells.

Supplementary Fig. 1

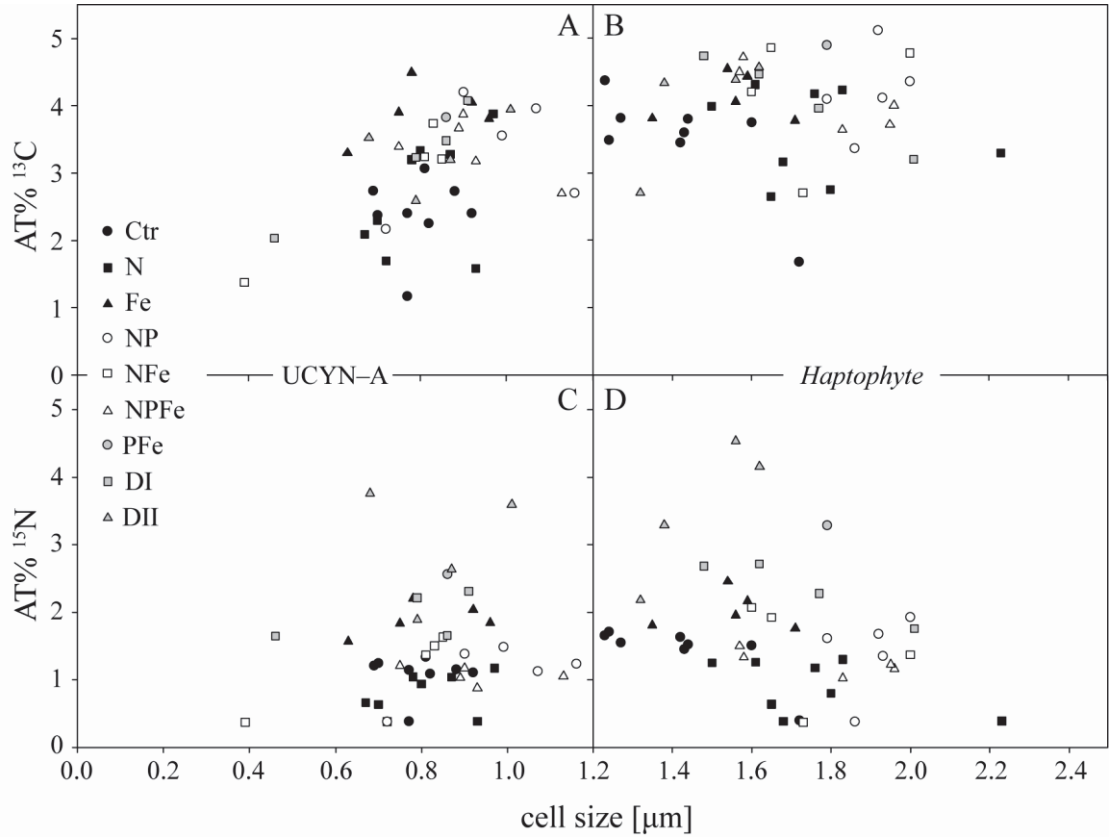

Supplementary Fig. 2

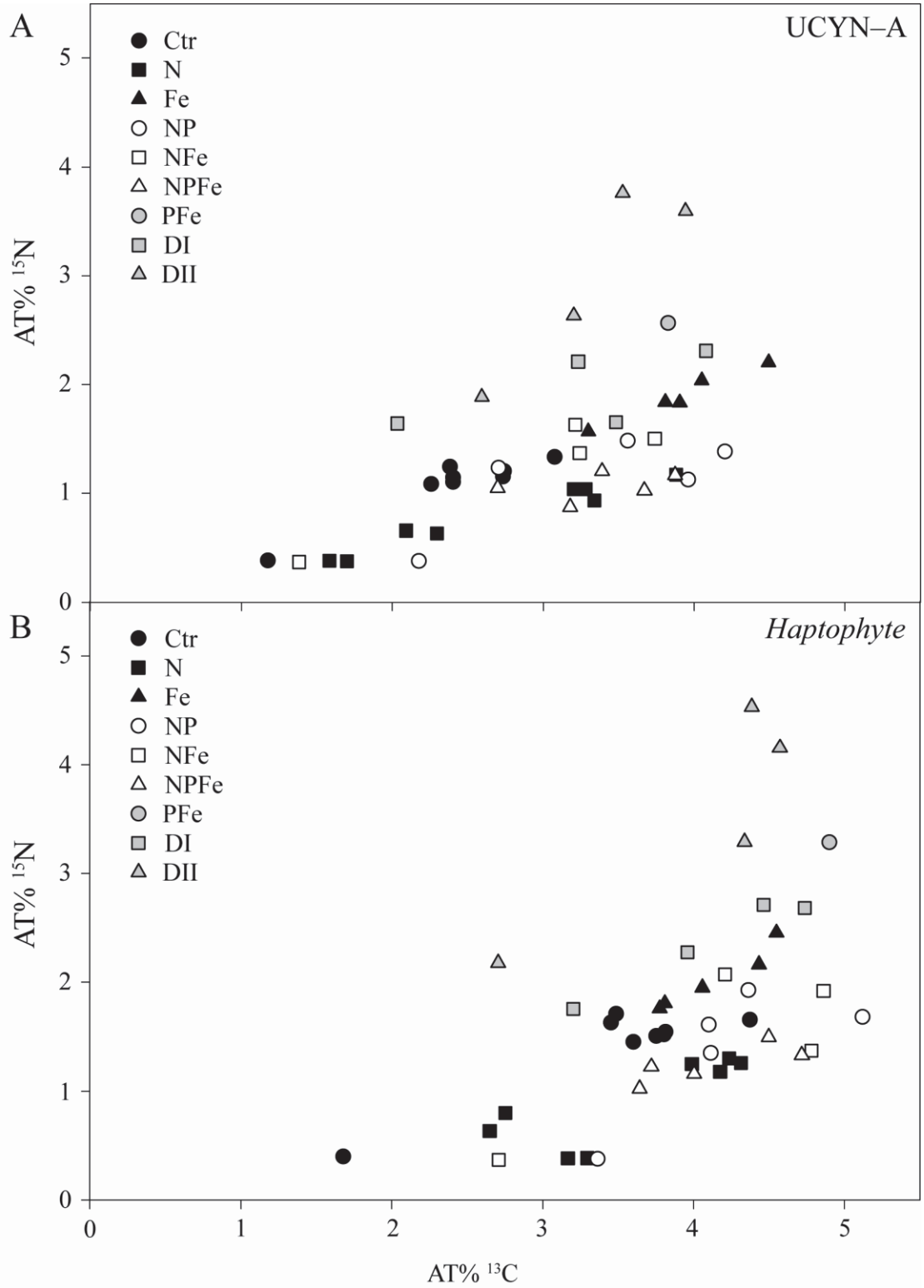

Supplementary Fig. 3

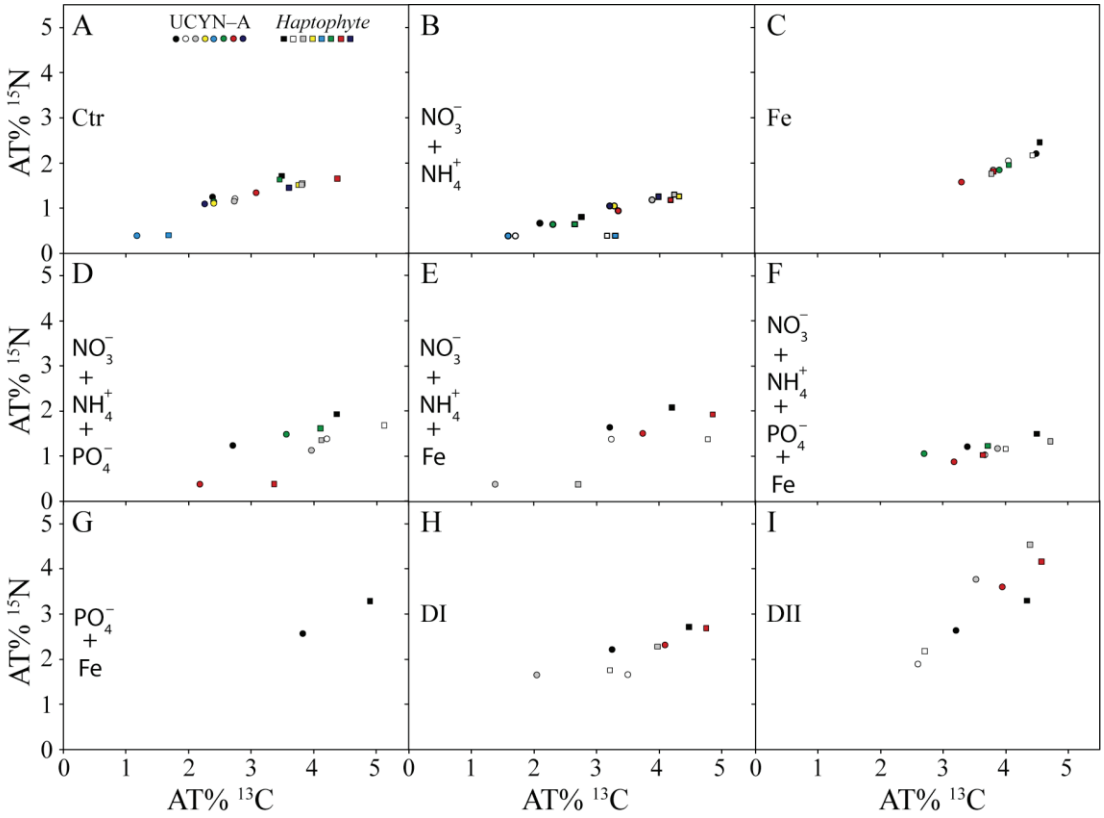

3 General Discussion and outlook

Unicellular cyanobacteria have been shown to be globally distributed in the marine environment, and they play a major role in the marine nitrogen cycle (Zehr et al., 2001; Montoya et al., 2004). Despite their wide distribution, only a few representative open ocean diazotrophs have been brought into culture, which makes it difficult to study these groups of microorganisms. In particular, the uncultured unicellular cyanobacteria group UCYN–A can dominate diazotrophic communities, indicated by high group specific *nifH* gene copy abundances (Church et al., 2008; Moisander et al., 2010). The N_2 fixation activity of UCYN–A is usually inferred from *nifH* gene expression pattern, which exhibit elevated transcripts during the day (Church et al., 2005b). These findings are unusual for unicellular cyanobacteria; typically, N_2 fixation is carried out during the night to prevent the nitrogenase enzyme from inactivation through oxygen–evolving photosynthesis (Mitsui et al., 1987; Toepel, 2009; Mohr et al., 2010a; Sherman et al., 2010). Thus far, the physiology of UCYN–A has been studied via environmental genome analysis, and has revealed an enigmatic genetic repertoire different from other cyanobacteria, e.g. lacking genes for CO_2 fixation, which likely prevents these microbes from living autotrophically (Tripp et al., 2010). These findings help to explain observed UCYN-A *nifH* gene expression during the day, but they also raise additional question as to how these microorganisms thrive in the environment.

UCYN–A living in symbiosis. The development of a 16S rRNA oligonucleotide probe that targeted UCYN–A cells and its successful application on environmental samples allowed us to image their metabolic activity within individual cells for the first time (Manuscript I and II). We found UCYN–A cells living in association with calcifying nanoplankton, e.g. *Braarudosphaera bigelowii*, and we demonstrated a transfer of carbon and nitrogen compounds between these two partner cells, providing insight into how these diazotrophs thrive in open ocean environments. Next, using double CARD–FISH assays, we provided quantitative information on the cellular abundance of UCYN–A in the North Atlantic Ocean and showed that the majority of these diazotrophs live in association with a *Haptophyta* versus free–living cells (Manuscript III). Interestingly, UCYN–A cells were also detected in association with non–calcifying microorganisms and eukaryotes that were not *Haptophyta*, raising questions of the host specificity. We hypothesize that UCYN–A can associate with a variety of eukaryotes, giving it a much better ecological advantage when environmental conditions change. This is supported by the fact that UCYN–A is more broadly distributed than other diazotrophs and can be found in diverse marine regimes (Short and Zehr, 2007; Rees et al., 2009; Moisander et al., 2010). Future work that focuses on identifying subgroups

of *Haptophyta* that appear in association with UCYN–A, as well as other eukaryotes that associate with UCYN-A, will allow us to address questions about host specificity. Parallel investigations that gather genomic data on these host cells will provide helpful information on potential nutrient transfer mechanisms within these unique associations.

Carbon and nitrogen transfer between UCYN–A and Haptophyta cells. The UCYN–A association is uncultivated, which means that our knowledge about the physiological interactions between these two partner cells, as well as the environmental factors that constrain its N_2 fixation activity are based on field studies. To investigate the effects of nutrient additions (including iron, phosphorus, ammonium–nitrate and iron-rich Saharan Dust) on the carbon and nitrogen exchange between UCYN–A and *Haptopyhta* cells, we conducted various field incubation experiments (Manuscript IV). Single cell measurements showed that UCYN–A N_2 fixation is limited by phosphate and iron addition (including Saharan dust), whereas the metabolic activity of the *Haptophyta* partner cells was mainly ammonium–nitrate, phosphate and iron limited. Independent of nutrient treatment, we demonstrated a tight coupling in carbon and nitrogen transfer within individual associations, suggesting that UCYN–A cells play an important role in regulating the growth of partner *Haptophyta* cells by transferring substantial amounts of fixed nitrogen. It remains unclear, yet intriguing, what carbon source is transferred between UCYN–A and their partner cell to support this N_2 fixation activity. The combination of stable isotope incubation experiments using ^{13}C labelled substrate and subsequent Fourier–Transform ion cyclotron resonance mass spectrometer (FT–ICR–MS) analysis provides one promising approach for identifying the carbon compound(s) exchanged in the partnership. This technology can precisely determine atomic masses of single organic carbon molecules and derive their molecular structure (Koch et al., 2005; Dittmar and Paeng, 2009). Such an analysis would not only provide insight into the carbon compounds exchanged in this association, but it also might provide the key to cultivation attempts through the identification of carbon compounds that are critical to the growth of UCYN–A.

Interestingly, we found that UCYN–A N_2 fixation activity is not inhibited when inorganic nitrogen (i.e. ammonium and nitrate) was added (Manuscript IV). Other diazotrophs are typically restricted to nitrate depleted waters, and their activity is inhibited by the presence of nitrate (Ramos and Guerrero, 1983; Mulholland et al., 2001). The cultured unicellular diazotroph *Crocosphaera watsonii* exhibited a similar response to UCYN–A under the presence of nitrate (Dekaezemacker and Bonnet, 2011; Großkopf and LaRoche, 2012). The ability to take up inorganic nitrogen is believed to increase the competitive fitness of these

organisms and might give UCYN–A an advantage in mixed communities of non–diazotrophic populations (Agawin et al., 2007). This work emphasizes the diverse physiological capabilities of different diazotrophic populations, and the need to incorporate these metabolic differences into global N_2 fixation models (Sanz–Alférez and del Campo, 1994; Großkopf and LaRoche, 2012).

Oxygen protection in unicellular diazotrophs. The nitrogenase enzyme works best under reduced conditions (Postgate, 1982; Fay, 1992), even though diazotrophs are constantly exposed to high levels of oxygen in pelagic waters of the subtropical and tropical oceans. The development of strategies to prevent nitrogenase inhibition through oxygen contact is crucial for survival. UCYN–A *nifH* gene expression peaks during the day, indicating that N_2 fixation depends on the energy supply through photosynthetically–derived reducing equivalents and implying that both processes need to occur at the same time. Nonetheless, exact mechanisms that protect nitrogenase from oxygen inactivation within the UCYN–A association remain unclear.

Increased respiratory activity during the dark period is believed to be one mechanism to remove intracellular oxygen to establish anoxic conditions (Peschek et al., 1991; Bergman et al., 1993). The diazotroph *Azotobacter vinelandii* reveals elevated activity of certain cytochromes (i.e. *bd* oxidase) under high oxygen concentrations in order to scavenge respiratory electrons and therefore, keep oxygen concentrations low (Robson and Postgate, 1980; Poole and Hill, 1997). In addition, the Mehler reaction may reduce intracellular oxygen concentrations of diazotrophic microorganisms by scavenging oxygen (Mehler, 1951; Berman–Frank et al., 2001b). *Autoprotection* is another strategy to reduce intracellular oxygen concentrations (Oelze, 2000). Future studies that investigate how UCYN–A achieves oxygen protection, including examination of the third cellular structure observed in the UCYN–A–*Haptophyta* association (Manuscript IV) and its putative role in metabolic partitioning, are necessary to understand these intricate processes.

Future approaches for studying the UCYN-A symbiosis. The metabolic activity of diazotrophs with respect to CO_2 and N_2 fixation has been shown to be regulated by circadian rhythms (Chen et al., 1996; Mohr et al., 2010a). Therefore, additional incubation experiments that assess the carbon and nitrogen metabolism of symbiotic UCYN–A cells should encompass multiple time points to monitor nutrient exchange and growth rates accurately. Since we depend on field samples to assess N_2 fixation activity of the UCYN–A association, the diel periodicity needs to be considered for planning and carrying out field experiments. Further, direct comparisons between *in situ* activity (i.e. N_2 fixation) and specific *nifH* gene

expression could give information on the relationship between functional gene abundance and actual metabolic response. In manuscript IV we applied the new $^{15}N_2$ tracer method (Mohr et al., 2010b; Großkopf et al., 2012) that gave more reliable results, but likely underestimated N_2 fixation activity of UCYN–A compared to previous studies (Manuscript I and II) (Thompson et al., 2012; Krupke et al., 2013). Future nitrogen budget calculations will also benefit from this improved methodology.

The results from chapter 5 demonstrate complex physiological responses under varying environmental stimuli and reveal single cell heterogeneity. Our knowledge about regulatory factors that affect N_2 fixation is mainly based on population level analysis, whereas recent cell specific rates indicate phenotypic variation in N_2 fixation activity (Taniuchi et al., 2008; Foster et al., 2013; Mohr et al., 2013). Studying single cell heterogeneity within the UCYN–A association is an interesting aspect for future investigations. Finally, UCYN–A cells can associate with globally abundant calcifying microorganisms, implying a significant role in carbon sequestration in open ocean environments as suggested for associations between diazotrophs and diatoms (Foster et al., 2011; Karl et al., 2012). Future studies should look to compare the specific impact on carbon sequestration in respect to carbonate based UCYN–A associations and silica based diatom–diazotroph associations. Investigating spatial–temporal differences between these types of associations and understanding environmental factors (e.g. temperature, nutrient concentrations or grazing) controlling the ecological fate of these associations are necessary to develop accurate models of global N_2 fixation.

In addition to the ecological importance of N_2 fixation in marine systems, the UCYN–A association represents an intriguing form of symbiosis from an evolutionary perspective. It could be that it represents an early stage in endosymbiosis that led to chloroplast development; these are organelles mostly found in plants, where CO_2 fixation occurs, and evolved from symbiotic cyanobacteria that have been incorporated into their host cells. Understanding the physiological mechanisms within this unique association has economic implications through biotechnological applications, providing novel pathways to establish symbiotic relationships between diazotrophic microorganisms and plants. Such scientific findings can be utilized for agricultural purposes where the N_2 fixing symbionts enhance the supply of fixed nitrogen to the plant, thus generating higher crop yields.

N_2 fixation in future oceans. The protection from oxidative stress in diazotrophic cells to perform N_2 fixation draws attention to marine environments that are characterized by low oxygen levels, i.e. oxygen minimum zones (OMZs). These areas are critical for the marine nitrogen inventory because they account for ~30–50% nitrogen–loss mainly due to

denitrification and anaerobic oxidation of ammonium (Codispoti et al., 2001; Gruber, 2004; Kuypers et al., 2005). The oxygen depletion in these regions (due to the degradation of sinking organic matter) can be assigned to habitat loss for species at higher levels (Stramma et al., 2011). OMZs have also been thought to form potential hot spots for N_2 fixation, as suggested by Deutsch et al. (2007). The co–occurrence of denitrification and N_2 fixation activity in an alpine lake has also been demonstrated (Halm et al., 2009). OMZs are expected to expand in the future due to climate change, which could have implications on the marine nitrogen inventory and ecosystems (Stramma et al., 2008). Increased N_2 fixation could possibly lead to increased input of fixed nitrogen, counteracting nitrogen–loss in these regions. Understanding the balance between nitrogen–loss and nitrogen–gain processes is essential to assessing the regulation of nitrogen–cycling in these regions.

The impact of a changing climate, such as rising CO_2 concentrations, will alter N_2 fixation activity. Studies on *Trichodesmium* and *Crocosphaera watsonii* showed increased N_2 fixation activity under elevated CO_2 levels (Barcelos e Ramos et al., 2007; Hutchins et al., 2007; Fu et al., 2008), implying that open ocean diazotrophs could fuel the *biological carbon pump* by increasing the supply of nitrogen for primary producers. Increasing CO_2 levels can also cause opposite effects by inhibiting growth and reducing N_2 fixation rates (Czerny et al., 2009). Additional environmentally-induced changes, such as regional differences in mineral dust deposition that affect iron availability in surface waters, as well as the release of phosphorus and nitrogen compounds from dust, might alter N_2 fixation and overall primary production (Baker et al., 2007; Rijkenberg et al., 2008).

Global change accompanied by increasing atmospheric CO_2, increasing OMZs (and their elevated denitrification), as well as elevated anthropogenically–induced flux of fixed nitrogen species towards the oceans represent a few examples of environmental factors that will influence diazotrophs. The identification of a novel association between UCYN-A and a eukaryotic partner cell, as well as the discovery that these types of associations are widespread, opens up a new arena for assessing N_2 fixation in the world's ocean. Organismal interactions likely play a critical role in determining the flux of carbon and nitrogen in the marine environment, as indicated by the observed transfer of compounds between the partner cells in this dissertation. Furthermore, the discovery of heterotrophic N_2 fixing organisms, which are widely distributed and appear in oceanic regions where other autotrophic diazotrophs are absent (e.g. deep water zones), indicates that additional studies are necessary to determine which diazotrophs are present in the world's oceans and the extent of their metabolic activity. Understanding vertical and biogeographic distributions of different

diazotrophic groups, as well as their physiological activity will provide insight into determining how these microorganisms influence marine ecosystems and ultimately, how they influence the *biological carbon pump*. In order to make predications on future ocean scenarios, we need to deepen our understanding about marine N_2 fixation in the present-day ocean.

3.1 References

Agawin, N.S., Rabouille, S., Veldhuis, M., Servatius, L., Hol, S., van Overzee, H.M.J., and Huisman, J. (2007) Competition and facilitation between unicellular nitrogen–fixing cyanobacteria and non–nitrogen–fixing phytoplankton species. *Limnol Oceanogr* **52**: 2233–2248.

Baker, A.R., Weston, K., Kelly, S.D., Voss, M., Streu, P., and Cape, J.N. (2007) Dry and wet deposition of nutrients from the tropical Atlantic atmosphere: Links to primary productivity and nitrogen fixation. *Deep-Sea Res Pt I* **54**: 1704–1720.

Barcelos e Ramos, J., Biswas, H., Schulz, K.G., LaRoche, J., and Riebesell, U. (2007) Effect of rising atmospheric carbon dioxide on the marine nitrogen fixer *Trichodesmium*. *Glob Biogeochem Cycles* **21**: 1–6.

Bergman, B., Siddiqui, P.J.A., Carpenter, E.J., and Peschek, G.A. (1993) Cytochrome oxidase: Subcellular distribution and relationship to nitrogenase expression in the nonheterocystous marine cyanobacterium *Trichodesmium thiebautii*. *Appl Environ Microbiol* **59**: 3239–3244.

Berman–Frank, I., Lundgren, P., Chen, Y.–B., Küpper, H., Kolber, Z., Bergman, B., and Falkowski, P. (2001) Segregation of nitrogen fixation and oxygenic photosynthesis in the marine cyanobacterium *Trichodesmium*. *Science* **294**: 1534–1537.

Chen, Y.–B., Zehr, J.P., and Mellon, M. (1996) Growth and nitrogen fixation of the diazotrophic filamentous nonheterocystous cyanobacterium *Trichodesmium* sp. IMS 101 in defined media: Evidence for a circadian rhythm. *J Phycol* **32**: 916–923.

Church, M.J., Short, C.M., Jenkins, B.D., Karl, D.M., and Zehr, J.P. (2005) Temporal patterns of nitrogenase gene (*nifH*) expression in the oligotrophic North Pacific Ocean. *Appl Environ Microbiol* **71**: 5362–5370.

Church, M.J., Björkman, K.M., Karl, D.M., Saito, M.A., and Zehr, J.P. (2008) Regional distributions of nitrogen–fixing bacteria in the Pacific Ocean. *Limnol Oceanogr* **53**: 63–77.

Codispoti, L.A., Brandes, J.A., Christensen, J.P., Devol, A.H., Naqvi, S.W.A., Paerl, H.W., and Yoshinari, T. (2001) The oceanic fixed nitrogen and nitrous oxide budgets: Moving targets as we enter the anthropocene? *Scientia Marina* **65**: 85–105.

Czerny, J., Barcelos e Ramos, J., and Riebesell, U. (2009) Influence of elevated CO_2 concentrations on cell division and nitrogen fixation rates in the bloom–forming cyanobacterium *Nodularia spumigena*. *Biogeosciences* **6**: 1865–1875.

Dekaezemacker, J., and Bonnet, S. (2011) Sensitivity of N_2 fixation to combined nitrogen forms ($NO_3^-$and NH_4^+) in two strains of the marine diazotroph *Crocosphaera watsonii* (Cyanobacteria). *Mar Ecol Prog Ser* **438**: 33–46.

Deutsch, C., Sarmiento, J.L., Sigman, D.M., Gruber, N., and Dunne, J.P. (2007) Spatial coupling of nitrogen inputs and losses in the ocean. *Nature* **445**: 163–167.

Dittmar, T., and Paeng, J. (2009) A heat–induced molecular signature in marine dissolved organic matter. *Nat Geosci* **2**: 175–179.

Fay, P. (1992) Oxygen relations of nitrogen fixation in cyanobacteria. *Microbiol Mol Biol Rev* **56**: 340–373.

Foster, R.A., Sztejrenszus, S., and Kuypers, M.M. (2013) Measuring carbon and N_2 fixation in field populations of colonial and free–living unicellular cyanobacteria using nanometer-scale secondary ion mass spectrometry. *J Phycol*: 1–15.

Foster, R.A., Kuypers, M.M.M., Vagner, T., Paerl, R.W., Musat, N., and Zehr, J.P. (2011) Nitrogen fixation and transfer in open ocean diatom–cyanobacterial symbioses. *ISME J* **5**: 1484–1493.

Fu, F.–X., Mulholland, M.R., Garcia, N.S., Beck, A., Bernhardt, P.W., Warner, M.E. et al. (2008) Interactions between changing pCO_2, N_2 fixation, and Fe limitation in the marine unicellular cyanobacterium *Crocosphaera*. *Limnol Oceanogr* **53**: 2472–2484.

Großkopf, T., and LaRoche, J. (2012) Direct and indirect costs of dinitrogen fixation in *Crocosphaera watsonii* WH8501 and possible implications for the nitrogen cycle. *Front Aquat Microbiol* **3**: 1–10.

Großkopf, T., Mohr, W., Baustian, T., Schunck, H., Gill, D., Kuypers, M.M.M. et al. (2012) Doubling of marine dinitrogen-fixation rates based on direct measurements. *Nature* **488**: 361–364.

Gruber, N. (2004) The dynamics of the marine nitrogen cycle and its influence on atmospheric CO_2 variations. In *The ocean carbon cycle and climate*: Springer, pp. 97–148.

Halm, H., Musat, N., Lam, P., Langlois, R., Musat, F., Peduzzi, S. et al. (2009) Co–occurrence of denitrification and nitrogen fixation in a meromictic lake, Lake Cadagno (Switzerland). *Environ Microbiol* **11**: 1945–1958.

Hutchins, D.A., Fu, F., Zhang, Y., Warner, M.E., Feng, Y., Portune, K. et al. (2007) CO_2 control of *Trichodesmium* N_2 fixation, photosynthesis, growth rates, and elemental ratios: Implications for past, present, and future ocean biogeochemistry. *Limnol Oceanogr* **52**: 1293–1304.

Karl, D.M., Church, M.J., Dore, J.E., Letelier, R.M., and Mahaffey, C. (2012) Predictable and efficient carbon sequestration in the North Pacific Ocean supported by symbiotic nitrogen fixation. *P Natl Acad Sci USA* **109**: 1842–1849.

Koch, B.P., Witt, M., Engbrodt, R., Dittmar, T., and Kattner, G. (2005) Molecular formulae of marine and terrigenous dissolved organic matter detected by electrospray ionization Fourier transform ion cyclotron resonance mass spectrometry. *Geochim Cosmochim Acta* **69**: 3299–3308.

Krupke, A., Musat, N., LaRoche, J., Mohr, W., Fuchs, B.M., Amann, R.I. et al. (2013) *In situ* identification and N_2 and C fixation rates of uncultivated cyanobacteria populations. *Syst Appl Microbiol* **36**: 259–271.

Kuypers, M.M.M., Lavik, G., Woebken, D., Schmid, M., Fuchs, B.M., Amann, R. et al. (2005) Massive nitrogen loss from the Benguela upwelling system through anaerobic ammonium oxidation. *P Natl Acad Sci USA* **102**: 6478–6483.

Mehler, A.H. (1951) Studies on reactions of illuminated chloroplasts: I. Mechanism of the reduction of oxygen and other hill reagents. *Arch Biochem Biophys* **33**: 65–77.

Mitsui, A., Cao, S., Takahashi, A., and Arai, T. (1987) Growth synchrony and cellular parameters of the unicellular nitrogen fixing marine cyanobacterium, *Synechococcus* sp. strain Miami BG 043511 under continuous illumination. *Physiol Plantarum* **69**: 1–8.

Mohr, W., Intermaggio, M.P., and LaRoche, J. (2010a) Diel rhythm of nitrogen and carbon metabolism in the unicellular, diazotrophic cyanobacterium *Crocosphaera watsonii* WH8501. *Environ Microbiol* **12**: 412–421.

Mohr, W., Großkopf, T., Wallace, D.W.R., and LaRoche, J. (2010b) Methodological underestimation of oceanic nitrogen fixation rates. *PLoS ONE* **5**: e12583.

Mohr, W., Vagner, T., Kuypers, M.M.M., Ackermann, M., and LaRoche, J. (2013) Resolution of Conflicting Signals at the Single–Cell Level in the Regulation of Cyanobacterial Photosynthesis and Nitrogen Fixation. *PLoS ONE* **8**: e66060.

Moisander, P.H., Beinart, R.A., Hewson, I., White, A.E., Johnson, K.S., Carlson, C.A. et al. (2010) Unicellular cyanobacterial distributions broaden the oceanic N_2 fixation domain. *Science* **327**: 1512–1514.

Montoya, J.P., Holl, C.M., Zehr, J.P., Hansen, A., Villareal, T.A., and Capone, D.G. (2004) High rates of N_2 fixation by unicellular diazotrophs in the oligotrophic Pacific Ocean. *Nature* **430**: 1027–1032.

Mulholland, M.R., Ohki, K., and Capone, D.G. (2001) Nutrient controls on nitrogen uptake and metabolism by natural populations and cultures of *Trichodesmium* (Cyanobacteria). *J Phycol* **37**: 1001–1009.

Oelze, J. (2000) Respiratory protection of nitrogenase in *Azotobacter* species: Is a widely held hypothesis unequivocally supported by experimental evidence? *FEMS Microbiol Rev* **24**: 321–333.

Peschek, G.A., Villgrater, K., and Wastyn, M. (1991) "Respiratory protection" of the nitrogenase in dinitrogen–fixing cyanobacteria. *Plant Soil* **137**: 17–24.

Poole, R., and Hill, S. (1997) Respiratory protection of nitrogenase activity in *Azotobacter vinelandii*–roles of the terminal oxidases. *Biosci Rep* **17**: 303–317.

Postgate, J.R. (1982) *The fundamentals of nitrogen fixation*. Cambridge University Press.

Ramos, J.L., and Guerrero, M.G. (1983) Involvement of ammonium metabolism in the nitrate inhibition of nitrogen fixation in *Anabaena* sp. strain ATCC 33047. *Arch Microbiol* **136**: 81–83.

Rees, A.P., Gilbert, J.A., and Kelly–Gerreyn, B.A. (2009) Nitrogen fixation in the western English Channel (NE Atlantic ocean). *Mar Ecol Prog Ser* **374**: 7–12.

Rijkenberg, M.J.A., Powell, C.F., Dall'Osto, M., Nielsdottir, M.C., Patey, M.D., Hill, P.G. et al. (2008) Changes in iron speciation following a Saharan dust event in the tropical North Atlantic Ocean. *Mar Chem* **110**: 56–67.

Robson, R.L., and Postgate, J.R. (1980) Oxygen and hydrogen in biological nitrogen fixation. *Annu Rev Microbiol* **34**: 183–207.

Sanz–Alférez, S., and del Campo, F.F. (1994) Relationship between nitrogen fixation and nitrate metabolism in the *Nodularia* strains M1 and M2. *Planta* **194**: 339–345.

Sherman, L.A., Min, H., Toepel, J., and Pakrasi, H.B. (2010) Better Living Through *Cyanothece*–Unicellular Diazotrophic Cyanobacteria with Highly Versatile Metabolic Systems. *Adv Exp Med Biol* **675**: 275–290.

Short, S.M., and Zehr, J.P. (2007) Nitrogenase gene expression in the Chesapeake Bay Estuary. *Environ Microbiol* **9**: 1591–1596.

Stramma, L., Johnson, G.C., Sprintall, J., and Mohrholz, V. (2008) Expanding oxygen–minimum zones in the tropical oceans. *Science* **320**: 655–658.

Stramma, L., Prince, E.D., Schmidtko, S., Luo, J., Hoolihan, J.P., Visbeck, M. et al. (2011) Expansion of oxygen minimum zones may reduce available habitat for tropical pelagic fishes. *Nature Climate Change* **2**: 33–37.

Taniuchi, Y., Murakami, A., and Ohki, K. (2008) Whole–cell immunocytochemical detection of nitrogenase in cyanobacteria: Improved protocol for highly fluorescent cells. *Aquat Microb Ecol* **51**: 237–247.

Thompson, A.W., Foster, R.A., Krupke, A., Carter, B.J., Musat, N., Vaulot, D. et al. (2012) Unicellular cyanobacterium symbiotic with a single–celled eukaryotic alga. *Science* **337**: 1546–1550.

Toepel, J. (2009) Transcriptional analysis of the unicellular, diazotrophic cyanobacteria *Cyanothece* sp. ATCC 51142 grown under short day/night cycles. *J Phycol* **45**: 610–620.

Tripp, H.J., Bench, S.R., Turk, K.A., Foster, R.A., Desany, B.A., Niazi, F. et al. (2010) Metabolic streamlining in an open–ocean nitrogen–fixing cyanobacterium. *Nature* **464**: 90–94.

Zehr, J.P., Waterbury, J.B., Turner, P.J., Montoya, J.P., Omoregie, E., Steward, G.F. et al. (2001) Unicellular cyanobacteria fix N_2 in the subtropical North Pacific Ocean. *Nature* **412**: 635–637.

4 Appendix

4.1 Responses of the coastal bacterial community to viral infection of the algae *Phaeocystis globosa*

A.R. Sheik[1*], C.P.D. Brussaard[2], G. Lavik[1], P. Lam[1], N. Musat[3], A. Krupke[1], S. Littmann[1], M. Strous[1], M.M.M. Kuypers[1]

[1]Max Planck Institute for Marine Microbiology, Celciusstraße 1, Bremen, Germany.
[2]Department of Biological Oceanography, NIOZ – Royal Netherlands Institute for Sea Research, Texel, The Netherlands.
[3]Department of Isotope Biogeochemistry, Helmholtz Centre for Environmental Research–UFZ, Permoserstraße 15, Leipzig, Germany.
[*]Corresponding author. E–mail: arsheik@mpi–bremen.de

Accepted in: *Environmental Microbiology*

Keywords: *Alteromonas* and *Roseobacter*, carbon remineralization, nanoSIMS, *Phaeocystis globosa*, pyrosequencing, viral lysis

Contribution: AK conducted nanoSIMS measurements and data acquisition.

Abstract

Algal cell lysis upon infection is thought to be the significant process how lytic viruses structure bacterial communities and affect biogeochemical fluxes. We show that organic matter leakage or excretion by infected yet intact algal cells is already largely responsible for shaping North Sea bacterial community composition and enhanced bacterial substrate assimilation. Prior to algal cell lysis, the application of nano–scale secondary–ion mass spectrometry (nanoSIMS) showed a high transfer of infected ^{13}C and ^{15}N–labelled *Phaeocystis globosa* biomass, which stimulated substrate assimilation by *Alteromonas* cells and triggered its attachment to the infected algal host 'phycosphere'. The leakage or enhanced excretion in response to algal viral infection was not reported previously and represents a so far undocumented way of viruses facilitating bacterial substrate assimilation. The bacterial response to algal viral lysis itself was very rapid with a temporal succession of *Alteromonas* and *Roseobacter* populations and distinct bacterial phylotypes relative to non–infected control cultures. Additionally, our results show that viral lysis of *P. globosa* single cells results in the formation of aggregates which are colonized densely with bacteria. Subsequent bacteriophage lysis appeared to be responsible for aggregates dissolution and ultimately led to substantial regeneration of dissolved inorganic carbon (55% of the particulate ^{13}C–organic carbon). These findings reveal a critical role of viruses in the leakage or excretion of algal biomass upon infection, which provides an ecological niche for specific bacterial populations and potentially redirects carbon availability.

4.2 Draft genome sequence of marine alphaproteobacterial strain HIMB11, the first cultivated representative of a unique lineage within the Roseobacter clade possessing a remarkably small genome

Bryndan P. Durham[1,2], Jana Grote[1,3], Kerry A. Whittaker[1,4], Sara J. Bender[1,5], Haiwei Luo[6], Sharon L. Grim[1,7], Julie M. Brown[1,8], John R. Casey[1,3], Antony Dron[1,9], Lennis R. Florez–Leiva[1,10], Andreas Krupke[1,11], Catherine M. Luria[1,12], Aric H. Mine[1,13], Santhiska Pather[1,14], Agathe Talarmin[1,15], Emma K. Wear[1,16], Thomas S. Weber[1,17], Jesse M. Wilson[1,18], Matthew J. Church[1,3], Edward F. DeLong[1,19], David M. Karl[1,3], Grieg F. Steward[1,3], John M. Eppley[1,19], Nikos C. Kyrpides[1,20], Stephan Schuster[1,21], and Michael S. Rappé[1,22]*

[1]Center for Microbial Oceanography: Research and Education, 2011 Summer Course in Microbial Oceanography, SOEST, University of Hawaii, Honolulu, Hawaii, USA
[2]Department of Microbiology, University of Georgia, Athens, Georgia, USA
[3]Department of Oceanography, SOEST, University of Hawaii, Honolulu, Hawaii, USA
[4]Graduate School of Oceanography, University of Rhode Island, Kingston, Rhode Island, USA
[5]School of Oceanography, University of Washington, Seattle, Washington, USA
[6]Department of Marine Sciences, University of Georgia, Athens, Georgia, USA
[7]University of Delaware, Newark, Delaware, USA
[8]Cornell University, Ithaca, New York, USA
[9]Observatoire Océanologique Villefranche, Villefranche–sur–Mer, France
[10]University of Concepcion, Concepcion, Chile
[11]Max Plank Institute Marine Microbiology, Bremen, Germany
[12]Brown University, Providence, Rhode Island, USA
[13]University of Chicago, Chicago, Illinois, USA
[14]University of Massachusetts Dartmouth, Dartmouth, Massachusetts, USA
[15]Center of Oceanology of Marseilles, La–Seyne–sur–Mer, France
[16]University of California Santa Barbara, Santa Barbara, California, USA
[17]University of California Los Angeles, Los Angeles, California, USA
[18]University of California Merced, Merced, California, USA
[19]Department of Civil and Environmental Engineering, Massachusetts Institute of Technology, Cambridge, Massachusetts, USA

[20]Department of Energy Joint Genome Institute, Walnut Creek, California, USA
[21]Center for Comparative Genomics and Bioinformatics, Pennsylvania State University, University Park, Pennsylvania, USA
[22]Hawaii Institute of Marine Biology, SOEST, University of Hawaii, Kaneohe, Hawaii, USA

[*]Corresponding author. E–mail: rappe@hawaii.edu

In preparation for: *Standards in Genomic Sciences*

Keywords: marine bacterioplankton, roseobacter, aerobic anoxygenic phototroph, dimethylsulfoniopropionate

Contribution: A.K. was involved in detecting genes encoding transporters for ammonium and other various nitrogen–containing substrates (e.g. amino acids, polyamines, glycine betaine, taurine)

Abstract

Strain HIMB11 is a planktonic marine bacterium isolated from coastal seawater of the tropical North Pacific Ocean that belongs to the ubiquitous and versatile Roseobacter clade of the alphaproteobacterial family *Rhodobacteraceae*. Here we describe the preliminary characteristics of strain HIMB11, including annotation of the draft genome sequence and comparative genomic analysis with other members of the Roseobacter lineage. The 3,098,747 bp draft genome is arranged in 34 contigs and contains 3,183 protein–coding genes and 54 RNA genes. Phylogenomic and 16S rRNA gene analyses indicate that HIMB11 represents a unique sublineage within the Roseobacter clade. Comparison with other publicly available genome sequences from members of the Roseobacter lineage reveals that strain HIMB11 has the genomic potential to utilize a comparatively wide variety of energy sources (e.g. light, carbon monoxide), while also possessing a reduced number of substrate transporters.

4.3 *In situ* oxygenic photosynthesis fuels aerobic oxidation of methane in the anoxic water of Lago di Cadagno

Carsten J. Schubert [1,3*], Jana Milucka[2,3], Mathias Kirf[1], Andreas Krupke[2], Phyllis Lam[2], Marcel M.M. Kuypers[2]

[1]Dept. Surface Waters–Research and Management, Swiss Federal Institute of Aquatic Science and Technology (Eawag), Seestrasse 79, CH–6047 Kastanienbaum, Switzerland
[2]Department of Biogeochemistry, Max Planck Institute for Marine Microbiology, Celsiusstrasse 1, 28359 Bremen, Germany
[3]These authors contributed equally to this work

[*]Corresponding author. E–mail: Carsten.Schubert@eawag.ch

In preparation for: *The ISME Journal*

Keywords: Aerobic methanotrophs, freshwater, Lago di Cadagno, methane oxidation

Contribution: A.K. collected samples during the field trip in 2009, measured various physical–chemical parameters, prepared samples for IRMS and performed CARD–FISH assays on purple and green sulphur bacteria.

Abstract

Freshwater lakes represent large methane reservoirs which contribute up to 13% of all methane emissions to the atmosphere. Unlike in marine settings where sulfate is the main oxidant, the full variety of processes responsible for methane removal in lacustrine environments is still not understood. Here we investigated methane oxidation in the water column of a permanently stratified lake, Lago di Cadagno, in which methane is almost completely oxidized before reaching the water surface. Highest rates of methane oxidation were measured at and below the oxycline and the process was accompanied by a high carbon isotopic fractionation of methane (α_C=1.035). Interestingly, known anaerobic methanotrophic archaea (ANME) could not be detected in these anoxic waters. Instead we found abundant alpha– and gamma–proteobacterial aerobic methanotrophic bacteria (MOB) in all investigated water depths. Gamma–MOB were active under anoxic conditions and assimilated methane carbon. In contrast, alpha–MOB did not take up any methane–derived carbon and they might feed on excretion products of e.g. algae, with which they associate. The measured geochemical profiles and *in vitro* incubations revealed that of all tested potential electron acceptors only oxygen additions resulted in increased rates of methane oxidation. Similar effect was observed when the samples were incubated in the light, presumably due to oxygen production by photosynthesis. Given the widespread distribution of shallow stratified lakes, we propose that photosynthesis–driven aerobic methane oxidation might be a common mechanism for methane removal from anoxic lacustrine environments.

4.4 Experimental and single cell approaches to understanding microbial life in subsurface sediments underlying the extremely oligotrophic South Pacific Gyre

Anand Patel[1], Tim G. Ferdelman[2], Andreas Krupke[2], Wiebke Ziebis[1*]

[1]University of Southern California
[2]Max–Planck–Institute for Marine Microbiology

[*]Corresponding author. E–mail:wziebis@usc.edu

In preparation for: *Frontiers in Microbiology*

Keywords: Sub–seafloor, nitrogen–uptake, single cell activity, oligotrophic, nanoSIMS

Contribution: A.K. supervised HISH–SIMS assays, performed nanoSIMS measurements and data acquisition.

Abstract

The South Pacific Gyre (SPG) is the largest oceanic province on our planet, yet very little is known about microbial life at and below the seafloor of this extremely oligotrophic region. In the better–studied continental margins, sediments have very different biological processes at play. Chlorophyll concentrations in the water column and carbon burial rates at the seafloor within the gyre are the lowest in the Ocean. Within the gyre, the seafloor is thinly draped with sediments comprised mostly of deep–sea red clay or nanofossil carbonate ooze (with water depths of 3500 to 5700 m and sediment thickness of ~70 m at the edges to < 2 m in the very center). During IODP Expedition 329 seafloor drilling, sediment cores were recovered along 2 transects at 6 sites spanning from the gyre edges to its ultra–oligotrophic center, plus a 7th site just to the south of the gyre. The main goal of the expedition was to explore the nature of the sub–seafloor habitats and the microbial communities of this vast ocean area. Onboard studies documented that oxygen and nitrate penetrated the entire sediment column within the gyre, whereas at the outside station oxygen was depleted within the top 1.5 m, exhibiting a mainly anoxic sediment column, typical of less oligotrophic ocean regions. Microbial cell abundances were very low within the gyre sediments, with values at the detection limit and became undetectable with greater depth. To explore and compare the metabolic activities of these entirely oxic sub–seafloor habitats, sediments samples were taken from drill cores at 3–4 different sediment depths over the entire thickness of the sediment cover at each site. We performed onboard incubation experiments, using stable and radio–isotopic labeled substrates, to test for potential autotrophic versus heterotrophic metabolisms (^{14}C–carbon dioxide, ^{14}C–acetate), as well as for nitrogen turnover and uptake (^{15}N–dinitrogen, ^{15}N–ammonium). A protocol was developed and tested to efficiently (80–90%) extract and concentrate intact cells from these very low–abundance habitats for single cell analyses using nanoSIMS. Initial examination of our cell extracts, using FISH, indicated that bacterial cells dominate. NanoSIMS analyses showed strong incorporation of ^{15}N–ammonium into bacterial cells. We are currently performing statistical comparisons to explore a possible trend of uptake rates across the gyre and with depth. The results of our investigations will provide a significant step towards understanding microbial life underneath oligotrophic open ocean gyres.

5 Acknowledgements

The past five years at this Max Planck Institute have been a unique opportunity! Obtaining the doctoral degree usually happens once in your life and I don't aspire to do it twice ☺
This period of time here has been eye-opening and life-changing for me and I am grateful to a lot of people that believed in me and supported me on different levels throughout these years.

To begin with, I would like to thank Prof. Dr. Marcel Kuypers for accepting me as one of his PhD students and giving me the possibility to conduct my thesis project. The scientific input and feedback that I received over the past five years including the time as a Master student was immensely helpful in making my research work successful. I feel privileged for saying that I have been supervised by you, Marcel, and unaccountably happy for this chance. I also want to acknowledge PD Dr. Bernhard Fuchs, who supported and accompanied my scientific development from the very beginning five years ago until the end of my doctoral thesis. Marcel and Bernhard, I am indebted and thankful to both of you for critical, but constructive guidance, and motivating ideas, especially in methodological issues.

I would further like to thank Dr. Niculina Musat, Dr. Timothy G. Ferdelman, Dr. Gaute Lavik, Dr. Rachel Foster, Prof. Dr. Ir. Marc Strous and Prof. Dr. Rudolf Amann. Every one of you had a tremendous impact on my thesis work and I lack the exact words to express how much it means to me. Your constant care and support helped me to cross the finish line of my doctoral thesis work.

Being part of the Biogeochemistry Department was an amazing experience and at this point I want to thank the technical assistants in this group for their kind support regarding laboratory work and great interactions, especially Gabriele Klockgether, Daniela Franzke, Tomas Vagner, Daniela Nini and Sten Littmann. I also want to send a special thank you to technical assistants from the Department of Molecular Ecology for their help, patience and consistent support throughout all these years, especially Jörg Wulf and Silke Wetzel.

I want to assign my gratitude to people from the logistics and administration departments for exceptional organizational skills in helping me before, during and after field expeditions as well as for various other matters including conference trips etc, particularly Thomas Wilkop and Ulrike Tietjen.

Further, I want to say thank you to my MarMic class 2012, especially my office mates Jessika Füssel, Hannah Marchant and Zainab Beiruti. Likewise, to Dr. Karl-Heinz Blotevogel and Dr. Christiane Glöckner. You guys made my *MarMic* experience unforgettable!

I want to express a special thank you to great companions, old and new friends, which make my social life amazing: Abdul Rahiman Sheik, Philipp Hach, Soeren Heinrich Ahmerkamp, Birgit Adam, Marcel Günther, Stefan Zwiebel Thiele, Thomas Holler, Andre Kubetin, Martin Thiele, Nino Kipp, Lukas Galla, Thomas Weber, Santhiska Pather, Bryndan P. Durham, Kerry A. Whittaker and many more!

I dedicate my doctoral thesis to five persons, who mean a lot to me. Each one of them played a significant role in my life and enriched it with beautiful thoughts and memories every single day: Liebe Mama und lieber Papa, danke dafür dass ihr so wundervolle Eltern seid und ihr mich die ganzen Jahre über bedingungslos unterstützt habt und mir immer den Rücken gestärkt habt, in jeglicher Lebenssituation. Liebe Julia, danke, dass ich dich als Schwester haben darf und mit dir so viele schöne Erinnerung teile. Lieber Ulf, eine bessere *broschaft* kann ich mir nicht vorstellen…in diesem Sinne *Hausten*! Liebe Sara, ich bin die sehr dankbar für dein Verständnis, Zuneigung und Unterstützung über die letzten Jahre…du bist einzigartig und ich danke dir, dass du es mit mir aushältst! Jeder Einzelne von euch weckt Emotionen, die das Leben lebenswert machen! Danke, dass ich euch habe!

6 Erklärung

Name: Andreas Krupke
Anschrift: Prangenstraße 92, 28203 Bremen
Datum: 16.08.2013

Erklärung

Hiermit versichere ich, dass ich

1. die Arbeit ohne unerlaubte fremde Hilfe angefertigt habe,
2. keine anderen als die von mir angegebenen Quellen und Hilfsmittel benutzt habe und
3. die den benutzten Werken wörtlich oder inhaltlich entnommenen Stellen als solche kenntlich gemacht habe.

Bremen, den 16.08.2013

_____

(Unterschrift)